Experimental evolution and characterisation of glyphosate resistance in green alga *Chlamydomonas reinhardtii*

Erika M Hansson

A thesis submitted for the degree of Doctor of Philosophy

The University Of Sheffield.

The University of Sheffield
Faculty of Science
School of Biosciences

July 2022

To R. Lethbridge,
U. Lethbridge
and S. Bug

Acknowledgements

Above all, thank you to my supervisors Andrew Beckerman and Dylan Childs. I could not have done this without you. Thank you for teaching me your approach to science, supporting me and helping me keep my spirits up when things didn't work out as planned, and inspiring me to always think one step further. Your guidance has made me the scientist I am today and will influence me for the rest of my career.

A very special thanks to Heather Walker for helping me turn what was supposed to be a quick side-question into a full-blown chapter and tirelessly answering all my questions. Thank you to Mike Burrell for introducing me to the wonders of mass spectrometry, and thank you to Alex Williams for taking the time to give advice on compound and pathway identification strategies.

Thank you to the generations of postdocs, PhDs and master students in the Beckerman and Childs lab groups whose time here have overlapped with mine, for advice and making the work days fun. Special thanks to Holly for running the first pilot of the clumping assay method for me.

Thank you to the departmental technical staff, especially Allison, Lynsey, Timo and Andy, for general advice, keeping track of equipment and samples and help maintaining algal stocks throughout the years — including a maternity leave and a pandemic.

Thank you to the rotifer experts in the Butlin lab — Aga, Joe and Nathan — for advice and letting me steal some shelf space for my stocks. Thank you to the Brockhurst lab for letting me use and abuse their machines, and Megan and Rosanna specifically for teaching me how to use the machines and providing settings and trouble shooting.

Thank you to my department for funding my research, and thank you to the FoS Mass Spectrometry Centre for providing me with a voucher allowing me to use their time and resources.

Lastly, thank you to my family — husband, daughter, cat, parents and siblings – for all the support and putting up with being talked at about algae.

Author's declaration

The research presented in this thesis is my own and it has not been submitted for any other award at this or any other institution.

CHAPTER 2

This chapter has been published as:

Hansson, E.M., Childs, D.Z. and Beckerman, A.P. (2022). Mesostats — A multiplexed, low-cost, do-it-yourself continuous culturing system for experimental evolution of mesocosms. PLoS ONE 17(7): e0272052. DOI:10.1371/journal.pone.0272052

The manuscript is reproduced fully in the thesis with minor formatting alterations. The data presented in this chapter, along with relevant code, is available at DOI:10.5281/zenodo.6786427. EMH, APB and DZC conceived the study. EMH performed the experiments and collected the data. EMH performed the statistical analyses with contributions from APB and DZC. EMH wrote the manuscript with contributions from APB and DZC.

CHAPTER 3

This chapter is currently in preparation for submission to Proceedings of the Royal Society B as:

Hansson, E.M., Childs, D.Z. and Beckerman, A.P. (2022). Glyphosate resistance evolution to lethal and sublethal doses in chemostat populations of model organism *Chlamydomonas reinhardtii*.

The manuscript is reproduced fully in the thesis with minor formatting alterations. EMH, APB and DZC conceived the study. EMH performed the experiments and collected the data. EMH performed the statistical analyses with contributions from APB and DZC. EMH wrote the manuscript with contributions from APB and DZC.

CHAPTER 4

This chapter is currently in preparation for submission to Functional Ecology as:

Hansson, E.M., Childs, D.Z. and Beckerman, A.P. (2022). Evidence for a trade-off between glyphosate resistance and anti-grazer defence in green alga *Chlamydomonas reinhardtii*.

The manuscript is reproduced fully in the thesis with minor formatting alterations. EMH, APB and DZC conceived the study. EMH performed the experiments and collected the data. EMH performed the statistical analyses with contributions from APB and DZC. EMH wrote the manuscript with contributions from APB and DZC.

CHAPTER 5

This chapter is currently in preparation for submission to Current Biology as:

Hansson, E.M., Walker, H.J., Childs, D.Z. and Beckerman, A.P. (2022). Metabolomic profiling of glyphosate resistance evolution in green alga *Chlamydomonas reinhardtii*.

EMH, HJW, APB and DZC conceived the study. EMH performed the experimental evolution and sample collection, EMH and HJW performed the mass spectrometry and collected the data. EMH performed the statistical analyses with contributions from APB and DZC. EMH wrote the manuscript with contributions from APB, DZC and HJW.

Thesis abstract

Modern agriculture is completely dependent on chemical weed control to ensure crop yields, but the widespread and persistent use of herbicides has led to both a strong selective pressure for weeds to evolve resistance and pollution of non-target ecosystems. Understanding the evolutionary dynamics of herbicide resistance is pivotal to managing both aspects as they determine how weeds and organisms within non-target ecosystems will respond through time. Microbial model organisms like green alga *Chlamydomonas reinhardtii* provide the opportunity to control and monitor resistance evolution in action in the lab, as well as representing a major group of non-target organisms exposed to herbicide pollution. The dynamics of evolving glyphosate resistance in *C. reinhardtii* were thus here characterised by continuous flow-through cultures exposed to lethal and sublethal doses of glyphosate and continuous assaying through time to determine when resistance evolved, the extent of the increase in resistance, test for intrinsic and extrinsic fitness consequences, as well as creating a fingerprint of the changing cellular metabolic state. The results show rapid evolution to the lethal dose, with tentative evidence for the sublethal dose populations exhibiting the same pattern but at a delay. While intrinsic fitness consequences were indicated to be low or non-existent, an extrinsic fitness consequence was found in the form of increased variance in the ability to deploy anti-grazer defences. The metabolomics screen revealed extensive disruption of cellular machinery in response to glyphosate that was mitigated by the evolution of resistance, as well as strong evidence of a persisting secondary effect of glyphosate through oxidative damage after resistance evolved. This thesis thus emphasises the necessity of considering resistance evolution as a complex process with multiple components, the timing of which may matter to the outcome of management strategies aiming to prevent resistant weeds or conserve natural ecosystems.

Table of Contents

List of Figures

List of Tables

CHAPTER 1

General introduction

1.1 THE PROBLEM WITH HERBICIDES

1.1.1 THE AGE OF HERBICIDES – A SUCCESS STORY FEEDING THE WORLD

The invention of the first synthetic herbicide in the early 1940s marked the start of an agricultural revolution (Shaner, 2014; Timmons, 1970). While humans have relied on many methods for protection of crop yields against weeds and other pests throughout the history of agriculture, the first commercially available herbicide — plant hormone analogue 2,4-D (Quastel, 1950) — ushered in a new era with a fundamentally changed agricultural strategy and management outlook. As a direct result of the increasing use of chemical crop protection, there was a significant reduction in the need for human, animal or mechanical power in pest management, while crop yields boomed (Timmons, 1970). The discovery of new herbicides in the following decades continued at an exponential rate, going from 15 commercially available formulations in 1940 to 120 by 1969 (Timmons, 1970).

1.1.1.1 HOW AND WHY HERBICIDES WORK

Weeds are unwanted plants that risk outcompeting crops and depleting space and resources unless managed. The threat to crop yields from weeds is considerable and with the highest potential of causing loss out of all pests, in modern times often resulting in losses around 10% for major crops (Oerke, 2006). The projected losses without management, however, is estimated at four times as much (Oerke, 2006). Chemical weed control has also allowed new forms of agriculture like vast monocultures or very high use of fertiliser to increase crop yield, systems that would otherwise be at extreme risk from weeds (Shaner, 2014; Timmons, 1970).

Herbicides control weeds by causing growth arrest, defoliation or death, and may be selective (e.g. targeting dicot weeds while having little effect on monocot crops) or non-selective, having a broad-spectrum effect on all plants. Non-selective herbicides may be used for clearing land, or they may be used with crops genetically engineered to be resistant. In general, herbicides are highly effective, usually killing 90-99% of the target weed (Délye *et al.*, 2013), while non-chemical methods require the combination of several, generally highly labour intensive, strategies to reach the same efficacy (Bastiaans *et al.*, 2008). Herbicides can be further divided into groups based on their mode of action (MoA) – i.e. the molecular effect on the target organism (Table 1.1). Out of the huge range of possible targets within a cell, any given herbicide will have a highly specific effect that then has a knock-on effect on the overall cellular machinery by either enabling light activation of reactive oxygen species, disrupting cellular metabolism, or inhibiting cellular division and growth (HRAC, 2022).

Weed management is pivotal to keeping the world fed and the economy stable, making herbicides foundational to modern agriculture as the main tool. A failed harvest has consequences reaching far beyond the individual farmer, impacting the whole community depending on it for food and labour. Furthermore, modern farms are often part of a complex supply chain, and main crops like soybeans and cotton are not grown for human consumption but for sustaining livestock and

Table 1.1: HRAC herbicide mode of action classification groups as of 2022 (HRAC, 2022).

HRAC group	Mode of Action	Target Pathway/Process
1	Inhibition of ACCase	Amino acid synthesis
2	Inhibition of ALS	Fatty acid synthesis
3	Inhibition of microtubule assembly	Microtubule organisation
4	Auxin mimics	Hormone based gene regulation
5	Inhibition of photosynthesis PS II (Serine 264)	Photosynthesis
6	Inhibition of photosynthesis PS II (Histidine 215)	Photosynthesis
9	Inhibition of EPSP synthase	Amino acid synthesis
10	Inhibition of glutamine synthease	Amino acid synthesis
12	Inhibitions of PDS	Photosynthesis
13	Inhibition of DOXP synthase	Photosynthesis
14	Inhibition of PPO	Photosynthesis
15	Inhibition of VLCFAs	Fatty acid synthesis
18	DHP inhibition	Tetrahydrofolate synthesis
19	Auxin transport inhibitors	Hormone transport
22	PS I electron diversion	Photosynthesis
23	Inhibition of microtubule organisation	Microtubule organisation
24	Uncouplers	ATP synthesis
27	Inhibition of HPPD	Photosynthesis
28	Inhibition of dihydroorotate dehydrogenase	Pyrimidine synthesis
29	Inhibition of cellulose synthase	Cell wall synthesis
30	Inhibition of fatty acid thioesterase	Fatty acid synthesis
31	Inhibition of serine/threonine proteine phosphatase	Cell signalling
32	Inhibition if solanesyl diphosphate synthase	Photosynthesis
33	Inhibition of homogentisate solanesyltransferase	Photosynthesis
34	Inhibition of lycopene cyclase	Photosynthesis

textile production. The herbicide industry was as a result estimated at $33.65 billion in 2020, and projected to grow to $47.09 billion in 2025 (Business Wire, 2021).

1.1.2 HERBICIDE RESISTANT WEEDS — LIFE FINDS A WAY

The widespread and persistent use of herbicides however also represents a strong selective pressure for weeds to evolve resistance. Continued application of herbicides in the face of mutations and drift invariably lead to phenotypes that might resist the herbicide, and this phenotype will then spread in the population, rendering the given herbicide and dose combination useless against that weed.

1.1.2.1 THE SCALE OF THE PROBLEM

Herbicide resistant weeds was always a known, theoretical risk (Harper, 1956), but when the first case was recorded in 1957 in wild carrot (*Daucus corota* L.) (Mithila *et al.*, 2011; Whitehead & Switzer, 1963) the focus was instead on insecticide-resistant insects and plants were still thought to be of less concern as their comparatively longer life-cycles should slow down the adaptation process (Shaner, 2014). It was not until 1968, when triazine-resistant common groundsel (*Senecio vulgaris* L.) was first discovered (Ryan, 1970), that some weed scientists started to worry. However, as there was a considerable fitness penalty to this resistance phenotype (Conard & Radosevich, 1979; Warwick & Black, 1981) and there were still few recorded instances in response to the over 100 formulations on the market, the threat was not considered pressing by industry or academia (Shaner, 2014).

By 1980, 41 weeds had been recorded to have evolved resistance to at least one herbicide, and most of those were resistant to triazine (Heap, 2022). By 2020, that number was 509 (Figure 1.1). This dramatic increase has been attributed to general increased herbicide use along with the introduction of new herbicide formulations, first ACCase and ALS inhibitors in the early 1980s, and later EPSPS-inhibitor glyphosate combined with genetically engineered glyphosate resistant crops in 1996 (Duke & Powles, 2008; Shaner, 2014; Shaner, 1995). In common for these herbicides is their ease of use and efficacy, leading to rapid and widespread adoption by farmers. And as the herbicide use increased, so did the selective pressure for weeds to evolve resistance. As the use of herbicides continues to increase worldwide, the link between level of use and the number of resistant populations becomes even more apparent, and complex forms of resistance involving multiple mutations and resistance to multiple herbicides and modes of action have increased with time (Gaines *et al.*, 2020; Heap, 2022; Shaner, 2014). This has resulted in several concerted efforts to develop methods to manage and prevent the emergence of herbicide resistance.

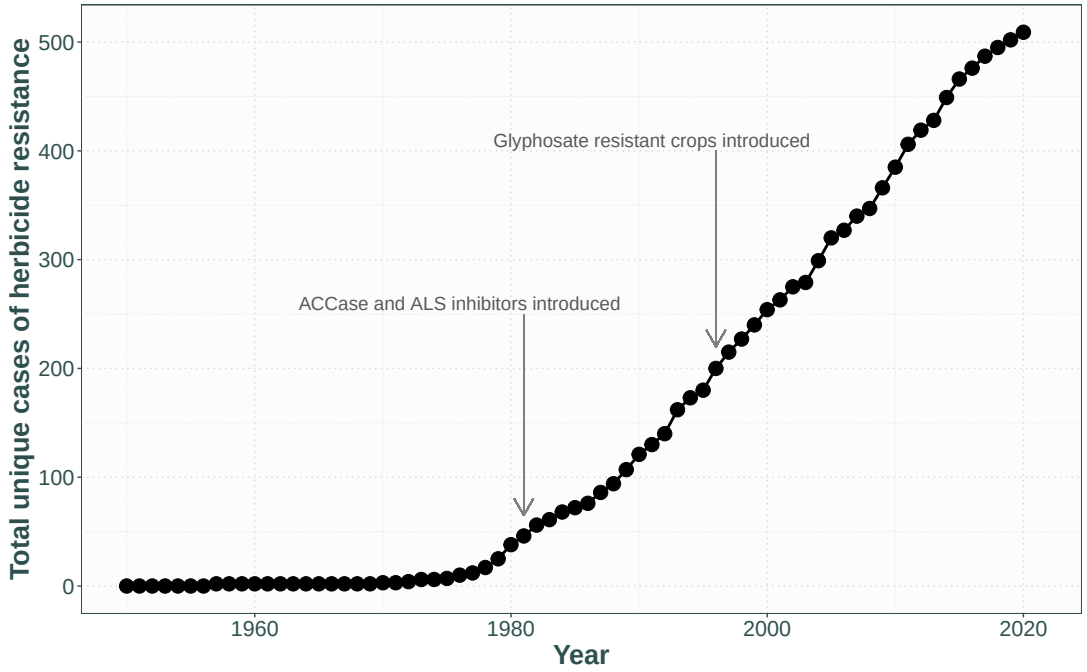

Figure 1.1: Unique cases of herbicide resistant weeds worldwide by year. Adapted from (Heap, 2022).

1.1.2.2 HERBICIDE RESISTANCE MECHANISMS AND THE LIMITS OF HUMAN INVENTION

Herbicide resistance mechanisms can be divided into two classes: target-site resistance (TSR) and non-target-site resistance (NTSR) (Gaines *et al.*, 2020; Powles & Yu, 2010). TSR mechanisms are specialist and limit the herbicide impact by changes to the herbicide target. This may be mutations directly changing the herbicide target, changing its structure and limiting the herbicide-molecule's ability to bind to it (Gaines *et al.*, 2020; Murphy & Tranel, 2019; Powles & Yu, 2010). Alternatively, the target's expression may be up-regulated through gene multiplication or increased transcriptions, increasing the required dose for the herbicide to be effective (Gaines *et al.*, 2020). It is worth noting that the resistance mechanism is most often not in response to the specific herbicide molecule, but to its MoA. Thus evolved resistance to one herbicide will generally be effective against other herbicides sharing that MoA. And while new herbicide formulations regularly make it to market, the rate of discovery for MoAs has declined and is now a relatively rare event, with only two new MoAs discovered recently after a gap of over 30 years (Dayan, 2019; Rüegg *et al.*, 2007; Shino *et al.*, 2018).

NTSR mechanisms instead limit the dose of herbicide reaching the target (Gaines *et al.*, 2020; Powles & Yu, 2010; Yuan *et al.*, 2007). This may be through decreased herbicide absorption into the plant, limited translocation of the herbicide through the plant, sequestration of the herbicide molecule into the metabolically inactive vacuole, or developing the ability to metabolise the herbicide. NTSR mechanisms have further potential for generalist resistance affecting multiple herbicides as they may involve gene families for general stress response and transport, which also makes their role more difficult to identify (Gaines *et al.*, 2020). Currently cytochrome P450 monooxygenases and GSH *S*-transferases have been identified as the most important gene families involved in NTSR (Cummins *et al.*, 2011; Gaines *et al.*, 2020; Werck-Reichhart *et al.*, 2000).

All of these mechanisms can be combined to create a more robust resistance, as well as confer resistance to multiple herbicides (Gaines *et al.*, 2020; Powles & Yu, 2010). Herbicides thus constitute a limited resource where evolution risks outpacing human invention.

1.1.2.3 RESISTANCE MANAGEMENT — OR HOW WE LEARNED TO STOP WORRYING AND LOVE EVOLUTION

When a weed becomes resistant to a given dose of a herbicide, an increased dose may still be effective, depending on the underlying resistance mechanism. Otherwise, a different herbicide with a different MoA has to be used for future weed management. However, either of these options will inevitably repeat the process of resistance evolution to the new weed management method. Rather than attempting to reactively mitigate the impact of herbicide resistant weeds, modern weed management strategies thus focus on pro-actively delaying resistance evolution (Beckie, 2006; Gressel, 2009; Hamill *et al.*, 2004; Powles, 2008) but this requires detailed understanding of the evolutionary process.

How long evolution of resistance takes for a given species depends on the selective pressure, i.e. the herbicide MoA and the dose, as well as the genetics of the population (Gressel, 2009). If resistance is already present as part of the standing genetic variation at a high enough frequency in a population, it may only take a few generations for it to become the dominant phenotype. If the incidence of resistant genotypes in the population is largely absent, resistance evolution will instead be dependent on *de novo*-mutations. How common either route to resistance is in natural populations is still poorly understood (Jasieniuk *et al.*, 1996; Neve *et al.*, 2009; Preston & Powles, 2002; Vila-Aiub *et al.*, 2009a). Population size plays a considerable role in the case of *de novo*-mutations, and weeds tend to have large population sizes (Jasieniuk *et al.*, 1996), but the specific mutations themselves also matter as different parts of the genome have different mutation rates (Futuyma, 2009; Orr, 2000). Furthermore, the number of possible mutations conferring resistance

and how many mutations are required for effective resistance will further influence the rate at which resistance will evolve (Neve *et al.*, 2009).

The exact genetics of the resistance mechanism also matters. Many herbicide resistance alleles contain a single point mutation, but it is possible this is due to the generally strong selective pressure herbicides exert not being conducive to accumulation of smaller fitness effect mutations (Powles & Yu, 2010). While sublethal doses may favour accumulation of minor resistance traits (Busi & Powles, 2009; Busi *et al.*, 2013; Norsworthy *et al.*, 2021) and have been suggested to select for a higher degree of NTSR mechanisms (Powles & Yu, 2010), it has also been hypothesised that the chronic stress of low herbicide doses might lead to increased mutation rates, and instead increase generation of large impact mutations (Cairns *et al.*, 2022; Gressel, 2011; Love & Wagner, 2022). Furthermore, the population structure as well as level of gene flow and the mode of inheritance will further affect the dynamics of resistance evolution (Jasieniuk *et al.*, 1996; Neve *et al.*, 2009).

As all of the above are still poorly characterised for most weed populations and are thus difficult to exploit for management, modern weed management strategies designed to mitigate the effects of herbicide resistance are all underpinned by the basic assumption of evolutionary theory that any new adaptation will confer a fitness cost in the ancestral environment (Vila-Aiub *et al.*, 2009a). The resistance trait is expected to result in a fitness penalty that puts it under negative directional selection in the absence of the herbicide, and thus heterogeneous selection environments are created to slow down the pace of the evolutionary process through changing herbicides in a sequence, cycling between different herbicides or through using herbicide mixtures (Beckie, 2006). This cost may be intrinsic – within the organism – in the form of trade-offs with normal cell function and enzyme activity (Chevillon *et al.*, 1995; Cohan *et al.*, 1993; Groeters *et al.*, 1994), or through increased investment in resistance trading off with resources available for growth or reproduction (Chapin *et al.*, 1993; Coley *et al.*, 1985; Herms & Mattson, 1994). Alternatively, the cost may be extrinsic – outwith the organism – conferring an ecological cost through changed interspecific interactions or compromised performance in different environments or when challenged by competition or other stressors (Gassmann, 2005; Menchari *et al.*, 2007; Pedersen *et al.*, 2007; Strauss *et al.*, 2002; Vila-Aiub *et al.*, 2009a). However, the long-term efficacy of these strategies is poorly understood (Beckie, 2006; Gressel & Segel, 1990; Gressel, 2009; Jasieniuk *et al.*, 1996; Lagator *et al.*, 2013a,b; Neve, 2008; Vogwill *et al.*, 2012), especially as costs are not universal and depend not only on the genetics of the species and the specifics of the selective pressure, but also both the specific mechanism (Vila-Aiub *et al.*, 2005) and allele (Menchari *et al.*, 2007) of resistance, the genetic background (Giacomini *et al.*, 2014; Menchari *et al.*, 2007; Paris *et al.*, 2008), the dominance of the trait (Roux *et al.*, 2004), the herbicide MoA target enzyme (Ashigh & Tardif, 2007; Purrington & Bergelson, 1999; Yu *et al.*, 2010), as well as the biotic and abiotic environment (Ashigh & Tardif, 2009, 2011; Gassmann & Futuyma, 2004; Gassmann, 2005; Menchari *et al.*, 2007; Pedersen *et al.*, 2007; Purrington & Bergelson, 1999; Vila-Aiub *et al.*, 2009b). Furthermore, if multiple resistance mechanisms coexist, the costs conferred by each one may be difficult to untangle, and in specific cases, herbicide resistance alleles might instead confer fitness advantages (Vogwill *et al.*, 2012; Wang *et al.*, 2010).

1.1.3 CONTAMINATION OF NON-TARGET ECOSYSTEMS — A TANGLE OF UNINTENDED CONSEQUENCES

The causes and consequences of resistance within the management of weeds is not isolated to agricultural systems because agriculture is not an isolated system. As the agricultural industry applies increasing amounts of herbicides to increase crop yield and grapple with herbicide resistance, the amount of herbicides reaching non-target ecosystems also increases, contributing to the anthropogenic pollution of natural communities that is implicated in a world-wide biodiversity crisis (Annett *et al.*, 2014; Fugère *et al.*, 2020; Helander *et al.*, 2012; Van Bruggen *et al.*, 2018). As most herbicides are not biodegradable, they first accumulate in the soil (Gill & Garg, 2014; Hussain *et al.*, 2009; Van Bruggen *et al.*, 2018). And as they are seldom specific to only the weeds

they are meant to target, they affect the soil community, having an effect on its overall biomass and composition, in turn affecting biochemical processes like soil nitrification, decomposition and the recycling of nutrients (Boldt & Jacobsen, 1998; Hussain *et al.*, 2009; Lupwayi *et al.*, 2009; Sofo *et al.*, 2012).

From the soil, the herbicides may then enter the ground and surface water through runoff or drainage (Blann *et al.*, 2009; Hébert *et al.*, 2019; Larson *et al.*, 2019; Van Bruggen *et al.*, 2018), where the potential to affect non-target communities of microorganisms (Motta *et al.*, 2018; Saxton *et al.*, 2011), plants (Helander *et al.*, 2012), amphibians (Brühl *et al.*, 2013; Christin *et al.*, 2013; Forson & Storfer, 2006; Relyea, 2003, 2005a, 2012), fish (Kelly *et al.*, 2010; Pereira *et al.*, 2013; Scholz *et al.*, 2012; Tierney *et al.*, 2010), birds (Guerrero *et al.*, 2012; Mitra *et al.*, 2011; Parsons *et al.*, 2010), annelids (Pelosi *et al.*, 2014), arthropods (Amalin *et al.*, 2009; Kevan, 1999) and humans (Dawson *et al.*, 2010; Gill & Garg, 2014), becomes a serious risk. The specific effects depend on the herbicide and species but include organ damage (Pelosi *et al.*, 2014; Pereira *et al.*, 2013), reduced ability to withstand parasite infection or predation (Christin *et al.*, 2013; Forson & Storfer, 2006; Kelly *et al.*, 2010; Lürling *et al.*, 2011; Lürling, 2011), behavioural changes (Mitra *et al.*, 2011; Pelosi *et al.*, 2014; Tierney *et al.*, 2010), reduced reproduction (Parsons *et al.*, 2010; Pelosi *et al.*, 2014) and increased overall mortality of both adult and juvenile organisms (Relyea, 2005a,b). Higher trophic levels are often affected by the herbicides impacting the growth and availability of their food resources (Relyea *et al.*, 2005; Relyea, 2005b), and bioaccumulation of the herbicides in the tissues of primary producers or prey animals allows them to move up through the trophic levels (Bessa da Silva *et al.*, 2016; Pereira *et al.*, 2013). The overall ecosystem effect is generally a restructuring of the makeup of the community as the herbicide has differing effects on different species and organism classes, which may lead to a loss in overall biomass (Motta *et al.*, 2018; Pelosi *et al.*, 2014; Relyea, 2005b), but sometimes it instead leads to a biomass increase as competition is lifted (Saxton *et al.*, 2011). Often this is not solely attributable to the damage caused by the herbicides to individual organisms, but also to the destabilising effects of disrupted natural inter-species interactions (Relyea *et al.*, 2005; Relyea, 2005b). Furthermore, this may have a direct effect on agriculture as the affected non-target species may be pollinators (Kevan, 1999; Motta *et al.*, 2018) or the natural enemies of pests (Amalin *et al.*, 2009). This makes understanding the ecological effects of herbicide use pivotal to sustainable agriculture and food security.

1.2 MODEL SYSTEMS FOR HERBICIDE RESEARCH

While the introduction of herbicides to agriculture led to a considerable increase in crop yield, levels of loss have remained at roughly 10% for major crops since the 1960s (Oerke, 2006). This suggests that the new formulations, MoAs and management strategies developed since then have only served to keep the loss levels steady, and that we find ourselves in an evolutionary arms race against herbicide resistant weeds (Neve *et al.*, 2009). Experimental research thus remains pivotal for revealing herbicide impacts on agriculture and non-target ecosystems. It is necessary to reveal the mechanisms by which resistance can evolve and provide insight into regulatory and management strategies that benefit agricultural production and minimise costs to non-target systems. This in particular means understanding the evolutionary dynamics of herbicide resistance, looking at the process through time to understand how early events like the available standing genetic variation and availability and fitness distribution of resistance-conferring mutations interacts with the ecological context it is in and affects the later stages of the process (Gressel, 2009; Neve *et al.*, 2009; Preston & Powles, 2002). Furthermore, it requires detailed investigation of the assumed fitness costs of resistance, whether they are intrinsic or extrinsic, as their presence will interact with the selective pressures to set the pace of evolution. This has relevance to both agriculture and ecosystem management, but as higher plants grow slowly the majority of studies on herbicide resistance focus on characterising populations where resistance has already emerged, missing out on the evolutionary process leading to resistance (Powles & Yu, 2010).

Similarly, the majority of studies looking at herbicide pollution of natural ecosystems tend to focus on the acute effects on either a specific species or a community as a whole, and do not allow adaptation to the stressor. This is a particularly prevalent shortcoming in studies focusing on multiple stressors that may interact (Baselga-Cervera *et al.*, 2016), especially if one of those stressors is biotic as inter-species interactions are dynamic (Ellner & Becks, 2011; Yoshida *et al.*, 2003). The species interacting assert fluctuating selective pressures on each other and thus both will be affected by any trade-offs between traits integral to that interaction and the ability to cope with the herbicide stress, and interacting consumer-resource populations may see the pattern of their consumer-resource cycles perturbed, or even completely disrupted, depending on the form of the trade-off (Kasada *et al.*, 2014).

In both cases, characterising the adaptation process to herbicides is essential to understanding how it will affect both agriculture and non-target ecosystems long-term. The possible impacts of various factors such as distribution of resistance mutations, gene flow, fitness costs as well as particular management strategies have been evaluated using mathematical models (Diggle *et al.*, 2003; Gressel & Segel, 1990; Jasieniuk *et al.*, 1996; Neve *et al.*, 2011; Neve, 2008), however this relies on the assumptions based in evolutionary theory that are being made are indeed applicable to the system the predictions are being made for. To truly bridge the gap between models and the real world, these assumptions need to be evaluated.

1.2.1 MICROBIAL MODEL SYSTEMS

Experimental evolution using model organisms provides a framework to deal with these issues by testing the evolutionary theory that underpins resistance. In the context of herbicide research, plants like *Arabidopsis thaliana* and *Lemna minor* have been used to evaluate resistance mutation frequency (Jander *et al.*, 2003), and costs (Roux *et al.*, 2004, 2005; Roux & Reboud, 2005), metabolic effects of herbicide application (Kostopoulou *et al.*, 2020; Sikorski *et al.*, 2019) and evaluation of herbicide modes of action (Gomes & Juneau, 2016), but still require considerable resources and space to grow under lab conditions for enough generations. A recent exciting development has been the use of algal model systems as single-celled microorganisms provide an unparalleled opportunity for the study of evolutionary dynamics due to their combination of short generation time, simple genetics and ability to fit huge population sizes in a small space (Elena & Lenski, 2003). The path of evolutionary adaptation can thus be replicated and tightly controlled in real time in the lab, allowing new insights into the mechanisms of adaptive evolution and testing of predictions from theory. Tests may be performed on subsets of the evolving populations in real time but it is also possible to create a 'fossil record' of the adaptation process through freezing the cells or using preservatives like Lugol's solution (Elena & Lenski, 2003). This may then be returned to to perform further tests, such as employing -omics methods to characterise the genetic or metabolomic underpinnings of the observed phenotypes.

1.2.1.1 EXPERIMENTAL EVOLUTION USING CHEMOSTATS

Experimental evolution using microorganisms has in the past largely depended on batch culture propagation (Elena & Lenski, 2003). This is a conceptually simple and easily scalable method where small population subsets are moved to growth medium with abundant nutrients and grown to stationary phase before a new subsample is taken and moved to fresh medium. This process is repeated serially for as long as is necessary for the experiment. However, the cells are put through "boom and bust"-cycles at every transfer where as the population grows the nutrients gradually deplete, along with changes in oxygen, light and pH levels. Eventually the cells will cease growth and division and waste products will build up. This results in a highly complex selective environment, as any subsamples taken from these populations will be growth phase specific, with associated effects on the cellular metabolism and physiology (Gresham & Dunham, 2014; Van den Bergh *et al.*, 2018). Furthermore, each subsample transfer constitutes an evolutionary bottleneck,

where the reduction in population size affects the genetic diversity and mutational space available in the next batch (Lenski *et al.*, 1991; Van den Bergh *et al.*, 2018; Vogwill *et al.*, 2012; Wahl & Gerrish, 2001), giving an increased role to genetic drift in the evolutionary outcome (Elena & Lenski, 2003).

Chemostats are continuous flow-trough, chemically stable cultures kept at a fixed volume by feeding fresh medium and nutrients in at a constant rate while also allowing efflux of excess culture (Monod, 1950; Novick & Szilard, 1950). The specific growth rate of the population is thus matched to the dilution rate, and the populations are maintained in a state of exponential growth, where mixing keeps the environment homogeneous. This allows precise control of selective pressures in the long-term, making it possible to isolate which have an effect on the evolutionary outcome and in what way (Gresham & Dunham, 2014). Furthermore, population fluctuations in response to experimental treatments including several species or strains may be followed in the long term and be modelled as a function of the flow rate (Yoshida *et al.*, 2003). This, along with technological progress making them easier to construct, has resulted in increased interest in chemostats for experimental evolution and systems biology (Bull, 2010; Gresham & Hong, 2014).

1.2.2 THE THESIS MODEL SYSTEM: *CHLAMYDOMONAS REINHARDTII* AND GLYPHOSATE

Here I introduce a model system for the study of evolution of resistance using algae and chemostats. The system comprises model species *Chlamydomonas reinhardtii* exposed to growth-inhibiting herbicide glyphosate and a robust system for monitoring populations exposed to herbicide through time while allowing for assessment of molecular, evolutionary and ecological detail.

1.2.2.1 *C. REINHARDTII*

C. reinhardtii is a single-celled flagellate green alga widely occurring in soil and fresh water around the world (Harris *et al.*, 1989). It can grow both through photosynthesising and in the dark when supplied with acetate and while it generally reproduces asexually through cell division, nitrogen starvation induces a sexual phase and spore formation (Harris *et al.*, 1989). *C. reinhardtii* is easy to culture under laboratory conditions and has thus become a popular and well-studied model organism, particularly as a eukaryotic alternative for experimental evolution and has had its genome fully sequenced (Salomé & Merchant, 2019).

As *C. reinhardtii* shares much of its cellular biochemistry with higher plants it has been used for molecular analysis of herbicide resistance mutations (Erickson *et al.*, 1984, 1989; Fedtke, 1991; Galloway & Mets, 1984; Hartnett *et al.*, 1987; James & Lefebvre, 1989; James *et al.*, 1993; Randolph-Anderson *et al.*, 1998) as well as experimental evolution of herbicide resistance (Lagator *et al.*, 2013a,b; Melero-Jiménez *et al.*, 2021; Reboud *et al.*, 2007; Reboud, 2002; Vogwill *et al.*, 2012). Furthermore, as a commonly occurring primary producer, *C. reinhardtii*'s response to herbicides is directly relevant to the effects on non-target ecosystems as it will be one of the species affected by herbicide pollution. *C. reinhardtii* also has a well-studied and easily identifiable form of inducible defence – clumping (de Carpentier *et al.*, 2019; Harris *et al.*, 1989; Lürling & Beekman, 2006) – in response to grazing zooplankton and has thus been used in several eco-evolutionary studies modelling consumer-resource cycles, including how they are affected by fitness trade-offs (Ellner & Becks, 2011; Kasada *et al.*, 2014; Yoshida *et al.*, 2003).

1.2.2.2 GLYPHOSATE: MODE OF ACTION

With its highly effective and specific MoA and a lack of natural resistance in higher plants, glyphosate (*N*-phosphonomethyl glycine) has been described as 'a once-in-a-century herbicide' (Duke & Powles, 2008). Glyphosate blocks the shikimate pathway by competitively binding to enzyme 5-enolpyruvylshikimate-3-phosphate synthate (EPSPS) (Figure 1.2), outcompeting intended substrate phosphoenolpyruvate (PEP) and hindering the production of aromatic amino acids phenylalanine, tyrosine and tryptophan as well as other downstream products of chorismate metabolism (Steinrücken & Amrhein, 1980). As mutations to the EPSPS gene to change its structure and lower the affinity for the glyphosate molecule also tend to result in lowered affinity for PEP, and thus impair normal cell function, resistant phenotypes in natural populations are rare (Duke & Powles, 2008; Gaines *et al.*, 2020; Sammons & Gaines, 2014). It is unclear whether it is the depletion of the aromatic amino acids that results in growth inhibition and death in the plant, or whether it is due to the loss of the downstream feedback control of carbon flow into the shikimate pathway disrupting other cellular pathways (Duke & Powles, 2008; Maroli *et al.*, 2015, 2018). Secondary effects on other cellular processes have also recently been documented, including disruption of photosynthesis and increased production of reactive oxygen species (ROS) (Ahsan *et al.*, 2008; de María *et al.*, 2005; Gomes & Juneau, 2016; Maroli *et al.*, 2015; Sergiev *et al.*, 2006; Servaites *et al.*, 1987).

Figure 1.2: The shikimate pathway and the glyphosate primary mode of action. The aromatic amino acids tyrosine, phenylalanine and tryptophan are synthesised from chorismate.

As glyphosate is non-selective, its widespread adoption beyond pre-planting weed clearance was only made possible with the invention of genetically engineered glyphosate resistant crops (Powles, 2008). As these were introduced in 1996, glyphosate rapidly became foundational to the production of several major crops, including soybean, maize, canola and cotton, and thus hugely economically important (Benbrook, 2016; Cerdeira & Duke, 2006; Duke & Powles, 2008; Powles, 2008). Furthermore, it was assumed to have a relatively low environmental impact compared to the herbicides and management strategies preceding it, and not affect organisms lacking a shikimate pathway (i.e. animals) (Duke & Powles, 2008). And as glyphosate use increased, so did the selective pressure for resistance to evolve in weeds, which soon became a rapidly growing problem (Heap, 2022). Furthermore, the over-reliance on glyphosate for weed control increased the levels of contamination to natural ecosystems, along with the discovery that it is not environmentally neutral and may still affect animals and humans (Annett *et al.*, 2014; Fugère *et al.*, 2020; Helander *et al.*, 2012; Motta *et al.*, 2018; Relyea, 2005a; Van Bruggen *et al.*, 2018).

Four general types of resistance mechanisms against glyphosate have so far been identified across 55 unique cases of resistance in wild weed populations (Heap, 2022), two TSR involving nucleotide substitutions and enzyme amplification and two NTSR involving reduced translocation and

glyphosate degradation (Gaines *et al.*, 2020; Sammons & Gaines, 2014). Most of these confer complex fitness costs, and their effects appear species dependent. Furthermore, TSR and NTSR mechanisms have repeatedly been found to coexist within the same plant. Generally these combinations are associated with a more robust resistance (Bracamonte *et al.*, 2018; Chen *et al.*, 2020; Dominguez-Valenzuela *et al.*, 2017; Gherekhloo *et al.*, 2017; Mao *et al.*, 2016) although have been found to confer a notable fitness cost in at least one case (Fernández-Moreno *et al.*, 2017).

Mutations to the EPSPS gene in most cases involve the Pro-106 residue, with single nucleotide substitutions changing the proline codon to alanine (P106A), leucine (P106L), serine (P106S) or threonine (P106T) (Sammons & Gaines, 2014). However, this changed enzyme structure generally confers low resistance and impairs normal function (Healy-Fried *et al.*, 2007). So far one instance of a change to Thr-102 has been recorded, with a substitution to serine (T102S) reducing the affinity for glyphosate while increasing the affinity for PEP, however it is unclear whether this results in any other fitness trade-offs (Li *et al.*, 2018). A number of multiple nucleotide substitutions have also been identified in the wild in recent years – TIPS (T102I and P106S), TIPT (T102I and P106T) and TAP-IVS (T102I, A103V and P106S). Generally these multiple substitutions result in a considerably more robust resistance to glyphosate (the TIPS mutation is also the genetically engineered EPSPS used in glyphosate resistant maize) (Alcántara-de la Cruz *et al.*, 2016; Dill, 2005; Funke *et al.*, 2009; García *et al.*, 2019; Perotti *et al.*, 2019; Sidhu *et al.*, 2000; Takano *et al.*, 2020; Yu *et al.*, 2015), but the fitness costs have either not been evaluated yet or appear to be complex and depending on genetic structure and competition (Han *et al.*, 2017). The fact that the same residue location changes are involved across many species highlights the problem with relying on a single, non-selective herbicide with a single primary MoA. Together with the existence of multiple resistance mechanism phenotypes this also demonstrates how rapidly resistance to glyphosate evolves where it is asserting a strong selective pressure.

EPSPS amplification has been detected both in the form of up-regulated expression (Baerson *et al.*, 2002) and gene multiplication (Gaines *et al.*, 2019; Patterson *et al.*, 2018). The underlying genetic mechanisms appear to be varied (Gaines *et al.*, 2016; Jugulam *et al.*, 2014; Koo *et al.*, 2018; Patterson *et al.*, 2019), along with the associated fitness costs ranging from none (Vila-Aiub *et al.*, 2014) to trading off with growth and reproduction (Yanniccari *et al.*, 2016), while varying with the genetic background (Martin *et al.*, 2017) and life history stage (Osipitan & Dille, 2017).

Multiple forms of reduced translocation of glyphosate have been identified, through changing its distribution through tissues (Feng *et al.*, 2004; Lorraine-Colwill *et al.*, 2002), reducing penetration of glyphosate (Michitte *et al.*, 2007; Nandula *et al.*, 2013; Vila-Aiub *et al.*, 2012) and increasing vacuolar sequestration (Ge *et al.*, 2010, 2011, 2012; Peng *et al.*, 2010; Yuan *et al.*, 2010). The molecular bases for these are unknown, but increased vacuolar sequestration in particular seems to trade-off with the ability to withstand cold temperatures (Ge *et al.*, 2011; Vila-Aiub *et al.*, 2013) and competition (Pedersen *et al.*, 2007) as well as being generally costly (Preston & Wakelin, 2008; Wakelin & Preston, 2006). The 'phoenix phenomenon' is a particularly dramatic example of reduced translocation, where rapid cell death sacrifices leaves that have been exposed so that the glyphosate never reaches the meristem (Moretti *et al.*, 2018; Van Horn *et al.*, 2018).

While the main metabolic product of glyphosate, aminomethylphosphonic acid (AMPA) has been repeatedly detected in higher plants (de Carvalho *et al.*, 2012; Duke, 2011), it is only recently that the pathway facilitating the degradation has been identified. In *Echinochloa colona* aldo-ketoreductase, a family of enzymes with broad substrate specificity found in many prokaryotes and eukaryotes, was found to confer the evolved ability to metabolise glyphosate (Pan *et al.*, 2019; Vemanna *et al.*, 2017), in contrast to the previously known glyphosate oxidoreductase pathway found in bacteria. However, the fitness consequences of this mechanism have yet to be investigated, and other candidate pathways remain to investigate for other species (Leslie & Baucom, 2014).

1.2.2.3 PREVIOUS STUDIES ON *C. REINHARDTII* AND GLYPHOSATE

C. reinhardtii and glyphosate have been used together as a model system for a number of studies to date dealing with evolution of resistance. Bruggeman *et al.* (2014) genetically engineered resistance in *C. reinhardtii* using a glyphosate acyltransferase gene (modified from *Bacillus*), intended for use with glyphosate in commercial-scale algal production facilities, but found that the resistant strain still experienced reduced growth when glyphosate was applied. Lagator *et al.* (2013a,b) investigated the evolutionary dynamics of resistance evolution under mixing and cycling regimes, including ones with glyphosate and found that a high level of resistance to glyphosate alone evolved in 3.5 weeks on average. While this resistance trait resulted in reduced growth in the ancestral environment, this cost disappeared when cycled for longer periods with atrazine. No evidence was found for glyphosate resistance conferring cross-resistance to other herbicides. Similarly, Vogwill *et al.* (2012) found no evidence for cross-resistance resulting from glyphosate resistance but instead a positive correlation was found between the degree of resistance and fitness in the ancestral environment, and the fitness cost of resistance decreased with increasing bottleneck size. They suggested this was either due to there being a range of resistance conferring mutations with varying degrees of antagonistic pleiotropy, and their occurrence being sufficiently random that populations relying on a small mutation space were more likely to fix ones with large fitness costs, whereas populations with a larger mutational space would be more likely to fix ones with smaller costs. Alternatively, the larger mutational space could be conducive to fixing further mutations ameliorating the costs of resistance. Lastly, Melero-Jiménez *et al.* (2021) used a ratchet protocol on several algal species to test their ability to withstand, and evolve resistance, to glyphosate and found that *C. reinhardtii* had a higher degree of both natural tolerance and evolved tolerance to glyphosate than the other species tested. This suggests *C. reinhardtii* might be favoured in communities experiencing glyphosate contamination as competition with other species is removed. However, they also recorded smaller cell sizes as well as lower growth rates and photosynthetic performance in the ancestral environment for the resistant strains, whereas there was no difference in photosynthetic pigment concentration.

1.3 AIMS OF THIS THESIS

This thesis connects fundamental evolutionary theory with the herbicide resistance challenges facing agriculture and natural ecosystems through characterising the dynamics of resistance evolution in a specific species–herbicide model system: *C. reinhardtii*–glyphosate. Specifically I:

- Develop a tractable DIY multiplexed chemostat array system for longitudinal experimental evolution studies using algae (dubbed "mesostats") that is cheap and easy to build as well as run and maintain by one person.
- Use the mesostat system to evolve glyphosate resistance in *C. reinhardtii* in response to lethal and sublethal levels of glyphosate and characterise the population level fluctuations throughout to determine when resistance has evolved.
- Test the effects of glyphosate resistance evolution in action on growth in a range of doses of glyphosate as well as the ancestral environment to characterise the level of resistance as well as possible intrinsic fitness costs.
- Test the effects of evolved herbicide resistance on *C. reinhardtii* anti-grazer defences by introducing a second model organism: freshwater rotifer *Brachionus calyciflorus*, evaluating both the ability to deploy the defence in response to *B. calyciflorus* infochemicals and ability to withstand grazing by live rotifers.
- Use targeted metabolomic fingerprinting analysis to determine the effect of evolving and evolved glyphosate resistance on shikimate pathway compounds, possible glyphosate degradation pathway products and the amino acid pool, to gain insight into the evolutionary process and possible resistance mechanisms.

- Use exploratory metabolomic fingerprinting analysis to identify compounds that may be associated with evolving or evolved glyphosate resistance, to gain insight into effects on the cell metabolome beyond the shikimate pathway as well as possible resistance mechanisms.

CHAPTER 2

Mesostats — A multiplexed, low-cost, do-it-yourself continuous culturing system for experimental evolution of mesocosms

2.1 ABSTRACT

Microbial experimental evolution allows studying evolutionary dynamics in action and testing theory predictions in the lab. Experimental evolution in chemostats (i.e. continuous flow through cultures) has recently gained increased interest as it allows tighter control of selective pressures compared to static batch cultures, with a growing number of efforts to develop systems that are easier and cheaper to construct. This protocol describes the design and construction of a multiplexed chemostat array (dubbed "mesostats") designed for cultivation of algae in 16 concurrent populations, specifically intended for studying adaptation to herbicides. We also present control data from several experiments run on the system to show replicability, data illustrating the effects of common issues like leaks, contamination and clumps, and outline possible modifications and adaptations of the system for future research.

2.2 INTRODUCTION

Microorganisms provide an unparalleled opportunity for the study of evolutionary dynamics due to their combination of short generation time, simple genetics and ability to fit huge population sizes in a small space. The path of evolutionary adaptation can thus be replicated and tightly controlled in real time in the lab, allowing exciting new insights into the mechanisms of adaptive evolution and testing of predictions from theory (Barrick & Lenski, 2013; Good *et al.*, 2017; Kawecki *et al.*, 2012; Lang & Desai, 2014; Van den Bergh *et al.*, 2018).

The most common way of growing microorganisms for experimental evolution is as batch cultures. This involves serial repetition of small cell population subsets being moved to fresh medium and grown to stationary phase before being transferred again to fresh medium to allow new growth and, with time, adaptation. This is a simple, cheap and scalable method, but its drawback is the resulting fluctuating environment as the cells go through “boom and bust”-cycles at every transfer resulting in a complex selective environment (Gresham *et al.*, 2008; Gresham & Dunham, 2014; Van den Bergh *et al.*, 2018). As the nutrients in the medium gradually run out, the cells will arrest growth and division while waste products build up. Oxygenation, light levels and pH will also fluctuate with population density. All of this affects cellular metabolism and physiology and subsamples taken from such populations will be growth phase specific, making it difficult to define and isolate the selective pressures acting on the populations (Gresham & Dunham, 2014). Furthermore, there is an evolutionary bottleneck at each transfer, where the considerable reduction in population size associated with transfer to the next batch affects the genetic diversity and mutational space available (Lenski *et al.*, 1991; Van den Bergh *et al.*, 2018; Vogwill *et al.*, 2012; Wahl & Gerrish, 2001), giving an increased role to genetic drift in the evolutionary outcome (Elena & Lenski, 2003).

Chemostats – continuous flow-through, chemically stable cultures where growth medium and treatments are fed into the fixed-volume populations at a constant rate – solve these issues as the specific growth rate of the population at steady state is matched to the dilution rate (Monod, 1950; Novick & Szilard, 1950). The populations are maintained in exponential growth and constant mixing ensures a homogeneous environment, allowing precise control of the relevant selective pressures compared to the complex dynamics present in batch cultures (Gresham & Dunham, 2014). This unique opportunity for experimental manipulation offers a high-throughput chance to pick apart evolution in action and, as a result, chemostats have recently seen a renaissance in experimental evolution and systems biology as new technological advancements make them easier to maintain than ever before (reviewed in Bull, 2010; Gresham & Hong, 2014). Chemostats also allow following population fluctuations and evolutionary dynamics in response to experimental treatments in the long term, where equilibria and population cycles including several species and strains can be described as a function of the flow rate (e.g. Becks *et al.*, 2012; Declerck *et al.*, 2015; Fussmann *et al.*, 2000; Hiltunen *et al.*, 2014; Yoshida *et al.*, 2003). Multiplexed arrays, where the dilution rate is set by a single pump, and medium sources can be shared, further minimise variation between population chambers (Dénervaud *et al.*, 2013; Ekkers *et al.*, 2020; Miller *et al.*, 2013; Skelding *et al.*, 2018; Tonoyan *et al.*, 2020; Toprak *et al.*, 2013; Wong *et al.*, 2018).

Here we describe a multiplexed small-scale DIY chemostat array system (dubbed "mesostats") adapted from the ministat array developed by Miller *et al.* (2013) to suit experimental evolution of algae, in contrast to the so far described designs specifically intended for yeast (Dénervaud *et al.*, 2013; Miller *et al.*, 2013; Wong *et al.*, 2018) and bacterial cultures (Tonoyan *et al.*, 2020; Toprak *et al.*, 2013). Our system uses common algal model species *Chlamydomonas reinhardtii*, with the specific goal to use it as a herbicide resistance evolution model. *C. reinhardtii* is an established model species for herbicide resistance evolution (Lagator *et al.*, 2013a,b; Reboud *et al.*, 2007; Vogwill *et al.*, 2012) and molecular analysis of herbicide resistance mutations (Erickson *et al.*, 1984, 1989; Randolph-Anderson *et al.*, 1998), but all studies to date have used batch cultures. We present the full protocol for assembling and maintaining a 16-chamber mesostat array by a single person as well as control data illustrating the ability of the system to track trends and variability in the abundance of organisms among replicates. We also present pilot data illustrating the ability to use the mesostats to evolve resistance in *C. reinhardtii* to growth inhibiting herbicide glyphosate. Furthermore, we have included data from this system illustrating the signal of common problems like leaks, contamination and cell clumping, showing how to distinguish it from biological variation as well as how to prevent and address these problems if they occur. We also outline the ways in which this system could be further modified and avenues of future research.

2.3 METHODS

The protocol described in this chapter is published on protocols.io `https://dx.doi.org/10.17504/protocols.io.6qpvr6q1bvmk/v1` as part of the publication of the chapter with PLOS ONE, but has been included in full below for the purposes of this thesis.

2.3.1 AN OVERVIEW OF THE DESIGN

The mesostat array consists of four main parts: (1) the medium line, (2) the culture chambers, (3) the overflow chambers and the (4) aeration line. Medium is pumped from the medium containers via a peristaltic pump into the culture chambers (mesocosms) where the experimental organisms are grown. Air is pumped through a gas washing bottle into the culture chambers via the aeration needle to ensure mixing and create pressure so liquid flows out through the efflux needle and the culture stays a fixed volume. The efflux line leads to an overflow chamber, and the volume collected in these is regularly measured to ensure equal flow rates between all culture chambers.

Samples for analysis can be obtained from the overflow, but this only samples from the top of the culture and the environment in the collection receptacle may differ from the culture chambers. To allow sampling from lower levels of the culture, sampling needles have been fitted to the culture chambers. The sampling needle can also be used for inoculation or addition of treatments to the chambers. The entire setup can be kept in a controlled temperature room which ensures low levels of evaporation, but the culture temperature can also be maintained by other methods such as a light table or a water bath. When growing photosynthetic organisms such as algae, even light levels for all chambers are best maintained by a light table as well as fitting strip lights around the chambers. An overview of the full design is seen in Figure 2.1 and Figure 2.2A, as well as full assembly schematics in section 2.4 Figure 2.3–2.5. The control conditions are summarised in Table 2.1.

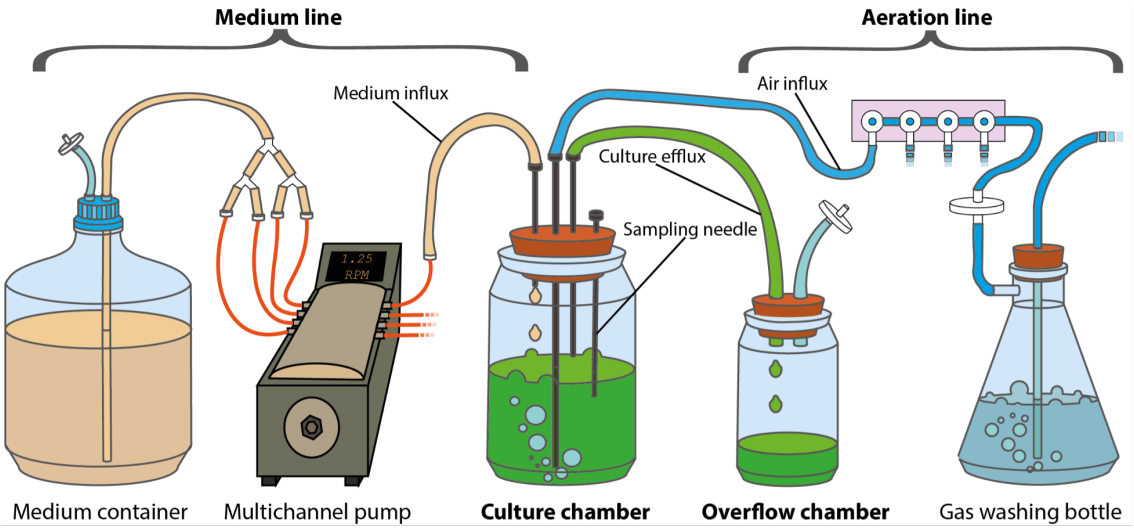

Figure 2.1: Simplified schematic overview of the mesostat system showing medium containers, the pump, the culture chamber with sampling needle, the overflow bottle, the gas washing bottle along with the medium and air influx lines and the culture efflux line.

2.3.1.1 THE MEDIUM CONTAINERS

The volume and number of medium containers depends on the experimental design and number of treatments. When the experimental design calls for different treatments applied via the medium, culture chambers sharing a treatment share a medium source. The volume of the medium containers should be chosen to allow sufficient medium to supply all its chambers for at least 5 days, to ensure the time to prepare new sterile medium before changing is needed. The depletion rate of the medium will depend on the number of chambers sharing a container and the flow rate.

The medium container should be sealed with a lid or stopper with a hole that allows air to escape through a filter. If the medium outflow can be through either a tap at the bottom of the container, or tubing through the lid siphoning medium from the bottom.

For the data presented in this thesis, a single 20 L autoclaveable glass container, fitted with a silicone stopper and a filter (0.45 µm) on top and a tap connected to large silicone tubing (inner/wall diameter: 12.5/2.25 mm) at the bottom, is used when all 16 chambers are receiving the same medium.

For data obtained from experiments where different treatment levels were present, 5 L or 2 L autoclaveable glass bottles are used for the treatments, each fitted with medium silicone tubing (inner/wall diameter: 6.5/1.5 mm) siphoning the medium out through holes in the lids alongside tubing ending in a filter to allow air to escape the bottle (Figure 2.2B). For example, as seen in

Figure 2.2A, 6 different herbicide concentrations are applied through the medium to two chambers each from 2L bottles, and the control treatment is supplied to four chambers from a 5L bottle.

2.3.1.2 THE PUMP AND THE MEDIUM LINES

The medium is pumped from its container(s) by a multichannel peristaltic pump. Our design employed a Watson-Marlow 205S/CA16 (16 channels) and pumped liquid through small silicone tubing (inner/wall diameter: 3/1 mm), connected to the medium container tubing with a reducing connector. The tubing is split using Y-connectors before the pump so that each culture chamber has its own media line. The same tubing is used throughout the mesostat array (Figure 2.2A), except for the tubing mounted in the pump itself which is autoclaveable marprene tubing (Watson-Marlow, orange/orange, 0.88 mm bore), connected to the silicone tubing using cut off and blunted hypodermic needles (18 G, 50 mm) inserted into the pump tubing and connected to the silicone tubing using male luer locks (Figure 2.2C).

2.3.1.3 THE CULTURE CHAMBERS

Each culture chamber consists of a 500 ml glass jar, sealed with a rubber bung. The rubber bung has four hypodermic needles inserted through it (Figure 2.2D): a medium influx needle (18 G, 50 mm) connected to the tubing running through the pump, an aeration needle (16G, 203 mm) connected to the aeration system allowing constant mixing of the culture, a sampling needle (16 G, 203 or 101 mm depending on sampling needs), and an efflux needle (16 G, 101 mm) which sets the culture volume.

Tubing is connected to the medium influx, aeration, and efflux needles using male luer locks. A sterile syringe is used with the sampling needle to pull samples out of the chamber or for injections, which is kept sealed with a male luer cap when not in use.

2.3.1.4 THE AERATION SYSTEM

The culture chambers have a constant influx of air for mixing to prevent the organisms – in our case algae – from sedimenting, and to create pressure for the efflux of liquid so that the culture is kept at a constant volume. Air can be supplied by lab/building infrastructure, e.g. air supply taps, or by an aquarium pump with high enough pressure. The air passes through a filter (0.2 µm) into a gas washing bottle to prevent evaporation. The gas washing bottle consists of a 1L flask with a sidearm, with the incoming air being passed through a glass pipette into distilled water. The air is pushed from the gas washing bottle through 4-port manifold connectors (180° rotation), splitting the air supply to tubing for each culture chamber and passing it through a second filter (0.45 µm). This tubing connects to the aeration needle fitted in the culture chamber bung. The air supply can be controlled using an adjustable clamp fitted to the tubing between the gas washing bottle and the manifold connector.

2.3.1.5 THE OVERFLOW CHAMBERS AND THE EFFLUX LINE

The efflux line from each culture chamber leads to an overflow chamber consisting of a 175 ml glass bottle sealed with a rubber bung (Figure 2.2E). The efflux tubing is connected to a hole in the rubber tubing using a female luer lock. A second female luer lock is also fitted on the opposite side of the hole on the underside of the bung, to serve as a funnel for the incoming liquid. A second hole connected with a female luer lock to tubing ending with a filter (0.45 µm) allows air to escape the collection chamber. This chamber should be emptied regularly and can be used to control

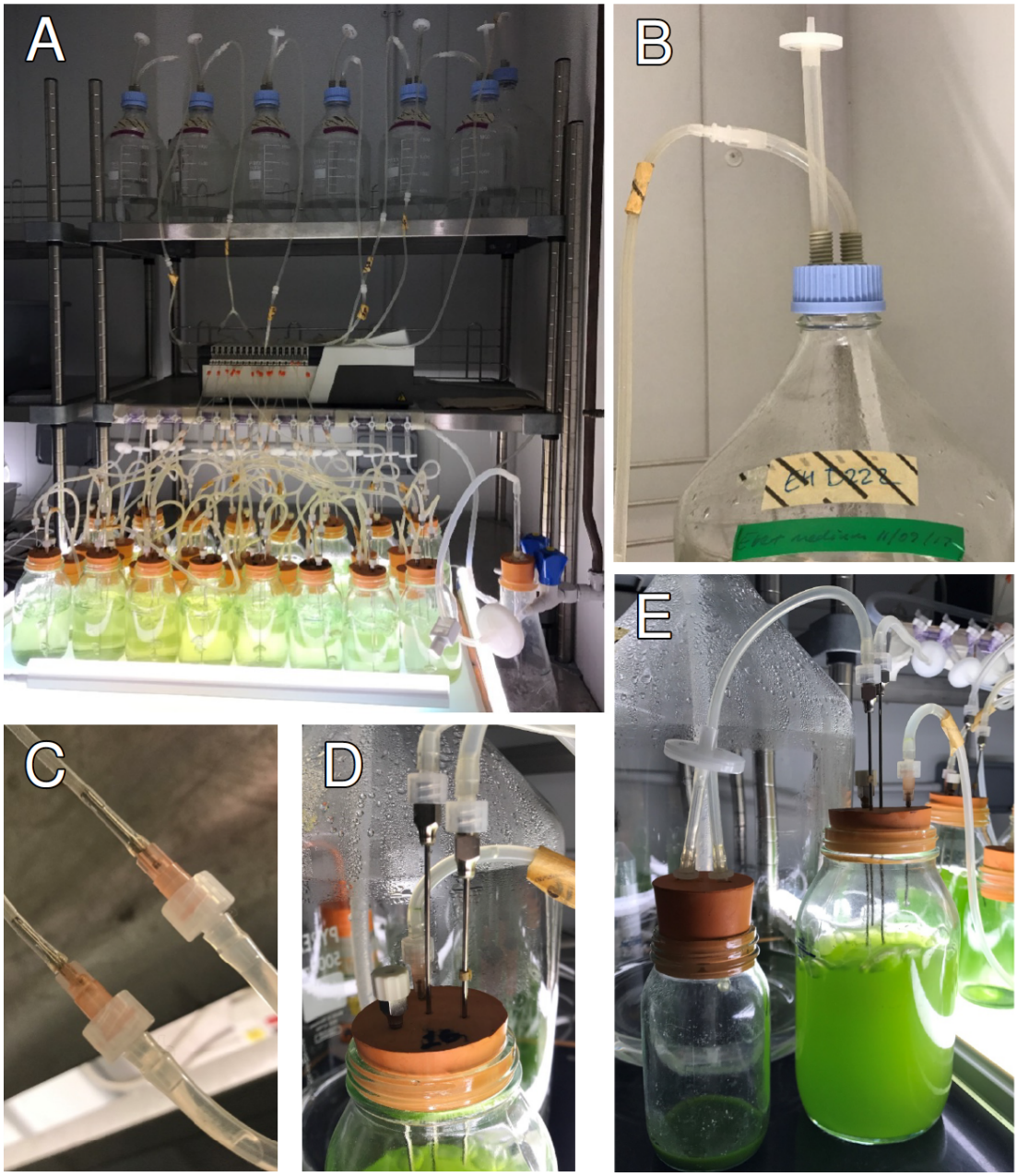

Figure 2.2: A) The complete setup just after inoculation with algae, running an experiment with six levels of treatments applied through the media lines. B) Close-up of medium siphon through medium container lid. C) Close-up of connection between pump tubing and silicone tubing used throughout array. D) Close-up of culture chambers rubber bung with the four hypodermic needles, capped sampling needle to the left in foreground, steel efflux needle to the right in foreground, steel aeration needle in the middle, and pink plastic medium influx needle in the background. E)The overflow chamber (left) and the culture chamber at steady state (right) with the efflux line running between them.

that the flow rate remains equal between the culture chambers. Samples can be obtained from the overflow chamber, but the environment in the overflow chamber will be different from the culture chambers. With a low flow rate and a high temperature environment, the culture will evaporate quickly when its volume is low. The overflow chamber is also not being diluted with fresh medium, meaning the cells are no longer kept in exponential growth or connected to the aeration line, often

resulting in sedimentation and stratification of the culture.

2.3.2 THE LIGHT SYSTEM

The light is provided by white light LED strip lights mounted around the chambers and between the two rows of chambers, as well as a DIY light box consisting of white light LED strip lights and a semi-transparent plastic top to diffuse the light. Equal light from all angles is essential to ensure even algal growth in the chambers. A light box is not necessary, but convenient and can be used for providing light to batch cultures or growth assays of subsamples.

2.3.3 MATERIALS AND EQUIPMENT

Here we present a complete list of materials required to construct a 16-chamber array. Note that the media containers and associated lids are listed as optional, as exact size and number needed depend on the experimental design. If the company and product code is not listed, the part was not acquired new and the exact same product is no longer sold. Other than the pump and pump tubing, all of the pieces are fairly standard pieces found in many wet labs and similar products can be obtained easily from all major scientific suppliers.

1. Small tubing, 20 m (Fisherbrand™ Silicone Tubes; inner/wall diameter: 3.0/1.0 mm, Fisher Scientific, 10111801)
2. Medium tubing, 20 m (Fisherbrand™ Silicone Tubes; inner/wall diameter: 6.5/1.5 mm, Fisher Scientific, 10549201)
3. Large tubing, 10 m (Fisherbrand™ Silicone Tubes; inner/wall diameter: 12.5/2.25 mm, Fisher Scientific, 10726931)
4. Reducing connector, 10 (Reducing Connector PVDF; 1/4" to 1/8", Cole Parmer, EW-30703-50)
5. Male luer lock, 100 (Cole-Parmer ADCF Male Luer to 1/8" L Barb Adapter, Cole Parmer, WZ-30800-24)
6. Female luer lock, 50 (Cole-Parmer ADCF Female Luer to 1/8" L Barb Adapter, Cole Parmer, WZ-30800-08)
7. Y-connector, 40 (Barbed Y Connector; PVDF; 1/8", Cole Parmer, WZ-30633-44)
8. Straight connector, 10 (Barbed fittings; Straight Connector; Kynar; 1/4" ID Cole Parmer, WZ-30703-05)
9. Gas washing bottle, 1 (1L flask with sidearm tubulation)
10. Glass pipette, 1 (10 ml glass pipette)
11. 4-port Manifold, 4 (Polycarbonate individual manifolds with luer locks; 4 ports; 180° rotation Cole Parmer, EW-06464-85)
12. 0.45 µm filters, 100 (PTFE Nonsterile Syringe Filters; 0.45 micron; 25 mm dia, Cole Parmer, WZ-02915-22)
13. 0.2 µm filters, 1 (AcroVent 0.2µm PTFE, Pall Corporation, 4249)
14. Air tubing clamp, 1 (Adjustable tubing clamp)
15. Multiplexed peristaltic pump, 1 (205S/CA16 16 Cartridge pump, Watson-Marlow, 020.3716.00A)

16. Pump tubing, 18 (Autoclaveable marprene manifold pump tubing; orange/orange; 0.88 mm bore, Watson-Marlow, 978.0088.00+)
17. Culture chamber jars, 16 (Clear glass powder jars; 500 ml)
18. Culture chamber rubber bungs, 16 (Fisherbrand™ Solid Rubber Stoppers; 45 mm bottom; 51 mm top Fisher Scientific, 41122502)
19. Aeration needle, 16 (Central Surgical Company™ Stainless Steel Needle; 16 G; 203 mm, Fisher Scientific, 12329259)
20. Media influx needle, 48 (B Braun™ Hypodermic Needles Pink 1.2 mm 18 G 50 mm, Fisher Scientific, 10722784)
21. Efflux needle, 16 (Central Surgical Company™ Stainless Steel Needle; 16 G; 101 mm, Fischer Scientific, 12339259)
22. Sampling needle, 16 (Central Surgical Company™ Stainless Steel Needle; 16 G; 101 mm, Fischer Scientific, 12339259 *or* Central Surgical Company™ Stainless Steel Needle; 16 G; 203 mm, Fisher Scientific, 12329259)
23. Male luer cap, 16 (Male Luer Lock Plug; Nylon, Cole Parmer, WZ-45505-56)
24. Collection chamber jars, 32 (Clear glass powder jars; 175 ml)
25. Collection chamber rubber bungs, 16 (Fisherbrand™ Solid Rubber Stoppers; 37 mm bottom; 42.5 mm top, Fisher Scientific, 41122502)
26. 20 L medium container, 2 *optional*
27. Silicone stopper for 20 L medium container, 2 *optional*
28. 5 L medium container, 2 (Pyrex™ Borosilicate Glass Reagent Bottles with Polypropylene Cap and Pouring Ring; 5000 mL, Fisher Scientific, 12094637) *optional*
29. 2 L medium container, 20 (Pyrex™ Borosilicate Glass Reagent Bottles with Polypropylene Cap and Pouring Ring; 2000 mL, Fisher Scientific, 11922629) *optional*
30. Lids with holes for 5 L and 2 L medium containers, 14 (GL45 Screw cap for Pyrex GL 45 media-lab bottle, Fisher Scientific, 15173927) *optional*
31. Syringes, 100 (BD Discardit™ Eccentric Luer-Slip Two-Piece Syringe, Fisher Scientific, 10152534)
32. Linear LEDs (LEDVANCE, 600 10 W, 3000 K warm white)

2.3.4 PROTOCOLS

2.3.4.1 ASSEMBLING THE MESOSTATS FOR THE FIRST TIME

See section 2.4 Figure 2.3–2.5 for visual representation of how the parts connect. A more detailed description with possible variations in design is given below. Place all vessels and machinery in their intended location before cutting the tubing to ensure sufficient lengths and to minimise mistakes.

- Medium container(s):
    1. Prepare the medium container lids.
        (a) If using silicone stoppers:

i. If the medium container has a tap, the silicone stopper only needs a hole for air to escape. Drill a hole large enough to squeeze medium size tubing through but ensuring a tight seal so that no air can escape around the edges. Attach a short piece of tubing, sticking out about 1 cm on the underside of the stopper and 5 cm on top. Attach a 0.45-micron filter to the tubing.

ii. If the medium container does not have a tap, a medium siphon is also needed. Drill a second hole in the silicone stopper of the same size and squeeze through medium size tubing long enough to reach the bottom of the container and sticking up about 5 cm on top of the stopper.

(b) If using screwtop lids with holes, first insert a short piece of medium size tubing through one hole so that it ends just inside the lid and sticks out about 5 cm on top. Attach a 0.45-micron filter to the tubing. For the medium siphon, insert a piece of medium size tubing, long enough to reach the bottom of the container and stick out about 5 cm on top of the lid.

2. Attach the lid or stopper to the medium container.

   (a) If there is a medium siphon, attach the long piece of tubing to a reducing connector.

   (b) If there is no medium siphon and the medium container has a tap, attach a short piece of appropriate size tubing to the tap and attach this to a reducing connector.

- Media lines:

3. Attach a short piece of small size tubing to the other side of the reducing connector and attach it to a Y-connector. Split the medium line into as many channels as needed by connecting short (2—3 cm) pieces of small tubing and Y-connectors. Channels receiving the same treatment should share a medium source.

4. For each channel, attach small size tubing of sufficient length to reach the pump and end with a male luer lock.

5. For each channel, cut off two 18G hypodermic needles to 0.5 cm and insert them into the ends of a piece of pump tubing. Be careful to not cut up the inside of the pump tubing, if pieces detach, they will cause blockages. The ends of the needles may need additional blunting or filing to reduce sharpness. A damaged piece of pump tubing can easily be cut off.

6. Connect the pump tubing to the media lines by screwing the needle luer end to the male luer lock. Screw another male luer lock to the other end of the pump tubing.

7. Cut a piece of small size tubing long enough to reach from the pump to the culture chamber with some slack. Plan carefully where each chamber is going to sit, if multiple treatments are used they should be distributed randomly throughout the array to avoid effects of e.g. differing light level. Attach this piece of tubing to the male luer lock at the end of the pump tubing, and end with another male luer lock.

8. Label the tubing with autoclave tape so you know which chamber it should connect to.

- Culture and overflow chambers:

9. For each chamber, prepare the culture chamber rubber bung by drilling four 1 mm holes, one for each hypodermic needle. This aids pushing the needles through, but the seal around them should still be very tight.

10. Push through one 18 G short needle (medium influx), one 18 G 20 cm needle (air influx) and two 18 G 10 cm needles (culture efflux and sampling needle). A longer sampling needle can be used if desired.

11. Label the rubber bung so you know which chamber it belongs to.

12. Mark the 500 ml glass jar at the desired volume (380 ml) as well as ±19 ml (±5%) to make the magnitude of any volume inconsistencies easier to judge by eye.

13. Attach the media line to the medium influx needle.

14. Cover the sampling needle with a male luer cap.
15. Attach a male luer lock to the culture efflux needle and set the needle at the height required for the desired culture volume, i.e. it should be skimming the surface of the culture.
16. For each culture chamber, prepare an overflow chamber. For each overflow chamber, prepare a rubber bung by drilling two holes large enough to squeeze the lock end of female luer locks into (approximately 2.5 mm in diameter). Connect one hole with a small size of tubing to the male luer lock on the culture efflux needle, and attach another female luer lock on the underside of the bung as a funnel. Attach a short piece of small size tubing to the other hole and end with a 0.2-micron filter.
17. Attach a male luer lock and push the air influx needle down to touch the bottom of the chamber.
18. Mount lights around the chambers and/or place the chambers on a light table, using a light meter to ensure light levels are even.

- Aeration system:

19. Mount the 4-port manifold(s) above the chambers using clamps or tape so that the aeration tubing will be held up without kinks.
20. Attach a short piece of small size tubing and a 0.2-micron filter to each active port on the manifold.
21. Connect a small size tube to the air influx needle long enough to reach the 4-port manifold and attach to the other side of the filter.
22. Prepare the gas washing bottle rubber bung by drilling a hole large enough to push the long glass pipette through, but tight enough that no air can escape around it. Push the pipette through down to the bottom of the flask. If needed, use a sealant around edges of the hole.
23. Connect the top of the glass pipette to the air supply (building supply or an aquarium pump) with appropriate size tubing.
24. Put dH2O in the gas washing bottle. The water level should be so that the water sufficiently covers the air outflow from the pipette, but not so that water enters the sidearm when the air is on. Mark upper and lower water levels on the gas washing bottle.
25. Connect the sidearm to a 0.2-micron filter with a short piece of medium size tubing and the filter to the manifold with a longer piece of medium size tubing. A clamp can be placed on this part of the tubing to control air flow if needed.

2.3.4.2 AUTOCLAVING

All parts that will come into contact with the medium need to be sterilised before use:

1. Medium container(s):
   (a) Disconnect the reducing connector on media line between the medium container and the pump tubing.
   (b) Prepare the medium and place in the container as it should be autoclaved with the medium inside.
   (c) Place a filter in the open tubing on the medium container.
   (d) Seal tightly with autoclave bags and autoclave tape around all filters.
   (e) Autoclave at 121 (15psi) for 30 min (longer might be necessary for larger containers).

2. Media line:
    (a) Disconnect at male luer locks to media influx needle.
    (b) Neatly roll up each media line and secure with autoclave tape.
    (c) Place all pieces of tubing in an autoclave bag. Autoclave at 121 (15 psi) for 30 min.
3. Culture chamber and collection chamber bungs:
    (a) Disconnect filters from tubing to 4-port manifold, and disconnect the male luer locks to the efflux line.
    (b) Place the rubber bungs with the needles and tubing in place into autoclaveable trays.
    (c) Place the trays in autoclave bags and seal with autoclave tape, taking care to not let the needles pierce the bag.
    (d) Autoclave at 121 (15 psi) for 30 min.
4. Culture chamber and collection chamber jars:
    (a) These jars are not autoclaveable. Sterilise using 70% IMS and rinse with dH2O.

2.3.4.3 PREPARING FOR AN EXPERIMENT

1. Reconnect all parts after sterilising. Wear gloves washed with 70% IMS at all times, and wear eye protection when handling the hypodermic needles.
2. When the array is assembled, start the pump to fill up the chambers and turn on the aeration system. At max speed (90 RPM) the flow rate is 2.92 ml/minute, meaning it will take approximately 2 hours and 10 minutes to fill the chambers to 380 ml.
3. When the chambers are full, ensure medium levels are equal and set pump to experiment speed. Adjust the efflux needle as necessary and monitor the overflow bottles to ensure efflux is equal.
4. Turn on the lights and ensure control conditions for light level, internal culture and ambient temperatures are met (see Table 2.1).

Table 2.1: Control conditions for *C. reinhardtii* cultures.

Light level	75 µmol m^{-2} s^{-1}, 24 h, all directions
Internal culture temperature	30°C
CT room ambient temperature	25°C
Medium flow rate	0.15/day, 1.25 RPM pump speed
Sampling frequency and volume	1.5 ml day
Medium	Ebert algal medium ((Ebert, 2013))

2.3.4.4 INOCULATING WITH ALGAE

Inoculating with *C. reinhardtii* from static stock culture:

1. Fill up a couple of 15 ml falcon tubes with stock solution and centrifuge at 2000 RPM for approximately 20 minutes. If there is a red layer on top of the green pellet, remove it as this is bacterial contamination. Pour out the supernatant and mix the pellet with fresh, sterile medium. Repeat washing procedure twice.

2. Use a sterile syringe to push an equal amount of freshly washed algal cells into each chamber through the sampling needle. Note: The inoculation volume will vary depending on the amount of stock algae available, the stock density and the desired starting density for the cultures.
3. Allow cultures to reach steady state before applying experimental treatments. See below for methods for how to sample to estimate concentration.

2.3.4.5 APPLYING TREATMENTS

Treatments can be applied gradually through the medium line by adding the compound directly to the medium or as shock injections through the sampling needle. The two methods can also be combined. For shock injection:

1. Prepare a mixture of medium and compound at as high a concentration as practical to ensure the volume injected into the chamber is as small as possible and reducing the effects of dilution of the culture.
2. Before injection, remove culture at a volume corresponding to the intended injection volume by using a sterile syringe to pull it out through the sampling needle. This so the treatment can be adequately mixed into the culture, and to avoid a sudden rush of culture through the efflux line.
3. Inject the treatment in through the sampling needle using a sterile syringe. All chambers should receive the same injection volume, including controls.

2.3.4.6 DAILY MAINTENANCE

To ensure equal conditions in all chambers, the mesostat array must be attended to daily according to the daily maintenance protocol:

1. Check water level in gas washing bottle is between max and min markings. Top up with distilled water if running low. Avoid going over the max marking, as this will cause water to bubble into the airflow tubing which can lead to blocked filters.
2. Check culture chamber airflow is satisfactory and equal. If a culture chamber has low airflow, check if the filters are blocked, first the filter on the adjoining collection chamber, then the filter connecting to the manifold, and replace if necessary. The most common cause of filter blockage is them becoming wet, either by an efflux blockage or low pressure resulting in the culture entering the aeration needling and tubing, or by high ambient humidity. Make a note of airflow problems data is being collected if it is possible the problems have been present for more than an hour. If filters are often blocked, consider changing the ambient humidity.
3. Check for leaks around connectors and luer locks. If leaking, first try tightening. If that does not help, replace with a new part (sometimes autoclaving can warp the luer locks), taking care to sterilise the new part with 70% IMS.
4. Check culture levels are even and do not deviate from the 380 ml line. If the medium level is too low, check the media influx tubing and needle for blockages. The most likely points for blockages are inside the pump tubing and any needles due to their narrow gauges. If medium influx is normal, adjust the efflux needle, and check if the level is back to normal in a couple of hours (time needed to wait dependent on flow rate and total volume deviation). If the level is too high, examine the efflux tubing and needle for blockages, along with the collection chamber filter. When unblocked, the culture chamber level should return to normal volume relatively quickly. Always make a note of culture level changes if data is being collected.

5. Check collection bottle levels are even, and measure volume of a few to ensure the flow rate is correct. Empty the collection bottles and note the time, so that flow rate can be calculated when the bottles are next emptied.

2.3.4.7 SAMPLING AND MONITORING

1. Temporarily restrict the airflow using the adjustable clamp on the tubing. This prevents liquid from bubbling up through the sampling needle.
2. Wearing gloves washed with 70% IMS, unscrew the cap on the sampling needle and use a sterile syringe to extract liquid.
3. Put the sample in a labelled Eppendorf tube and put the cap back on the sampling needle, ensuring it is screwed on tightly. Clean up any spillage.
4. Repeat for each chamber.
5. Do not forget to turn the airflow back on.
6. The samples may be stored for later processing or counting, either through flash freezing with LN_2 and subsequent storage at -80°C, or by mixing with Lugol's solution and storing in a fridge at 4°C depending on the intended use for the samples.

2.4 ASSEMBLY SCHEMATIC

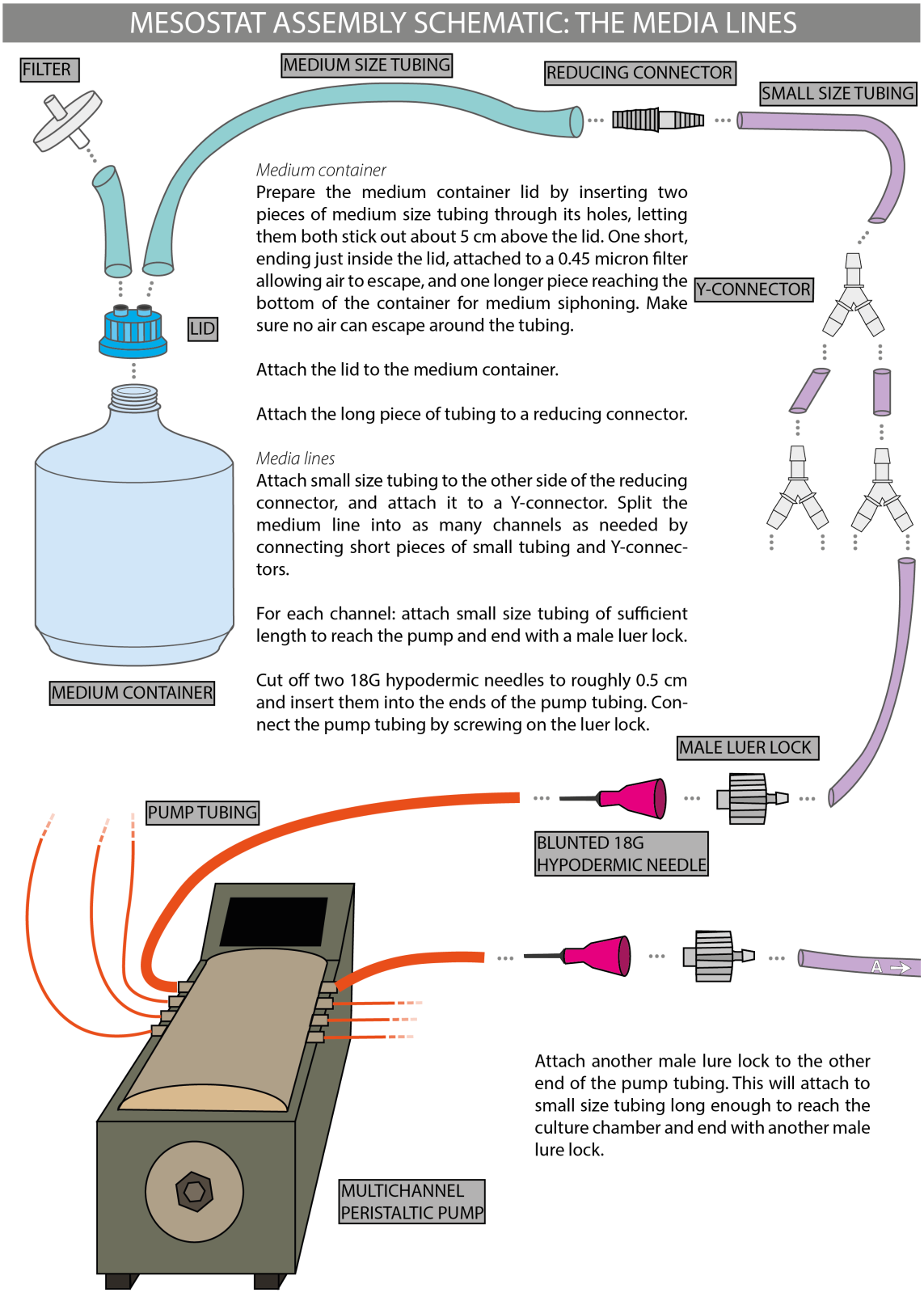

Figure 2.3: Assembly schematic part 1, the media lines.

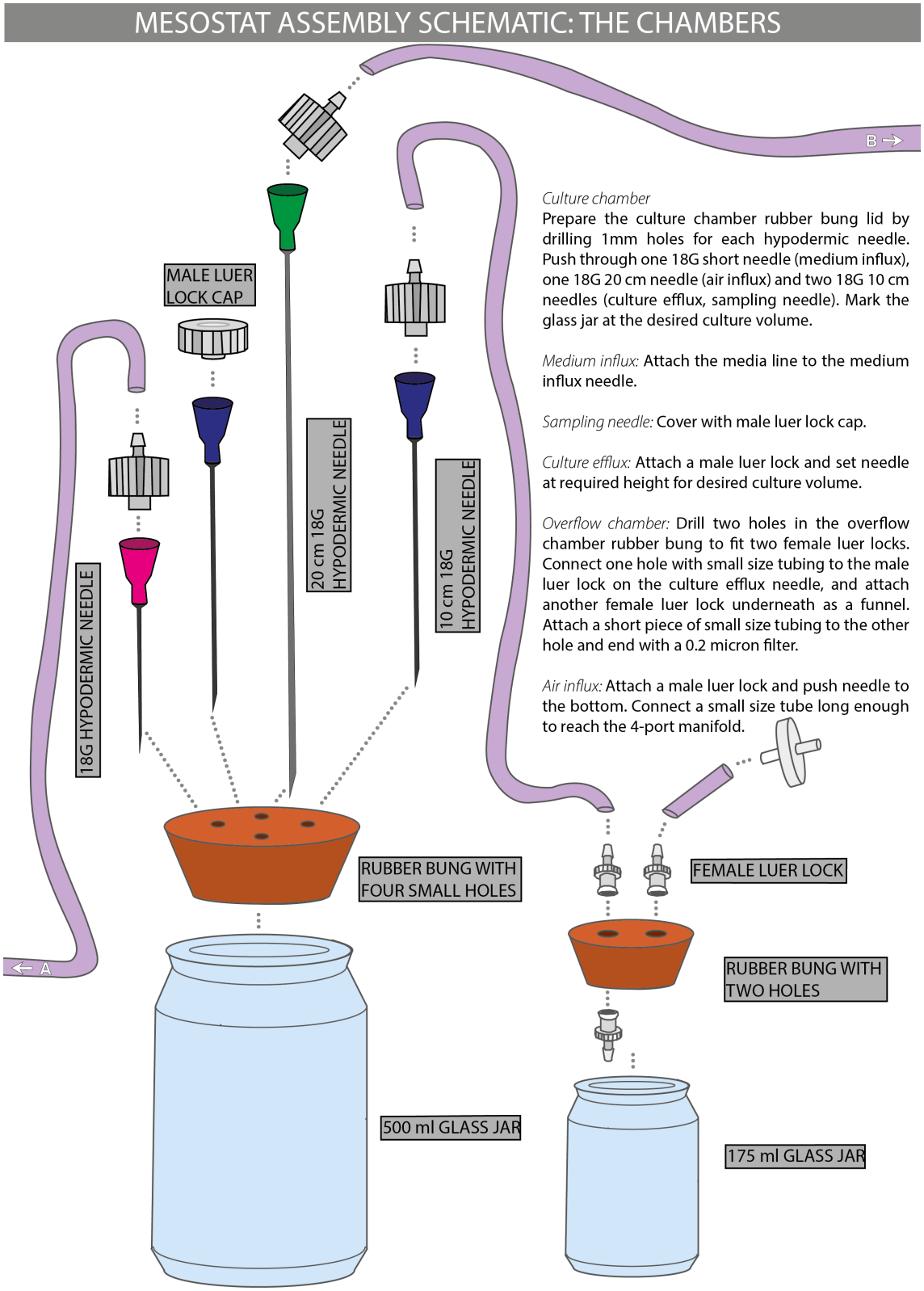

Figure 2.4: Assembly schematic part 2, the chambers.

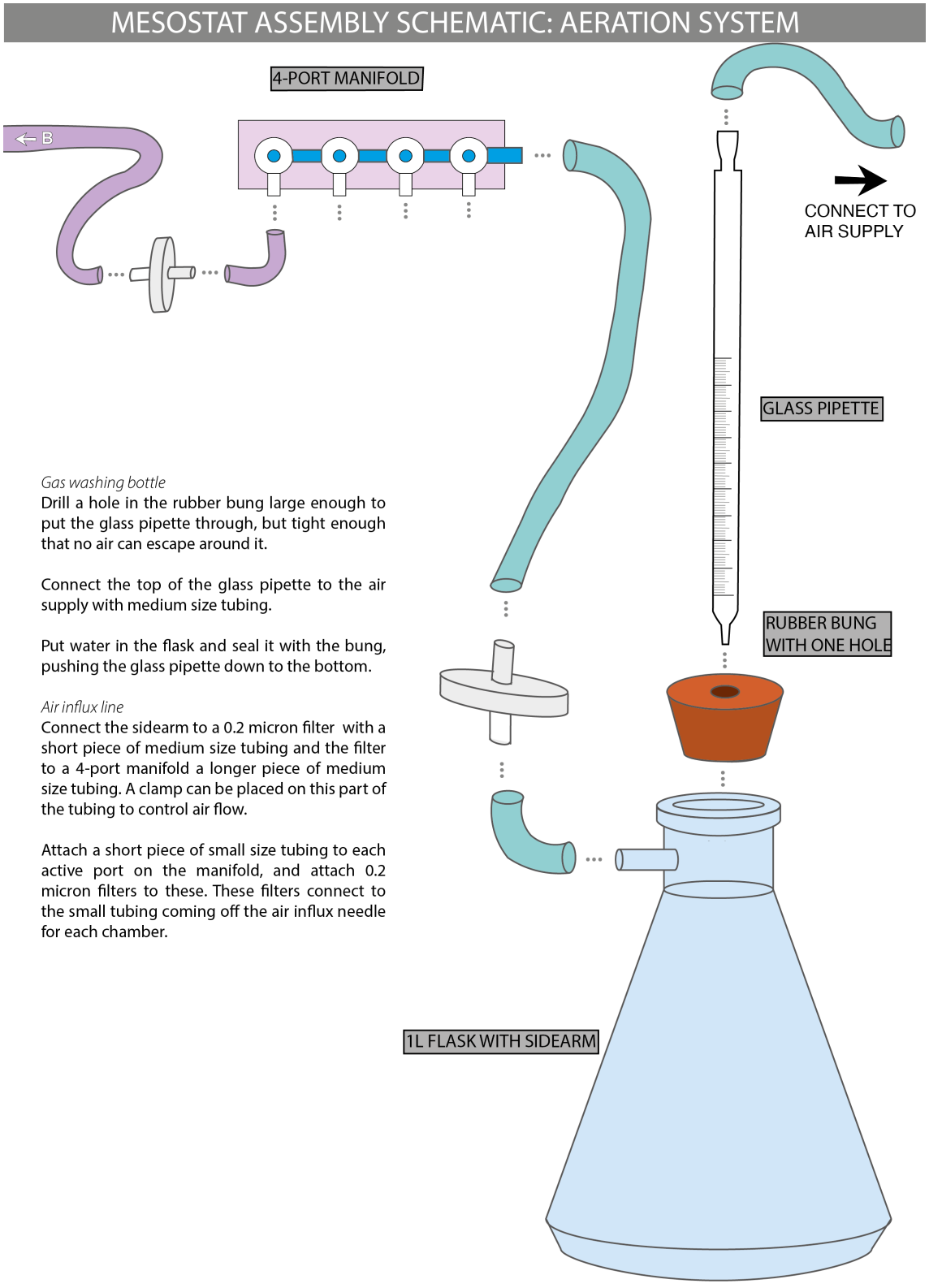

Figure 2.5: Assembly schematic part 3, the aeration system.

2.4.1 EXPERIMENTAL DESIGN FOR VALIDATION DATA

2.4.1.1 REPLICABILITY

Presented below are control data from four separate experiments using the linked protocol to show replicability. The conditions and relevant differences for these experiments are summarised in Table 2.2, unless otherwise stated the experimental conditions correspond to those outlined in the protocol. In all of the presented experiments, *Chlamydomonas reinhardtii* strain Sager's CC-1690 wild-type 21 gr was used, obtained from the *Chlamydomonas* Resource Centre (University of Minnesota, St Paul, MN, USA) core collection. Two different dilution rates were used in the experiments: 0.3/day and 0.15/day. The former was based on the dilution rates used in previous experiments using chemostat populations of similar species that this system was designed for (e.g. Becks *et al.*, 2012; Yoshida *et al.*, 2003), the latter was used as an alternative lower rate to decrease the consumption of growth medium as well as wear and tear on the pump tubing.

Table 2.2: Summary of experimental conditions and properties of data used in Figure 2.6–2.10. Data from all four experiments were used to generate Figure 2.6, whereas data from experiment C was used for Figure 2.7, and experiment D data were used for Figure 2.8, Figure 2.9 and Figure 2.10

Experiment	n	Dilution rate	Time window	Initial density
A	16 (day 1–10) then 4	0.3/day	Days 1–20	50 000 cells/ml
B	16 (day 1–7) then 4	0.3/day	Days 1–28	30 000 cells/ml
C	7 (day 3–11) then 2	0.15/day	Days 3–35	50 000 cells/ml
D	16 (day 5–16) then 6	0.15/day	Days 5–76	30 000 cells/ml

2.4.1.2 APPLICABILITY TO EXPERIMENTAL HERBICIDE RESISTANCE EVOLUTION

Six mesostat chambers in experiment C were allowed a week to reach steady state before the glyphosate treatment was introduced. Shock injections of 38 ml were performed as described in the protocol bringing two chambers each to concentrations of 0 mg/L (controls), 100 mg/L and 150 mg/L glyphosate (analytical standard, PESTANAL®). Both of the chosen glyphosate concentrations are above the minimum inhibitory concentration for *C. reinhardtii* of 97.5 mg/L (Lagator *et al.*, 2013b).

2.4.1.3 COMMON PROBLEMS

We have provided data from three common problems that present with this type of system: a leak, contamination and algal clumping, all from experiment D. These were spontaneous events and the data presented here aims to show how to identify their signal in the population density data and distinguish it from normal variation among populations. The leak in this example resulted in elevated dilution of a single chamber for roughly four hours due to a clamp securing the pump tubing cassette coming undone. In the case of the contamination event, all of the presented six chambers had been disconnected from the array six days before bacterial contamination was observed under the microscope in four chambers, with the remaining two unaffected by the contamination

event. The clumping phenotype was not receiving control medium but presented in a population undergoing treatment with a sublethal dose of glyphosate.

2.4.2 SAMPLE PROCESSING

Population density was in all cases determined through flow cytometry (Beckman Coulter CytoFLEX), using CytExpert (Beckman Coulter) to gate and count events detected in the PerCP-A channel (Excitation: 488nm, Emission: 690/50 BP). This channel is used to detect chlorophyll *a* and represents a robust method for estimating algal density (Kadono *et al.*, 2004) which was further validated against manual haemocytometer counts for this system.

2.4.3 DATA HANDLING

All statistical analyses were carried out in R (version 4.0.5, (R Core Team, 2021)), using the `lme4` package (Bates *et al.*, 2015) to fit a linear mixed effects model with log-transformed population density as the response, dilution rate and experiment as fixed effects, and day and chamber as random effects with varying intercepts. The significance of the fixed effects was tested using the Anova() function from the `car` package (Fox & Weisberg, 2019) and confirmed through parametric bootstrapping using the `pbkrtest` package (Halekoh & Højsgaard, 2014).

The slope of population density decline was estimated between days 6–16 with the package `emmeans` (Lenth, 2022) after fitting a linear mixed effects model with the log-transformed population density as the response, treatment and day as fixed effects as well as day and chamber as random effects with varying intercepts.

2.5 RESULTS

2.5.1 REPLICABILITY

Across the experiments presented here, there is no difference between the mean population densities after steady state has been reached ($\chi^2 = 2.1$, DF = 3, p = 0.6, Figure 2.6). Furthermore, there was no difference in steady state population density whether the dilution rate is 0.3 or 0.15/day ($\chi^2 = 0.4$, DF = 1 p = 0.5). The length of the establishment batch phase before steady state is reached will differ depending on the conditions and inoculate density. The dynamics during this phase has the potential to affect the makeup of the population and thus later dynamics, and it is thus advisable to let the cultures reach steady state before introducing treatments. However, all experiments presented here reached steady state within the first week and it was maintainable for several weeks thereafter.

The level of variation observed in this data set is normal for this type of system (Becks *et al.*, 2012; Fussmann *et al.*, 2000; Yoshida *et al.*, 2003) and can be divided into among population variation and day-to-day variation. Among population variation is primarily caused by the biology of the system as these are separate, genetically heterogeneous populations on separate evolutionary trajectories. Day-to-day variation is however at least partly caused by limitations in sample processing. Both are discussed in more detail in the Discussion section, as well as how to reduce or circumvent the latter in particular.

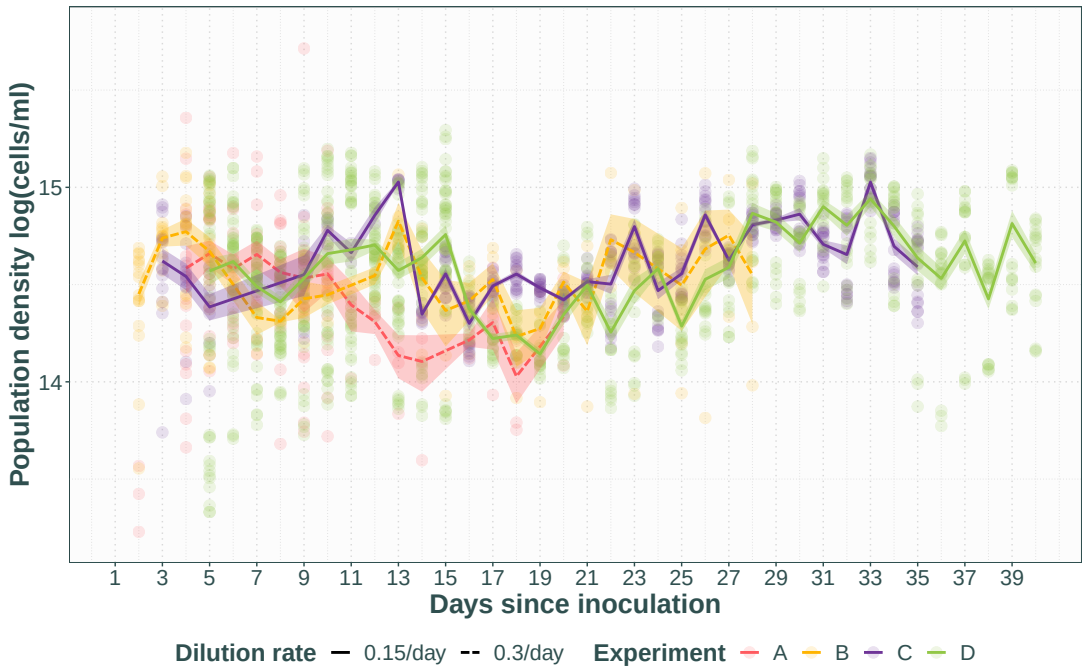

Figure 2.6: Population density with time in four separate runs of the mesostat system. Transparent points represent technical replicates and opaque lines with standard error represent average across populations for experiment. Experiments A and B had a dilution rate of 0.3/day (dashed line), whereas experiments C and D had a dilution rate of 0.15/day (solid line). Note that all have runs have a brief and rapid decline in population density between day 11 and 16. This corresponds to an injection of additional medium as part of the experiment the data is from.

2.5.2 APPLICABILITY TO EXPERIMENTAL HERBICIDE RESISTANCE EVOLUTION

Figure 2.7 shows the population densities of the four glyphosate treated populations and two control populations for 24 days following glyphosate treatment introduction. The glyphosate treated chambers exhibit population decline at a rate approximate to (150 mg/L, slope = -0.14, SE = 0.006) or below (100 mg/L, slope = -0.098, SE = 0.006) the dilution rate of 0.15/day. In the same timespan, the control populations exhibit an overall slight increase in population density (slope = 0.022, SE = 0.006), possibly reflecting adaptation to the mesostat environment. The onset of the population decline appears to be immediate for the 150 mg/L glyphosate treatment, whereas it occurs roughly 5 days after the glyphosate injection for the 100 mg/L glyphosate treatment. This is likely due to the 100 mg/L glyphosate treatment being just on the cusp of the minimum inhibitory concentration, enabling the populations to maintain growth for a short while before the herbicidal action is apparent. After 15 and 18 days respectively of population density decline, the 100 mg/L populations increase in cell density again, suggesting the populations have evolved resistance to the glyphosate, whereas the 150 mg/L populations never show evidence of resistance.

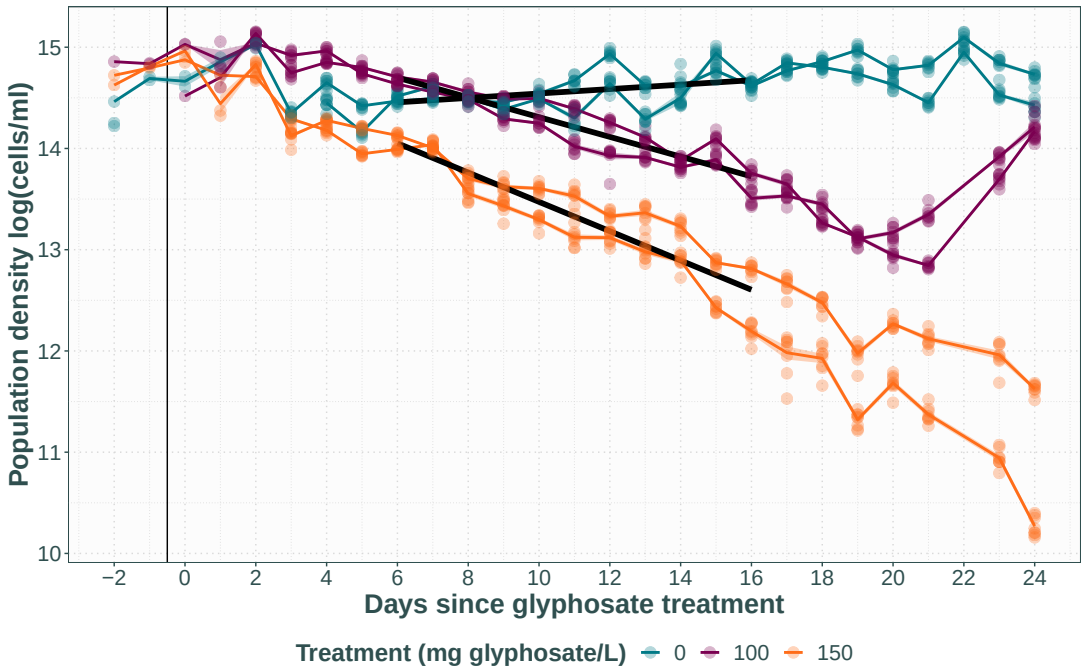

Figure 2.7: Population density with time in populations receiving 0, 100 or 150 mg/L glyphosate. Transparent points represent technical replicates, with opaque lines for population average with standard error transparent ribbon. Thick black lines represent the fitted linear model and the thin black vertical line shows start of the treatment.

2.5.3 COMMON PROBLEMS

2.5.3.1 LEAKS

Figure 2.8 shows the population density in chamber F after a major leak causing over-dilution. Compared to the expected among population and within-population day-to-day variation observed in the chambers that did not experience a leak, three crucial differences together make this the characteristic signal of over-dilution: 1) While similarly large day-to-day fluctuations in the measured density occur in the presented data set, day effects present across chambers. The rapid reduction in population density for chamber F between days 34 and 35 is only apparent in that chamber, whereas a similar reduction between days 37 and 38 is seen in all of chambers A–E. 2) The reduction in population density in chamber F results in a lower population density than otherwise observed in the data set (by roughly 3×10^5 cells/ml). 3) The reduced population density is observed in chamber F for several days after day 35, rather than recovering by the next day like seen for chambers A–E after day 38.

2.5.3.2 CONTAMINATION

Figure 2.9 shows the gradual population density decline in four chambers where bacterial contamination was observed under the microscope compared to two chambers that were unaffected by the contamination event. While the average population density of the contaminated chambers starts

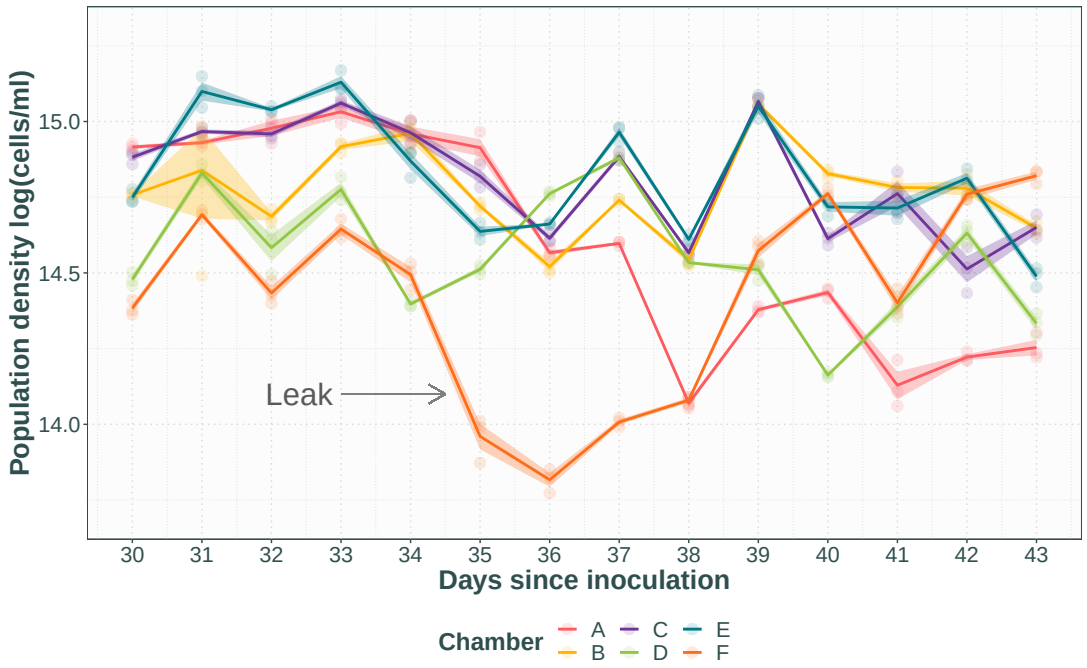

Figure 2.8: Population density with time after a major leak. Transparent points represent technical replicates with opaque lines for population average with standard error. The leak caused overdilution of chamber F between days 34 and 35 (indicated by arrow), compared to the unaffected chambers A—E.

to trend lower a few days after the contamination event, the full effect on the population density is not clear until several days after the contamination had been observed under the microscope. Furthermore, while there is considerable variation among all populations, the signal of contamination in the data is clearly distinguished from the expected among population variation and day-to-day variation by the fact that it is a consistent, long-term population-density decline without recovery 12 days after the contamination event.

2.5.3.3 CLUMPING

Figure 2.10 shows flow cytometry population density estimates from a population exhibiting a clumping phenotype compared to non-clumping populations undergoing the same treatment. The data signal here is an artefact of the limitations of the instrument being unable to accurately distinguish individual cells within aggregates, resulting in huge fluctuations in estimated cell density considerably larger than and out of step with the day-to-day variation observed in the other populations.

2.6 DISCUSSION

Chemostats offer a number of advantages over batch cultures for long-term experimental evolution research. Precise control of selective pressures in a chemically constant environment without evol-

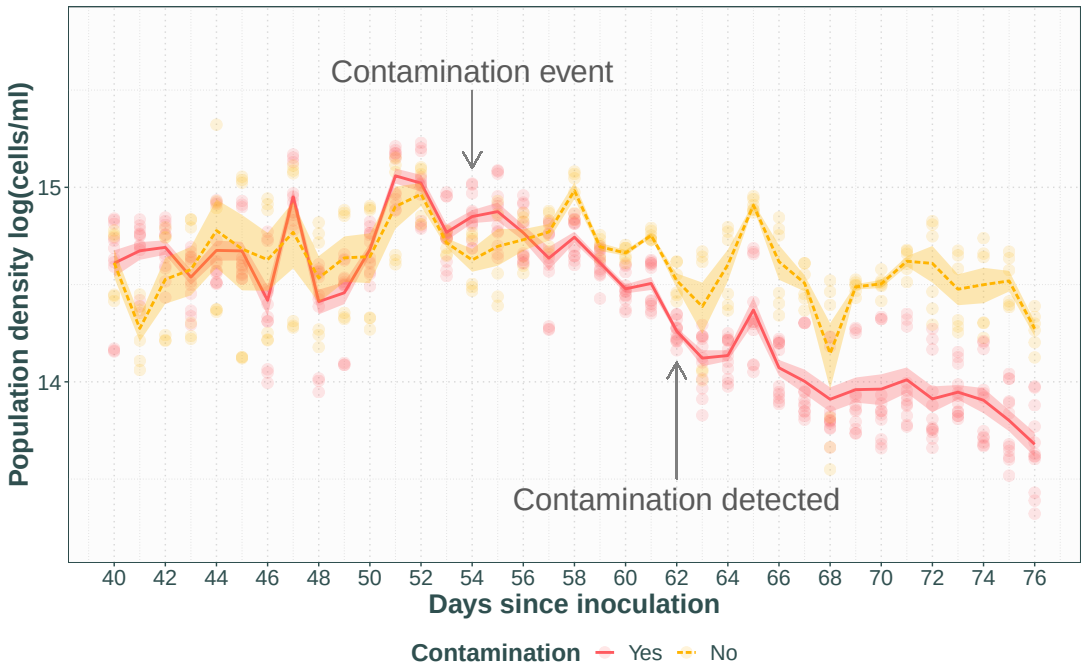

Figure 2.9: Population density with time after a contamination event. Transparent points represent technical replicates with opaque lines with standard error for average of contaminated (solid line) vs. non-contaminated (dashed line) populations. Contamination is likely to have entered the system at day 54 (indicated by arrow), and bacterial contamination was found in 4 out of 6 chambers on day 62 (indicated by arrow).

utionary bottlenecks along with a link between growth rate and dilution rate constitute a useful conceptual framework for modelling evolutionary adaptation and population dynamics. This system adds to the small, but growing, number of efforts to produce simple but scalable, multiplexed DIY chemostats from cheaper materials that are possible to build and maintain by a single person (Dénervaud *et al.*, 2013; Ekkers *et al.*, 2020; Miller *et al.*, 2013; Skelding *et al.*, 2018; Tonoyan *et al.*, 2020; Toprak *et al.*, 2013; Wong *et al.*, 2018), and is the first of its kind for experimental evolution of algae, specifically the evolution of herbicide resistance in model species *C. reinhardtii*. There are three substantive changes from the Miller *et al.* (2013) ministats, one system specific and two generic changes to suit experimental evolution with continuous sample extraction. Firstly the system was adapted to suit the study species *C. reinhardtii*, including light and a lower dilution rate, which distinguishes the system from previous DIY chemostat arrays developed for maintenance of yeast (Dénervaud *et al.*, 2013; Miller *et al.*, 2013; Wong *et al.*, 2018) and bacterial cultures (Tonoyan *et al.*, 2020; Toprak *et al.*, 2013). Secondly, a needle and syringe system was added to facilitate easy, sterile access to the culture for the removal of samples. This allows sampling from the middle of the active culture rather than relying on the overflow. The efflux only samples from the top and the overflow chamber constitutes a wholly different environment without continuous dilution, build-up of waste products and increased evaporation, making them unrepresentative samples of the chamber populations. Furthermore this simplifies addition of cells or treatment compounds directly to the chambers, eliminating the risk of contamination that comes with disconnecting the medium influx or efflux channels. While sampling ports have been described before (e.g. Ekkers *et al.*, 2020; Tonoyan *et al.*, 2020) our simplification and combination with syringe extraction allows manual sampling with minimal contamination. The third change is an increase in the chamber volume to allow larger population sizes and possible future introduction of several

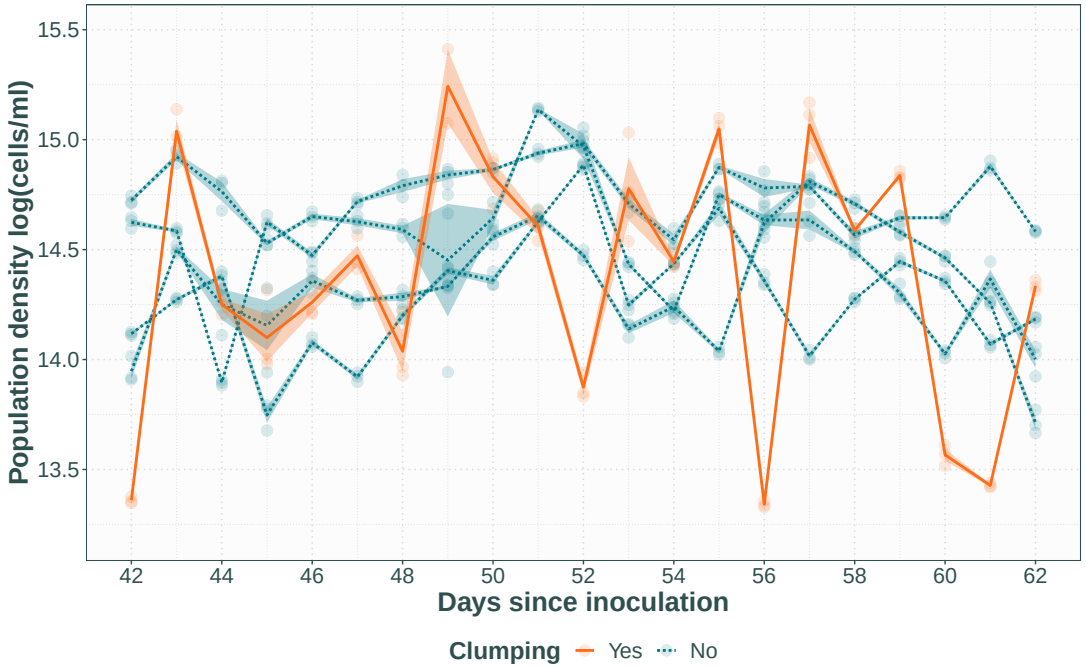

Figure 2.10: Population density with time in a population exhibiting a clumping phenotype. Clumping population shown with solid line, compared to four other populations receiving the same treatment that did not exhibit clumping in dashed line. Transparent points represent technical replicates, with the lines for population averages with standard error.

trophic levels. Furthermore, this increases increases the amount of sample that can be extracted on a regular basis, extending the possibilities for the types of assays that can be performed to characterise evolution in action, as most of the previous DIY chemostat arrays have been limited by their small working sizes (Ekkers *et al.*, 2020; Miller *et al.*, 2013; Tonoyan *et al.*, 2020). Lastly, there were several changes to specific materials to lower the overall costs.

2.6.1 SOURCES OF VARIATION AND HOW TO MINIMISE IT

The data presented here illustrates the expected variation between cultures and how to identify the signal of equipment failure, such as a leak, or contamination. We also demonstrate that the system can be used to evolve resistance to growth inhibiting herbicide glyphosate, and that the signal of herbicidal action is apparent as a population density decline, followed by an increase after the population has evolved resistance. The herbicidal effect is clearly distinguishable from the expected variation under control conditions, and given enough time, the resistant population is expected to settle at a new steady state.

The variation among replicate populations observed here is normal (Becks *et al.*, 2012; Fussmann *et al.*, 2000; Yoshida *et al.*, 2003) and expected as they constitute separate, genetically heterogeneous populations on separate evolutionary trajectories. Even when using a single founder population, the genetic bottleneck caused by splitting it between populations as well as the dynamics during the establishment phase of batch-like growth dynamics (Gresham *et al.*, 2008) will result in similar but distinct populations by the time they reach steady state. Effort should be made to ensure that

all chambers receive the same levels of light and aeration as well as consistent dilution with the same medium, and starting variation could be eliminated through starting with clone populations at a high enough concentration to effectively avoid the establishment phase. However, the among population variation is generally of scientific interest to experimental evolution studies and should be investigated rather than eliminated.

Conversely, while day-to-day variation within a population is also normal for this type of system, it is also partly caused by limitations to the sampling protocol. The data presented here was obtained from measurements performed on living cells that had the opportunity to grow and divide between sample extraction from the mesostat chambers and sampling processing. While this is an unavoidable source of variation, it can however be reduced by minimising the time that passes and working in a controlled temperature environment. If the experimental design allows, the cells can be immobilised by using e.g. Lugol's solution before counting with flow- or haemocytometry. It is also possible to control for this variation by including sampling day as a source of error in statistical models applied to the data.

The among population and day-to-day within population variation are however both clearly distinguishable from the data signal of common faults like leaks, contamination and clumping. While these faults are likely to be detected before they become apparent in the population density data, leaks causing significant over-dilution are apparent within a few hours while clumping and contamination can be observed under a microscope, it is important to understand how they affect the data so that an informed decision can be made on how to handle it. While the population density is always expected to quickly return to steady state after over-dilution, the increased flushing out of cells constitutes an evolutionary bottleneck and the changed growth conditions may affect other traits of the population not visible in the population density data and data collected subsequent to a major leak should thus be treated with caution. The leak presented here was caused by equipment failure resulting in over-dilution, but smaller leaks often occur as the pump tubing wears out with long term use, which can lead to under-dilution of the connected chambers. Both are best prevented by regular inspection of the pump parts for irregularities.

Bacterial contamination is another common risk in long-running continuous cultures (Gresham & Hong, 2014), and is best prevented by working in a sterile environment and minimising the points at which contamination can enter the system. The main contamination risk presents when disconnecting any part of the array, such as when switching medium containers, or when extracting samples, and particular care should be taken to keep the connecting parts sterilised during. The example presented here is the only instance of contamination observed across eight separate experiments each lasting more than a month and happened when the chambers were disconnected from the array for a longer period of time and removed from the sterile environment. Even so, only four out of six chambers showed evidence of contamination under the microscope 12 days after the contamination event, despite all of the chambers in question sharing a medium source. This suggests that the system is robust in terms of contamination not spreading between the chambers. While regular microscopy inspection of cell samples for contamination is recommended, this can be laborious with a large number of replicates and the characteristic population density decline provides another opportunity to detect and isolate the problem.

Lastly, chemostat populations being under a selective pressure to evolve phenotypes reducing their risk of being flushed out is an often cited issue with the method (Gresham & Dunham, 2014; Gresham & Hong, 2014), presenting as adhesion to the chamber walls and cell flocculations. While this phenomenon has as of yet never been observed under control conditions with this protocol, there was one instance of cells exhibiting a clumping phenotype while under treatment with a sublethal dose of glyphosate, making it possible it was a response to the treatment rather than the mesostat environment. In *C. reinhardtii* there are two distinct types of clumping: cell aggregations of separate cells and palmelloid colonies that share a cell wall (de Carpentier *et al.*, 2019; Harris *et al.*, 1989; Lürling & Beekman, 2006). Both have been found to be an induced response as well as heritable (Harris *et al.*, 1989; Iwasa & Murakami, 1968; Khona *et al.*, 2016; Lürling & Beekman, 2006; Olsen *et al.*, 1983), meaning that once they become common in a population they may be hard to get rid of (Harris *et al.*, 1989). Palmelloids are small enough that they will not

cause blockages, but due to the shared cell wall they cannot be disassociated through bubbling or by vortexing a sample. Cell aggregations can be considerably larger, however they are also possible to break apart through vortexing, and vigorous bubbling of the cultures often prevents their formation (Gresham & Dunham, 2014). How much of a problem clumping is depends on the experiment, i.e. it becomes a problem if it hinders sample processing and when it is thought to be an artefact of the chemostat environment rather than in response to the applied treatment. For population density measurements by flow cytometry as presented here, clumping considerably reduces the accuracy of the measurements as each clump is counted as a single particle, increasing day-to-day variation. In this case, manual haemocytometry could give a better estimate but this is considerably more laborious.

2.6.2 OTHER POSSIBLE ISSUES AND LIMITATIONS

Despite the many advantages of chemostat cultures, there are limitations to their application and caveats to how the data may be interpreted. While the system described in this protocol was explicitly designed to be maintainable by one person as well as cheaper than the Miller *et al.* (2013) ministats it is based on by choosing alternative materials and using parts not purpose bought for this experiment, it is still considerably more expensive than batch cultures. While it is theoretically possible to run very large cultures indefinitely, the cost of the medium or treatment components will limit the lifespan of the experiment as they will be consumed faster than in a batch culture design. One way to conserve medium and treatment components is to lower the dilution rate, which in the experiments presented here had no effect on population density in the chambers. However, this changes the selection pressures experienced by the populations as well as their doubling rate (Gresham & Hong, 2014). The logistics of the system and any cost saving measures must therefore be carefully balanced against the resulting biology, taking into account the desired selective pressure, cell cycle stage and generation time.

This design introduced sampling needles to allow sampling directly from the culture as an alternative to sampling from the overflow chamber, as the environment therein will be different from the culture chamber, or redirecting the overflow, as the low flow rate made sampling a slow process and the high temperature caused high levels of evaporation. However, sampling directly from the culture does perturb the steady state and change the dynamics within the chamber by temporarily reducing the culture volume and thus pausing dilution (Fischer *et al.*, 2014). The frequency and volume of samples should thus be carefully considered against the disruption they may cause.

Another potential problem involves insufficient aeration or efflux blockages causing over- or under-pressure in the chambers. Provided the air supply is sufficient, the most common reason for low or uneven bubbling is blocked air filters, usually because they have become damp. If the air filters frequently become damp, the ambient humidity may be too high. Not enough bubbling may cause sedimentation and stratification of the culture, as well as selection for phenotypes that sink so they avoid being flushed out, or it may instead cause the culture to rise through the aeration needle instead of through the efflux needle, changing the effective dilution rate. Clogging of the media line is uncommon, but can occur if not properly sterilised and contamination is allowed to grow. This is often apparent as a reduction in flow into and out of the affected chambers. The daily maintenance part of the protocol outlines how to spot and address these problems.

Lastly, in terms of studying the dynamics of adaptive evolution, chemostat systems are highly specific environments. When transplanted out, chemostat populations are often found to grow poorly in their ancestral environment compared to the ancestral strain (Gresham & Hong, 2014; Wenger *et al.*, 2011), as they have had intense selection on a specific part of the growth cycle in an environment of constant dilution that is not reflective of natural populations. However, this is also part of their usefulness and beauty, by keeping the adaptive environment as simple and specific as possible, we can isolate fitness effects and allow fine-tuned investigation of their mechanics and dynamics.

2.6.3 HOW TO IMPROVE OR MODIFY

Several further modifications are possible for this system. A light table that does not transfer heat to the cultures would allow the internal culture temperature to be set solely by the ambient temperature in the controlled temperature room while maintaining low evaporation. As the chamber lids are relatively large, sensors to monitor e.g. pH or CO_2 levels could also be fitted through additional ports (see Ekkers *et al.*, 2020).

While the pump and pump-tubing are integral to the design and also the most expensive parts, all other parts could be easily substituted depending on availability or cost constraints. The materials list provided in the protocol can be used as a guide for the dimensions and properties of the part, but primarily aims to illustrate how this type of system can be built from parts already found in most wet labs rather than buying a pre-made set. Any water-tight, sterilisable container can be used for culture chambers if suitable lids can be manufactured, such as falcon tubes (Tonoyan *et al.*, 2020) or commonly available lab glassware (Ekkers *et al.*, 2020). The controlled temperature room can be replaced with water baths (note however that this requires mounting the lights up on the sides of the water baths), and portable aquarium pumps can be used instead of building infrastructure, increasing flexibility in where the system can be housed.

The light system here is rudimentary but sufficient for *C. reinhardtii* growth (Harris *et al.*, 1989), using white light LED strip lights mounted around the chambers along with a DIY light box also consisting of white light LED strip lights and a semi-transparent plastic top to diffuse the light. The light box is not necessary, but convenient for maximising light from all angles. Under control conditions 24h light was used, but it is possible to fit a timer to the outlet connecting the lights to instead provide a diurnal light cycle. Coloured semi-transparent plastic could be used to provide light only from a specific part of the light spectrum, but it would also be possible to mount specialist lighting around the mesostats if tuning for a specific photosynthetic organism or experiment is desired.

2.6.4 FUTURE RESEARCH OPPORTUNITIES

We have used this system for experimental evolution of herbicide resistance in algae by adding glyphosate as a shock injection and then continuously through the growth medium, however, this setup is also easily adaptable depending on the research question. The herbicide treatment could also be applied gradually through the medium or through series of shock injections in a ratchet protocol (Reboud *et al.*, 2007) and investigate to what level the resistance can be pushed and at what speed. The dilution rate and thus the cell growth rate is set by the pump speed, tubing thickness and culture volume, so running chambers with different dilution rates simultaneously would be possible with different pump tubing thicknesses, multiple pumps or multiple culture volumes, depending on the range required. Furthermore, the use of multiple light tables with opaque partitions between cultures would allow testing for an interaction with light level, or the chambers could be kept in water baths at different temperatures to determine the effect of temperature.

In addition to testing the effect of abiotic factors such as temperature or light, or manipulating the specific cell cycle stage of the population, a particularly interesting future application would be to use the system to ask focused questions about eco-evolutionary dynamics. In particular, introducing several trophic levels in the culture chambers to study the ecosystem and food web effects of herbicides and evolving herbicide resistance. The predator-prey cycles of rotifer *Brachionus calyciflorus* and *C. reinhardtii* as well as *Chlorella vulgaris* have been successfully studied and modelled using chemostat environments (e.g. Becks *et al.*, 2012; Yoshida *et al.*, 2003) and our setup allows simplified simultaneous replication for this type of system that can be maintained by one person. Competition could also be introduced to the system through using multiple algal strains and monitoring their frequencies or through expanding the culture ecosystem to include other algal species or bacteria (Raatz *et al.*, 2018).

CHAPTER 3

Glyphosate resistance evolution to lethal and sublethal doses in chemostat populations of model organism *Chlamydomonas reinhardtii*

3.1 ABSTRACT

Herbicide resistant weeds are an increasing economic and ecological problem worldwide. Evolutionary theory and insight from experiments testing this theory are now a central part of solving resistance problems. More specifically, experimental evolution, where populations are allowed to evolve under specific conditions, can offer substantial insights into the trade-offs that govern the pace at which resistance arises. Here we leverage the green alga *Chlamydomonas reinhardtii* facing glyphosate as a model plant system to evaluate such theory, monitoring the level of evolved resistance and associated fitness costs throughout the course of adaptation. On a gradient of lethal and sub-lethal doses of glyphosate, we found evidence for evolved resistance but limited evidence for classic growth rate trade-offs that are expected to affect the pace of resistance evolution.

3.2 INTRODUCTION

The widespread and persistent use of herbicides worldwide has resulted in a strong selective pressure for resistant phenotypes (Powles & Yu, 2010). To date, 266 different weed species have evolved resistance to 164 different herbicides (Heap, 2022), all while the rate of discovery of new herbicide modes of action (functional changes at a cellular level in response to exposure) is declining (Heap, 2022; Rüegg *et al.*, 2007). This is a growing problem, both ecologically and economically. Weeds are already responsible for ca. 10% of crop yield loss worldwide and with evolved resistance to herbicides constitute a higher potential threat to crop yield than any other pest (Oerke, 2006).

Resistance is an evolutionary process, and an understanding of the evolutionary ecology of herbicide resistant weeds at both an organism and population level is pivotal to enable sustainable use of herbicides in the future (Neve *et al.*, 2009, 2014). The evolutionary dynamics of herbicide resistance have thus emerged as a central part of the toolset for managing the impact of weeds and on crop plants. The evolutionary theory that drives this centres on the fitness consequences of resistance in the presence and absence of herbicides (Purrington, 2000; Vila-Aiub *et al.*, 2009b). Resistance is predicted to confer theoretical intrinsic fitness costs based on trade-offs with normal cell function or resource investment that decreases resources available for growth or reproduction (Gaines *et al.*, 2020; Powles & Yu, 2010). As a population evolves resistance to herbicide its performance while herbicide-exposed increases as well as the minimum inhibitory concentration (MIC) of the herbicide, resulting in a flatter dose-response slope (Figure 3.1). An associated change in performance in the ancestral environment would thus be evidence of an intrinsic fitness cost. Resistance management strategies are largely based on the expectation that resistance will incur a sufficient fitness cost that the absence of herbicide will put it under negative directional selection (Purrington, 2000). However, costs are rarely found to be universal and often have an extrinsic, ecological component through compromising performance in specific environments (Vila-Aiub *et al.*, 2009a) meaning their effect on the pace of evolution may be hard to estimate without

empirical evidence to underpin the theory. Furthermore, the dynamics of the adaptation process will depend on the strength of the selective pressure, i.e. the herbicide dose applied (Gressel, 2009; Powles & Yu, 2010), but as the majority of studies focus on weed populations experiencing high doses designed to kill the vast majority of the population, the effects of lower doses are poorly understood (Busi *et al.*, 2013; Gressel, 2011; Neve & Powles, 2005). Experimental evolution under tightly controlled conditions in the lab allows us to connect when shifts in resistance level and performance emerge with the overall pace and dynamics of evolution by monitoring resistance evolution in action with continuous testing of both the level of resistance and intrinsic fitness costs in the ancestral environment.

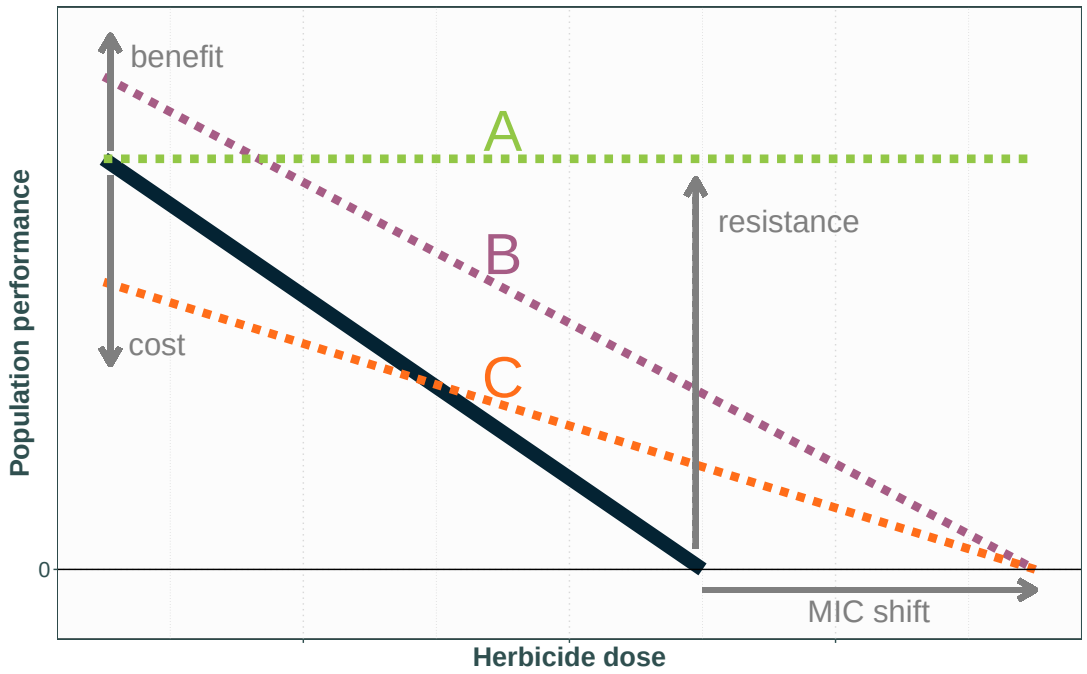

Figure 3.1: A) As the ancestral population represented by the black line evolves resistance to herbicide its performance while herbicide-exposed increases as well as the MIC of the herbicide, resulting in a flatter dose response slope, possibly associated with a change in performance in the ancestral environment. Examples of evolutionary outcomes are represented by the dotted lines: A has evolved resistance to herbicide at no cost to performance in the ancestral environment, and the magnitude of increased performance at high doses suggests a large shift in the MIC; B has evolved increased resistance to herbicide but with a slope suggesting a smaller shift in the MIC with a fitness benefit to performance in the ancestral environment; C has evolved increased resistance but this confers a cost in the ancestral environment.

Glyphosate has since the introduction of glyphosate resistant crops become the world's most commonly used herbicide, and is thus of particular economic importance (Duke & Powles, 2008). Due to the widespread use of glyphosate, documented resistant strains of weeds have rapidly increased in number (Heap, 2022) and become a serious problem for agriculture, as well as a major source of pollution for non-target ecosystems (Van Bruggen *et al.*, 2018). Glyphosate blocks the shikimate pathway by competitively binding to enzyme 5-enolpyruvylshikimate-3-phosphate synthate (EPSPS), outcompeting intended substrate phosphoenolpyruvate (PEP) and hindering aromatic amino acid synthesis (Steinrücken & Amrhein, 1980). Secondary effects on other cellular processes have also been documented, including disruption of photosynthesis and increased production of reactive oxygen species (de María *et al.*, 2005; Gomes & Juneau, 2016; Servaites *et al.*,

1987). However, while the glyphosate mode of action is relatively well understood, we have little insight into how fundamental evolutionary theory regarding fitness costs drive pace and direction of evolving glyphosate resistance; the level of resistance and the costs of resistance appear largely dependent on the species and the specific molecular mechanism (Gaines *et al.*, 2020; Sammons & Gaines, 2014). Furthermore, factors like trait dominance (Han *et al.*, 2017), genetic background (Martin *et al.*, 2017) and life history stage (Osipitan & Dille, 2017) as well as other stressors present in the environment like temperature (Ge *et al.*, 2011) or competition (Pedersen *et al.*, 2007) have a considerable effect on the phenotype. In some cases, resistance appears to be fitness neutral (Vila-Aiub *et al.*, 2014) or even confer a fitness benefit (Vogwill *et al.*, 2012).

Here we experimentally evolve resistance to lethal and sublethal doses of glyphosate in populations of unicellular green alga *Chlamydomonas reinhardtii* using continuous flow-through chemostats. We use this system to evaluate the theory of intrinsic costs underpinning the pace of evolution of resistance. Using chemostats rather than batch cultures allows the populations to be kept at a steady state of constant exponential growth, removing effects of incidental nutritional stress or over-dilution as well as evolutionary bottlenecks. With its short generation time, small size and sensitivity to multiple commonly used herbicides (Reboud *et al.*, 2007; Reboud, 2002), *C. reinhardtii* has already been used to study efficacy of resistance management strategies (Lagator *et al.*, 2013a,b), characterising fitness costs (Vogwill *et al.*, 2012), comparisons of evolutionary potential in communities of algae (Melero-Jiménez *et al.*, 2021) and molecular analysis of herbicide resistance mutations (Erickson *et al.*, 1989; Randolph-Anderson *et al.*, 1998). Furthermore, algal populations worldwide are still affected when herbicide contamination reaches non-target ecosystems through agricultural run-off (Van Bruggen *et al.*, 2018) and as key primary producers their ability to evolve resistance and associated fitness costs may have far reaching consequences (Annett *et al.*, 2014; Fugère *et al.*, 2020). While the ability for many algal species to evolve resistance to herbicide pollution is well documented, understanding the dynamics of that process with any associated trade-offs in fitness is an important missing piece of the puzzle to be able to understand the effects pollution may have on ecosystems and community assemblages (Baselga-Cervera *et al.*, 2016; Melero-Jiménez *et al.*, 2021).

We hypothesise that both glyphosate treatments should cause growth-inhibition leading to continuous population decline and that the evolution of resistance should thus lead to population density resurgence. We test whether this corresponds to increased population growth rate in a range of glyphosate doses compared to the susceptible control strain throughout the course of adaptation to assess the level of resistance. Furthermore we test the hypothesis that there is an intrinsic cost to glyphosate resistance through continuous assaying of the population growth rate in the ancestral environment to assess whether the evolution of resistance is associated with a trade-off in performance. The expected possible outcomes here correspond to those set out in Figure 3.1.

3.3 METHODS

3.3.1 EXPERIMENTAL DESIGN

3.3.1.1 ALGAL STRAIN AND CHEMOSTAT SETUP

Chlamydomonas reinhardtii strain CC-1690 was obtained from the Chlamydomonas Resource Centre core collection. This strain has been previously used in experimental evolution studies, including for herbicide resistance evolution (Lagator *et al.*, 2013a,b; Vogwill *et al.*, 2012). All *C. reinhardtii* populations were cultured in continuous flow through chemostats (see chapter 2 or Hansson *et al.*, 2022, for detailed protocol) in Ebert algal medium at a dilution rate of 0.15/day with a shared multichannel peristaltic pump (Watson-Marlow 205S/CA16) controlling the flow for all culture chambers, maintaining a culture volume of 380ml±5%. The populations were kept on a

light box providing white light from below and surrounded on all sides with white light fluorescent bulbs at a light level of 75 µmol m^{-2} s^{-1} 24 h a day. The cultures were heated by the light box to an internal temperature of 30°C, and kept in a controlled temperature room with an ambient temperature of 25°C. The cultures were continuously mixed by bubbling with air supplied from the building's air supply taps. The 16 experimental *C. reinhardtii* populations were allowed 14 days to reach steady state and acclimate to control conditions to ensure equal and high starting population sizes of approximately 2.5×10^5/ml.

3.3.1.2 HERBICIDE CONCENTRATIONS AND REPLICATION

10 out of the 16 populations were exposed to glyphosate (PESTANAL®, analytical standard) at a concentration of either 100 mg/L (lethal dose) and 50 mg/L (sublethal dose) 14 days after initial inoculation, with five chambers receiving each dose. 100 mg/L glyphosate completely inhibits population growth in batch cultures over at least 4 days (Lagator *et al.*, 2013a,b), whereas 50 mg/L glyphosate results in a population growth rate reduction. The remaining 6 chambers continued to receive the control medium.

3.3.2 POPULATION DENSITY AND GROWTH RATE ASSAYS

The culture chambers were sampled daily from the middle of the culture to monitor population density through flow cytometry (Beckman Coulter CytoFLEX) starting 5 days after initial inoculation.

Growth assays were performed 1, 8, 22, 29, 36 and 43 days after glyphosate introduction. As the resistance trait is likely to be in the form of increased ability to grow in a given dose rather than complete insensitivity to glyphosate, i.e. a MIC will still exist, the resistance level was tested at five doses of glyphosate, ranging from sublethal to far above lethal for a naive strain and glyphosate resistance was defined as increased population growth rate in the presence of glyphosate compared to control population growth under the same conditions. Intrinsic trade-offs were assessed through comparing the population growth rate in the ancestral environment to the control population growth rate in the ancestral environment, defining a cost as a reduction in population growth rate under control conditions associated with increased resistance. A washed subsample from each population consisting of approximately 2.5×10^7 cells was allowed to acclimate to the ancestral environment in 30 ml of control medium for 72 hours to allow at least one generation of growth without the herbicide treatment for cells permanently growth-inhibited by glyphosate to die and thus be removed from the subsample, as well as acclimation to the batch environment of the assays. The resistance and trade-off assays were carried out simultaneously with 10 µl of each washed sample added to 250 µl control medium containing 150, 125, 100, 75, 50 and 0 mg glyphosate/L respectively with 3 replicates of each. The fluorescence intensity (excitation: 485nm, emission: 670nm) for each sample was measured as a proxy for population density at 0, 6, 12 and 24 hours using a Tecan Spark 10M Multimode Microplate Reader. These time points adequately captured the log phase of growth both in control medium and under acute glyphosate stress in pilot studies. Between measurements, the assay populations were kept under the same temperature and light conditions as the chemostat populations.

3.3.3 POPULATION DENSITY THROUGH TIME ANALYSIS

All data were analysed using R (version 4.0.5) and CytExpert (Beckman Coulter). CytExpert was used to gate and count events detected in the PerCP-A channel (excitation: 488nm, emission: 690/50 BP) to determine population density. This channel is used to detect chlorophyll *a* and represents a robust method for estimating algal density (Kadono *et al.*, 2004) which was further

validated against manual haemocytometer counts for this system. Data from one of the control chambers and one of the 50 mg/L glyphosate chambers were removed after a malfunction (resulting in $n = 5$ for controls and $n = 4$ for 50 mg/L for the latter half of the data set). Growth-inhibition due to glyphosate was defined as a continuous decline in population density for at least 3 days following the addition of the herbicide. A continuous increase in population following this decline to eventually reach a steady state was considered evidence of a newly resistant population.

Day-to-day growth rate for each chamber was calculated as $GR = log(N_t - N_t - 1)/\Delta t$, where GR denotes growth rate, N is the population density at a given time-point and the preceding time-point, and Δt is the time elapsed between measurements. To test whether the day-to-day growth rate exhibited a pattern different from a flat fit, i.e. if there was a noticeable population decline and recovery coinciding with glyphosate treatment, R package `mgcv` (Wood, 2011) was used to run a hierarchical generalised additive model (hGAM) following (Pedersen *et al.*, 2019). The hGAM framework was chosen to allow modelling of the average treatment effect on the full time series while taking into account the differences between individual chamber populations, capturing the non-linear dynamics of the system. Day-to-day growth rate was modelled as a function of the interactions between time and glyphosate treatment as well as time and population. Populations within the same glyphosate treatment were assumed to have a similar functional form over time but with some intergroup variation and were thus fit with a shared smoothing parameter, whereas each glyphosate treatment was fit with independent smoothing parameters to allow for differences in wiggliness (Pedersen *et al.*, 2019). In both cases thin plate regression splines were used. Day was also included as a random effect smooth (equivalent to a random intercept) to account for day-to-day variation. The first 7 days of the experiment were excluded from the model to improve the fit as the population establishment phase is inherently different in its dynamics to the steady state and thus introduced unnecessary noise. The model residuals were also assessed for temporal autocorrelation within each chamber and were judged to be independent, and as such no correlation term was included in the model.

3.3.4 RESISTANCE LEVEL AND FITNESS TRADE-OFF ANALYSIS

Times series were constructed of maximum growth rates for all replicates in the growth assays, where the growth rate for each day was the maximum growth rate measured within each 24h period of sampling. Mixed-effects models with this daily maximum growth rate as the response were fit with R `lme4` package (Bates *et al.*, 2015) to assess the change in slope (i.e. resistance level) and intercept (i.e. associated cost in ancestral environment) throughout the course of resistance evolution for each population. Dose, day and treatment were fit as fixed effects and chamber as a random effect with varying intercept. Both growth rate and dose were scaled and centred to improve fit. R `emmeans` package (Lenth, 2022) was used to estimate the dose response trends and intercepts obtained from the model.

As the populations never exhibited growth in 125 or 150 mg/L glyphosate and would reach a fluorescence intensity consistent with a population consisting of dead cells within 12 hours, these assays were excluded from the linear mixed-effects models to improve fit. The growth rate in these assays 43 days after glyphosate introduction were instead analysed as death rate assays using an ANOVA to determine if there was evidence for a higher growth rate (i.e. slower rate of death) to higher doses associated with the evolution of glyphosate resistance suggesting increased tolerance.

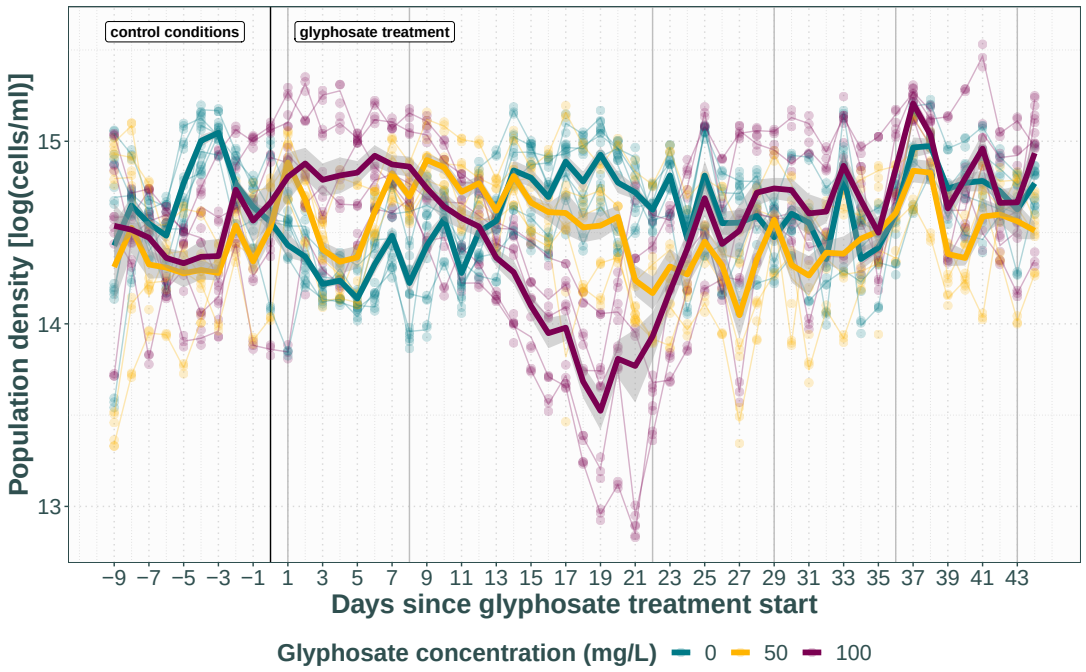

Figure 3.2: Population density throughout the experiment. Each point is a technical replicate, thin lines represent average chamber population density. Thick lines with SE represent average densities for the treatment groups. Grey vertical lines indicate growth assay sampling points.

3.4 RESULTS

3.4.1 POPULATION DENSITY SHOWS EVIDENCE OF RESISTANCE 19 DAYS INTO LETHAL DOSE TREATMENT

While each population represents a separate evolutionary trajectory, there are clear overall patterns shared by the populations receiving the same treatment (Figure 3.2). All the populations receiving the lethal treatment exhibit a clear density decline where the day-to-day growth rate consistently averages below 0 for at least 3 consecutive days starting after the treatment was introduced, but the exact onset of this decline and its slope varies by chamber. All chambers at some point during the mortality phase have a growth rate around or below -0.15, i.e. the expected population density change if all cell growth and division is arrested while the population is diluted by the continuous inflow of media. This suggests that the populations are not just being diluted as cell division is suspended, but that cells are dying at a faster rate than division can take place. The mortality phase is immediately followed by a recovery phase where the growth rate consistently averages above 0 for several consecutive days, suggesting the population has evolved resistance. The earliest instance of this is 19 days after the treatment was applied, and all populations have entered the recovery phase by 22 days. This pattern is not apparent in the controls or sublethal glyphosate populations, and is reflected in the hGAM of the day-to-day growth rate. The control populations and those receiving sublethal glyphosate treatment average day-to-day growth rates of zero after day 7, resulting in a flat fit by the hGAM (control $F_8 = 0$, $p = 0.5$; sublethal $F_8 = 0$, $p = 0.7$). By contrast, the model fit a smooth function significantly different from a flat fit for

the populations receiving the lethal glyphosate treatment ($F_8 = 7.9$, $p < 0.001$).

3.4.2 GROWTH ASSAYS SHOW NO EVIDENCE FOR INCREASED LEVEL OF RESISTANCE

43 days after the introduction of glyphosate there is no evidence of increased resistance to any of the tested doses or a shifted MIC, in direct contrast with the population density data indicating resistance has evolved 24 days prior. While there is an effect of dose ($F_1 = 454.1$, $p < 0.001$), treatment ($F_2 = 18.7$, $p < 0.001$) and day ($F_5 = 73.2$, $p < 0.001$), as well as their two-way (Dose*Treatment $F_2 = 21.1$, $p < 0.001$; Dose*Day $F_5 = 49.3$, $p < 0.001$; Treatment*Day $F_{10} = 147.5$, $p < 0.001$) and three-way interactions ($F_{10} = 21.7$, $p = 0.02$), on the growth rate, the dose-response relationships are indistinguishable between treatment lines (Figure 3.3) by the end of the experiment (Figure 3.4, Table 3.1). The intercepts of the dose response are also not significantly different between treatments, indicating no evidence of a fitness cost in the ancestral environment.

The death assays also reveal no differences in population performance between treatments at very high doses of glyphosate, with no effect of dose ($F_1 = 1.8$, $p = 0.2$), treatment ($F_2 = 2.5$, $p = 0.1$) or their interaction ($F_2 = 0.2$, $p = 0.8$) on growth rate. This further suggests no increased tolerance or shifted MIC as a result of either glyphosate treatment.

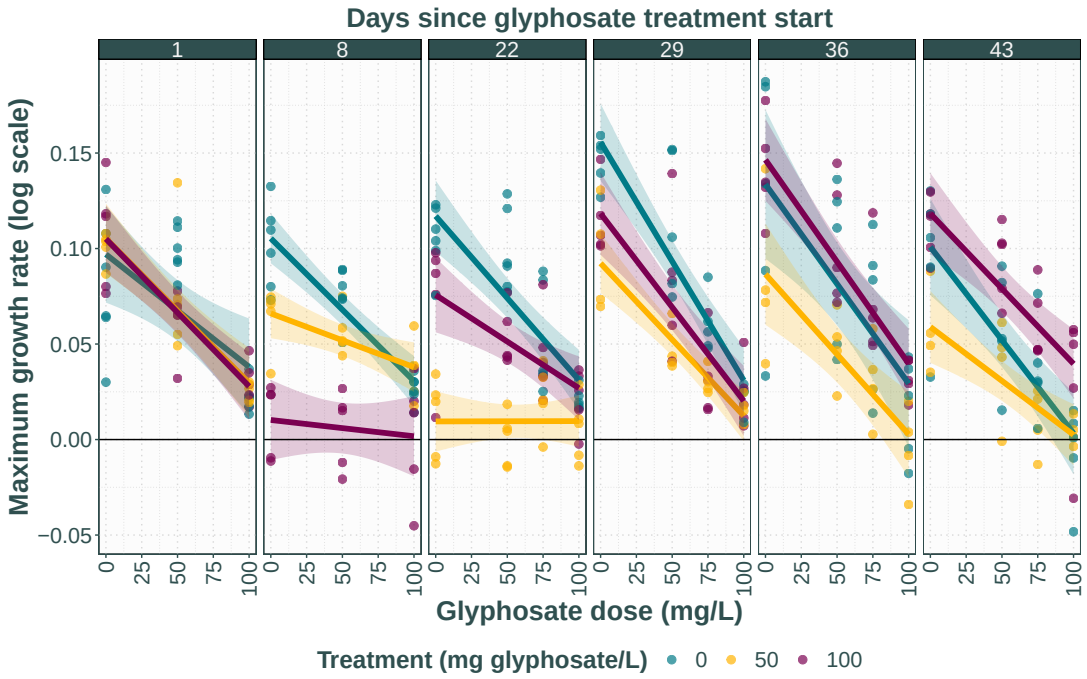

Figure 3.3: Maximum log growth rate in control medium and range of glyphosate doses for each growth assay. Each point is the average growth rate of a chamber, with lines and 95% confidence intervals representing the average for each treatment group.

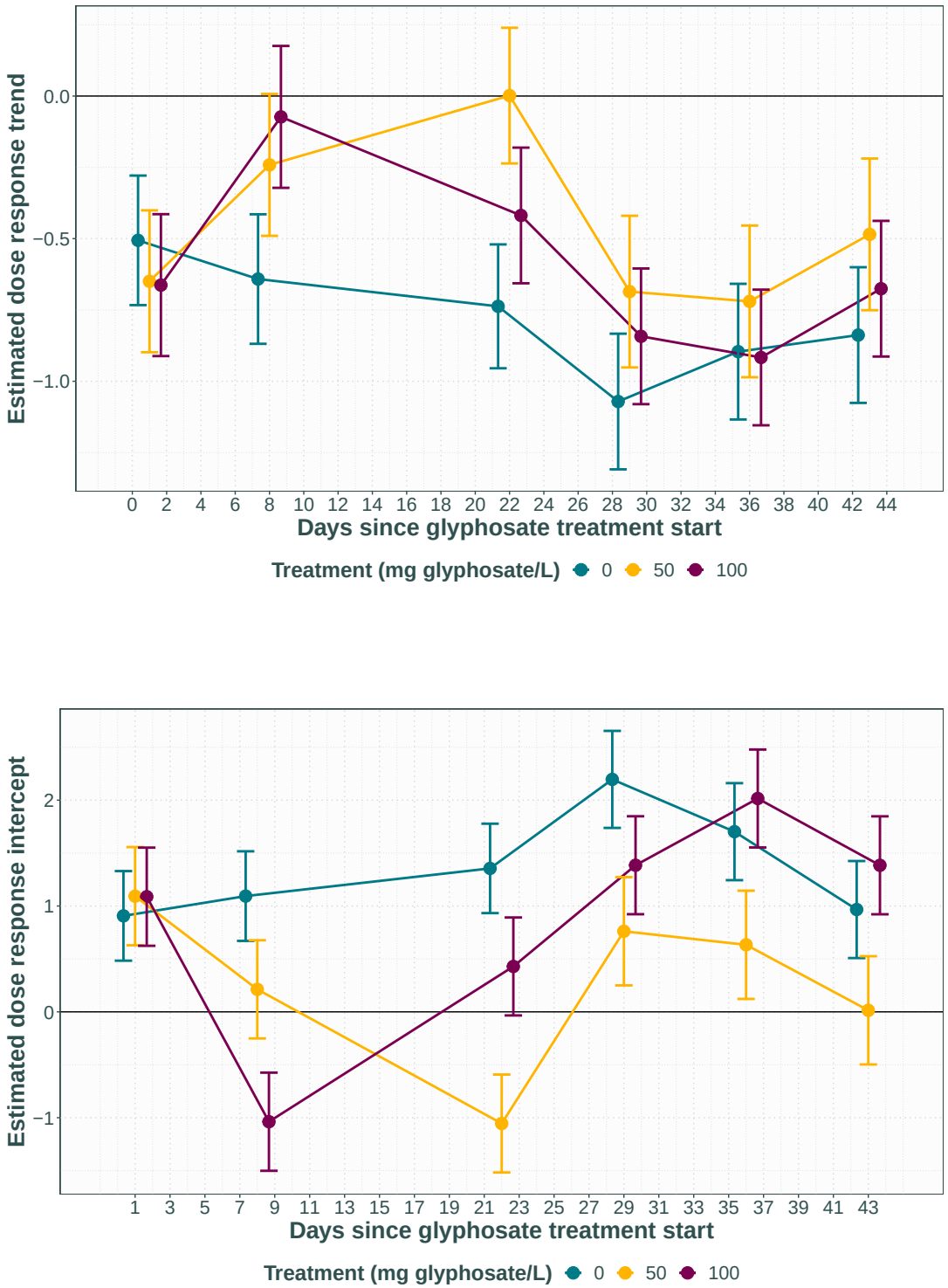

Figure 3.4: Dose response trend (top) and intercepts (bottom) with 95% CI through time as estimated by linear mixed effects model.

Table 3.1: Within-day pairwise contrasts of linear mixed effects model fixed effect term slopes and intercepts.

Contrast		**Slope**			**Intercept**		
Day	*Treatments*	*df*	*t-ratio*	*p-value*	*df*	*t-ratio*	*p-value*
1	0 - 50	279.1	0.8	> 0.9	158.4	-0.6	> 0.9
	0 - 100	279.1	0.9	> 0.9	158.4	-0.6	> 0.9
	50 - 100	279.1	0.08	> 0.9	158.4	0.06	> 0.9
8	0 - 50	279.1	-2.3	0.7	158.4	2.7	0.4
	0 - 100	279.1	-3.3	0.09	158.4	6.7	< 0.001
	50 - 100	279.1	-0.9	> 0.9	158.4	3.7	0.03
22	0 - 50	279.1	-4.5	0.001	157.5	7.5	< 0.001
	0 - 100	279.1	-1.9	0.9	157.5	2.9	0.3
	50 - 100	279.1	2.4	0.6	157.5	-4.4	0.002
29	0 - 50	279.1	-2.1	0.8	185.0	4.1	0.007
	0 - 100	279.1	-1.3	> 0.9	169.3	2.4	0.6
	50 - 100	279.1	0.9	> 0.9	173.5	-1.8	> 0.9
36	0 - 50	279.1	-1.0	> 0.9	185.0	3.1	0.2
	0 - 100	279.1	0.1	> 0.9	169.3	-0.9	> 0.9
	50 - 100	279.1	1.1	> 0.9	173.5	-3.9	0.01
43	0 - 50	279.1	-1.9	0.9	185.0	2.7	0.4
	0 - 100	279.1	-0.9	> 0.9	169.3	-1.3	> 0.9
	50 - 100	279.1	1.0	> 0.9	173.5	-3.9	0.02

3.4.3 GLYPHOSATE TREATED POPULATIONS SHOW DECREASED INITIAL ASSAY PERFORMANCE IN ALL DOSES

After comparable performance for all treatments right after the introduction of glyphosate, all glyphosate treated populations show a decrease in overall growth rate compared to the controls in the growth assays performed at 8 and 22 days post-glyphosate introduction (Figure 3.4, Table 3.1). Concurrent with the population decline apparent in the population density for the lethal treatment, the slopes flatten and the intercepts decrease, reflecting decreased performance in all doses of glyphosate tested. This is followed by the slopes and intercepts returning to the same levels as those of the controls. Notably, while no evidence was found for a population density decline in the sublethal treatment populations, they exhibit the same slope and intercept patterns as the lethal populations, albeit lagging by roughly two weeks.

3.5 DISCUSSION

To manage resistance to economically vital herbicides like glyphosate, we need to understand the underlying evolutionary dynamics. Model organisms such as green alga *C. reinhardtii* provide the opportunity to test the evolutionary theory under controlled lab conditions with huge population sizes and fast generation times, giving insight both to weed science and evolutionary biology (Baucom, 2019; Reboud *et al.*, 2007). We here for the first time use chemostat cultures to evolve glyphosate resistance in *C. reinhardtii* to both a lethal and sublethal dose and monitor the effects on population density, resistance level and growth in the ancestral environment throughout the course of resistance evolution.

3.5.1 EVIDENCE FOR RAPID RESISTANCE EVOLUTION

The population density data shows rapid evolution of resistance to glyphosate in populations experiencing a lethal dose, with the inflection point between the mortality phase and the recovery phase reflecting the point at which resistance becomes dominant appearing in the population as early as 19 days after the treatment was initiated. This is somewhat faster than the average pace of adaptation of 3.5 weeks for this system found in other studies (Lagator *et al.*, 2013a; Melero-Jiménez *et al.*, 2021), likely owing to the larger population sizes and lack of evolutionary bottlenecks.

By contrast, the dose response relationship by the end of the experiment for this treatment line does not indicate a shift in the MIC as it is not significantly different from the control treatment. Instead we see a marked decrease in growth rate at all glyphosate doses as well as in the absence of glyphosate coinciding with the morbidity phase, followed by a recovery. This is likely due to the populations comprising multiple, co-existing genetic lineages with different adaptive strategies, a consistent finding in evolution experiments using chemostats (Gresham & Hong, 2014; Maharjan *et al.*, 2012). This population structure is largely attributed to soft selective sweeps and proportion fluctuations being more common than hard sweeps to fixation of any allele (Gresham & Hong, 2014). As such, when measuring overall population performance, as opposed to isolating and testing labelled clones, the result is an average of those genetic lineages, and the performance of individual lineages is obscured. A new, fitter genotype will only have a noticeable signal in the assays once it has reached a larger proportion of the population. Thus, there is likely to be a lag between the emergence of a new lineage and its detectability in the growth assays as performed here, and the coexistence of less fit lineages means the true fitness of any new mutation is likely to be underestimated. Furthermore, cells that are growth-inhibited by the glyphosate will remain in the population until they die or are flushed out, and these cells will lower the average population performance in the assays. A considerable proportion of the population being growth-inhibited at the beginning of the experiment may be why the treated lineages perform poorly in the growth assays, while growth is indeed detectable in the population density measurements.

The sublethal glyphosate dose treatment appears to have a negligible effect on population density, likely due to the dilution rate allowing a moderate reduction in growth rate without resulting in over-dilution or the model lacking the statistical power to pick up subtler effects. While there is no evidence for a shifted MIC in the growth assays, the decrease in performance with a subsequent recovery suggests the populations have evolved. This pattern lags behind that of the lethal dose by roughly two weeks, consistent with the sublethal dose constituting a weaker selective pressure providing an alternate path to resistance through accumulation of minor gene traits to result in moderate resistance (Busi *et al.*, 2013; Neve & Powles, 2005).

3.5.2 IMPLICATIONS FOR INTRINSIC COSTS AND THE RESISTANCE MECHANISM

For a reduction in growth rate in the ancestral environment to represent the signal of a likely trade-off with glyphosate resistance, it should be observed in conjunction with increased resistance. While the evolution of increased resistance to the lethal dose treatment as evidenced by the population density data must necessarily reflect a shift of the MIC, the fact that the dose response trends show such a strong signal of the growth-inhibited portion of the population makes it difficult to draw conclusions about any associated fitness costs. However, the fact that the estimated intercept for the lethal treatment populations is not significantly different from the control populations by the last assay suggests that the fitness cost of resistance in the ancestral environment is either small or non-existent. This is also the case for the sublethal dose populations as their evolution of resistance is only inferred by exhibiting a similar pattern in the growth assays. As two of the previous studies examining the fitness costs of glyphosate resistance in *C. reinhardtii* found

evidence of a minor (Lagator *et al.*, 2013a) and major (Melero-Jiménez *et al.*, 2021) growth rate reduction in the ancestral environment associated with evolved resistance, and the third found a positive correlation between resistance level and fitness (Vogwill *et al.*, 2012), our results suggest that fitness costs are not universal in this system and that the resistance trait in all studies to date may be conferred by different molecular mechanisms.

Given the growth-inhibiting action of glyphosate, the resistance mechanism for the lethal dose populations is likely initially based on standing genetic variation rather than *de novo*-mutations. While mutations may have accumulated subsequently to improve resistance, the short time frame of the experiment limits the likelihood of polygenic resistance mechanisms. Furthermore, sequential point mutation genotypes changing the structure of EPSPS tend to render it highly insensitive to glyphosate and confer very high resistance (García *et al.*, 2019; Mendes *et al.*, 2020; Perotti *et al.*, 2019; Yu *et al.*, 2015), meaning we would then have expected to see a reduction in death rate, if not evidence of growth, at the very high doses of glyphosate tested in the death assays. A single substitution causing a structural change to EPSPS may instead cause a moderate resistance increase at variable cost depending on species (Beres *et al.*, 2020; Fonseca *et al.*, 2020; Healy-Fried *et al.*, 2007; Kaundun *et al.*, 2008; Li *et al.*, 2018). Incidences of these genotypes are expected to be rarely occurring as part of standing genetic variation as the structure of EPSPS is highly conserved, although they may arise quickly under strong directional selective pressure (Powles & Yu, 2010). An amplification of EPSPS (Baerson *et al.*, 2002; Patterson *et al.*, 2018), however, may possibly be present already in a large population (Powles & Yu, 2010), while conferring moderate resistance (Gaines *et al.*, 2016) to no detectable resistance cost (Vila-Aiub *et al.*, 2014). Similarly, resistance mechanisms affecting other parts of the cellular machinery to reduce the dose reaching EPSPS such as increased vacuolar sequestration (Ge *et al.*, 2011; Pedersen *et al.*, 2007; Preston & Wakelin, 2008; Vila-Aiub *et al.*, 2013) or glyphosate degradation (Pan *et al.*, 2019) could theoretically have evolved in only a few generations, resulting in a medium level of resistance without obvious intrinsic fitness consequences (Powles & Yu, 2010).

While the lethal and sublethal dose treatments appear to be following the same growth assay pattern, the respective treatments are likely selecting for different fitness optima and may thus be selecting for different resistance mechanisms. Most cases of herbicide resistant weeds documented in the field exhibit major single gene mechanisms of resistance, due to high herbicide doses only selecting for sufficiently high resistance mutations (Powles & Yu, 2010). Lower doses instead select for a range of mutations conferring a greater variety in level of resistance, and previous studies indicate that sublethal doses may favour accumulation of minor resistance traits as well as polygenic traits (Busi *et al.*, 2013; Neve & Powles, 2005; Norsworthy *et al.*, 2021). However, it has also been suggested that the chronic stress of low herbicide doses might lead to increased mutation rates, and thus increase generation of large impact mutations (Gressel, 2009, 2011; Love & Wagner, 2022).

3.5.3 BROADER IMPLICATIONS AND FUTURE RESEARCH

While this experiment covers only the initial dynamics of glyphosate resistance evolution in *C. reinhardtii*, these early stages are likely to determine the later outcome of the process (Neve *et al.*, 2009) and the application of chemostats to the chosen system allowed tight control of the specific selective pressures (Gresham & Hong, 2014) as well as monitoring the dynamics through time. These results also add to the increasing number of studies emphasising the potential *C. reinhardtii*, along with other algae, have for a rapid evolutionary response to herbicides, demonstrating their usefulness as a link between weed science and evolutionary biology (Lagator *et al.*, 2013a,b; Melero-Jiménez *et al.*, 2021; Vogwill *et al.*, 2012).

The results reported here also have direct implications for wild *C. reinhardtii* and other algae as agricultural runoff has led to glyphosate being a widely occurring pollutant of non-target ecosystems (Van Bruggen *et al.*, 2018). As the dose reaching non-target ecosystems will vary, the indication that a sublethal dose at half the MIC may still lead to relatively rapid resistance evolution is of

particular interest. Further investigation of the effects of even lower doses could determine how dose affects both the pace of evolution and the particular resistance trait selected for, both which may determine the overall outcome for the ecosystem (Annett *et al.*, 2014; Fugère *et al.*, 2020).

Future research should also investigate the evolutionary dynamics of longer term effects of glyphosate exposure as further adaptation and refinement of the resistance mechanism is likely. Increased replication would also allow for refining the hGAM to add in more terms to explain variation, e.g. to control for perturbations to the steady state caused by sampling events, thus creating a more sensitive model able to detect subtler effects of lower doses of glyphosate. Furthermore, isolation of the genotypes present in the evolving populations along with competition assays would allow detailed characterisation of the resistance level and associated fitness costs, whereas -omics analyses could reveal whether sublethal and lethal doses select for different resistance mechanisms or merely provide different paths to the same goal.

CHAPTER 4

Evidence for a trade-off between glyphosate resistance and anti-grazer defence in green alga *Chlamydomonas reinhardtii*

4.1 ABSTRACT

The widespread and persistent use of herbicides has selected for dramatically increased levels of herbicide resistance in the weed populations they were designed to control. Experimental evolution using microbes offers the opportunity to explore basic evolutionary theory, including testing for the existence of intrinsic and extrinsic fitness trade-offs, and connect them to the patterns observed in both natural and agricultural populations. We here use green alga *Chlamydomonas reinhardtii* adapted to high and moderate levels of glyphosate to test for an extrinsic cost to glyphosate resistance in the form of a trade-off with clumping, the inducible anti-grazer defence deployed against gape-limited micrograzers. Through exposing the algae to freshwater rotifer *Brachionus calyciflorus* as well as their isolated info-chemicals, we test whether glyphosate resistance affects ability to deploy defences as well as ability to withstand grazing compared to control populations. Our results find an increase in variation rather than uni-directional effect of glyphosate treatment, with treated populations exhibiting both lower and higher degree of anti-grazer defence compared to controls. Furthermore, our data suggests there are at least three different glyphosate resistant phenotypes present, with two conferring different extrinsic costs in the form of trade-off with anti-grazer defence.

4.2 INTRODUCTION

Herbicides are used worldwide to protect crops by controlling weed populations. However, this widespread and persistent use also constitutes a strong selective pressure for weeds to evolve resistance to herbicides, and herbicide resistant weeds is an increasingly costly problem, both economically and ecologically (Gaines *et al.*, 2020; Powles & Yu, 2010). As this is an evolutionary process, emphasis has been placed on the necessity of evolutionary thinking, not only in trying to characterise the problem but in trying to manage it (Neve *et al.*, 2009, 2014).

Classic evolutionary theory states that increased fitness in a new environment should trade off with fitness in the original environment, a cost of adaptation based on negative pleiotropic effects of the alleles involved (Purrington, 2000; Vila-Aiub *et al.*, 2009b). Characterising fitness costs is not only important for understanding the resistance trait and its mechanism, but to understand how they constrain adaptation by maintaining polymorphisms or preventing fixation of new alleles (Futuyma & Moreno, 1988; Futuyma, 2009; Rainey *et al.*, 2000). This will affect the outcome of any attempt to manage herbicide resistance evolution as well as allow answering wider questions about plant adaptation (Baucom, 2019). Fitness costs may be intrinsic — to do with processes within the organism, or extrinsic — arising primarily through the exposure to external stressors. Intrinsic mechanisms include diverted energy allocation from growth and reproduction to the new trait (Purrington, 2000; Vila-Aiub *et al.*, 2009b), or involve disruption of normal cell function (Eschenburg *et al.*, 2002; Fonseca *et al.*, 2020; Funke *et al.*, 2009; Healy-Fried *et al.*, 2007).

By contrast, extrinsic fitness costs only become apparent in certain environments, either due to resource allocation costs affecting stress tolerance or interference with specific molecular processes (Reznick *et al.*, 2000; Strauss *et al.*, 2002). This could be reduced performance in extreme conditions, like cold temperatures (Ge *et al.*, 2011; Vila-Aiub *et al.*, 2013), or by changing vital ecological interactions such as competition (Pedersen *et al.*, 2007), disease response (Salzmann *et al.*, 2008) or anti-herbivore defence (Gassmann & Futuyma, 2004; Gassmann, 2005).

Here we use green alga *Chlamydomonas reinhardtii* populations adapted to lethal and sublethal concentrations of growth-inhibiting herbicide glyphosate to test for the existence of an extrinsic cost to glyphosate resistance in the form of a trade-off with deployment of anti-grazing defences. Experimental evolution using microbes offers an opportunity to explore basic evolutionary ideas and connect them to the patterns observed in both natural and managed populations (Barrick & Lenski, 2013; Elena & Lenski, 2003; Good *et al.*, 2017; Kawecki *et al.*, 2012; Lang & Desai, 2014; Van den Bergh *et al.*, 2018). With its short generation time, small size and sensitivity to multiple commonly used herbicides (Reboud *et al.*, 2007), *C. reinhardtii* has already been used to study herbicide resistance evolution (Lagator *et al.*, 2013a,b; Reboud *et al.*, 2007; Reboud, 2002; Vogwill *et al.*, 2012) and molecular analysis of herbicide resistance mutations (Erickson *et al.*, 1984, 1989; Randolph-Anderson *et al.*, 1998).

C. reinhardtii has a well-studied and easily identifiable form of inducible anti-grazer defence, clump formation which limits ingestion by grazers (de Carpentier *et al.*, 2019; Harris *et al.*, 1989; Lürling & Beekman, 2006). *C. reinhardtii* forms clumps through two processes: palmelloid colony formation and flocculation (de Carpentier *et al.*, 2019; Harris *et al.*, 1989; Lürling & Beekman, 2006). Palmelloid colonies consist of between 4–16 non-motile cells sharing a cell wall (Harris *et al.*, 1989; Lürling & Beekman, 2006; Nakamura *et al.*, 1978), indicating that they are formed through a modified form of mitosis where the daughter cells do not fully hatch from the walls of the mother cell rather than aggregation by formerly motile, independent cells. Palmelloid formation has been found in response to abiotic (Iwasa & Murakami, 1968; Khona *et al.*, 2016; Olsen *et al.*, 1983) and biotic stressors, including gape-limited micrograzing zooplankton like rotifers and cladocerans (Lürling & Beekman, 2006). Furthermore, when the triggering stress disappears, the cells disassociate rapidly (Khona *et al.*, 2016). Similar clumping strategies having been documented in other green algae such as *Scenedesmus* (Hessen & Van Donk, 1993; Lürling & Van Donk, 1996, 1997) and *Chlorella* (Boraas *et al.*, 1998; Fisher *et al.*, 2016) suggests it might be a conserved trait (de Carpentier *et al.*, 2019; Pančić & Kiørboe, 2018). Flocculation refers to a larger structure comprising up to thousands of cells, held together by an extra-cellular mucous matrix (Fan *et al.*, 2017; Goff *et al.*, 2013; Lürling & Beekman, 2006; Sathe & Durand, 2016; Visviki & Santikul, 2000). Flocculations of previously free-swimming cells have been observed in response to grazing protist *Peranema* (Sathe & Durand, 2016), but flocculation in response to grazing rotifers appears to require active growth as they only form in the presence of light, suggesting a separate formation strategy involving mitosis (Lürling & Beekman, 2006). The exact genetic mechanism underlying clumping in *C. reinhardtii* is unknown, involving up- and down-regulated transcription of several genes, although the exact genes may differ depending on the exact ecological context (Becks *et al.*, 2012).

In addition to serving as a model for connecting theory and management strategies, the effects of herbicide resistance evolution in algae on their stress responses and anti-grazer defences has real world impact: algal populations worldwide are still affected when herbicide contamination reaches non-target ecosystems through agricultural run-off (reviewed in Van Bruggen *et al.*, 2018). While a few studies have looked at the short term effects of the combined stress of herbicides and predation (Fischer *et al.*, 2012), it is necessary to consider the impact of adaptation to either stressor to assess the full impact of herbicide contamination of aquatic ecosystems (Baselga-Cervera *et al.*, 2016).

In the present experiment we compare the degree of clumping in response to freshwater rotifer *Brachionus calyciflorus* kairomones between glyphosate-adapted and naive strains *C. reinhardtii*, hypothesising that a trade-off between glyphosate resistance and anti-grazer defences should present as decreased clumping compared to the naive strain. Furthermore, we test whether the clear-

ance rate of live rotifers is affected by which strain they are feeding on to evaluate whether any differences in ability to clump translate to an effect on ability to defend against the actual grazers.

4.3 METHODS

4.3.1 ALGAL STRAIN AND CULTURE CONDITIONS

16 *Chlamydomonas reinhardtii* strain Sager's CC-1690 wild-type 21 populations were cultured in a continuous flow through chemostats ("mesostats", see chapter 2 or Hansson *et al.*, 2022, for detailed description of setup) in sterile Ebert algal medium (Ebert, 2013) at a dilution rate of 0.15/24h with a shared multichannel peristaltic pump (Watson-Marlow 205S/CA16). Cultures were maintained at a volume of 380ml±5%. The cultures were kept on a light box providing white light from below and surrounded on all sides with white light fluorescent bulbs giving a light level of 75 µmol m^{-2} s^{-1} 24h a day. The internal temperature of the cultures was 30°C, heated by the light box and the controlled temperature room they were kept in, and they were continuously mixed by bubbling.

4.3.1.1 HERBICIDE TREATMENT AND EVOLUTION OF HERBICIDE RESISTANCE

The *C. reinhardtii* populations were allowed to reach steady state in control medium free from glyphosate to ensure equal and high starting population sizes of approximately 250 000 cells/ml before glyphosate treatments were introduced 14 days after initial inoculation. 10 out of the 16 culture chambers were exposed to treatment consisting of glyphosate (PESTANAL®, analytical standard) at 100 mg/L (lethal) and 50 mg/L (sublethal) respectively, with five chambers receiving each dose. Glyphosate inhibits growth through blockage of the shikimate pathway (Steinrücken & Amrhein, 1980) and 100 mg/L glyphosate completely inhibits population growth, whereas 50 mg/L glyphosate results in a population growth reduction in batch culture. The remaining 6 chambers continued to receive the control medium free from herbicides.

The full experimental design as well as analysis of the effects of the glyphosate treatment on population density and growth rate are presented in chapter 3 of this thesis. Briefly, population densities for each replicate were monitored using flow cytometry (Beckman Coulter CytoFLEX). As glyphosate inhibits growth, resistance to glyphosate was defined as a continuous decline in population density followed by a recovery to steady state (Figure 4.1). CytExpert (Beckman Coulter) was used to gate and count events detected in the PerCP-A channel (Excitation: 488nm, Emission: 690/50 BP) to determine population density. R (version 4.0.5, R Core Team, 2021) was used along with package `mgcv` (Wood, 2011) to construct a hierarchical generalised additive model (hGAM) with the day-to-day growth rate for each population as the response. While the pattern associated with resistance evolution could be detected in the lethal dose populations, the model resulted in a flat fit for the sub-lethal populations comparable to the control populations. However, growth assays performed throughout the course of the treatment detected a signal of evolving resistance in the sublethal populations similar to the lethal populations at a two week delay.

Samples for clumping and feeding assays were obtained 36 days after introduction of the glyphosate treatment, when all populations in both treatment groups were at steady state and roughly 17 days after the first evidence of glyphosate resistance in the lethal treatment populations (Figure 4.1).

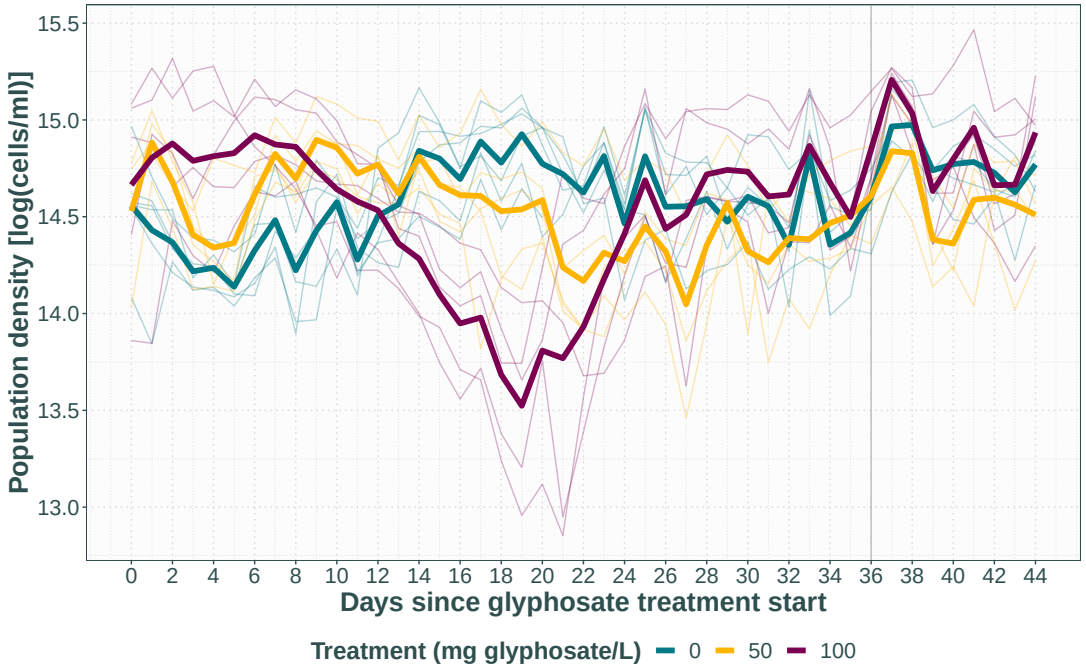

Figure 4.1: Data from chapter 3. Average population density for each replicate population is shown in transparent thin lines, averages for each treatment are shown in thick opaque lines. The grey line at day 36 represents when samples for clumping and feeding assays were extracted.

4.3.2 ROTIFER CULTURES AND ROTIFER WATER PREPARATION

Freshwater rotifer *Brachionus calyciflorus* resting eggs were obtained from Florida Aqua Farms, Inc. The rotifers were kept under standardised stock conditions in jars of 400 ml hard artificial pond water ("ASTM", ASTM, 1989), with 24h 75 µmol m^{-2} s^{-1} warm, white light from above and below at a temperarature of 25°C. They were fed 50 µl of *Nannochloropsis* paste (Seahorsebreeder) every 24 hours.

Experimentally triggering a clumping response requires water that has had rotifers in it. This long established method works because metabolites from the rotifer grazers represent kairomone signals of risk to the algae from the grazers (Lürling & Van Donk, 1997). Rotifer water ("RW") was prepared from the water of a 14 days old population where the population density averaged 100 rotifers/ml the 5 days before water collection and filtered using a vacuum pump through 0.2 micron filters to prevent introduction of algae or bacteria from the rotifer culture (Lürling & Van Donk, 1997). The water was then serially diluted with ASTM water to the desired concentrations and stored frozen for a month before the experiment.

4.3.3 DETERMINING THE EFFECT OF GLYPHOSATE RESISTANCE ON CLUMP FORMATION

The ability of *C. reinhardtii* cells from each treatment line to form clumps was tested in response to *B. calyciflorus* kairomones but in the absence of live rotifers. Four replicates of 7500 algal cells

from each *C. reinhardtii* mesostat population were washed with ASTM water and placed in RW corresponding to a density of 100, 50 or 25 rotifers/ml or ASTM water for controls. We measured clumping using confluence as a proxy with a plate reader (Tecan Spark 10M Multimode Microplate Reader) at 96 hours after inoculation. Confluence is a measure of surface cover and the number of gaps within and between cover in the well, and a higher degree of cell aggregation as well as larger cells should result in more coverage with fewer gaps and thus higher confluence. Pilot data using microscopy and flow cytometry indicate a strong prositive relationship between confluence and clumping (ME Sorensen, pers. comm., April 2018). The populations were kept next to the mesostat populations to ensure as similar conditions as possible, in 30°C with 24h light provided by the light box and white light fluorescent bulbs at 75 µmol m^{-2} s^{-1}.

4.3.3.1 STATISTICAL ANALYSIS OF CONFLUENCE DATA

All data were analysed using R (version 4.0.5, R Core Team, 2021). The effect of glyphosate treatment line and rotifer concentration as well as their interaction on confluence was analysed with linear mixed-effects models using the `lme4` package (Bates *et al.*, 2015), with population chamber fit as a random effect with a varying intercept. The Anova() function from the `car` package (Fox & Weisberg, 2019) was used to test the significance of the fixed and random effects and confirmed through parametric bootstrapping using the `pbkrtest` package (Halekoh & Højsgaard, 2014). The `emmeans` package (Lenth, 2022) was used to do pairwise comparisons of the means estimated from the mixed-effects model and effect sizes were estimated using the `effectsize` package (Ben-Shachar *et al.*, 2020).

4.3.4 FEEDING ASSAYS

Feeding assays were carried out to establish whether the ability of *C. reinhardtii* to withstand grazing by live *B. calyciflorus* was affected by glyphosate treatment. Three replicates of 2×10^5 cells from each *C. reinhardtii* mesostat population were washed with and suspended in 5 ml of hard ASTM water with 40 adult pregnant *B. calyciflorus* females as well as three control replicates with no rotifers. The populations were monitored at 0, 24, 48 and 72h to ensure live rotifers were still present and 400µl of the population was removed so cell density could be characterised through flow cytometry (Beckman Coulter CytoFLEX).

4.3.4.1 STATISTICAL ANALYSIS OF FEEDING ASSAY DATA

All data were analysed using R (version 4.0.5, R Core Team, 2021). R packages `flowCore` and `ggcyto` (Ellis *et al.*, 2020) were used to gate and count events detected in the PerCP-A channel (Excitation: 488nm, Emission: 690/50 BP) to determine population density. These counts were validated against manual haemocytometer counts.

Rotifer clearance rate between the 0 and 72 hour timepoints was calculated according to Equation 4.1.

$$CR = log[(Y_{\mathrm{t}} - Y_{\mathrm{t\text{-}1}})/\Delta t] - log[(N_{\mathrm{t}} - N_{\mathrm{t\text{-}1}})/\Delta t] \tag{4.1}$$

where CR denotes clearance rate, N is the population density at a given timepoint and the preceding timepoint in the absence of rotifers, Y is the population density at a given timepoint and the preceding timepoint in the presence of rotifers, and Δt is the time elapsed between measurements.

The effect of *C. reinhardtii* glyphosate treatment line on rotifer clearance rate using the absolute values of clearance rate was analysed using the `lme4` package (Bates *et al.*, 2015), with population

chamber fit as a random effect with a varying intercept. Bartlett's test was used to test the effect of glyphosate treatment line on variation in the clearance rate, with clearance rates square root-transformed to meet the test's normality assumption.

Linear regression was used to test the relationship between the mean confluence for each population at the maximum RW concentration and the clearance rate for rotifers feeding on the cells, aiming to confirm that a higher confluence level translated to an effective defence and thus lower clearance rate.

4.4 RESULTS

4.4.1 GLYPHOSATE TREATMENT EFFECT ON CLUMPING RESPONSE VARIES BY POPULATION

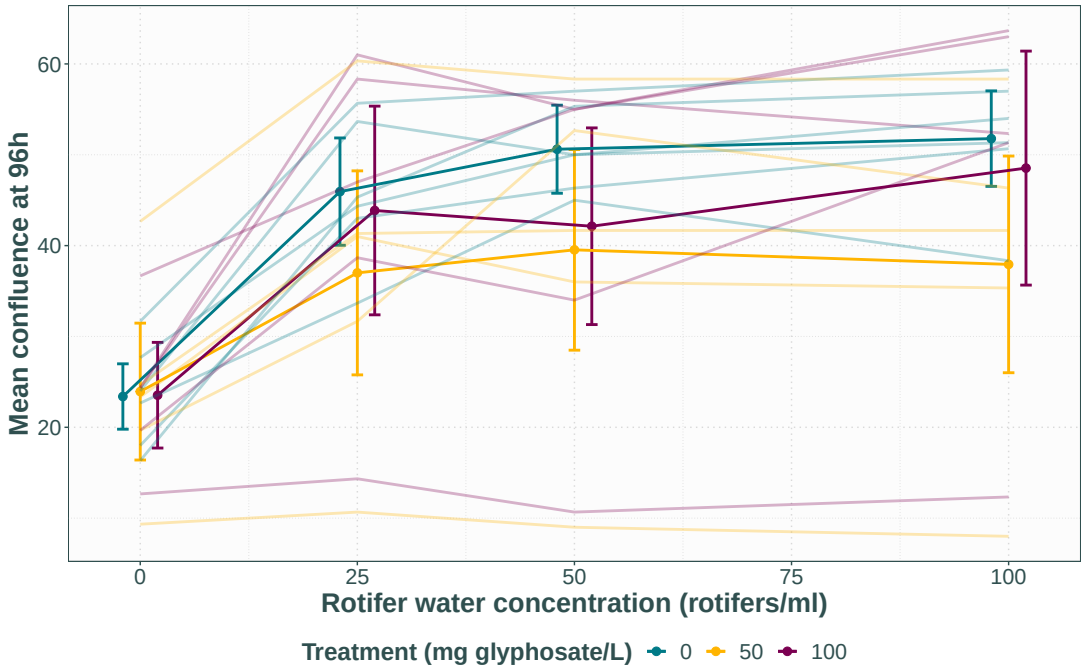

Figure 4.2: Mean confluence after 96 hours for each glyphosate treatment line in response to each rotifer water treatment. Opaque points with 95% CI represent the average for each glyphosate treatment, with transparent lines representing each replicate population.

RW concentration had a strong effect on confluence ($\chi^2 = 131.7$, DF $= 2$, p < 0.001, $\eta^2 = 0.4$), with considerably higher confluence recorded in all treatments containing rotifer kairomones compared to the control RW treatment for all populations but two (Figure 4.2, Table 4.1). Although the interaction between glyphosate treatment and RW concentration was not significant, the pairwise contrasts identified a smaller effect in the glyphosate treated populations (INTERACTION RW*GLYPHOSATE $\chi^2 = 9.9$, DF $= 6$, p $= 0.1$, $\eta^2 = 0.06$, Table 4.1), suggesting that the evolution of glyphosate resistance on average reduces clumping. However, there was no difference between glyphosate impacts within the RW treatment ($\chi^2 = 1.1$, DF $= 2$, p $= 0.6$, $\eta^2 = 0.08$), with pair-

wise comparisons between controls and either herbicide treatment at the highest RW concentration showing no significant effect (Table 4.1).

There was also significant among population variation with population replicate as a random effect had a highly significant effect ($\chi^2 = 98.3$, DF = 1, $p < 0.001$). Two populations, one from the lethal glyphosate treatment and one from the sublethal glyphosate treatment, instead show consistently low levels of confluence both in the presence and absence of rotifers suggesting they are not responding to the rotifer kairomones. Furthermore, the lower levels of confluence for these two populations in the control RW treatment may indicate they also have a reduced growth rate.

Table 4.1: Selected pairwise contrasts of linear mixed-effects model fixed effect term means as estimated by the `emmeans` package for R. RW signifies RW concentration, H signifies glyphosate concentration

Contrast	estimate	SE	df	t-ratio	p-value
RW0H0–RW100H0	-28.4	3.7	167.0	-7.7	< 0.001
RW0meanH50H100–RW100meanH50H100	-19.5	2.9	167.0	-6.8	< 0.001
RW100H0–RW100H50	13.8	8.7	17.9	1.6	0.1
RW100H0–RW100H100	3.2	8.7	17.9	0.4	0.7

4.4.2 GLYPHOSATE TREATMENT EFFECT ON ROTIFER CLEARANCE RATE VARIES BY POPULATION

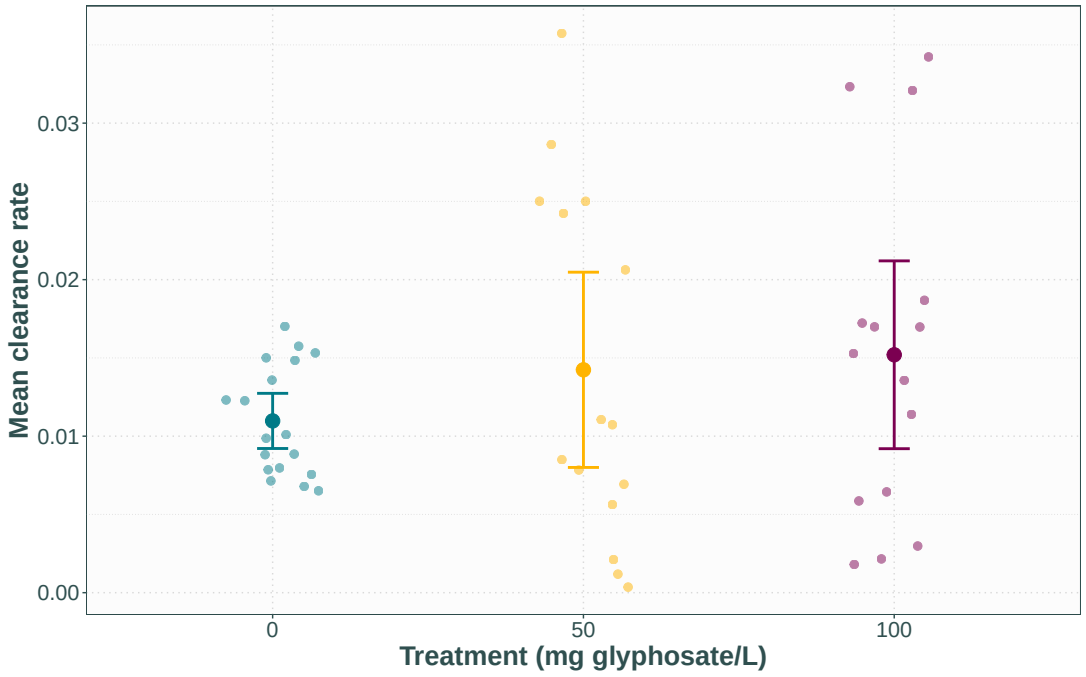

Figure 4.3: Mean clearance rate by *B. calyciflorus* feeding on algae from each glyphosate treatment line. Opaque points with 95% CI represent glyphosate treatment averages, with transparent points representing each assay replicate.

Glyphosate treatment did not have an effect on mean clearance rate ($\chi^2 = 0.6$, DF = 2, $p = 0.7$, $\eta^2 =$

0.05), but it did have an effect on its variance ($K^2 = 18.1$, DF = 2, p-value < 0.001), with increased variance including both higher and lower clearance rates experienced by the glyphosate treated populations compared to the controls (Figure 4.3). Biological replicates from each population cluster together with similar clearance rate levels, and likelihood ratio testing of the random effect found a highly significant effect of population chamber ($\chi^2 = 67.0$, DF = 1, $p < 0.001$), suggesting that the increase in variance is due to each population representing an individual evolutionary trajectory and exhibiting different strategies rather than an increase in noise.

4.4.3 HIGH CONFLUENCE CORRELATES WITH LOW CLEARANCE RATE IN MOST, BUT NOT ALL, POPULATIONS

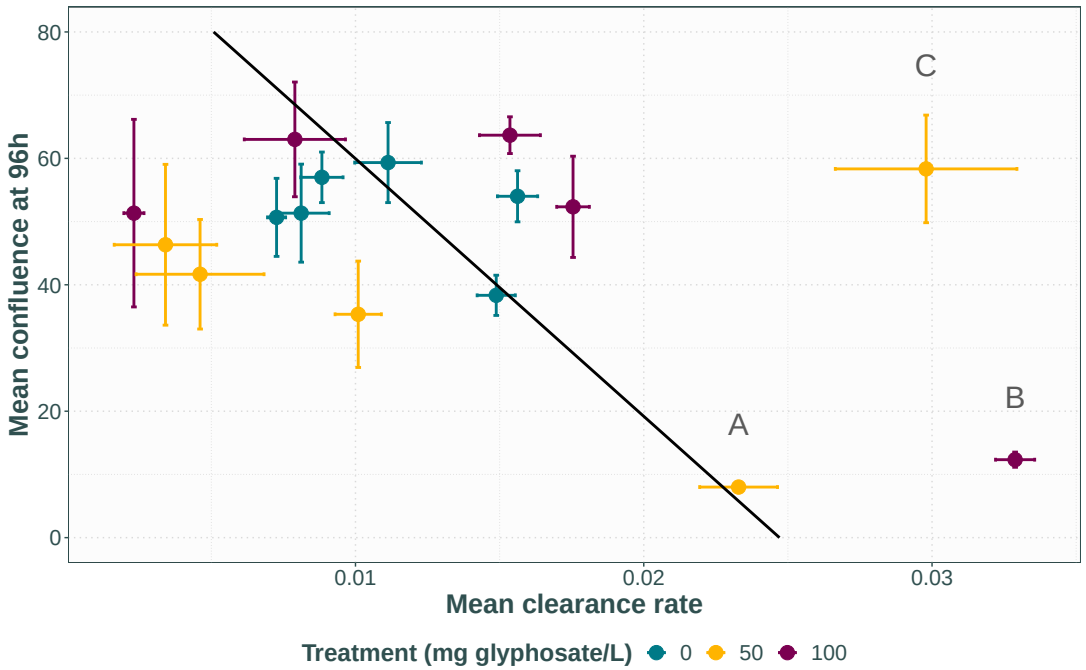

Figure 4.4: Mean confluence at 96h in the highest RW concentration plotted against mean clearance rate by *B. calyciflorus* for each given population with error bars for standard error. Regression line in black with equation $y = 0.0247092 - 0.0002454x$. Three outlier populations of interest have been labelled with letters.

There was a marginally significant but large effect of confluence on clearance rate ($F = 3.5$, DF = 1,14, $p = 0.08$, $\eta^2 = 0.2$), with a negative relationship between confluence and clearance rate (Figure 4.4) indicating that in most cases, confluence level indicates an adequate defence against grazing. The two outlier populations with lower confluence levels (A and B) do indeed experience higher clearance rates as expected. However, a third outlier population (C) from the sublethal glyphosate treatment line with similarly high confluence as the controls also experienced a higher clearance rate, suggesting that there is a separate mechanism involved.

4.5 DISCUSSION

To manage herbicide resistance, we need to understand its evolutionary dynamics, including the fitness consequences of resistance in different ecological contexts as costs may be intrinsic — to do with processes within the organism, or extrinsic — arising primarily through the exposure to external stressors. Model organisms such as *C. reinhardtii* provide the opportunity to test the underpinning evolutionary theory under controlled lab conditions with huge population sizes and fast generation times, giving insight both to weed science and evolutionary biology. We here focused on extrinsic costs, by testing the ability of *C. reinhardtii* populations adapted to lethal and sublethal concentrations of glyphosate to deploy anti-grazer defences and withstand grazing by rotifer *B. calyciflorus*.

4.5.1 ADAPTATION TO GLYPHOSATE INCREASES VARIATION IN ABILITY TO DEPLOY ANTI-GRAZER DEFENCE: IMPLICATIONS FOR TRADE-OFF

The effect of glyphosate treatment line on the ability to both clump in response to rotifer kairomones and withstand grazing by live rotifers is not consistent among replicates. Instead evolution under glyphosate exposure increased variation in defence strategies compared to controls. Notably, two populations, one from the lethal glyphosate treatment and one from the sublethal, lost their ability to clump in response to rotifer kairomones, which was associated with an increased clearance rate by live rotifers. The other glyphosate treated populations appeared to generally clump at the same level as the controls, but the associated clearance rates by live rotifers were both lower and, in one case, much higher.

This is consistent with each population representing a separate evolutionary trajectory, with different responses to the glyphosate treatment based on both extent of standing genetic variation and chance. Increased flocculation and wall-adhering phenotypes is a common problem in long-term chemostat populations (Gresham & Hong, 2014; Harris *et al.*, 1989), but the performance of the control populations in both assays is tightly clustered, suggesting that adaptation to the chemostat environment itself has thus far into the experiment not had any effect on the clumping trait in response to grazers. Flocculations were observed in the chamber for one of the sublethal dose populations, but this was not one of the outlier populations, suggesting that any changes in flocculation induction in this population did not carry over to the assays.

From the assays presented here, three distinct patterns have emerged in performance by the glyphosate treated lines: 1) performance comparable to controls, suggesting no trade off between the glyphosate resistance trait and anti-grazer defence, 2) reduced ability to both clump and withstand grazing, indicating a trade-off with glyphosate resistance, and 3) ability to clump comparable to control lines but reduced ability to withstand grazing, indicating a different trade-off with glyphosate resistance. This suggests there are at least three different dominant resistance mechanisms in the populations tested, two of which confer an extrinsic cost.

The glyphosate treated populations will at the time of these assays have been heterogeneous and comprising several coexisting lineages, a typical feature of experimental chemostat populations (Gresham *et al.*, 2008; Hong & Gresham, 2014; Kao & Sherlock, 2008; Kinnersley *et al.*, 2009; Kvitek & Sherlock, 2011; Maharjan *et al.*, 2006, 2012; Wenger *et al.*, 2011), as well as early on in the stages of adapting to glyphosate, having experienced the treatment for only 36 days. While there was evidence for evolved resistance in the lethal glyphosate treatment populations at this point, it was only by inference from patterns common to the lethal and sublethal populations that we could conclude the same for the sublethal populations. Furthermore, there was no conclusive evidence for the level of resistance increase or intrinsic trade-offs for growth for either treatment.

As the assays are testing subsets of a heterogeneous population rather than isolated clones we expect the assay results to be averages of all the phenotypes present, rather than exact reflections of any given novel genotype. We can however expect the underlying genotypes to share a few characteristics, with the the short time frame of adaptation meaning that 1) single substitutions to the target enzyme or up and down regulation of relevant metabolic pathways are more likely than resistance mechanisms dependent on sequential mutations (Gaines *et al.*, 2020; Powles & Yu, 2010), 2) they will still be far away from the fitness optimum (Gresham & Hong, 2014), and 3) changes in performance in these assays is likely to be due to pleiotropy of the glyphosate resistance trait rather than the result of neutral mutation accumulation.

The mechanism for either trade-off cannot be determined conclusively without knowing the mechanism of resistance, but there are a few ways we could expect known costs and mechanisms glyphosate resistance and the known costs and mechanisms of clumping to intersect. Any theoretical resistance mechanism could lead to a general resource allocation cost (Chapin *et al.*, 1993; Coley *et al.*, 1985; Herms & Mattson, 1994; Purrington, 2000; Vila-Aiub *et al.*, 2009a) and in the case of single nucleotide substitutions to the target enzyme, reduced binding affinity for the intended substrates often leads to impaired cell functioning (Eschenburg *et al.*, 2002; Fonseca *et al.*, 2020; Funke *et al.*, 2009; Healy-Fried *et al.*, 2007) affecting resource availability. Similarly, the clumping trait likely confers a cost in reduced nutrient uptake both due to the extra-cellular mucous matrix reducing diffusion of vital nutrients (Becks *et al.*, 2012) and due to larger cell sizes in general being correlated with lowered metabolic activity (Marañón, 2015; Raven & Kubler, 2002), but this is often only observed to confer a cost under nutrient limited conditions (Becks *et al.*, 2012; Pančić & Kiørboe, 2018). Both flocculation and palmelloid formation in *C. reinhardtii* in response to *B. calyciflorus* is linked to cell division (Harris *et al.*, 1989; Lürling & Beekman, 2006), so any negatively pleiotropic effects on growth may also impair clumping ability, resulting in a negative feedback loop where lack of growth impairs clumping and the clumping that does occur further slows down growth. Furthermore, a secondary effect of glyphosate is increased production of reactive oxygen species (ROS), causing lipid peroxidation (Ahsan *et al.*, 2008; de María *et al.*, 2005; Gomes & Juneau, 2016; Maroli *et al.*, 2015; Sergiev *et al.*, 2006), evolved resistance against which could involve membrane lipid composition.

While the relationship between reduced clumping and reduced ability to withstand grazing can be assumed to be straightforward, a genotype being less effective at withstanding grazing while not having a reduced ability to clump in response to the kairomones of those grazers suggests that the clump formation itself is less robust. This could also be due to lacking resources to allocate to production of the adhesive mucus, leading to increased disassociation when disturbed. Alternatively, part of the anti-grazer defence could be unrelated to colony formation and instead to cell wall structure (Hamm *et al.*, 2003; Harvey *et al.*, 2015; Liu *et al.*, 2016; Pondaven *et al.*, 2007; Van Donk *et al.*, 1997), cell hardness (DeMott, 1995) or the mucous envelope surrounding the cell (Porter, 1975) allowing the cells to pass through the rotifer gut without being digested. If instead this is trading off against the glyphosate resistance trait rather than colony formation, we could expect the pattern seen for the third outlier population. This trade-off could also be caused by limits on resource allocation, or perhaps a resistance mechanism like reduced absorption into the cell, although this is a rarely documented resistance mechanism and tends to be accompanied by other mechanisms (Gaines *et al.*, 2020; Nandula *et al.*, 2013). Similarly, changes to the cell wall or cell structure resulting in increased resistance to digestion or changes to the extra-cellular mucus provides a putative mechanism for the populations experiencing a lower clearance rate without an associated increase in clumping.

An alternative explanation is that the three outlier populations have evolved resistance against the shikimate pathway-inhibiting primary effect of glyphosate but not the ROS producing secondary effects and lipid peroxidation (Ahsan *et al.*, 2008; de María *et al.*, 2005; Gomes & Juneau, 2016; Maroli *et al.*, 2015; Sergiev *et al.*, 2006), whereas the other treated populations have evolved to withstand both. This suggests that the stage of resistance evolution may be a strong influence on the ability to respond adequately to additional stressors.

4.5.2 BROADER IMPLICATIONS AND FUTURE RESEARCH

The trade-offs between herbicide resistance and anti-grazer defence has only been the subject of a limited number of studies of a single plant–herbivore–herbicide interaction (*Amaranthus hybridus*–*Disonycha glabrata*–triazine, Gassmann & Futuyma, 2004; Gassmann, 2005), and in general little is known about whether there are generalisable patterns to how these traits affect each other or if it is specific to the interaction or agricultural context. This study indicates that it may also be context dependent, possibly only being present at particular stages in the adaptation process or with particular resistance mechanisms.

The effects particular to the system studied here are however directly relevant to wild aquatic ecosystems as glyphosate contamination from agricultural runoff is an increasing problem (Van Bruggen *et al.*, 2018). If adaptation to glyphosate contamination has the ability to disrupt anti-grazer defences in *C. reinhardtii*, it might have far reaching effects on food webs where it is an important primary producer as selective grazing by gape-limited grazers like *B. calyciflorus* can restructure communities, and may in turn affect the course of adaptation to glyphosate.

This study contributes one piece of the puzzle for the possible trade offs between anti-grazer clumping and glyphosate resistance in *C. reinhardtii*. Future studies should investigate the outcome of adaptation to glyphosate with rotifers present, as well as perform assays in the presence and absence of glyphosate, especially as glyphosate may have a stimulating effect on sexual reproduction in *B. calyciflorus* (Xi & Feng, 2004). As the data presented here represents only one stage throughout the process of adaptation, a longer running study assaying the effects on clumping and anti-grazer defence would be useful to determine later stage effects and whether there is a pattern to where and when a trade-off is or is not seen. Furthermore, microscopy analysis of the aggregates and cells could distinguish whether it is flocculation or palmelloid formation that is primarily affected, and analysis of the extra-cellular mucus could determine whether its composition is affected (Roccuzzo *et al.*, 2020).

CHAPTER 5

Metabolomic profiling of glyphosate resistance evolution in green alga *Chlamydomonas reinhardtii*

5.1 ABSTRACT

The widespread use of glyphosate has led to a rapid increase in glyphosate resistant weeds at a considerable cost to agriculture. Furthermore, agricultural run-off means non-target, natural ecosystems are also being affected. Resistance may arise both through mutations to target enzyme EPSPS in the shikimate pathway that generate insensitivity to glyphosate and through non-target site mutations that regulate the dose of glyphosate reaching the shikimate pathway, and this resistance mechanism may trade-off against normal cell functioning. Here, using experimental evolution of replicated *Chlamydomonas reinhardtii* populations facing glyphosate, we apply untargeted metabolomic screens throughout the course of resistance evolution to reveal the metabolomic fingerprint of both glyphosate action and emerging resistance, as well as testing for the underlying molecular mechanism and potential fitness costs. We find evidence of buildup of shikimate pathway metabolites, a characteristic signal of glyphosate action, that disappears as resistance evolves. Concurrent with this is evidence of cell wide disruption of pathways including amino acid synthesis and glycolysis, that stabilises as resistance evolves. While we could not determine the resistance mechanism, we found evidence of effects of glyphosate on membrane lipids and increased levels of reactive oxygen species persisting after resistance had evolved. This suggests a considerable effect of the recently described secondary effect of glyphosate: oxidative damage. These data highlight the necessity of understanding the full molecular effects of a herbicide to be able to predict its population- and ecosystem-level effects.

5.2 INTRODUCTION

Herbicides are used to control weeds and ensure high levels of crop production. However, the persistent use of herbicides worldwide has constituted a strong selective pressure for the evolution of herbicide resistant weeds, presenting an increasingly costly problem both ecologically and economically (Gaines *et al.*, 2020; Powles & Yu, 2010). As this is an evolutionary process, evolutionary thinking is necessary both to understand and manage it (Neve *et al.*, 2009, 2014). In addition to understanding how the fitness costs and benefits of resistance lead to rapid resistance in populations, it is vital to illuminate the molecular mechanisms that give rise, via mutations, to resistance (Purrington, 2000; Vila-Aiub *et al.*, 2009b).

Glyphosate (*N*-phosphomethyl glycine) is at the time of writing the world's most commonly used herbicide, and the over-reliance on glyphosate in combination with genetically engineered glyphosate resistant crops has resulted in a rapid increase in the number of characterised glyphosate resistant non-crop species as well as unique glyphosate resistance mechanisms (Gaines *et al.*, 2020; Heap, 2022). Glyphosate's mode of action is through blockage of the shikimate pathway, which is responsible for 30% of the carbon flow in plants, algae and bacteria (Maeda & Dudareva, 2012; Steinrücken & Amrhein, 1980). By competitively binding to enzyme 5-enolpyruvulshikimate-3-phosphate (EPSPS) instead of intended substrate phosphoenolpyruvate (PEP), production of the aromatic amino acids phenylalanine (Phe), tyrosine (Tyr) and tryptophan (Trp) as well as

other downstream products of chorismate metabolism is disrupted, leading to arrested growth and eventual death due to suspended cellular function. Furthermore, disruption of photosynthesis and increased production of reactive oxygen species (ROS) are documented secondary effects of glyphosate, leading to reduced growth and performance during benign and stressful conditions (Ahsan *et al.*, 2008; de María *et al.*, 2005; Gomes & Juneau, 2016; Maroli *et al.*, 2015; Sergiev *et al.*, 2006; Servaites *et al.*, 1987).

Single point mutations to EPSPS generally confer low resistance but impair normal enzyme function by lowered affinity for PEP (Eschenburg *et al.*, 2002; Fonseca *et al.*, 2020; Funke *et al.*, 2009; Healy-Fried *et al.*, 2007; Kaundun *et al.*, 2008; Li *et al.*, 2018; Yu *et al.*, 2006). While there are notable exceptions conferring higher resistance in specific species (Beres *et al.*, 2020; Li *et al.*, 2018), including sequential double (Alcántara-de la Cruz *et al.*, 2016; Mendes *et al.*, 2020; Yu *et al.*, 2015) and triple (García *et al.*, 2019; Perotti *et al.*, 2019) mutations that render EPSPS highly insensitive to glyphosate, the fitness consequences for most of these have yet to be tested. EPSPS amplification has been detected both in the form of up-regulated expression (Baerson *et al.*, 2002) and gene multiplication (Gaines *et al.*, 2019; Patterson *et al.*, 2018), and the underlying genetic mechanisms for this appear to be varied (Gaines *et al.*, 2016; Jugulam *et al.*, 2014; Koo *et al.*, 2018; Patterson *et al.*, 2019). Glyphosate resistance has also been found to be conferred through changes elsewhere in the cellular machinery to reduce the dose that reaches the target through reduced absorption (Michitte *et al.*, 2007; Nandula *et al.*, 2013; Vila-Aiub *et al.*, 2012) and increased vacuolar sequestration (Ge *et al.*, 2010, 2011, 2012; Peng *et al.*, 2010; Yuan *et al.*, 2010) have been found to confer glyphosate resistance but the molecular basis for either is unknown. Furthermore, aminomethylphosphonic acid (AMPA), the main metabolic product of glyphosate, has been detected in many higher plants (de Carvalho *et al.*, 2012; Duke, 2011) and has recently been identified in one species to be produced from breakdown of glyphosate by aldo-keto reductase, in contrast to the known glyphosate oxidoreductase pathway found in some bacteria (Pan *et al.*, 2019; Vemanna *et al.*, 2017).

The last two decades have seen a huge increase in the application of multiple -omics methods to characterise herbicide effects on cellular processes, and by extension their associated resistance mechanisms (Duke *et al.*, 2013). Metabolomics provides a snapshot of the cellular state by quantifying the metabolites present at the time of sampling, thereby connecting genotype to phenotype. This allows us to differentiate between genetically programmed and environmentally induced cellular processes, such as stress responses, and observe how they change with time (Fiehn, 2001, 2002; Patti *et al.*, 2012; Sumner *et al.*, 2003). However, most of these studies have focused on comparing resistant to susceptible individuals, missing out on characterising the metabolomic signals of resistance evolution in action. Furthermore, most metabolomic studies target known compounds in pathways expected to be affected based on previous knowledge of the particular herbicide's mode of action, introducing a bias that may mischaracterise the full effects of the herbicide. Untargeted metabolomic fingerprinting is a general approach that measures a wider spectrum to give an as comprehensive as possible profile of the metabolome at a given time. This makes it a powerful hypothesis generating tool for identifying the overall metabolomic effects of a herbicide as well as resistance mechanisms and their fitness costs (Fiehn, 2002; Overy *et al.*, 2005).

Here we evaluate the effects of glyphosate resistance evolution on the metabolome of green alga *Chlamydomonas reinhardtii* through untargeted metabolomic fingerprinting at regular intervals of cells from populations undergoing adaptation to a high dose of glyphosate. Unicellular green algae provide a fruitful model system for experimental evolution as their small size and short generation times allow monitoring and manipulating evolution in huge populations in the lab. With its sensitivity to many commonly used herbicides (Reboud, 2002), *C. reinhardtii* as already been used to study efficacy of resistance management strategies (Lagator *et al.*, 2013a,b), characterising fitness costs (Vogwill *et al.*, 2012), comparisons of evolutionary potential in communities of algae (Melero-Jiménez *et al.*, 2021) and molecular analysis of herbicide resistance mutations (Erickson *et al.*, 1984, 1989; Fedtke, 1991; Galloway & Mets, 1984; Hartnett *et al.*, 1987; James & Lefebvre, 1989; James *et al.*, 1993; Randolph-Anderson *et al.*, 1998). Furthermore, while not the primary target of commercial herbicide application, algal populations worldwide are still affected through agricultural

runoff (reviewed in Van Bruggen *et al.*, 2018) and as such the molecular and metabolomic dynamics underlying their adaptation to herbicides has relevance to natural ecosystems as well.

To capture the fingerprint of glyphosate resistance evolution, associated fitness costs, as well as determine the resistance mechanism, we focus on three targeted hypotheses relating to specific compounds selected *a priori* that are all expected to change in abundance depending on whether resistance has evolved and by what mechanism: shikimate pathway functioning, glyphosate and its breakdown products, and amino acid pool composition (Figure 5.1). Furthermore, we perform further exploratory analysis to identify the largest differences in the data set between glyphosate-treated and control populations to extend the fingerprint beyond the targeted compounds and identify other cellular processes affected by either glyphosate or glyphosate resistance and thus give insight into the resistance mechanism or potential trade-offs.

5.2.1 SHIKIMATE PATHWAY FUNCTIONING: THE RESISTANCE EVOLUTION TIMELINE FINGERPRINT

Firstly, to conclude glyphosate resistance has evolved we must see evidence of glyphosate inhibition of the shikimate pathway followed by a return to pathway functioning, presenting as an initial build-up of upstream pathway metabolites that returns to lower levels as resistance evolves (Figure 5.1A Aristilde *et al.*, 2017; de María *et al.*, 2006; Felline *et al.*, 2019; Kostopoulou *et al.*, 2020; Maroli *et al.*, 2015, 2018; Oikawa *et al.*, 2006; Sikorski *et al.*, 2019; Wang, 2001; Zabalza *et al.*, 2017; Zhong *et al.*, 2018). The post-resistance functioning of the shikimate pathway also gives an indication of the level of resistance as well as potential trade-offs with cell functioning, with upstream metabolite levels remaining elevated post-resistance suggesting glyphosate still has some inhibiting effect (Figure 5.1C) or that the resistance mechanism involves mutated EPSPS that is also less sensitive to its intended substrates (Figure 5.1B).

5.2.2 GLYPHOSATE AND ITS BREAKDOWN PRODUCTS: THE RESISTANCE MECHANISM FINGERPRINTS

Secondly, increased levels of intracellular glyphosate post-resistance is consistent with it being sequestered to the vacuole or that insensitive EPSPS is no longer binding it (Gaines *et al.*, 2020; Ge *et al.*, 2010, 2011, 2012), whereas decreased levels post-resistance could indicate decreased absorption into the cell (Gaines *et al.*, 2020) or possibly amplified EPSPS if the applied glyphosate dose is very high (Figure 5.1B). Presence of known primary breakdown products of glyphosate like AMPA, sarcosine and glyoxylate after resistance has evolved is evidence for it being at least partly conferred by glyphosate catabolism (Barrett & McBride, 2005; Dick & Quinn, 1995; Hove-Jensen *et al.*, 2014; Pizzul *et al.*, 2009), whereas their absence is evidence against (Figure 5.1B). Out of the four known pathways for glyphosate metabolism, those by glyphosate oxireductase and glyphosate oxidase result only in AMPA and glyoxylate by cleavage of the glyphosate C-N bond (Barry & Kishore, 1995; Pipke & Amrhein, 1988). Glyphosate degradation by cleavage of the glyphosate C-P bond by a C-P lyase has several intermediate steps with phosphate and sarcosine being the final product (Hove-Jensen *et al.*, 2014). Similarly, the complete breakdown of AMPA results in phosphate after a number of intermediate metabolites (Hove-Jensen *et al.*, 2014). Glyphosate degradation by aldo-keto reductase results in AMPA and glyoxylate, but is associated with possible breakdown of glyoxylate to glycine and 2-oxoglutarate as well as involvement of cinnamaldehyde and cinnamyl alcohol (Pan *et al.*, 2019). As such, if the primary glyphosate degradation products are detected, changes in the presence of these secondary breakdown products can distinguish between known breakdown pathways.

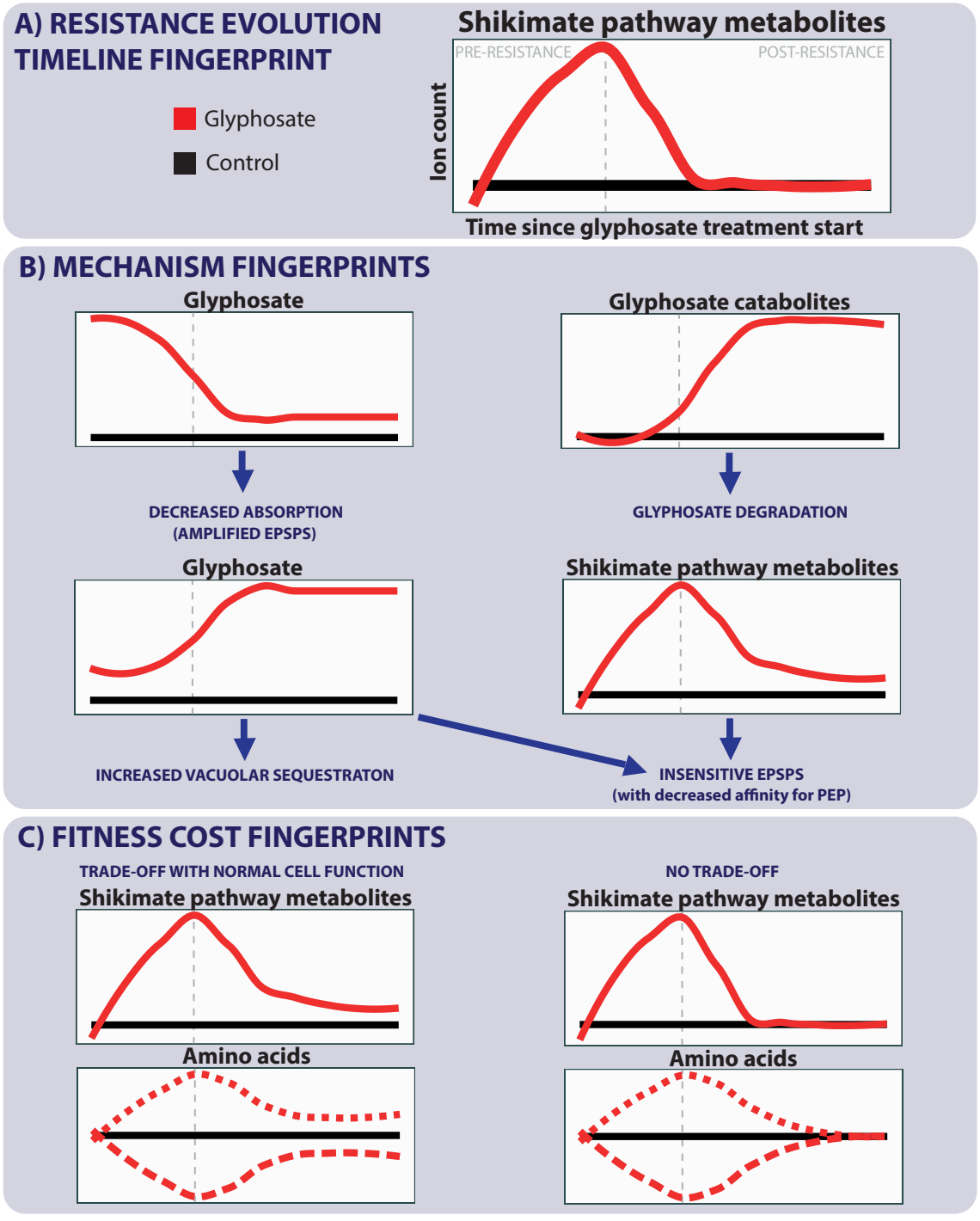

Figure 5.1: Overview of possible fingerprint outcomes for the three targeted hypotheses. All graphs show ion count vs time since glyphosate treatment start with glyphosate-treated line in red and control line in black. The vertical grey dashed line indicates boundary of pre- and post-resistance phase. A) The timeline of glyphosate resistance evolution is based on the shikimate pathway metabolites, the build-up and return to control levels of which define the pre- and post-resistance phases. B) Resistance mechanism fingerprints depend primarily on presence or absence of glyphosate and its catabolites. C) Trade-offs with normal cell function are determined by whether shikimate pathway metabolites and amino acid levels return to control levels or remain elevated after resistance has evolved.

5.2.3 AMINO ACID POOL COMPOSITION: THE FITNESS COST FINGERPRINT

Thirdly, we would expect perturbation of the amino acid pool during glyphosate inhibition, but for this effect to disappear after resistance has evolved (Figure 5.1C). Any remaining effects could be indicative of a trade-off between the resistance mechanism and normal cell function. While changes to the abundance of the aromatic amino acids Phe, Try and Tyr is another direct test of shikimate pathway functioning, the effects on the total amino acid pool and its composition is indicative of wider cell functioning throughout glyphosate resistance evolution as amino acids play multiple, integral roles in cell metabolism, not limited to just protein synthesis but also including signalling, regulation and stress response (Dinkeloo *et al.*, 2018; Fritz *et al.*, 2006; Häusler *et al.*, 2014; Hildebrandt *et al.*, 2015; Kostopoulou *et al.*, 2020; Less & Galili, 2008; Maeda & Dudareva, 2012; Moe, 2013). The effect of glyphosate inhibition on the amino acid pool differs depending on system, with evidence of both overall decreases in abundance reflective of widespread disruption to carbon metabolism (Aristilde *et al.*, 2017; Felline *et al.*, 2019), and overall increases of the pool of free amino acids or increases in specific amino acids (Böttcher *et al.*, 2007; Diaz Vivancos *et al.*, 2011; Kostopoulou *et al.*, 2020; Maroli *et al.*, 2015; Trenkamp *et al.*, 2009; Wang, 2001), suggested to be part of increased catabolism (Kostopoulou *et al.*, 2020) as a stress response or by shifts in production between pathways (Diaz Vivancos *et al.*, 2011).

5.2.4 EXTENDING THE METABOLOMIC FINGERPRINT OF EVOLVING GLYPHOSATE RESISTANCE

Furthermore, we identified other cell machinery changes that may be evidence of costs, trade-offs or other aspects of resistance such as shifting prioritisation between metabolic pathways or mechanisms specifically targeting the secondary effects of glyphosate. This extension of the metabolomic fingerprint of evolving glyphosate resistance used multivariate analyses to determine compounds of interest showing the largest differences between treatments in the data set and classifying when during resistance evolution these differences occurred. Compounds with differences between glyphosate-treated and control populations occurring only pre-resistance, during the glyphosate sensitive phase are likely involved in initial stress response, build up or dearth of certain compounds due to the blocked shikimate pathway as well as compounds related to cellular death and breakdown. Sustained differences in compound presence emerging post-resistance is however likely related to the resistance mechanism, including compounds that are up or down regulated as part of resource allocation for resistance, or may be due to later effects of chronic glyphosate exposure. Differences throughout the course of the experiment from the first application of the treatment suggests the compound is related to glyphosate action rather than resistance, such as a continued stress response to secondary effects.

5.3 METHODS

5.3.1 EXPERIMENTAL DESIGN

5.3.1.1 ALGAL STRAIN AND CHEMOSTAT SETUP

Chlamydomonas reinhardtii strain Sager's CC-1690 wild-type 21 gr was obtained from the *Chlamydomonas* Resource Centre (University of Minnesota, St Paul, MN, USA) core collection. Prior to the experiment, the algae had been kept in static stock cultures for two years (Ebert algal medium,

25°C, 24h light), with batches being transferred to fresh medium fortnightly, then in continuous flow culture for two months under the experiment control conditions detailed below.

Ten *C. reinhardtii* populations were cultured in a continuous flow through chemostats in sterile Ebert algal medium (Ebert, 2013) at a dilution rate of 0.15/24h with a shared multichannel peristaltic pump (Watson-Marlow 205S/CA16) controlling the flow for all culture chambers, maintaining a volume of 380ml±5% (see chapter 2 or Hansson *et al.*, 2022, for detailed protocol). The cultures were kept on a light box providing white light from below and surrounded on all sides with white light fluorescent bulbs giving a light level of 75 µmol m^{-2} s^{-1} 24h a day. The internal temperature of the cultures was 30°C, heated by the light box and the controlled temperature room they were kept in, and they were continuously mixed by bubbling. The *C. reinhardtii* populations were allowed to reach steady state in control medium free from herbicides to ensure equal and high starting population sizes of approximately 250 000 cells/ml before herbicide treatments were introduced 14 days after initial inoculation.

5.3.1.2 HERBICIDE CONCENTRATIONS AND REPLICATION

Five culture chambers were exposed to herbicide treatment consisting of glyphosate (PESTANAL®, analytical standard) at 100 mg/L, a concentration that completely inhibits population growth over seven days in batch cultures (Lagator *et al.*, 2013a,b). Five chambers received the control medium free from herbicides. The glyphosate was initially introduced to each population through a direct injection of 38 ml of sterile Ebert medium containing 38 mg glyphosate. The control chambers received 38 ml of sterile Ebert medium. Immediately before the treatment injection, 38 ml of the existing culture in the chamber was removed (10% of the total culture volume) to ensure the culture volume remained consistent.

5.3.2 CELL SAMPLE EXTRACTIONS

Algal samples for metabolomic analysis were removed at eight time points throughout the experiment: a sample of the founding population, a sample three days before the glyphosate treatment was applied and 1, 8, 16, 22, 29 and 36 days after glyphosate introduction. The cells were washed with sterile Ebert medium and centrifuged to produce a pellet of cells which was flash frozen with LN2 before storing in -80°C. The frozen algal pellets were added to 2.5 µl 80% ethanol/mg of cells and crushed with a ball bearing in a homogeniser at 6 m/s for 2 minutes. The samples were centrifuged at 14 kRPM for 15 minutes and 7.5 µl of the resulting supernatant was added to 30 µl 80% ethanol.

5.3.3 METABOLOMIC PROFILING USING MASS SPECTROMETRY

Direct injection electrospray ionisation (negative and positive modes) mass spectrometry was applied to the samples and analysed on a Waters Synapt G2-Si ToF mass spectrometer (Waters Corporation, United States). Injections were performed by a Waters Acquity UPLC (Waters Corporation, United States) and the MassLynx data system (Waters Corporation, United States) was used for instrument control and data acquisition. Each of the biological replicates (n = 5 glyphosate, n = 5 controls) was evaluated in triplicate (technical replicates) in both positive and negative modes and injected at a flow rate of 5 µl/min for 3 minutes. All spectra were measured from 50 to 1200 Da for both modes with a scan time of 1 scan/second. The conditions for sample introduction are summarised in Table 5.1.

Table 5.1: Conditions for sample introduction into mass spectrometer.

Condition	Negative mode	Positive mode
Capillary voltage	2.5 kV	2.8 kV
Sample cone	20 V	80 V
Source offset	80 V	20 V
Desolvation gas flow	300 L/h	500 L/h
Desolvation temperature	280°C	280°C
Source temperature	100°C	100°C

5.3.4 DATA PRE-PROCESSING

Peak lists of accurate masses (to four decimal places) and corresponding ion counts were exported as text files from the MassLynx data system and processed into a Microsoft Excel (Microsoft Corp, USA) spreadsheet using an in-house Visual Basic macro (detailed in Overy *et al.*, 2005). Briefly, this macro removes background noise by combining the spectra of the three replicate runs and selecting only peaks that are present in all three and are within an acceptable range of variation. This method avoids loss of peaks of interest where metabolites are consistently present but at relatively low concentrations. The mean mass for each metabolite in a sample is then calculated and the values binned to create a metabolite profile, with mass peak intensity normalised as percentage of the total ion count for that sample.

5.3.5 TARGETED ANALYSIS: SHIKIMATE PATHWAY COMPOUNDS, GLYPHOSATE, GLYPHOSATE BREAKDOWN PRODUCTS AND AMINO ACIDS

All data were analysed in R (version 4.0.5, R Core Team, 2021). The monoisotopic masses for relevant compounds related to the shikimate pathway, known glyphosate breakdown products as well as all amino acids were obtained from MetaCyc.org database (Caspi *et al.*, 2020). Their expected mass peaks (i.e. $[M+H]^+$ or $[M+H]^-$) putatively matched to mass bins in negative and/or positive mode dependent on the compound's likelihood of ionising under the given conditions. Compounds were accepted as a putative match to a mass bin if the error margin to actual detected masses in that bin was less than 60 Δppm Da. In order to get a measure of the total amino acid pool abundance, the percentage ion counts for all mass bins matched to an amino acid were summed for each population by sampling day.

The percentage total ion counts of the matched compound mass bins where then compared between the controls and the glyphosate-treated populations throughout the experiment by fitting mixed-effects models with each of the putative mass bin percentage ion counts as the response (arcsine transformed), treatment (glyphosate or control) and day (as a factor) as fixed effects and chamber as a random effect to account for repeated measurements using the `lme4` package (Bates *et al.*, 2015). The `emmeans` package (Lenth, 2022) was used to carry out pairwise comparisons between treatments within each sampling day. The `car` package function `Anova()` was used to test the significance of the fixed effects and confirmed through parametric bootstrapping using the `pbkrtest` package (Halekoh & Højsgaard, 2014). When the variance of the random effect was zero or near zero for some models, resulting in a singular fit or a convergence failure, these were refit as a linear model without the random effect to validate the robustness of the significance testing. Furthermore, as the ion count for any given mass bin may contain several mass peaks and thus compounds that cannot be distinguished, the presence of detected masses within the acceptable error margin of 60 Δppm Da was confirmed in the samples with the higher ion count wherever a significant difference was found.

5.3.5.1 METABOLITE IDENTIFICATION USING TANDEM MASS SPECTROMETRY

To validate the presence of the targeted compounds, tandem mass spectrometry (MS/MS) using direct injection at 10 µl/min for 1 min on the same system as above was applied to their respective matched mass bins. The general conditions were the same as listed in Table 5.1, but each mass of interest was checked for sensitivity and optimised if necessary to maximise the signal. Fragmentation patterns were resolved against MassBank spectra (Horai *et al.*, 2010) where available, with the exception of glyphosate which was validated against a standard of glyphosate diluted to 150 mg/L in dH2O. See Table B.1 for instrument settings, MassBank record IDs and matched peaks for each compound.

As the signal for some masses was very low, compounds were accepted as present in the sample as long as the reference spectrum peak with the highest intensity was detected. Compounds where MS/MS fragmentation patterns did not resolve against MassBank spectra were discarded from the analysis, but compounds where no reference spectra was available were still included. The complete list of compounds used to test each targeted hypothesis — shikimate pathway metabolite buildup, amino acid pool composition, and presence of glyphsoate and its breakdown products — is found in Table 5.2.

5.3.6 EXPLORATORY ANALYSIS TO EXTEND THE METABOLOMIC PROFILE OF EVOLVING RESISTANCE

In order to locate large differences of interest in the data set, the SIMCA (Umetrics, Umeå, Sweden) statistical package was used to carry out Principle Component Analyses (PCA) and supervised multivariate analyses using Orthogonal Partial Least Squares Discriminant Analysis (OPLS-DA). OPLS-DA is used to determine which variables have the largest power to discriminate (loading) between defined groups (explanatory variable) and is a commonly used -omics method for biomarker identification. We applied OPLS-DA models on the whole data set with the explanatory variable as either sampling day or glyphosate treatment, as well as glyphosate treatment as the explanatory variable to the data set subset by sampling day. For each model the 40 most discriminatory mass bins (i.e. the 20 highest and 20 lowest mean loadings) were extracted to create a list of peaks of interest. Any mass bin where the standard error was larger than the mean loading was removed from the list. Mixed effects models were then fit as above for each mass bin of interest. For mass bins where a significant pairwise difference between treatments within a sampling day were found, the detected masses within that bin were putatively matched to compounds using the MetaCyc.org *Chlamydomonas reinhardtii* database for $[M\text{-}H]^-$ ions in negative mode and $[M+H]^+$,$[M+Na]^+$ and $[M+K]^+$ ion adducts in positive mode, applying a maximum error margin of 60 Δppm Da. Additionally, for those compounds where no matches were found in the initial search $[M\text{-}2H]^{2-}$, $[M\text{-}3H]^{3-}$ and $[M\text{-}H_2O\text{-}H]^-$ ion adducts for negative mode and $[M+2H]^{2+}$, $[M+3H]^{3+}$, $[M+H\text{-}H_2O]^+$ and $[M+H\text{-}2H_2O]^+$ ion adducts for positive mode were also considered.

Furthermore, the presence of detected masses within the acceptable error margin of 60 Δppm Da was confirmed in the samples with the higher ion count wherever a significant difference was found to strengthen the assumption that they were driving the observed pattern. Lastly, MS/MS analysis was carried out as above for any putatively identified compounds where MassBank reference spectra were available Table B.1 and putative compound identities where the fragmentation pattern did not match reference spectra were discarded from further analysis.

Pairwise comparisons between treatments for each sampling day were carried out as above and the compounds were classified according to when significant differences in ion count were observed. Compounds where there was no difference between treatments by the last time point were classified as pre-resistance phase. Compounds where differences were still apparent by the last time point were classified as post-resistance phase if the differences emerged with resistance evolving, whereas those where differences were present from the application of the treatment were classified

Table 5.2: Compounds tested in targeted analysis along with chemical structure, metabolomic role, accurate mass and bin. Note that some compounds have the same monoisotopic mass and thus cannot be distinguished by the metabolite screen carried out here and have been listed together if part of the same hypothesis, and labelled with matching asterisks if part of separate hypotheses. Compounds labelled with a dagger share a mass bin but they do not have the same monoisoptic mass. The presence of all listed target compounds was confirmed through MS/MS except for those in *italics* for which no reference spectra were available.

Compound	**Formula**	**Accurate mass**	**Bin (mode)**
Hypothesis: Shikimate pathway functioning			
D-Erythrose-4P (E4P)	$C_4H_7O_7P$	200.0086	199(-)
Phosphoenolpyruvate (PEP)	$C_3H_2O_6P$	167.9824	167(-)
3-Deoxy-D-Arabino-Heptulosonate 7-Phosphate (DAHP)	$C_7H_{13}O_{10}P$	288.0246	287(-)
3-Dehydroquinate (3-DHQ)	$C_7H_9O_6$	190.0477	189(-)
3-Dehydroshikimate	$C_7H_7O_5$	172.0372	171(-)
Shikimate	$C_7H_9O_5$	174.0528	173(-)
Shikimate-3-Phosphate	$C_7H_8O_8P$	254.0192	253(-)
5-Enolpyruvoyl-Shikimate 3-Phosphate (EPSP)	$C_{10}H_9O_{10}P$	324.0246	323(-)
Chorismate/Prephenate	$C_{10}H_8O_6$	226.0477	225(-)
Hypothesis: Glyphosate and its degradation products			
Glyphosate	$C_3H_6NO_5P$	169.0140	168(-)
Aminomethyl-phosphonate (AMPA)	CH_5NO_3P	111.0085	112(+)
Sarcosine*	$C_3H_7NO_2$	89.0477	88(-), 90(+)
α-D-ribose-1-[N-(phosphonomethyl)glycine] 5-triphosphate	$C_8H_{13}NO1_8P_4$	540.9553	540(-), 542(+)
α-D-ribose-1-[N-(phosphonomethyl)glycine] 5-phosphate	$C_8H_{13}NO_{12}P_2$	381.0226	380(-), 382(+)
α-D-ribose 1,5-bisphosphate	$C_5H_8O_{11}P_2$	309.9855	309(-), 311(+)
5-phospho-α-D-ribose 1,2-cyclic phosphate	$C_5H_7O_{10}P_2$	291.9749	291(-), 293(+)
5-phospho-α-D-ribose 1-diphosphate	$C_5H_8O_{14}P_3$	389.9518	389(-), 391(+)
α-D-ribose 1-(acetamidomethylphosphonate) 5-triphosphate	$C_8H_{14}NO_{17}P_4$	524.9603	524(-), 526(+)
α-D-ribose-1-(2-N-acetamidomethylphosphonate) 5-phosphate	$C_8H_{14}NO_{11}P_2$	365.0277	364(-), 366(+)
Cinnamaldehyde†	C_9H_8O	132.0575	131(-)
Cinnamyl alcohol	$C_9H_{10}O$	134.0732	133(-), 135(+)
2-oxoglutarate‡	$C_5H_4O_5$	146.0215	145(-)
Hypothesis: Amino acid pool composition			
Alanine (Ala)*	$C_3H_7NO_2$	89.0477	88(-), 90(+)
Arginine (Arg)	$C_6H_{14}N_4O_2$	174.1117	173.2(-), 175.2(+)
Asparagine (Asn)†	$C_4H_8N_2O_3$	132.0535	131(-)
Aspartate (Asp)	$C_4H_7NO_4$	133.0375	132(-)
Glutamate (Glu)	$C_5H_9NO_4$	147.0532	146(-)
Glutamine (Gln)‡	$C_5H_{10}N_2O_3$	146.0691	145(-)
Glycine (Gly)	$C_2H_5NO_2$	75.0320	74(-), 76(+)
Histidine (His)	$C_6H_9N_3O_2$	155.0695	154(-), 156(+)
Isoleucine (Iso)/Leucine (Leu)	$C_6H_{13}NO_2$	131.0946	130(-), 132(+)
Lysine (Lys)	$C_6H_{14}N_2O_2$	146.1055	147.2(-)
Methionine (Met)	$C_5H_{11}NO_2S$	149.0510	150(+)
Phenylalanine (Phe)	$C_9H_{11}NO_2$	165.0790	164(-), 166(+)
Proline (Pro)	$C_5H_9NO_2$	115.0633	114(-), 116(+)
Tryptophan (Trp)	$C_{11}H_{12}N_2O_2$	204.0899	203(-), 205(+)
Tyrosine (Tyr)	$C_9H_{11}NO_3$	181.0739	180(-), 182(+)
Valine (Val)	$C_5H_{11}NO_2$	117.0790	116(-), 118(+)

as persistent differences. The MetaboAnalyst Pathway Analysis tool (Xia *et al.*, 2009) was used to identify pathways linking the putatively identified compounds within each classification.

5.4 RESULTS

5.4.1 SHIKIMATE PATHWAY METABOLITE BUILD-UP BEFORE, BUT NOT AFTER, RESISTANCE EVOLVES

We found strong evidence of disrupted shikmate pathway functioning in the form of initial metabolite build-up, as well as a clear indication of when resistance evolved as this build-up disappeared. Glyphosate treatment and its interaction with day had a strong effect on the ion counts in the mass bins matched to the three metabolites directly upstream of EPSPS (Figure 5.2, Table B.3). Blockage of the shikimate pathway by glyphosate action is apparent at 8 days after the introduction of the treatment and resulting in considerable build-up of 3-dehydroshikimate (Figure 5.2e, t-ratio = -7.9, DF = 52.6, $p < 0.001$), shikimate (Figure 5.2f, t-ratio = -10.2, DF = 56 $p < 0.001$) and shikimate-3-phosphate (Figure 5.2g, t-ratio = -7.2, DF = 53.6, $p < 0.001$) compared to the control populations, with a roughly 3.1-fold increase in 3-dehydroshikimate, 2.7-fold increase in shikimate and a 4.5-fold increase in shikimate-3-phosphate. While there on day 16 is no difference between controls and treated populations in levels of 3-dehydroshikimate (t-ratio = -0.79, DF = 52.6, $p > 0.9$) and shikimate (t-ratio = -1.7, DF = 56, $p > 0.9$), shikimate-3-phosphate increases to 12-fold that of controls (t-ratio = -10.8, DF = 53.6, $p < 0.001$) before returning to levels comparable to the controls. There is a marginally significant difference in ion counts for the shikimate mass bin on day 29 (t-ratio = -3.6, DF = 56, $p = 0.04$), but by day 36 it has once again returned to levels comparable to the controls (t-ratio = -2.3, DF = 56, $p = 0.5$), while the 3-dehydroshikimate mass bin has a marginally significant increase in ion counts again by day 36 (t-ratio = -3.6, DF = 52.6, $p = 0.04$), but at no point do they return to levels comparable to day 8. This is clear evidence of resistance evolving to neutralise the effect of glyphosate, allowing the shikimate pathway to function again. While the level of shikimate-3-phosphate is still elevated by 2.8-fold compared to controls on day 22 (t-ratio = -4.0, DF = 53.6 $p = 0.01$), there is no difference between controls and treated populations on days 29 (t-ratio = -3.0, DF = 53.6, $p = 0.2$) and 36 (t-ratio = -1.3, DF = 53.6, $p > 0.9$), suggesting there is little to no trade-off between normal EPSPS function and the resistance trait.

While glyphosate treatment had a significant effect on the mass bins for PEP (Figure 5.2b) and the metabolites upstream of 3-dehydroshikimate — E4P (Figure 5.2a), DAHP (Figure 5.2c) and DHQ (Figure 5.2d) — either as a main effect or through its interaction with day (Table B.3), the pairwise comparisons for PEP, DAHP and DHQ only found significant differences in ion counts between treatments on different sampling days. These differences are more likely to be due to daily fluctuations or adaptation to the chemostat environment and are thus not of interest to the hypotheses investigated here. E4P was found at lower ion counts for the glyphosate-treated populations on days 16 (t-ratio = 4.7, DF = 42.9, $p = 0.002$) and 22 (t-ratio = 5.1, DF = 42.9, $p < 0.001$) at roughly a 0.7-fold decrease compared to the controls. However, the fact it was also found to have similarly lower ion counts for the same populations on day -3 (t-ratio = 3.6, DF = 42.9, $p = 0.047$) before the glyphosate treatment was introduced makes it possible that the pattern is at least in part driven by a different compound in the same mass bin.

There was also an effect of the glyphosate treatment and day interaction on the mass bins for compounds downstream of EPSPS (Table B.3) — EPSP (Figure 5.2h) and chorismate/prephenate (Figure 5.2i). An increase in ion count in the chorismate/prephenate mass bin for the glyphosate-treated populations was found immediately after the start of the treatment on day 1, before the build-up of upstream metabolites is seen (t-ratio = -5.1, DF = 53.6, $p < 0.001$), but after that remains at levels comparable to the controls. No pairwise differences were found for the EPSP mass

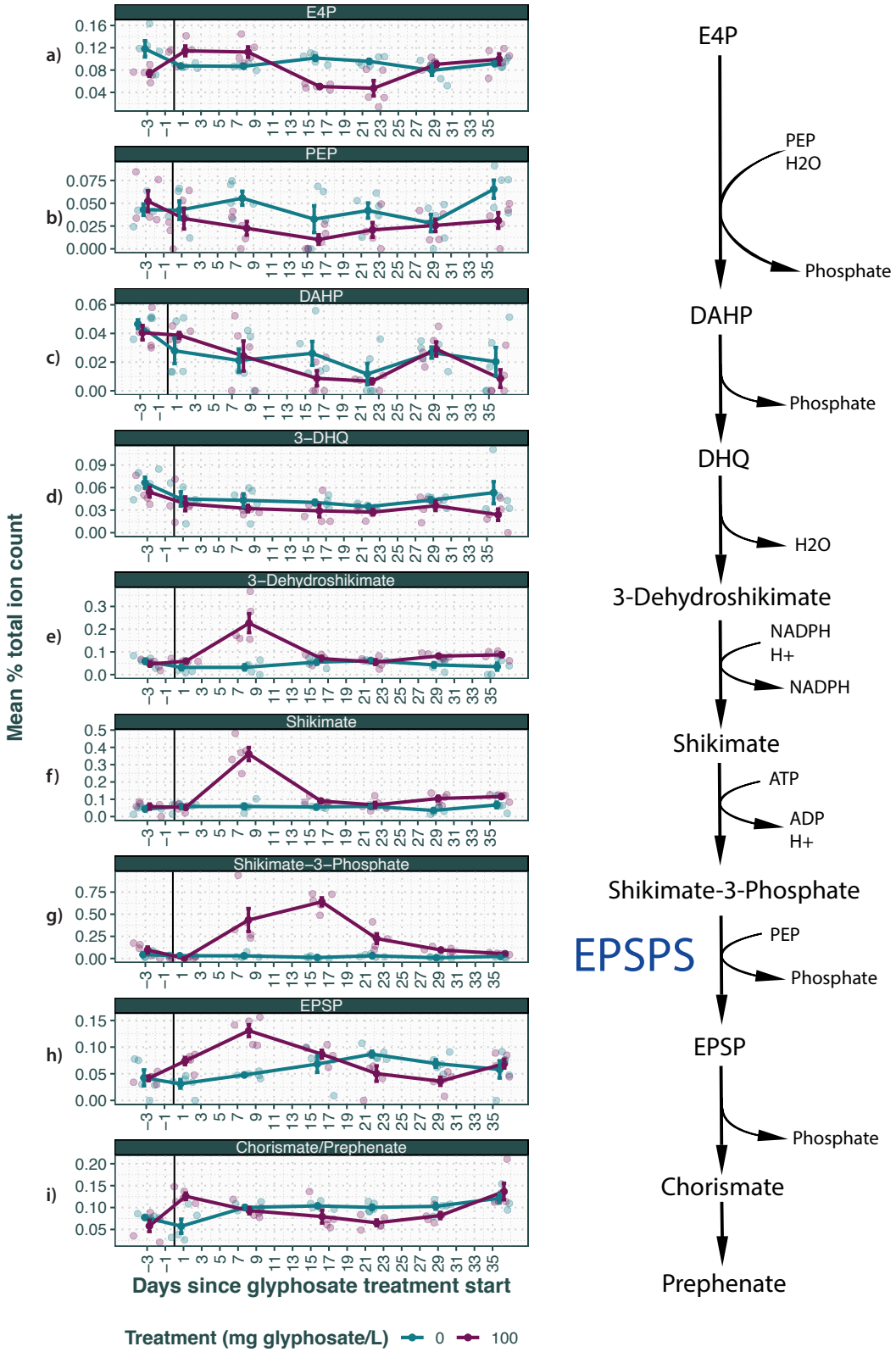

Figure 5.2: Mean % total ion count with standard error for the putative mass bin matches of compounds in shikimate pathway for control and glyphosate-treated populations throughout the course of the experiment. The compounds are ordered according to their position in the shikimate pathway, but note that PEP appears twice as a substrate. The black vertical line in the graphs indicates start of the glyphosate treatment.

bin, and neither EPSP (day 36, t-ratio = -1.1, DF = 54.5, $p > 0.9$) nor chorismate/prephenate (day 36, t-ratio = -0.84, DF = 53.6, $p > 0.9$) ion counts were different between treatments after resistance evolved.

5.4.2 NO EVIDENCE OF DIFFERENCES IN GLYPHOSATE LEVEL

Our data suggest that ion count fluctuations in the targeted mass bin are not linked to glyphosate itself. While glyphosate presence was confirmed through MS/MS in negative mode, the ion counts are low throughout (Figure 5.3), and there was no effect of glyphosate treatment or its interaction with day on the ion count (Table B.4), nor were pairwise differences found in ion counts between the glyphosate-treated populations and the controls on any given day (Table B.5). This makes it highly likely a different compound is responsible for the bulk of fluctuations seen in the ion counts in this bin, and that any glyphosate present in the glyphosate-treated cells is either bound to EPSPS or other enzymes.

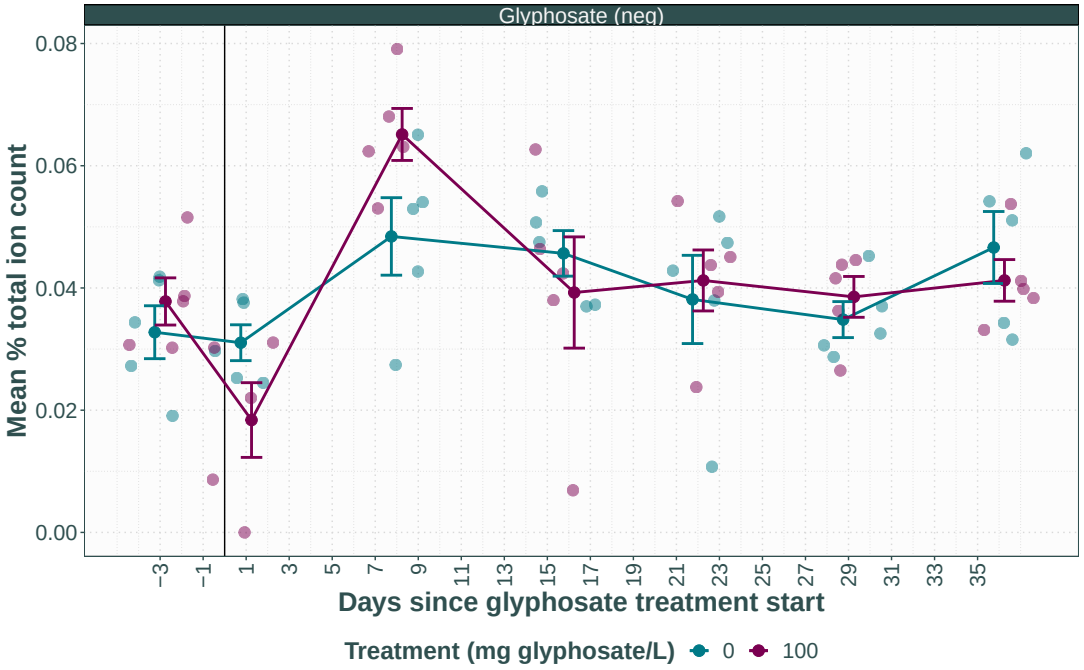

Figure 5.3: Mean % ion counts with standard error in negative and positive mode for the glyphosate mass bin. The raw data is shown in the background as transparent points and the black vertical line indicates introduction of the glyphosate treatment.

5.4.3 NO EVIDENCE OF GLYPHOSATE DEGRADATION IN RESISTANT POPULATIONS

Our data suggests there is no increase in presence of glyphosate degradation products after resistance has evolved. While a significant effect of either glyphosate treatment or its interaction with day was found on the mass bins matched to major glyphosate degradation products AMPA and sarcosine in positive mode (Table B.4), the effect is in the wrong direction for it to be compatible

with glyphosate degradation (Figure 5.4). In all instances where significant or marginally significant pairwise differences between the treatments were found (Table B.5), the higher ion counts were in the controls. This suggests the ion count fluctuations in the mass bin matched to AMPA actually reflects the changes in a different compound. The mass bins matched to sarcosine may also be picking up a different compound (e.g. Ala) or the differences reflect sarcosine's involvement in a different process unrelated to glyphosate degradation. There was also no evidence of an effect of glyphosate treatment or its interaction with day on the ion counts for the mass bins matched to AMPA or sarcosine in negative mode (Table B.4) and the presence of glyoxylate was ruled out by the MS/MS analysis (Table B.1). This strongly suggests glyphosate degradation does not have a role in the resistance mechanism in these populations.

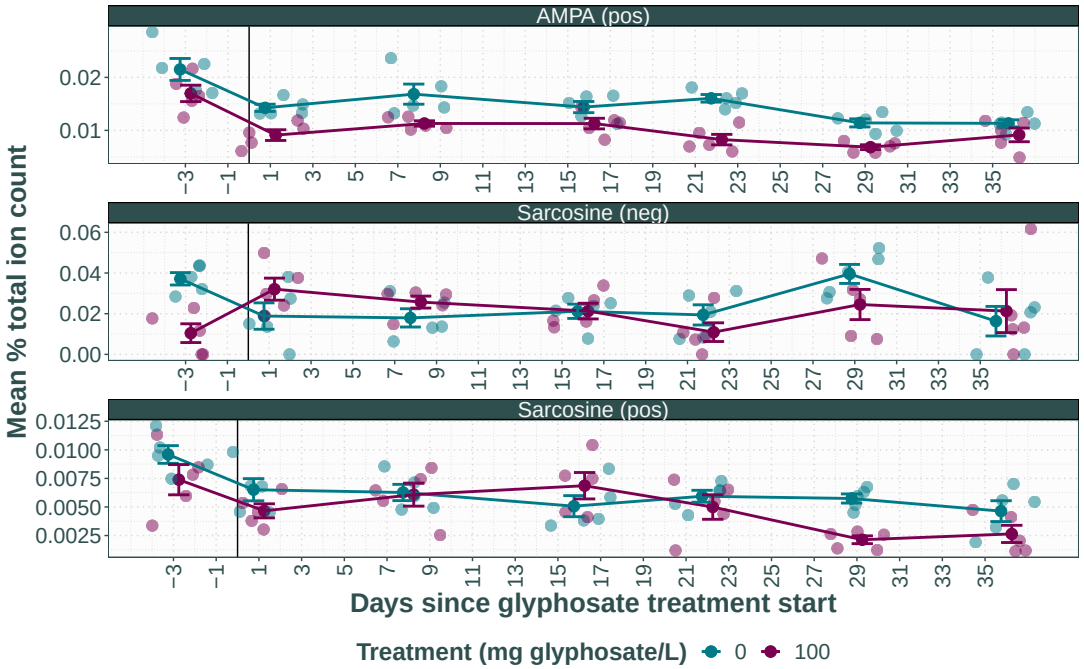

Figure 5.4: Mean % ion counts with standard error for mass bins matched to primary glyphosate degradation products in negative and positive mode. The raw data is shown in the background as transparent points and the black vertical line indicates introduction of the glyphosate treatment.

Further analysis of possible AMPA degradation products and glyphosate degradation products associated with C-P lyase or aldo-keto reductase also showed no evidence of glyphosate degradation, with the vast majority of matched mass bins showing no effect of glyphosate treatment or its interaction with day on the ion count (Table B.6, Figure B.1). Mass bin 524(-), matched to α-D-ribose-1-[N-(phosphonomethyl)glycine]-5-triphosphate, shows a sudden increase in ion count in the controls on days 22 and 29, but the direction and timing of the effect makes it unlikely that this is related to glyphosate degradation.

Our data for the mass bins matched to cinnamaldehyde and cinnamyl alcohol suggest that the pattern is likely an effect of glyphosate inhibition, rather than related to the resistance mechanism. Pairwise differences between treatments for these mass bins were observed on days 1 and 8 in negative mode (Table B.6, Figure B.1), with the ion counts being lower for the glyphosate-treated populations prior to glyphosate resistance has evolved, but returning to comparable levels to the controls after. The mass bin matched to 2-oxoglutarate also showed lower ion counts associated with the glyphosate treatment ranging the span of glyphosate inhibition and early after resistance

has evolved. As mentioned above, it shares a mass bin with Glu confounding the interpretation, but as the effect disappears with the evolution of resistance, it is likely to be due to a different cellular process than glyphosate degradation.

5.4.4 DECREASE IN AMINO ACID POOL ASSOCIATED WITH GLYPHOSATE TREATMENT, BUT EFFECT DISAPPEARS WHEN RESISTANCE EVOLVES

The effect of glyphosate on the overall amino acid pool size and composition provides further evidence of the cell wide disruptive effects of glyphosate action, but that this effect disappears as resistance evolves. The effect of glyphosate treatment on the ion counts of the mass bins matched to amino acids depends on compound, the mode and the day (summarised in Table 5.3, Table B.9, Table B.8, Table B.11, Table B.10). However, the overwhelming and consistent pattern is either no pairwise difference between glyphosate-treated populations and controls, or a decrease in ion count in the days associated with glyphosate inhibition (days 1–16) or early after resistance has evolved (day 22–29). The amino acids possibly affected in this time frame are the aromatic amino acid products of the shikimate pathway Trp and Tyr, as well as Glu, Gln, Pro and Val. The effect of glyphosate treatment during this period also reflected in the overall ion counts for the total amino acid pool (Figure 5.5). Our data also suggest that there may be other processes affecting the ion counts in some of the targeted mass bins. This is evidenced by significant pairwise differences on day -3, before the glyphosate treatment was introduced, for Arg, Phe, Pro and the total amino acid pool in positive mode. Note as well that Gln shares a mass bin with 2-oxoglutarate meaning any pattern observed here may be due to either or both compounds.

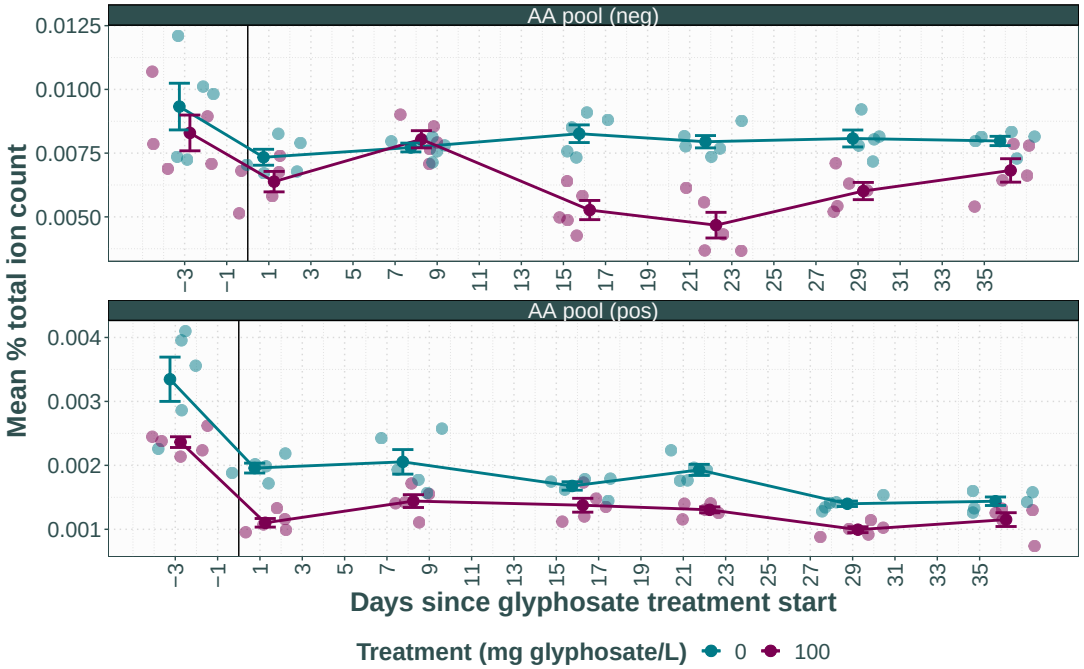

Figure 5.5: Mean % ion counts with standard error in negative and positive mode for the total AA pool in each population. The raw data is shown in the background as transparent points and the black vertical line indicates introduction of the glyphosate treatment.

For all compounds but one (Met) as well as the total amino acid pool, no differences were found between treatments by the end of the experiment (day 36, Table B.11), suggesting there may be little to no trade-off between glyphosate resistance and overall cell functioning at this point.

Table 5.3: Summary of significant pairwise differences between glyphosate-treated populations and controls for mass bins matched to amino acids as well as the total amino acid pool. See Table B.11 and Table B.10 for the associated test statistics. Arrows and fold changes (calculated as the average glyphosate-treated ion count divided by the average control ion count, i.e. a fold change of 0.8 means the treated population ion count is 0.8 that of the controls) indicate the average % total ion count for the glyphosate-treated populations as compared to the controls. Blacked out cells represent mass bins discarded from the analysis as the detected masses differed from the amino acid target expected masses by more than 60 Δppm or MS/MS analysis could not confirm the presence of the compound. Greyed out cells represent no difference found between treatments. * denotes that a significant pairwise difference was found but that the detected mass peaks difference from the expected mass in the relevant samples were above the 60 Δppm threshold but below 100 Δppm, ** denotes that a significant pairwise difference was found but that the detected mass peaks compared to the expected mass in the relevant samples were outwith an error margin of 100 Δppm.

Day / AA	Negative mode							Positive mode						
	-3	1	8	16	22	29	36	-3	1	8	16	22	29	36
Ala													↓*	
Arg								↓0.8				↓**		
Asn														
Asp														
Cys														
Glu		↓0.7		↓0.8	↓0.7									
Gln			↓0.7	↓0.5	↓0.5									
Gly														
His									↓**					
Iso/Leu														
Lys														
Met														↓0.7
Phe								↓0.8						
Pro								↓0.8	↓0.8			↓*		
Ser														
Thr														
Trp									↓0.6	↓0.7				
Tyr					↓0.9									
Val		↓0.4							↓**					
AA pool				↓0.8	↓0.8			↓0.8	↓0.8	↓0.8		↓0.8		

5.4.5 THE EXTENDED METABOLOMIC FINGERPRINT OF GLYPHOSATE RESISTANCE EVOLUTION DEPENDS ON TIME POINT

166 compounds were putatively matched to the mass bins forming the basis of the extended metabolic fingerprint of glyphosate resistance evolution. Out of a total of 156 unique mass bins of interest, 91 could not satisfactorily be matched to a putative identity (Table B.12). These masses likely reflect fragments of larger compounds or adducts not investigated here. The putative identities of the remaining 65 are listed in Table B.2, with several being matched to more than one identity.

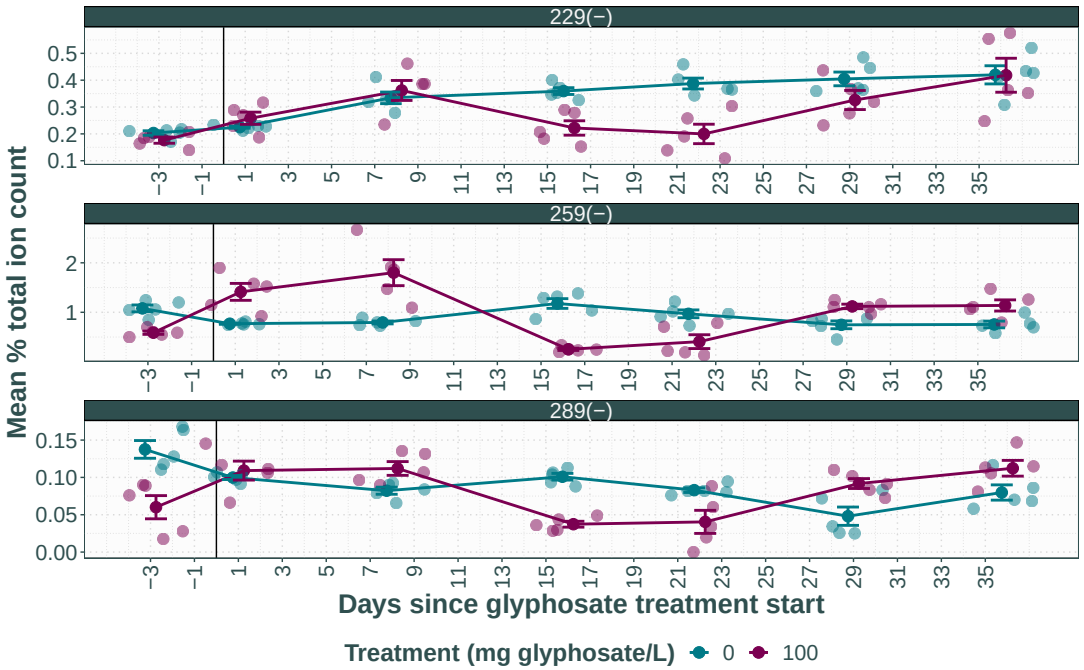

Figure 5.6: Mean % ion counts with standard error for mass bins with compound matches relating to carbon metabolism. The raw data is shown in the background as transparent points and the black vertical line indicates introduction of the glyphosate treatment. See Table B.2 for full list of compounds matched to each bin.

Most of the mass bins of interest were found to have a pre-resistance phase pattern (Table B.13, Table B.14), both out of the putatively identified and the unidentified compounds, suggesting the majority are related to glyphosate toxicity. The types of putatively identified compounds in this group are diverse, including lipids, fatty acids, sugars, pigments, hormones, vitamins and redox electron carriers. The pathways identified by MetaboAnalyst to link the putatively identified compounds included the pentose phosphate pathway, fructose and mannose metabolism, carbon fixation, linoleic acid metabolism, amino sugar and nucleotide sugar metabolism, as well as pentose and glucuronate interconversions. Of particular interest are bins 229(-), 250(-) and 289(-) (Figure 5.6) which were matched to a number of sugar phosphates — including D-ribose 5-phosphate, sedoheptulose 7-phosphate, D-ribulose 5-phosphate, β-D-fructose 6-phosphate, β-D-glucose 6-phosphate and D-xylulose 5-phosphate — as these are all involved in carbon metabolism.

The putatively identified compounds in the post-resistance phase or persistently different from the start of the treatment included electron-transfer quinols and carotenoids like menaquinol-6, menaquinol-9 and adonixanthin (Figure 5.7) suggesting the cells are responding to oxidative stress, along with several lipids and fatty acids. The pathways identified by MetaboAnalyst to link the putatively identified compounds here included linoleic acid metabolism, carotenoid biosynthesis and glycerophospholipid metabolism.

Furthermore, the presence of a persistent pattern also suggests there is a distinctive metabolite profile for *C. reinhardtii* cells experiencing glyphosate action, regardless of whether the population is resistant or susceptible.

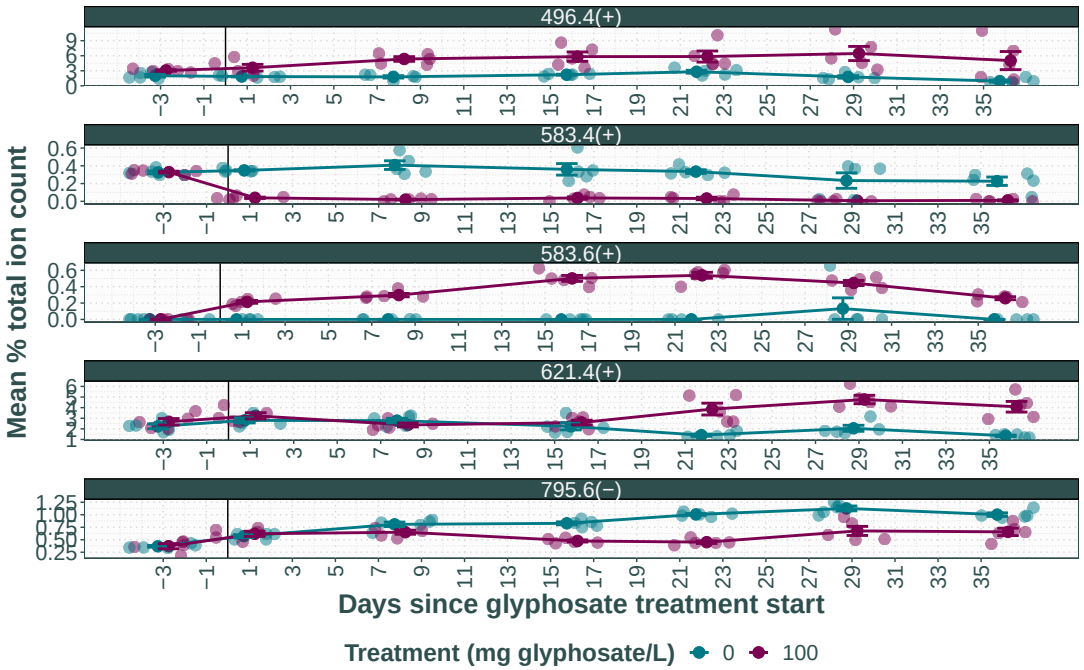

Figure 5.7: Mean % ion counts with standard error for mass bins with compound matches including carotenoids and quinols/quinones with a post-resistance or persistent pattern. The raw data is shown in the background as transparent points and the black vertical line indicates introduction of the glyphosate treatment. See Table B.2 for full list of compounds matched to each bin.

5.5 DISCUSSION

Herbicide resistance in weed populations is an increasing economic and ecological problem worldwide. To manage it, we need to understand its evolutionary dynamics, including the underlying molecular mechanisms. Here we for the first time characterise the effect of glyphosate resistance evolution in action on the metabolome of model species *C. reinhardtii*, from the first introduction of the herbicide to a naive population to after resistance has evolved, and use this metabolomic fingerprint to make inferences about the underlying resistance mechanism as well as associated fitness costs. We find a clear signal of evolving resistance in the form of disrupted shikimate pathway functioning that is then returned to control levels, as well as evidence of concurrent widespread cellular disruption which also disappears after resistance has evolved. Furthermore, while we could not determine the underlying resistance mechanism, we could rule out glyphosate degradation. We also found compelling evidence for secondary effects of glyphosate in the form of ROS and lipid peroxidation.

5.5.1 EVIDENCE FOR GLYPHOSATE RESISTANCE EVOLUTION

As in previous work with other organisms, we detected a strong effect of glyphosate action on the metabolites upstream of EPSPS in the shikimate pathway (Aristilde *et al.*, 2017; de María *et al.*, 2006; Felline *et al.*, 2019; Kostopoulou *et al.*, 2020; Maroli *et al.*, 2015, 2018; Oikawa *et al.*, 2006; Sikorski *et al.*, 2019; Wang, 2001; Zabalza *et al.*, 2017; Zhong *et al.*, 2018), that then returns to

a level comparable to the controls. This is not only strong evidence for glyphosate action, it is evidence for evolved resistance returning normal cell function, and gives a timeline for resistance evolving in this system.

Similarly, evidence of general disruption to the cellular machinery is seen through ion count decreases in bins matched to a number of amino acids as well as the overall amino acid pool coinciding with the blockage of the shikimate pathway. This too returns to levels comparable to the controls by the end of the experiment as resistance has evolved, further suggesting that the resistance mechanism is highly effective at lifting the negative, inhibitory effects of glyphosate without trading off against normal cell function. The general effects of glyphosate inhibition on the amino acid pool and its fluctuations is poorly understood, and appears to vary by system (Aristilde *et al.*, 2017; Böttcher *et al.*, 2007; Diaz Vivancos *et al.*, 2011; Felline *et al.*, 2019; Kostopoulou *et al.*, 2020; Maroli *et al.*, 2018; Trenkamp *et al.*, 2009), timing (Böttcher *et al.*, 2007; Trenkamp *et al.*, 2009) and the level of stress (Felline *et al.*, 2019). While our results are consistent with the many studies showing that the patterns of disruption differ depending on the specific amino acid, the majority of the mass bins matched to an amino acid see no effect of the glyphosate treatment at any point. We can thus not see any evidence of the overall triggering of parallel synthesis pathways or shifts toward more minor or more nitrogen rich amino acids to buffer against the effects of glyphosate inhibition found in other systems (Diaz Vivancos *et al.*, 2011; Felline *et al.*, 2019; Maroli *et al.*, 2018), especially as some of the amino acids we would then expect an increase in (e.g. Gln or Val) show the opposite pattern. However, the binning of mass peaks method used here may be too blunt an instrument to fully capture changes in amino acid abundances with the fluctuations in other compounds sharing their mass bin masking the effect, particularly as the signal for the relevant masses for many amino acids was low in the MS/MS analysis. The present study is also testing whole populations expected to consist of a heterogeneous mixture of phenotypes with different resistance strategies emerging at different times, which may further obscure effects that are not overwhelmingly unidirectional.

It is likely the decreases in Trp and Tyr is a direct effect of the blocked shikimate pathway as they are the downstream products. However, the third aromatic amino acid Phe does not see a decrease in ion count after the application of the treatment, only before. While this indicates a masking effect by other compounds, Phe synthesis may also be prioritised over Trp and Tyr to maintain downstream biosyntheses (Diaz Vivancos *et al.*, 2011). Several studies have also noted a decrease in Glu coupled to an increase in Gln, suggesting upregulation of Gln as an important nitrogen donor for amino acid synthesis as a possible reason for this shift (Diaz Vivancos *et al.*, 2011; Felline *et al.*, 2019; Maroli *et al.*, 2018), however here we found concurrent decreases in both Glu and Gln, suggesting a different mechanism may be involved, or a masking effect of Glu by e.g. 2-oxoglutarate.

The mass bins identified for the extended metabolic fingerprint overwhelmingly showed a pattern where large differences between populations attributable to glyphosate action are lifted as resistance evolves. Either this presents as an immediate return to control population levels on days 16 or 22, or it is more gradual. This gradual pattern likely reflects the fact that the populations tested comprise several, competing phenotypes with different strategies (Gresham *et al.*, 2008; Hong & Gresham, 2014; Kao & Sherlock, 2008; Kinnersley *et al.*, 2009; Kvitek & Sherlock, 2011; Maharjan *et al.*, 2006, 2012; Wenger *et al.*, 2011), and we are picking up the metabolomic signal of both the phenotypes that are resistant and those that are dying. As the resistant phenotypes become dominant in the population, and the susceptible phenotypes die off, we should see a shift away from the signal associated with glyphosate inhibition. It is also possible that mutations are accumulated sequentially to improve resistance, and that the gradual pattern is associated with several soft sweeps to fixation (Gresham *et al.*, 2008). There is also no straightforward connection between the relative abundance of a compound and the underlying reason. A compound may increase in abundance due to upregulation or due to buildup as downstream pathways are blocked or diverted, and a compound may decrease in abundance as it is downregulated, because it is used more or because it is being catabolised to divert the resources.

A considerable proportion of the putatively identified compounds are related to carbon capture and

metabolism, consistent with the shikimate pathway blockage disrupting the control of carbon flow, with knock-on disruptive effects on all related pathways (Aristilde *et al.*, 2017; Felline *et al.*, 2019; Kostopoulou *et al.*, 2020; Maroli *et al.*, 2015). Mass bins 229(-), 259(-) and 289(-) contain putative matches involved in the tightly connected pentose phosphate pathway, pentose and glucuronate interconversions, glycolysis, mannose and fructose metabolism and sugar nucleotide biosynthesis, and with significant differences between treatments before or around resistance evolving. The pattern seen for mass bin 259(-) in particular is consistent with the build-up of sugars as a result of shikimate pathway blockage observed by Maroli *et al.* (2015), suggested to be due to the PEP that is no longer bound by EPSPS during glyphosate inhibition. PEP and phosphate levels regulate the conversion of fructose-6-phosphate to fructose-1,6-biphosphate in glycolysis (Plaxton, 1996; Smyth *et al.*, 1984), and increased unused PEP will block this step, resulting in fructose-6-phosphate accumulation (Colombo *et al.*, 1998; Orcaray *et al.*, 2012). Similar secondary effects on other, linked pathways could explain the lower ion counts in the mass bin matched to 2-oxoglutarate as the tricarboxylic acid (TCA) cycle has also been found to be perturbed by glyphosate application (Aristilde *et al.*, 2017; Felline *et al.*, 2019; Kostopoulou *et al.*, 2020; Maroli *et al.*, 2015). The return to control levels for all of these mass bin ion counts indicates that resistance has restored not only shikimate pathway functioning, but lifted some of its secondary effects.

5.5.2 EVALUATION OF POSSIBLE RESISTANCE MECHANISMS

Given that the functioning of the shikimate pathway, the amino acid pool, sugars and other metabolites return to control population levels after resistance has evolved, without evidence of a trade-off against normal cell functioning, the resistance mechanism is likely highly efficient. This suggests that if there is a target mutation to EPSPS rendering it insensitive to glyphosate, it has not significantly reduced its sensitivity to the intended substrates (Eschenburg *et al.*, 2002; Fonseca *et al.*, 2020; Funke *et al.*, 2009; Healy-Fried *et al.*, 2007; Kaundun *et al.*, 2008; Li *et al.*, 2018; Yu *et al.*, 2006). Similarly if there is instead amplification of EPSPS, this is sufficiently large to fully release the inhibition of the pathway (Baerson *et al.*, 2002; Gaines *et al.*, 2019; Patterson *et al.*, 2018).

As each population represents a separate evolutionary trajectory, and likely comprises several phenotypes, we would not necessarily expect them to all exhibit the same dominant resistance mechanism, and there may be more than one mechanism present within each population as well as within each cell. However, as the level of inter-population variation found here is generally very low, and there is limited chance for *de novo*-mutation generation in a growth inhibited population, it is possible that at least the initial steps in resistance evolution are resulting from selection on standing genetic variation and that this is very similar in all the populations. Furthermore, the level of complexity of a chemostat population depends on the specific selective pressure it is experiencing (Gresham *et al.*, 2008). This means that it is also possible that there is a limited number of mutations that confer glyphosate resistance that quickly become dominant in the initial phase of glyphosate resistance evolution, even though later sequential mutations may have led to greater divergence between populations as the selective pressures change.

5.5.2.1 NO EVIDENCE FOR GLYPHOSATE DEGRADATION OR CHANGES IN GLYPHOSATE LEVEL

There was no indication of glyphosate degradation playing a role in resistance, with low ion counts in all the mass bins matched to potential breakdown products and the only significant effects treatment being in the wrong direction. This is not unexpected as while the breakdown products have been identified in some species, evidence for it being the primary resistance mechanism is highly limited (de Carvalho *et al.*, 2012; Duke, 2011; González-Torralva *et al.*, 2012; Pan *et al.*, 2019; Sammons & Gaines, 2014; Vemanna *et al.*, 2017).

However, presence of a compound in a metabolite screen is always stronger evidence than absence. A compound may still be present even if it is not detected in the expected mass bin as it may have formed an unexpected adduct or fractured into smaller molecules (Overy *et al.*, 2005). Furthermore, as the metabolite screen is designed to give as broad coverage as possible, the settings used are not optimal for picking up all compounds, and ion suppression – where the finite ionisation energy is utilised to a higher degree by the compounds that ionise easily, leaving little energy for other compounds – may reduce the signal for a compound in a mixture compared to it being injected on its own (Fiehn, 2002; Overy *et al.*, 2005). Targeted confirmatory analysis using e.g. LC-MS to isolate the compounds is thus needed to definitively rule out the presence of glyphosate breakdown products.

There was also no evidence for changes to the level of glyphosate itself. While the low ion counts in its mass bin may be accounted for by ion suppression, it is more likely due to it almost exclusively being present bound by EPSPS or other enzymes rather than freely. In the case of upregulated EPSPS, we would not expect to see any free glyphosate as it would all be bound by EPSPS (Gaines *et al.*, 2020). Similarly in the case of increased vacuolar sequestration, the glyphosate may be bound by other enzymes related to its transport (Ge *et al.*, 2010, 2011, 2012). While mutated EPSPS with a lower affinity for glyphosate could theoretically result in free glyphosate, the absence of an increase does not exclude this mechanism as it may be working in tandem with other mechanisms. Furthermore, as there is no indication of higher levels of glyphosate before resistance has evolved, we cannot conclude whether the level of absorption of glyphosate by the cell is involved in the resistance mechanism.

5.5.3 EVIDENCE FOR PERSISTING OXIDATIVE DAMAGE AND MEMBRANE CHANGES

While the evolution of resistance appears to lift the majority of the effects of glyphosate inhibition of the shikimate pathway, a number of mass bins still show marked differences between the treatments by the end of the experiment. Some have persisted from the first application of the treatment, suggesting they are direct effects of glyphosate itself, whereas some appear to emerge gradually or around the same time as resistance emerges, suggesting instead they may be related to costs of resistance. The putatively identified compounds found here mainly include lipids, fatty acids, electron-transfer quinols and carotenoids, suggesting the differences are related to cell membranes and oxidative damage.

While the disruption to carbon flow caused by the shikimate pathway blockage may be enough to upset the redox balance of the cell (Maroli *et al.*, 2015), and production of ROS is commonly found as a secondary effect of different stressors (Demidchik, 2015; Gauthier *et al.*, 2020; Liu *et al.*, 2020; Noctor *et al.*, 2015; Okamoto *et al.*, 2001; Pinto *et al.*, 2003), Gomes & Juneau (2016) found that glyphosate also interferes with the mitrochondrial electron transport chain to produce ROS. This mechanism may explain the reported effects of glyphosate on non-target organisms lacking a shikimate pathway (e.g. animals) (Liu *et al.*, 2021; Strilbyska *et al.*, 2022), and means that there is a potential for glyphosate to cause continued damage even if the inhibition of the shikimate pathway is lifted. This damage includes lipid peroxidation, the chain reaction of free radical propagation in which free radicals steal electrons from membrane lipids (Demidchik, 2015). Increased antioxidant activity has been found in glyphosate resistant strains in several systems (Maroli *et al.*, 2015; Unver *et al.*, 2010; Zhu *et al.*, 2008), and in some glyphosate continues to have an effect on germination through oxidative damage (Gomes *et al.*, 2017).

The electron-transfer quinols putatively identified are menaquinols and ubiquinols, compounds involved in electron transport and signalling across membranes, but also natural antioxidants shown to reduce damage from ROS and prevent lipid peroxidation (Fujimoto *et al.*, 2012; Goodwin, 1977; Landi *et al.*, 1984; Lichtenthaler, 1977; Vervoort *et al.*, 1997). The putatively identified 15-*cis*-phytoene is involved in early carotenoid biosynthesis (Brausemann *et al.*, 2017), and biosynthesis

of secondary carotenoids like the putatively identified adonixanthin and hydroxyspirilloxanthin is a known general stress response in algae, as well as a response to ROS production as they are singlet oxygen scavengers (Lemoine & Schoefs, 2010; Solovchenko, 2013). Immediate changes in the abundances of these compounds may reflect a plastic response to oxidative damage, whereas differences emerging post-resistance may reflect adaptation. While we cannot from the data presented here tell how effective this response is and if the level of ROS present in the cell or the damage being caused changes throughout the course of adaptation, their continued presence suggests that they present an ongoing stress response which cannot be attributed merely to the disruption caused by inhibition of the shikimate pathway. The putatively identified lipids are primarily involved in glycerophospholipid metabolism, producing the lipids involved in cellular membranes (Giroud *et al.*, 1988). Their changed abundances could either be a sign of continued stress and membrane degradation due to lipid peroxidation, or it may reflect changes to the membrane structure to limit either primary or secondary glyphosate damage (Pinto *et al.*, 2003; Stupak *et al.*, 2019).

Free fatty acids is another possible sign of membranes being degraded by lipid peroxidation (Noctor *et al.*, 2015; Okamoto *et al.*, 2001; Pinto *et al.*, 2003), but the mass bins putatively matched to fatty acids here all show a peak in abundance on days 16 and 22. This suggests that this signal is reflective of the widespread death and breakdown of glyphosate susceptible cells seen in the population at this point resulting from shikimate pathway blockage, and the stabilisation to control levels would then correspond to the majority of the population consisting of living, glyphosate resistant cells that are not experiencing the same levels of membrane damage regardless of ROS levels. *Myo*-inositols have also been identified as potential ROS scavengers (Noctor *et al.*, 2015), and while they were found as a putative match to mass bin 259(-), this mass bin is shared with the sugars phosphates that are expected to accumulate due to the shikimate pathway blockage as outlined above. This makes interpreting the pattern for this bin difficult, but it is possible that the initial ion count increase in the treated populations is due to sugar accumulation pre-resistance whereas the decrease found post-resistance could be driven by depletion of *myo*-inositols. Lastly, Pro, one of the amino acid mass bins we see a decrease in on day 1, plays a role in cellular redox-regulation (Liang *et al.*, 2013; Noctor *et al.*, 2015), and has been suggested as a possible first line of defence against ROS produced by heavy metal stress (Liu *et al.*, 2020; Sharma & Dietz, 2006). As the ion counts for the mass bin putatively matched to Pro return to control levels by the end of the experiment, its role in ROS levels might only be an initial response, where its stabilisation would reflect a shift to other mechanisms for redox control.

Targeted analysis of the implicated pathways, as well as analysis of levels of ROS and lipid peroxidation through targeting its likely products (Noctor *et al.*, 2015), would give more insight into the severity of the damage and thus the extent of selective pressure it entails. Furthermore, metabolomic analysis of resistant cells experiencing the ancestral, glyphosate free environment would allow untangling adaptive and plastic response, answering what part of the metabolomic profile can be attributed to ongoing glyphosate action and what is caused by the resistance trait.

5.5.4 LIMITATIONS, BROADER IMPLICATIONS AND FUTURE RESEARCH

Untargeted metabolomic screening as used here is a powerful and fast hypothesis generating tool for extracting as much information as possible out of a small sample, allowing a high throughput and unbiased broad spectrum analysis of altered biochemical pathways (Overy *et al.*, 2005). Limiting sample size is particularly important when analysing cells grown in chemostats for longitudinal studies as sampling is destructive and perturbs the populations (Fischer *et al.*, 2014). However, the method comes with a number of caveats such as risk of ion suppression and inability to conclusively identify the compounds causing the mass peaks as well as definitely rule out the presence of a given compound.

While MS/MS analysis was able to strengthen the evidence for the presence of a number of targeted

and putatively identified compounds, we were limited by the availability of MassBank reference spectra and could not test all the compounds of interest for this study. Targeted analysis using chromatography would allow both confirming the absence of specific compounds (e.g. glyphosate degradation products) and to with higher accuracy quantify others as a measure of pathway functioning (e.g. shikimate-3-phosphate). It is also worth noting that the extended metabolomic fingerprint analysis presented here is only the tip of the iceberg, as each analysed sample generates over 5700 mass bins, each comprising several mass peaks. More extensive data analysis would certainly reveal more mass bins with significant differences between treatments and putative identity matches that could shine further light on the involved pathways and generate more specific hypotheses for further testing and targeted analysis. In particular, targeted analysis of metabolites involved in membrane lipid production as well as cellular redox balance would provide more material for evaluating the persistent effects of glyphosate action as these have the potential to affect resistant crops as well as weeds and non-target species after resistance has evolved. Connecting the phenotype observed to a genotype through employing genomics and transcriptomics would also allow greater understanding of the genetic underpinnings of the resistance mechanism, specifically it would be useful to test for nucleotide substitutions in the EPSPS gene as well as measuring whether its transcription has been up-regulated (Baerson *et al.*, 2002; Eschenburg *et al.*, 2002; Fonseca *et al.*, 2020; Funke *et al.*, 2009; Gaines *et al.*, 2019; Healy-Fried *et al.*, 2007; Patterson *et al.*, 2018).

The data presented here is by design an average of multiple populations, each representing a separate evolutionary trajectory. However, the low variance found between replicates in the models fit for many compounds suggests the early stages of adaptation to glyphosate in this system are highly replicable, although whether that depends on selection being mostly on standing variation or through a few commonly occurring *de novo*-mutations is not possible to say. A longer running study, combined with exploratory analysis targeting mass bins where there is a high level of variance in the treated populations but not the controls, would reveal if there are later divergences in strategy as the populations continue to adapt to the glyphosate treatment. It could also reveal how persistent the oxidative damage of glyphosate is, and whether the populations evolve a more extensive defence against it.

Metabolomic fingerprinting is also a useful tool for monitoring of environmental pollutants in natural ecosystems (Bundy *et al.*, 2009), and the results here emphasise that adaptation to the pollutants needs to be taken into account and that the stage of evolution of resistance matters for the fingerprint associated with the pollutant. While the acute metabolomic response to glyphosate is the build-up of shikimate pathway products, this is not present in the profile of the resistant strain, a shift that happens relatively quickly. However, our results still suggest there is indeed a distinctive metabolite profile for *C. reinhardtii* cells experiencing glyphosate action, regardless of whether the population is resistant or susceptible, but that this is primarily related to oxidative damage and membrane lipids rather than the shikimate pathway.

In addition to implications for monitoring strategies, this has the potential for far reaching consequences in natural ecosystems exposed to glyphosate contamination, especially if this reflects permanent changes to the algal cells. Firstly, as primary producers, their biochemical composition determines their quality as food and this determines the energy transferred to other trophic levels (Pinto *et al.*, 2003). If the changes are sufficiently large, it may lead to changes in foraging behaviour of grazing species or ultimately, restructuring of food webs. Secondly, if the changes in membrane lipid content indeed corresponds to a change in membrane structure, this may affect the clumping anti-grazer response or the digestability of the cells (Becks *et al.*, 2012; DeMott, 1995; Hamm *et al.*, 2003; Harvey *et al.*, 2015; Liu *et al.*, 2016; Lürling & Beekman, 2006; Pondaven *et al.*, 2007; Porter, 1975; Van Donk *et al.*, 1997), which will have an effect of energy transfer to grazing species. Thirdly, as oxidative damage is a secondary effect found from many stressors (Noctor *et al.*, 2015), this provides a mechanism for interactive effects of stressors. It is possible that a strong evolved cellular machinery to cope with the oxidative damage from glyphosate may provide a generalist defence against damage related to other stressors, but it is also possible that a combination of stressors could have an additive or synergistic effect (Gomes *et al.*, 2019; Yu *et al.*,

2021).

Lastly, while the exact molecular mechanisms may be species dependent, this study highlights the necessity of tackling the problem of herbicide resistance and management as a continuous, population level evolutionary process. The effects of a herbicide will be dependent on when in the process of resistance evolution it is applied, and different resistance mechanisms will evolve sequentially, and continue to evolve with time. Particularly pertinent is understanding the full effects of the herbicide on a molecular level at all stages to be able to predict its population- and ecosystem-level effects, as secondary effects like oxidative damage may continue to affect the organism after resistance to the primary mode of action has evolved.

CHAPTER 6

General discussion

6.1 SUMMARY OF FINDINGS

Herbicide resistance is a major challenge to agricultural productivity, and an often overlooked but vital factor in the effects of herbicide contamination to non-target ecosystems. This is especially true in the case of glyphosate, which due to its widespread use is both hugely economically important and a strong selective pressure leading to the rapid evolution of new resistant species and new mechanisms of resistance. Understanding, managing and mitigating the consequences of herbicide resistant weeds as well as herbicide contamination requires detail on the evolutionary, ecological and molecular features of resistance. Experimental evolution using model systems like *Chlamydomonas reinhardtii* provides the opportunity to test the evolutionary theory under controlled lab conditions with huge population sizes and fast generation times, giving detailed insight both to weed science and evolutionary biology.

In this thesis, I:

- Develop a tractable DIY multiplexed chemostat array system for longitudinal experimental evolution studies using algae (dubbed "mesostats") that is cheap and easy to build as well as run and maintain by one person.
- Use the mesostat system to evolve glyphosate resistance in *C. reinhardtii* in response to lethal and sublethal levels of glyphosate and characterise the population level fluctuations throughout to determine when resistance has evolved.
- Test the effects of glyphosate resistance evolution in action on growth in a range of doses of glyphosate as well as the ancestral environment to characterise the level of resistance as well as possible intrinsic fitness costs.
- Test the effects of evolved herbicide resistance on *C. reinhardtii* anti-grazer defences by introducing a second model organism: freshwater rotifer *Brachionus calyciflorus*, evaluating both the ability to deploy the defence in response to *B. calyciflorus* infochemicals and ability to withstand grazing by live rotifers.
- Use targeted metabolomic fingerprinting analysis to determine the effect of evolving and evolved glyphosate resistance on shikimate pathway compounds, possible glyphosate degradation pathway products and the amino acid pool, to gain insight into the evolutionary process and possible resistance mechanisms.
- Use exploratory metabolomic fingerprinting analysis to identify compounds that may be associated with evolving or evolved glyphosate resistance, to gain insight into effects on the cell metabolome beyond the shikimate pathway as well as possible resistance mechanisms.

6.1.1 EVIDENCE FOR RAPID EVOLUTION OF GLYPHOSATE RESISTANCE

Evidence for evolving glyphosate resistance was consistently detected across experiments. Both the inhibiting herbicidal action and its subsequent release had an effect on growth in the evolving

populations, across a range of glyphosate doses and in the absence of glyphosate, as well as impacted the relative concentration of metabolic compounds in both the shikimate pathway and other vital cellular processes.

The population density data shows a decline in response to the lethal glyphosate dose, followed by a resurgence Figure 6.1. The sustained growth of the population and the establishment of a new stationary phase is evidence of evolved resistance and a necessarily increased minimum inhibitory concentration (MIC), although it does not reveal the extent of that shift or whether it is associated with any fitness consequences for other traits. The earliest inflection point is 19 days after the treatment was initiated, and the latest is 22 days. This is somewhat faster than what has been found in other studies using *C. reinhardtii* and glyphosate (Lagator *et al.*, 2013a; Melero-Jiménez *et al.*, 2021), likely owing to the very large population sizes and lack of evolutionary bottlenecks. As the populations are likely genetically heterogeneous, consisting of multiple, co-existing lineages (Gresham *et al.*, 2008; Hong & Gresham, 2014; Kao & Sherlock, 2008; Kinnersley *et al.*, 2009; Kvitek & Sherlock, 2011; Maharjan *et al.*, 2006, 2012; Wenger *et al.*, 2011), it is likely that the resistant phenotype was present earlier in the population, the inflection point merely reflects the point at which dividing cells carrying it became dominant over growth-inhibited cells.

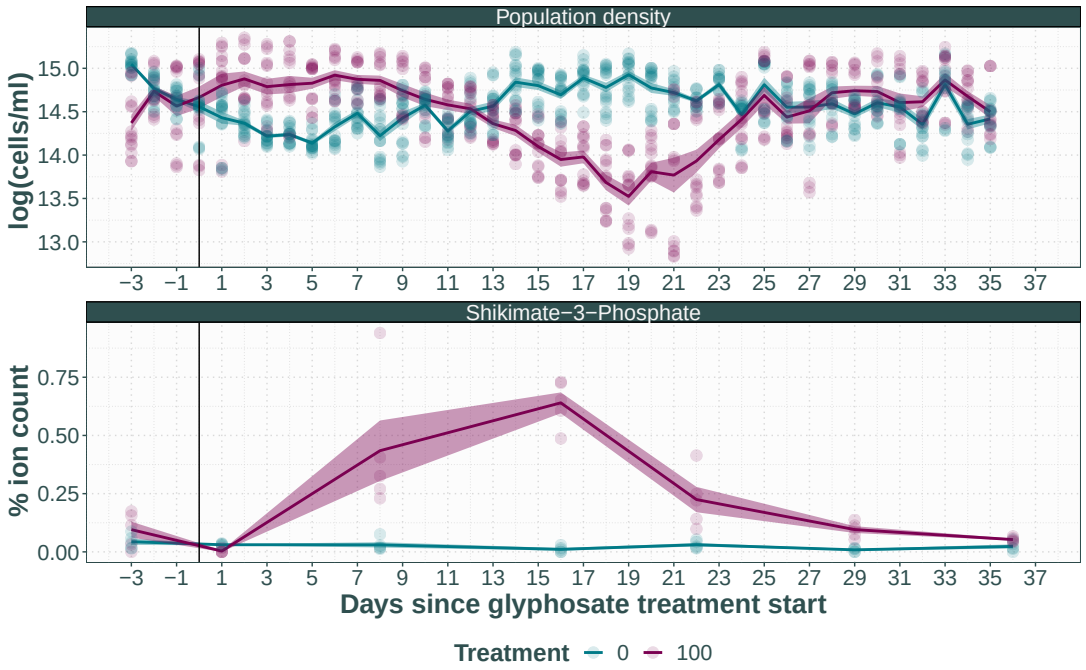

Figure 6.1: Population density (above) and the % ion count of shikimate-3-phosphate (below) in the evolving populations with time. Transparent points represent raw data, with opaque lines representing the treatment average with standard error transparent ribbon.

The results from the metabolomics screen provides further evidence to support initial growth inhibition followed by evolved resistance. This build-up of shikimate in particular is considered a hallmark of glyphosate toxicity, and its absence is strongly associated with resistance (Aristilde *et al.*, 2017; de María *et al.*, 2006; Felline *et al.*, 2019; Kostopoulou *et al.*, 2020; Maroli *et al.*, 2015, 2018; Oikawa *et al.*, 2006; Sikorski *et al.*, 2019; Wang, 2001; Zabalza *et al.*, 2017; Zhong *et al.*, 2018), and this exact pattern was found in the data presented in chapter 5. The mass bins matched to the shikimate pathway compounds upstream of EPSPS show significantly increased ion counts at the time points following the introduction of the lethal glyphosate dose, with a peak around

the same time as the inflection point in the population density data, before the return to control level as the population density goes through recovery and reaches a new steady state Figure 6.1. Furthermore, a number of mass bins matched to amino acids as well as those putatively matched to compounds in a wide range of metabolic roles, including several other pathways related to carbon metabolism, also show this pattern. This is evidence of the majority of the cells in each evolving population experiencing growth-inhibition and large scale disruption to cell functioning which is subsequently lifted by resistance. The pattern and pace of return of ion counts to control levels depends on the specific mass bin, and thus compound, with some being significantly different up until the last time point. This may be reflective of several mutations accumulating with time as the populations adapt, but it is also likely to be an artefact of the heterogeneous population genetics. Even after resistance has become the dominant phenotype, there will be a period during which a large proportion of the population is still growth-inhibited and dying cells, which is likely to present as a continued presence of compounds associated with cellular breakdown and death.

Evolved resistance is expected to confer increased growth at the dose of glyphosate the population was adapted to as well as in lower doses compared to the ancestral strain, indicated a shifted MIC. The growth assays tested the level of resistance throughout the course of the experiment, but failed to find evidence for an increased MIC at any point. Instead an unexpected pattern emerged, where the glyphosate-treated populations showed a decreased performance both in the presence and absence of glyphosate before returning to control levels by the end of the experiment. This is again a likely artefact of the heterogeneous populations, and the decreased performance the signal of a population consisting largely of growth-inhibited and dying cells. A new, fitter genotype will only have a noticeable signal in the assays once it has reached a larger proportion of the population and thus a lag between the emergence of a new lineage and its detectability in the growth assays as performed here is likely, and the coexistence of less fit lineages means the true fitness of any new mutation is likely to be underestimated. However, while this masking effect makes it impossible to detect the magnitude of the shifted MIC, the performance recovery and return to control levels still reflects that adaptation has taken place, particularly in the light of the other data sets.

While the sublethal dose populations did not show evidence of growth-inhibition and subsequent recovery in the population density data, and were not part of the metabolomics screen due to time constraints, they do exhibit the same pattern as the lethal dose populations in the growth assays – a decrease in overall performance, followed by a recovery, suggesting there is both a toxic effect of the glyphosate dose and adaptation to overcome it. However, this tentative evidence of evolving resistance also suggests it is at a slower pace, lagging by about two weeks, likely due to presenting a weaker selective pressure than the lethal dose. By the end of the experiment they had not returned to control levels, but this is more likely due to a trajectory being cut short than evidence of a trade-off.

6.1.2 EVIDENCE FOR FITNESS COSTS AND TRADE-OFFS

6.1.2.1 INTRINSIC FITNESS COSTS

Intrinsic fitness costs were defined as trade-offs within the cell, where the resistance trait interferes with normal cell function or limits resources available for allocation to growth or reproduction. Theory suggests that intrinsic costs underpin the evolution of resistance when resistant phenotypes bear a growth rate cost in their ancestral environment. Even though the hallmarks of resistance were detected, there was no evidence of intrinsic fitness costs. For a reduction in growth rate in the ancestral environment to be considered a likely trade-off with glypohosate resistance it should be observed in conjunction with increased resistance. Even though a shift in the MIC must have occurred based on the evidence from the metabolomics and population density data sets, the lack of a detectable MIC increase in the growth assays by the end of the experiment means that there is not sufficient evidence to conclusively determine the presence or absence of a trade-off with population growth. However, as the intercept of of the dose-response relationship

was not significantly different between the controls and the resistant populations (Figure 3.4), it does indicate that the fitness consequence may be small if it exists.

Intrinsic costs would also have been apparent in the metabolomics data in the form of continued disruption to cell functioning, particularly in the form of continued elevated levels of upstream shikimate pathway substrates. In contrast, the functioning of the shikimate pathway appears to be returned to control level functioning by the end of the experiment with no remaining build-up of upstream substrates. This strongly suggests the resistance mechanism does not interfere with normal cell function in the form of EPSPS with a lowered binding affinity for PEP (Gaines *et al.*, 2020). The other markers of disrupted cell machinery, such as amino acids and compounds associated with other carbon metabolism pathways, also return to control levels by the end of the experiment. This too suggests that cell function and resource allocation is not strongly affected by the resistance mechanism. However, it should be noted that the resistant cells were still being exposed to glyphosate and that their metabolomic state will reflect that. Intrinsic fitness costs could still be revealed through a metabolomic screen of resistant cells experiencing the ancestral, glyphosate free environment. Furthermore, a smaller number of putative compounds identified by the exploratory analysis – largely lipids, fatty acids and redox electron-carriers – showed a pattern where differences between treatments emerged around the time resistance evolved and persisted until the end of the experiment. As these differences are likely to be related to the resistance mechanism they also provide possible mechanisms for trade-offs, intrinsic or extrinsic.

6.1.2.2 EXTRINSIC COSTS

Extrinsic fitness costs were defined as costs emerging when the resistant strain faced an additional stressor. This may in the form of changed tolerance of abiotic stressors, like cold temperatures (Ge *et al.*, 2011; Vila-Aiub *et al.*, 2013), or it may be through changing vital ecological interactions such as competition (Pedersen *et al.*, 2007), immune response (Salzmann *et al.*, 2008) or anti-herbivore defence (Gassmann & Futuyma, 2004; Gassmann, 2005). Changed ecological interactions are of particular interest as they have the potential to affect entire ecosystems.

C. reinhardtii has a well-studied and easily observable anti-grazing response in the form of clumping, that could theoretically be affected by evolved glyphosate resistance through both resource allocation or structural mechanisms. However, the glyphosate resistant cells challenged here with *B. calyciflorus* kairomones as well as grazing by live rotifers did not show a unidirectional response, instead glyphosate resistance appeared to increase variation in defence induction compared to the controls. Notably, two populations, one from the lethal glyphosate treatment and one from the sublethal, lost their ability to clump in response to rotifer kairomones, which was associated with an increased clearance rate by live rotifers. The other glyphosate-treated populations appeared to generally clump at the same level as the controls, but the associated clearance rates by live rotifers were both lower and, in one case, much higher. This is the clearest evidence in the thesis of the separate evolutionary trajectories of the treated populations resulting in different phenotypes with the potential for completely separate outcomes in a natural ecosystem.

The observed trade-off could be due to resource allocation limits – while the resistance trait may not require enough extra resources that it affects growth in an environment with plentiful nutrients, it could still be too costly to allow enough resources to be available for a costly inducible trait like clumping (Becks *et al.*, 2012; Marañón, 2015; Raven & Kubler, 2002). Furthermore, the cells were transferred to water with very low levels of nutrients to perform the tests, which may have presented an extra challenge for the cells. Indeed, some studies suggest that resource allocation trade-offs only reveal themselves when resources are severely restricted (Becks *et al.*, 2012; Pančić & Kiørboe, 2018). However, the metabolomics screens provide some further insights into the possible mechanism(s) for the observed trade-offs. The cells may still be suffering the effects of increased ROS and lipid peroxidation as a secondary effect of glyphosate, preventing successful formation of clumps or reducing the robustness of the clumps through effects on the cell wall or the extracellular mucous matrix (Demidchik, 2015). This could also be assumed to have a potential effect

on the digestability of the cell (DeMott, 1995; Hamm *et al.*, 2003; Harvey *et al.*, 2015; Liu *et al.*, 2016; Pondaven *et al.*, 2007; Porter, 1975; Van Donk *et al.*, 1997). Alternatively, if the resistance mechanism includes cell wall changes to withstand the effects of ROS and lipid peroxidation this could be what is affecting clumping ability or the digestability of the cell (Pinto *et al.*, 2003; Stupak *et al.*, 2019).

6.1.3 DETERMINATION OF RESISTANCE MECHANISM

While none of the experiments presented in this thesis found clear evidence for any particular mechanism being responsible for the resistance trait, some mechanisms emerge as far more likely than others when the results are taken together. The metabolomics screen was able to rule out glyphosate degradation with some confidence along with finding no evidence for decreased absorption, increased vacuolar sequestration or glyphosate-insensitive EPSPS, although no conclusive evidence was found against these mechanisms. The population density and metabolomics data sets show that the glyphosate resistant phenotype becomes dominant quickly, and the population density data only shows one clear point in changed fitness. This would suggest a mechanism dependent on only one, or very few, changes at the genetic level and not the result of several, sequential mutations.

The metabolomic screens and the growth assays indicate that the intrinsic cost to the resistance mechanism is negligible, and is likely not one of the target-site mutations that results in EPSPS with a lower affinity for PEP (Gaines *et al.*, 2020). While it is possible for a single substitution to result in this phenotype (Beres *et al.*, 2020; Li *et al.*, 2018), it is more commonly the result of double or triple substitutions in sequential mutation events (Alcántara-de la Cruz *et al.*, 2016; García *et al.*, 2019; Mendes *et al.*, 2020; Perotti *et al.*, 2019; Yu *et al.*, 2015). It is possible that the gradual return of the ion count to control levels in the mass bin matched to shikimate-3-phosphate could be the result of stepwise accumulation of mutations, but it is also highly likely to be the signal of growth-inhibited cells remaining in the population until they die. However, while the MIC increase could not be accurately measured, the growth and death assays indicate that it may be relatively modest. This would suggest that double or triple mutants with a very strong insensitivity to glyphosate are not the underlying mechanism.

By process of elimination, EPSPS amplification thus remains as the mechanism most likely to be responsible for the resistance seen in these populations, conferring a low level of resistance sufficient for survival in the applied dose but not at higher doses and with fitness costs absent or complex (Baerson *et al.*, 2002; Gaines *et al.*, 2019; Martin *et al.*, 2017; Osipitan & Dille, 2017; Patterson *et al.*, 2018; Vila-Aiub *et al.*, 2014; Yanniccari *et al.*, 2016). However, as two distinct trade-off patterns with anti-grazer defences was observed in some populations but not all, it suggests there are at least three different dominant phenotypes present at that time point. If the extrinsic costs are due to a trade-off through the primary resistance mechanism, this may indicate that there are different resistance mechanisms at play, e.g. different degrees of amplification or different mechanisms of amplification may confer different resource allocation costs (Gaines *et al.*, 2016; Jugulam *et al.*, 2014; Koo *et al.*, 2018; Martin *et al.*, 2017; Osipitan & Dille, 2017; Patterson *et al.*, 2019; Vila-Aiub *et al.*, 2014; Yanniccari *et al.*, 2016). However if the trade-off is instead due to remaining secondary effects of the glyphosate through ROS and lipid peroxidation, it suggests that the populations not affected by this has evolved resistance against the secondary effects as well, which may be through a different mechanism than the one responsible for lifting the shikimate pathway blockage.

Lastly, it is important to keep in mind that while the lethal and sublethal dose populations show some common traits compared to the controls, they are experiencing different selective pressures and are thus likely to be on evolutionary trajectories headed for different fitness optima. This may mean that different resistance mechanisms are favoured under the different treatments (Busi & Powles, 2009; Busi *et al.*, 2013; Cairns *et al.*, 2022; Gressel, 2011; Love & Wagner, 2022;

Norsworthy *et al.*, 2021). Furthermore, all measures attempting to characterise the resistance mechanism presented in this thesis looks at the average of the whole population. Each population is likely to contain several coexisting genotypes of similar fitness that may have their resistance trait conferred by different mechanisms.

6.2 LIMITATIONS

There are two classes of potential limitations to the conclusions that can be drawn from this work: translating insights gained in one species across taxa as well as the implications of the experimental design.

6.2.1 TAXONOMIC LIMITATIONS

While a lab population of *C. reinhardtii* has many benefits as a model system making it more suitable for long-term experimental evolution in the lab, there are a number of factors that complicate translating the results to higher plants, and thus to agriculture. Higher plants are multi-cellular organisms with specialised tissues, meaning there is a potential for more ways the herbicide can affect the organism, as well as more possible resistance mechanisms against the herbicide (Gaines *et al.*, 2020; Powles & Yu, 2010). In fact, many non-target site resistance mechanisms in higher plants rely on protecting the meristem through translocating the herbicide to less vital tissues, a mechanism that is not possible in unicellular organisms like *C. reinhardtii* (Gaines *et al.*, 2020). As there may be a species effect on not just which resistance mechanism is favoured, but whether it confers a fitness cost and in which circumstances (Gaines *et al.*, 2020; Powles & Yu, 2010), the generalisability of some of the results presented in this thesis may be limited.

There are also genetic differences between higher plants and *C. reinhardtii* which may affect the dynamics of evolution. Firstly, *C. reinhardtii* is haploid (Harris *et al.*, 1989), while higher plants are diploid or polyploid. This means that there is no effect of trait dominance in *C. reinhardtii*, and while the fixation rate of dominant traits is expected to be the same in haploid and diploid organisms, a recessive allele is likely to see an increased rate of fixation in a haploid organism (Charlesworth, 1992). While the dominance of the resistance trait observed in the populations presented in this thesis is unknown, there is a distinct possibility other alleles may have been favoured in a diploid organism. Secondly, while some higher plants are able to self-fertilise, they generally reproduce sexually (Barrett, 2002), and all *C. reinhardtii* populations in this thesis were kept under conditions where they remained asexual. This difference may instead have slowed down the rate of adaptation, as sexual reproduction increases both genetic variation and the rate of fixation of dominant alleles (Agrawal, 2006; Colegrave, 2002). Taken together, these present a considerable caveat as dominant alleles appear to be more common among those characterised as conferring resistance in natural weed populations, and level of outcrossing has been suggested to be important in cases where several mutations are required for resistance (Powles & Yu, 2010).

6.2.2 EXPERIMENTAL DESIGN LIMITATIONS

Furthermore, the conditions of the lab with a monoculture, a single strong selective pressure, constant exponential growth and no gene flow between populations, presents another difference from the natural world, affecting the conclusions we can draw for both agricultural and non-target ecosystems. However, *C. reinhardtii* as a ubiquitously occurring species (Harris *et al.*, 1989) is likely to itself be affected by contamination of non-target ecosystems and more generally in trying to understand the overall effects on a community of species, understanding the effects on individual

species is an important piece of the puzzle. *C. reinhardtii*'s response to glyphosate exposure is also likely to be more generalisable to other green algae that may be affected by glyphosate pollution simply based on structural and genetic similarity.

While the chemostat environment is useful for simplifying some aspects of experimental evolution, in particular ensuring the constancy of the selective pressure and reducing the role of genetic drift through eliminating evolutionary bottlenecks (Gresham & Hong, 2014), they do present other caveats. A recurring finding in experimental evolution using chemostats is the long-term maintenance of heterogeneous populations of coexisting but genetically distinct lineages with differing fitness strategies, with soft sweeps to fixation being more common than hard ones (Gresham *et al.*, 2008; Hong & Gresham, 2014; Kao & Sherlock, 2008; Kinnersley *et al.*, 2009; Kvitek & Sherlock, 2011; Maharjan *et al.*, 2006, 2012; Wenger *et al.*, 2011). While batch cultures are by no means assumed to be genetically homogeneous, this will affect the interpretation of any comparisons of experiments. Furthermore, in batch cultures the evolutionary bottleneck at each transfer will be highly effective at removing dead or permanently growth-inhibited cells from the population as only a small number will be transferred and they will quickly be outnumbered by the cells that can grow. In the chemostat populations, they remain until they die or are flushed out, resulting in the possibility of a masking effect in assays such as the ones presented in this thesis, where the measures are of the population average. The growth assays in particular resulted in inconclusive results due to this limitation.

6.3 BROADER PERSPECTIVE

This thesis highlights the necessity of tackling the problem of herbicide resistance as a continuous, population level evolutionary process, the understanding of which needs to be based on a mixture of ecological, evolutionary and molecular data to make robust inferences about how and when resistance arises, and thus how to manage it. Furthermore, it shows the value of experimental evolution of model species as a tool to collect this type of data and create a profile of resistance evolution in action, connecting intrinsic and extrinsic mechanisms to make predictions for natural populations.

Particularly pertinent is also understanding the full effects of the herbicide on a molecular level to be able to predict its population- and ecosystem-level effects. The existence of non-universal extrinsic costs in the form of a trade-off with anti-grazer defence means the outcomes of adaptation to glyphosate pollution could have starkly different outcomes depending on the mechanism of resistance. The metabolomics data suggests that after the shikimate pathway blockage has been lifted, ROS continue to either have a direct effect or assert a selective pressure strong enough to result in changed redox activity and possibly membrane structure. This matches findings by Maroli *et al.* (2015, 2018) suggesting that even glyphosate resistant strains, including genetically engineered resistant crops, may still be negatively affected by glyphosate application which means management strategies may have to take into account direct effects of the herbicide application on the yield. Similarly, management strategies for pollution of natural ecosystems need to account for continued harmful effects even in cases where the non-target species evolve resistance.

Lastly, while the lethal and sublethal dose populations are experiencing different selective pressures and are thus likely to be on evolutionary trajectories headed for different fitness optima, they show common patterns in both the growth assays and the existence of possible trade-offs with anti-grazer defences. Furthermore, each population within the same treatment represents a separate evolutionary trajectory, yet there was little variation in the patterns identified in the population density, growth assays and metabolomics. The fact that the populations behave very similarly suggests there may be a limited number of first steps in the evolution of resistance for this system. As the populations were all established from the same founding population it is possible that e.g. variation in EPSPS copy number was present as part of standing variation in sufficient proportions to end up in all daughter populations, but it is also possible that a limited number of *de novo*-

mutations are both common enough and provide a large enough fitness benefit in early exposure that they tend to be the first to sweep to fixation (Gresham *et al.*, 2008; Gresham & Hong, 2014). While it is unclear whether the high replicability found in this system is reflected in higher plants, it highlights the necessity of studying and characterising populations under ongoing adaptation as that may inform the best strategy for preventing it in other populations of the same species.

6.4 FUTURE RESEARCH

The model system experimental evolution framework presented here allows theoretical endless replication of the course of resistance evolution where the selective pressures can be tightly controlled and varied to pick apart and test the basic assumptions of evolutionary theory. This is particularly powerful in combination with continuous sampling and the creation of a frozen "fossil record" of samples for molecular analysis (Elena & Lenski, 2003). The metabolomics analysis presented here generated several hypotheses for future work to test with targeted analysis and combining with genomics, transcriptomics and proteomics. The mechanism(s) of resistance should be conclusively determined and further investigation of the effects of ROS and lipid peroxidation, as well as induced or evolved resistance against it, prioritised. As the metabolomics data presented here only covers the lethal populations under acute exposure, future studies should compare to cells acclimated to ancestral environment as well as the effects of sublethal doses. This would allow a fuller understanding of which persistent effects are due to glyphosate exposure, and which are due to the resistance mechanism. Furthermore, characterisation of the level of standing genetic variation prior to exposure as well as the rate of resistance-conferring *de novo*-mutations would allow connecting these population traits to both the early and late events in the course of resistance evolution, and as the mesostat system was designed for long-term experimental evolution, eventual sequential refinement of the resistance trait could be monitored. It would be particularly interesting to reach more detailed understanding of the dynamics of arising single-gene vs. polygenic resistance traits, and isolation and tagging of separate resistant strains would allow competition assays to determine their relative fitness. As inducing sexual reproduction in *C. reinhardtii* is relatively straight-forward (Harris *et al.*, 1989), the effects of out-crossing vs. selfing on the dynamics of resistance evolution could also be tested.

Furthermore, the mesostat system was specifically designed for experimental evolution of algae with the explicit view to be able to introduce more planktonic species for the experimental evolution of whole mesocosms. Future work would continue to explore the *C. reinhardtii*-*B. calyciflorus*-glyphosate system to untangle how adaptation to one stressor affects the adaptation to the other with sequential exposure, and testing how simultaneous exposure to both may constrain and shape the course of adaptation. This should also include testing of the effects of independent glyphosate exposure on *B. calyciflorus* as well as introducing *B. calyciflorus* to be cultured with *C. reinhardtii* undergoing adaptation to glyphosate at different timepoints. It would be of particular interest to here also test the effects of a greater ranger of sublethal levels of glyphosate as their effects are particularly relevant to contaminated non-target ecosystems in terms of resistance mechanisms favoured and potential extrinsic trade-offs.

References

Agrawal, A. F. (2006). 'Evolution of Sex: Why Do Organisms Shuffle Their Genotypes?' *Current Biology* 16 (17), R696–R704.

Ahsan, N., Lee, D.-G., Lee, K.-W., Alam, I., Lee, S.-H., Bahk, J. D. & Lee, B.-H. (2008). 'Glyphosate-Induced Oxidative Stress in Rice Leaves Revealed by Proteomic Approach'. *Plant Physiology and Biochemistry* 46 (12), 1062–70.

Alcántara-de la Cruz, R., Fernández-Moreno, P. T., Ozuna, C. V., Rojano-Delgado, A. M., Cruz-Hipolito, H. E., Domínguez-Valenzuela, J. A., Barro, F. & De Prado, R. (2016). 'Target and Non-target Site Mechanisms Developed by Glyphosate-Resistant Hairy Beggarticks (*Bidens pilosa* L.) Populations from Mexico'. *Frontiers in Plant Science* 7, 1492.

Amalin, D., Peña, J., Duncan, R., Leavengood, J. & Koptur, S. (2009). 'Effects of Pesticides on the Arthropod Community in the Agricultural Areas near the Everglades National Park.' *Proceedings of Florida State Horticultural Society* 122, 429–37.

Annett, R., Habibi, H. R. & Hontela, A. (2014). 'Impact of Glyphosate and Glyphosate-Based Herbicides on the Freshwater Environment'. *Journal of Applied Toxicology* 34 (5), 458–79.

Aristilde, L., Reed, M. L., Wilkes, R. A., Youngster, T., Kukurugya, M. A., Katz, V. & Sasaki, C. R. S. (2017). 'Glyphosate-Induced Specific and Widespread Perturbations in the Metabolome of Soil *Pseudomonas* Species'. *Frontiers in Environmental Science* 5, 34.

Ashigh, J. & Tardif, F. J. (2007). 'An Ala_{205}Val Substitution in Acetohydroxyacid Synthase of Eastern Black Nightshade (*Solanum ptychanthum*) Reduces Sensitivity to Herbicides and Feedback Inhibition'. *Weed Science* 55 (6), 558–65.

Ashigh, J. & Tardif, F. J. (2009). 'An Amino Acid Substitution at Position 205 of Acetohydroxyacid Synthase Reduces Fitness under Optimal Light in Resistant Populations of *Solanum ptychanthum*'. *Weed Research* 49 (5), 479–89.

Ashigh, J. & Tardif, F. J. (2011). 'Water and Temperature Stress Impact Fitness of Acetohydroxyacid Synthase–Inhibiting Herbicide-Resistant Populations of Eastern Black Nightshade (*Solanum ptychanthum*)'. *Weed Science* 59 (3), 341–8.

ASTM (1989). 'Standard Guide for Conducting Acute Toxicity Tests with Fishes, Macroinvertebrates and Amphibians'. In: *Annual Book of ASTM Standards*. Vol. 11.04. ASTM International, West Conshohocken, PA, USA., 379–97.

Baerson, S. R., Rodriguez, D. J., Biest, N. A., Tran, M., You, J., Kreuger, R. W., Dill, G. M., Pratley, J. E. & Gruys, K. J. (2002). 'Investigating the Mechanism of Glyphosate Resistance in Rigid Ryegrass (*Lolium ridigum*)'. *Weed Science* 50.6, 721–30.

Barrett, K. A. & McBride, M. B. (2005). 'Oxidative Degradation of Glyphosate and Aminomethylphosphonate by Manganese Oxide'. *Environmental Science & Technology* 39 (23), 9223–8.

Barrick, J. E. & Lenski, R. E. (2013). 'Genome Dynamics During Experimental Evolution'. *Nature Reviews Genetics* 14 (12), 827–39.

Barry, G. & Kishore, G. (1995). *Glyphosate Tolerant Plants.* URL: `https://patents.google.com/patent/US5463175`.

Barrett, S. C. H. (2002). 'The Evolution of Plant Sexual Diversity'. *Nature Reviews Genetics* 3 (4), 274–84.

Bastiaans, L., Paoilini, R. & Baumann, D. T. (2008). 'Focus on Ecological Weed Management: What is Hindering Adoption?' *Weed Research* 48 (6), 481–91.

Baselga-Cervera, B., Lopez-Rodas, V., Balboa, G., Huertas Cabilla, E. I. & Costas, E. (2016). 'Mechanisms of Rapid Adaptation to Environmental Stressors in Phytoplankton'. *Journal of Environmental & Analytical Toxicology* 6 (5), 405.

Bates, D., Mächler, M., Bolker, B. & Walker, S. (2015). 'Fitting Linear Mixed-Effects Models Using `lme4`'. *Journal of Statistical Software* 67.1, 1–48.

Baucom, R. S. (2019). 'Evolutionary and Ecological Insights from Herbicide-Resistant Weeds: What Have We Learned About Plant Adaptation, and What is Left to Uncover?' *New Phytologist* 223 (1), 68–82.

Becks, L., Ellner, S. P., Jones, L. E. & Hairston, N. G. (2012). 'The Functional Genomics of an Eco-Evolutionary Feedback Loop: Linking Gene Expression, Trait Evolution, and Community Dynamics'. *Ecology Letters* 15 (5), 492–501.

Beckie, H. J. (2006). 'Herbicide-Resistant Weeds: Management Tactics and Practices'. *Weed Technology* 20 (3), 793–814.

Ben-Shachar, M. S., Lüdecke, D. & Makowski, D. (2020). '`effectsize`: Estimation of Effect Size Indices and Standardized Parameters'. *Journal of Open Source Software* 5.56, 2815. URL: `https://doi.org/10.21105/joss.02815`.

Benbrook, C. M. (2016). 'Trends in Glyphosate Herbicide Use in the United States and Globally'. *Environmental Sciences Europe* 28 (1), 3.

Beres, Z. T., Giese, L. A., Mackey, D. M., Owen, M. D. K., Page, E. R. & Snow, A. A. (2020). 'Target-Site EPSPS Pro-106-Ser Mutation in *Conyza canadensis* Biotypes with Extreme Resistance to Glyphosate in Ohio and Iowa, USA'. *Scientific Reports* 10 (1), 7577.

Bessa da Silva, M., Abrantes, N., Rocha-Santos, T., Duarte, A., Freitas, A., Gomes, A., Carvalho, A., Marques, J., Gonçalves, F. & Pereira, R. (2016). 'Effects of Dietary Exposure to Herbicide and of the Nutritive Quality of Contaminated Food on the Reproductive Output of *Daphnia magna*'. *Aquatic Toxicology* 179, 1–7.

Blann, K. L., Anderson, J. L., Sands, G. R. & Vondracek, B. (2009). 'Effects of Agricultural Drainage on Aquatic Ecosystems: A Review'. *Critical Reviews in Environmental Science and Technology* 39 (11), 909–1001.

Boldt, T. S. & Jacobsen, C. S. (1998). 'Different Toxic Effects of the Sulfonylurea Herbicides Metsulfuron Methyl, Chlorsulfuron and Thifensulfuron Methyl on Fluorescent Pseudomonads Isolated from an Agricultural Soil'. *FEMS Microbiology Letters* 161 (1), 29–35.

Boraas, M. E., Seale, D. B. & Boxhorn, J. E. (1998). 'Phagotrophy by Flagellate Selects for Colonial Prey: A Possible Origin of Multicellularity'. *Evolutionary Ecology* 12 (2), 153–64.

Böttcher, C., Centeno, D., Freitag, J., Höfgen, R., Köhl, K., Kopka, J., Kroymann, J., Matros, A., Mock, H.-P., Neumann, S., Pfalz, M., Roepenack-Lahaye, E. von, Schauer, N., Trenkamp, S., Zubriggen, M. & Fernie, A. R. (Nov. 2007). 'Teaching (and learning from) metabolomics: The 2006 PlantMetaNet ETNA Metabolomics Research School'. *Physiologia Plantarum* 0 (0), 136–49.

Brausemann, A., Gemmecker, S., Koschmieder, J., Ghisla, S., Beyer, P. & Einsle, O. (2017). 'Structure of Phytoene Desaturase Provides Insights into Herbicide Binding and Reaction Mechanisms Involved in Carotene Desaturation'. *Structure* 25 (8), 1222–32.e3.

Bracamonte, E., Silveira, H. M. da, Cruz, R. A.-d. la, Domínguez-Valenzuela, J. A., Cruz-Hipolito, H. E. & Prado, R. D. (2018). 'From Tolerance to Resistance: Mechanisms Governing the Differential Response to Glyphosate in *Chloris barbata*'. *Pest Management Science* 74 (5), 1118–24.

Brühl, C. A., Schmidt, T., Pieper, S. & Alscher, A. (2013). 'Terrestrial Pesticide Exposure of Amphibians: An Underestimated Cause of Global Decline?' *Scientific Reports* 3 (1), 1135.

Bruggeman, A. J., Kuehler, D. & Weeks, D. P. (2014). 'Evaluation of Three Herbicide Resistance Genes for Use in Genetic Transformations and for Potential Crop Protection in Algae Production'. *Plant Biotechnology Journal* 12 (7), 894–902.

Bull, A. T. (2010). 'The Renaissance of Continuous Culture in the Post-Genomics age'. *Journal of Industrial Microbiology and Biotechnology* 37 (10), 993–1021.

Bundy, J. G., Davey, M. P. & Viant, M. R. (2009). 'Environmental Metabolomics: A Critical Review and Future Perspectives'. *Metabolomics* 5 (1), 3–21.

Busi, R. & Powles, S. B. (2009). 'Evolution of Glyphosate Resistance in a *Lolium rigidum* Population by Glyphosate Selection at Sublethal Doses'. *Heredity* 103 (4), 318–25.

Busi, R., Neve, P. & Powles, S. (2013). 'Evolved Polygenic Herbicide Resistance in *Lolium rigidum* by Low-Dose Herbicide Selection Within Standing Genetic Variation'. *Evolutionary Applications* 6 (2), 231–42.

Business Wire (2021). *Global $47.09 Bn Herbicides Market to 2025 & 2030 - ResearchAndMarkets.com*. Accessed: 11-04-2022. URL: `https://www.businesswire.com/`.

Cairns, J., Jousset, A., Becks, L. & Hiltunen, T. (2022). 'Effect of Mutation Supply on Population Dynamics and Trait Evolution in an Experimental Microbial Community'. *Ecology Letters* 25 (2), 355–65.

Caspi, R., Billington, R., Keseler, I. M., Kothari, A., Krummenacker, M., Midford, P. E., Ong, W. K., Paley, S., Subhraveti, P. & Karp, P. D. (Jan. 2020). 'The MetaCyc Database of Metabolic Pathways and Enzymes – A 2019 Update'. *Nucleic Acids Research* 48 (D1), D445–D453.

Cerdeira, A. L. & Duke, S. O. (2006). 'The Current Status and Environmental Impacts of Glyphosate-Resistant Crops'. *Journal of Environmental Quality* 35 (5), 1633–58.

Chapin, F. S. I., Autumn, K. & Pugnaire, F. (1993). 'Evolution of Suites of Traits in Response to Environmental Stress'. *American Naturalist* 142, S78–S92.

Charlesworth, B. (1992). 'Evolutionary Rates in Partially Self-Fertilizing Species'. *The American Naturalist* 140 (1), 126–48.

Chen, J., Huang, H., Wei, S., Cui, H., Li, X. & Zhang, C. (2020). 'Glyphosate Resistance in *Eleusine indica*: EPSPS overexpression and P106A Mutation Evolved in the Same Individuals'. *Pesticide Biochemistry and Physiology* 164, 203–8.

Chevillon, C., Pasteur, N., Marquine, M., Heyse, D. & Raymond, M. (1995). 'Population Structure and Dynamics of Selected Genes in the Mosquito *Culex pipiens*'. *Evolution* 49 (5), 997–1007.

Christin, M. S., Ménard, L., Giroux, I., Marcogliese, D. J., Ruby, S., Cyr, D., Fournier, M. & Brousseau, P. (2013). 'Effects of Agricultural Pesticides on the Health of *Rana pipiens* Frogs Sampled from the Field'. *Environmental Science and Pollution Research* 20 (2), 601–11.

Cohan, M., King, E. C. & Zawadzki, P. (1993). 'Amelioration of the Deleterious Pleiotropic Effects of an Adaptive Mutation in *Bacillus subtilis*'. *Evolution* 48 (1), 81–95.

Coley, P. D., Bryant, J. P. & Chapin, F. S. I. (1985). 'Resource Availability and Plant Antiherbivore Defense'. *Science* 230 (4728), 895–9.

Colombo, S. L., Andreo, C. S. & Chollet, R. (1998). 'The Interaction of Shikimic Acid and Protein Phosphorylation with PEP Carboxylase From the C4 Dicot *Amaranthus viridis*'. *Phytochemistry* 48 (1), 55–9.

Colegrave, N. (2002). 'Sex Releases the Speed Limit on Evolution'. *Nature* 420 (6916), 664–6.

Conard, S. G. & Radosevich, S. R. (1979). 'Ecological Fitness of *Senecio vulgaris* and *Amaranthus retroflexus* Biotypes Susceptible or Resistant to Atrazine'. *The Journal of Applied Ecology* 16 (1), 171.

Cummins, I., Dixon, D. P., Freitag-Pohl, S., Skipsey, M. & Edwards, R. (2011). 'Multiple Roles for Plant Glutathione Transferases in Xenobiotic Detoxification'. *Drug Metabolism Reviews* 43 (2), 266–80.

Dawson, A. H., Eddleston, M., Senarathna, L., Mohamed, F., Gawarammana, I., Bowe, S. J., Manuweera, G. & Buckley, N. A. (2010). 'Acute Human Lethal Toxicity of Agricultural Pesticides: A Prospective Cohort Study'. *PLoS Medicine* 7 (10), e1000357.

Dayan, F. E. (2019). 'Current Status and Future Prospects in Herbicide Discovery'. *Plants* 8 (9), 341.

de María, N., de Felipe, M. R. & Fernández-Pascual, M. (2005). 'Alterations Induced by Glyphosate on Lupin Photosynthetic Apparatus and Nodule Ultrastructure and Some Oxygen Diffusion Related Proteins'. *Plant Physiology and Biochemistry* 43 (10–11), 985–96.

de María, N., Becerril, J. M., García-Plazaola, J. I., Hernández, A., Felipe, M. R. de & Fernández-Pascual, M. (2006). 'New Insights on Glyphosate Mode of Action in Nodular Metabolism: Role of Shikimate Accumulation'. *Journal of Agricultural and Food Chemistry* 54 (7), 2621–8.

de Carvalho, L. B., da Costa Aguiar Alves, P. L., González-Torralva, F., Cruz-Hipolito, H. E., Rojano-Delgado, A. M., De Prado, R., Gil-Humanes, J., Barro, F. & de Castro, M. D. L. (2012). 'Pool of Resistance Mechanisms to Glyphosate in *Digitaria insularis*'. *Journal of Agricultural and Food Chemistry* 60 (2), 615–22.

de Carpentier, F., Lemaire, S. D. & Danon, A. (2019). 'When Unity Is Strength: The Strategies Used by *Chlamydomonas* to Survive Environmental Stresses'. *Cells* 8 (11), 1307.

Declerck, S. A. J., Malo, A. R., Diehl, S., Waasdorp, D., Lemmen, K. D., Proios, K. & Papakostas, S. (2015). 'Rapid Adaptation of Herbivore Consumers to Nutrient Limitation: Eco-Evolutionary Feedbacks to Population Demography and Resource control'. *Ecology Letters* 18 (6), 553–62.

Délye, C., Jasieniuk, M. & Corre, V. L. (2013). 'Deciphering the Evolution of Herbicide Resistance in Weeds'. *Trends in Genetics* 29 (11), 649–58.

Demidchik, V. (2015). 'Mechanisms of Oxidative Stress in Plants: From Classical Chemistry to Cell Biology'. *Environmental and Experimental Botany* 109, 212–28.

DeMott, W. R. (1995). 'The Influence of Prey Hardness on *Daphnia*'s Selectivity for Large Prey'. *Cladocera as Model Organisms in Biology*, 127–38.

Dénervaud, N., Becker, J., Delgado-Gonzalo, R., Damay, P., Rajkumar, A. S., Unser, M., Shore, D., Naef, F. & Maerkl, S. J. (2013). 'A Chemostat Array Enables the Spatio-Temporal Analysis of the Yeast Proteome'. *Proceedings of the National Academy of Sciences* 110 (39), 15842–7.

Diaz Vivancos, P., Driscoll, S. P., Bulman, C. A., Ying, L., Emami, K., Treumann, A., Mauve, C., Noctor, G. & Foyer, C. H. (2011). 'Perturbations of Amino Acid Metabolism Associated with Glyphosate-Dependent Inhibition of Shikimic Acid Metabolism Affect Cellular Redox Homeostasis and Alter the Abundance of Proteins Involved in Photosynthesis and Photorespiration'. *Plant Physiology* 157 (1), 256–68.

Dick, R. E. & Quinn, J. P. (1995). 'Glyphosate-Degrading Isolates from Environmental Samples: Occurrence and Pathways of Degradation'. *Applied Microbiology and Biotechnology* 43 (3), 545–50.

Diggle, A. J., Neve, P. B. & Smith, F. P. (2003). 'Herbicides Used in Combination can Reduce the Probability of Herbicide Resistance in Finite Weed Populations'. *Weed Research* 43 (5), 371–82.

Dill, G. M. (2005). 'Glyphosate-Resistant Crops: History, Status and Future'. *Pest Management Science* 61 (3), 219–24.

Dinkeloo, K., Boyd, S. & Pilot, G. (Feb. 2018). 'Update on Amino Acid Transporter Functions and on Possible Amino Acid Sensing Mechanisms in Plants'. *Seminars in Cell & Developmental Biology* 74, 105–13.

Dominguez-Valenzuela, J. A., Gherekhloo, J., Fernández-Moreno, P. T., Cruz-Hipolito, H. E., Alcántara-de la Cruz, R., Sánchez-González, E. & De Prado, R. (2017). 'First Confirmation and Characterization of Target and Non-Target Site Resistance to Glyphosate in Palmer Amaranth (*Amaranthus palmeri*) from Mexico'. *Plant Physiology and Biochemistry* 115, 2012–18.

Duke, S. O. & Powles, S. B. (2008). 'Glyphosate: A Once-in-a-Century Herbicide'. *Pest Management Science* 64 (4), 319–25.

Duke, S. O., Bajsa, J. & Pan, Z. (2013). 'Omics Methods for Probing the Mode of Action of Natural and Synthetic Phytotoxins'. *Journal of Chemical Ecology* 39 (2), 333–47.

Duke, S. O. (2011). 'Glyphosate Degradation in Glyphosate-Resistant and -Susceptible Crops and Weeds'. *Journal of Agricultural and Food Chemistry* 59 (11), 5835–41.

Ebert, D. (2013). *Web-guide to Daphnia Parasites: Culturing Daphnia Food*. Accessed 13-10-2017. URL: `http://evolution.unibas.ch/ebert/lab/algae.htm`.

Ekkers, D. M., Branco dos Santos, F., Mallon, C. A., Bruggeman, F. & Doorn, G. S. van (2020). 'The Omnistat: A flexible Continuous-Culture System for Prolonged Experimental Evolution'. *Methods in Ecology and Evolution* 11.8, 932–42.

Elena, S. F. & Lenski, R. E. (2003). 'Evolution Experiments with Microorganisms: The Dynamics and Genetic Bases of Adaptation'. *Nature reviews. Genetics* 4 (6), 457–69.

Ellner, S. P. & Becks, L. (2011). 'Rapid Prey Evolution and the Dynamics of Two-Predator Food Webs'. *Theoretical Ecology* 4 (2), 133–52.

Ellis, B., Haaland, P., Hahne, F., Le Meur, N., Gopalakrishnan, N., Spidlen, J., Jiang, M. & Finak, G. (2020). *`flowCore`: Basic Structures for Flow Cytometry Data*. R package version 2.2.0.

Erickson, J. M., Rahire, M., Bennoun, P., Delepelaire, P., Diner, B. & Rochaix, J. D. (1984). 'Herbicide Resistance in *Chlamydomonas reinhardtii* Results from a Mutation in the Chloroplast Gene for the 32-kilodalton Protein of Photosystem II'. *Proceedings of the National Academy of Sciences of the United States of America* 81 (12), 3617–21.

Erickson, J. M., Pfister, K., Rahire, M., Togasaki, R. K. & Mets, L. (1989). 'Molecular and Biophysical Analysis of Herbicide-Resistant Mutants of *Chlamydomonas reinhardtii*: Structure-Function Relationship of the Photosystem II D 1 Polypeptide'. *The Plant Cell* 1, 361–71.

Eschenburg, S., Healy, M., Priestman, M., Lushington, G. & Schönbrunn, E. (2002). 'How the Mutation Glycine96 to Alanine Confers Glyphosate Insensitivity to 5-Enolpyruvyl Shikimate-3-Phosphate Synthase from *Escherichia coli*'. *Planta* 216 (1), 129–35.

Fan, J., Zheng, L., Bai, Y., Saroussi, S. & Grossman, A. R. (2017). 'Flocculation of *Chlamydomonas reinhardtii* with Different Phenotypic Traits by Metal Cations and High pH'. *Frontiers in Plant Science* 8, 1997.

Fedtke, C. (1991). 'Mode of Action Studies with Mefenacet'. *Pesticide Science* 33 (4), 421–6.
Felline, S., Coco, L. D., Kaleb, S., Guarnieri, G., Fraschetti, S., Terlizzi, A., Fanizzi, F. & Falace, A. (2019). 'The Response of the Algae *Fucus virsoides* (Fucales, Ochrophyta) to Roundup® Solution Exposure: A Metabolomics Approach'. *Environmental Pollution* 254, 112977.
Feng, P. C. C., Tran, M., Chiu, T., Sammons, R. D., Heck, G. R. & CaJacob, C. A. (2004). 'Investigations into Glyphosate-Resistant Horseweed (*Conyza canadensis*): Retention, Uptake, Translocation, and Metabolism'. *Weed Science* 52 (4), 498–505.
Fernández-Moreno, P. T., Cruz, R. A.-d. la, Smeda, R. J. & Prado, R. D. (2017). 'Differential Resistance Mechanisms to Glyphosate Result in Fitness Cost for *Lolium perenne* and *L. multiflorum*'. *Frontiers in Plant Science* 8, 1796.
Fiehn, O. (2001). 'Combining Genomics, Metabolome Analysis, and Biochemical Modelling to Understand Metabolic Networks'. *Comparative and Functional Genomics* 2 (3), 155–68.
Fiehn, O. (2002). 'Metabolomics – The Link Between Genotypes and Phenotypes.' *Plant Molecular Biology* 48 (1/2), 155–71.
Fischer, B. B., Roffler, S. & Eggen, R. I. L. (2012). 'Multiple Stressor Effects of Predation by Rotifers and Herbicide Pollution on Different *Chlamydomonas* Strains and Potential Impacts on Population Dynamics'. *Environmental Toxicology and Chemistry* 31 (12), 2832–40.
Fischer, R., Andersen, T., Hillebrand, H. & Ptacnik, R. (2014). 'The Exponentially Fed Batch Culture as a Reliable Alternative to Conventional Chemostats'. *Limnology and Oceanography: Methods* 12.7, 432–40.
Fisher, R. M., Bell, T. & West, S. A. (2016). 'Multicellular Group Formation in Response to Predators in the Alga *Chlorella vulgaris*'. *Journal of Evolutionary Biology* 29 (3), 551–9.
Fonseca, E. C. M., Costa, K. S. da, Lameira, J., Alves, C. N. & Lima, A. H. (2020). 'Investigation of the Target-Site Resistance of EPSP Synthase Mutants P106T and T102I/P106S Against Glyphosate'. *RSC Advances* 10 (72), 44352–60.
Forson, D. D. & Storfer, A. (2006). 'Atrazine Increases Ranavirus Susceptibility in the Tiger Salamander, *Ambystoma tigrinum*.' *Ecological applications : a publication of the Ecological Society of America* 16 (6), 2325–32.
Fox, J. & Weisberg, S. (2019). 'An R Companion to Applied Regression'. URL: `https://socialsciences.mcmaster.ca/jfox/Books/Companion/`.
Fritz, C., Mueller, C., Matt, P., Feil, R. & Stitt, M. (2006). 'Impact of the C-N Status on the Amino Acid Profile in Tobacco Source Leaves'. *Plant, Cell and Environment* 29 (11), 2055–76.
Fugère, V., Hébert, M.-P., Costa, N. B. da, Xu, C. C. Y., Barrett, R. D. H., Beisner, B. E., Bell, G., Fussmann, G. F., Shapiro, B. J., Yargeau, V. & Gonzalez, A. (2020). 'Community Rescue in Experimental Phytoplankton Communities Facing Severe Herbicide Pollution'. *Nature Ecology & Evolution* 4 (4), 578–88.
Fujimoto, N., Kosaka, T. & Yamada, M. (2012). 'Menaquinone as well as Ubiquinone as a Crucial Component in the *Escherichia coli* respiratory chain'. *Chemical biology* 10, 187–208.
Funke, T., Yang, Y., Han, H., Healy-Fried, M., Olesen, S., Becker, A. & Schönbrunn, E. (2009). 'Structural Basis of Glyphosate Resistance Resulting from the Double Mutation Thr97 → Ile and Pro101 → Ser in 5-Enolpyruvylshikimate-3-phosphate Synthase from *Escherichia coli*'. *Journal of Biological Chemistry* 284 (15), 9854–60.
Fussmann, G. F., Ellner, S. P., Shertzer, K. & Jr, N. H. (2000). 'Crossing the Hopf Bifurcation in a Live Predator-Prey System'. *Science* 290 (5495), 1358–60.
Futuyma, D. J. & Moreno, G. (1988). 'The Evolution of Ecological Specialization'. *Annual Review of Ecology and Systematics* 19 (1), 207–33.
Futuyma, D. J. (2009). *Evolution*. Vol. 2. Sinauer Associates.
Gaines, T. A., Barker, A. L., Patterson, E. L., Westra, P., Westra, E. P., Wilson, R. G., Jha, P., Kumar, V. & Kniss, A. R. (2016). 'EPSPS Gene Copy Number and Whole-Plant Glyphosate Resistance Level in *Kochia scoparia*'. *PLOS ONE* 11 (12), e0168295.
Gaines, T. A., Patterson, E. L. & Neve, P. (2019). 'Molecular Mechanisms of Adaptive Evolution Revealed by Global Selection for Glyphosate Resistance'. *New Phytologist* 223 (4), 1770–5.
Gaines, T. A., Duke, S. O., Morran, S., Rigon, C. A., Tranel, P. J., Küpper, A. & Dayan, F. E. (2020). 'Mechanisms of Evolved Herbicide Resistance'. *Journal of Biological Chemistry* 295 (30), 10307–30.

Galloway, R. E. & Mets, L. J. (1984). 'Atrazine, Bromacil, and Diuron Resistance in *Chlamydomonas*'. *Plant Physiology* 74 (3), 469–74.

García, M. J., Palma-Bautista, C., Rojano-Delgado, A. M., Bracamonte, E., Portugal, J., Cruz, R. A.-d. la & Prado, R. D. (2019). 'The Triple Amino Acid Substitution TAP-IVS in the EPSPS Gene Confers High Glyphosate Resistance to the Superweed *Amaranthus hybridus*'. *International Journal of Molecular Sciences* 20 (10), 2396.

Gassmann, A. J. & Futuyma, D. J. (2004). 'Consequence of Herbivory for the Fitness Cost of Herbicide Resistance: Pho tosynthetic Variation in the Context of Plant-Herbivore Interactions'. *Journal of Evolutionary Biology* 18 (2), 447–54.

Gassmann, A. J. (2005). 'Resistance to Herbicide and Susceptibility to Herbivores: Environmental Variation in the Magnitude of an Ecological Trade-Off'. *Oecologia* 145 (4), 575–85.

Gauthier, L., Tison-Rosebery, J., Morin, S. & Mazzella, N. (2020). 'Metabolome Response to Anthropogenic Contamination on Microalgae: A Review'. *Metabolomics* 16 (1), 8.

Ge, X., d'Avignon, D. A., Ackerman, J. J. & Sammons, R. D. (2010). 'Rapid Vacuolar Sequestration: The Horseweed Glyphosate Resistance Mechanism'. *Pest Management Science* 66 (4), 345–8.

Ge, X., d'Avignon, D. A., Ackerman, J. J., Duncan, B., Spaur, M. B. & Sammons, R. D. (Oct. 2011). 'Glyphosate-Resistant Horseweed Made Sensitive to Glyphosate: Low-Temperature Suppression of Glyphosate Vacuolar Sequestration Revealed by ^{31}P NMR'. *Pest Management Science* 67 (10), 1215–21.

Ge, X., d'Avignon, D. A., Ackerman, J. J. H., Collavo, A., Sattin, M., Ostrander, E. L., Hall, E. L., Sammons, R. D. & Preston, C. (2012). 'Vacuolar Glyphosate-Sequestration Correlates with Glyphosate Resistance in Ryegrass (*Lolium* spp.) from Australia, South America, and Europe: A ^{31}P NMR Investigation'. *Journal of Agricultural and Food Chemistry* 60 (5), 1243–50.

Gherekhloo, J., Fernández-Moreno, P. T., Alcántara-de la Cruz, R., Sánchez-González, E., Cruz-Hipolito, H. E., Domínguez-Valenzuela, J. A. & De Prado, R. (2017). 'Pro-106-Ser Mutation and EPSPS Overexpression Acting Together Simultaneously in Glyphosate-Resistant Goosegrass (*Eleusine indica*)'. *Scientific Reports* 7 (1), 6702.

Giacomini, D., Westra, P. & Ward, S. M. (2014). 'Impact of Genetic Background in Fitness Cost Studies: An Example from Glyphosate-Resistant Palmer Amaranth'. *Weed Science* 62 (1), 29–37.

Gill, H. K. & Garg, H. (2014). 'Pesticides: Environmental Impacts and Management Strategie.s'. *In M. L. Larramendy, & S. Soloneski (Eds.), Pesticides - Toxic Aspects.*

Giroud, C., Gerber, A. & Eichenberger, W. (1988). 'Lipids of Chlamydomonas reinhardtii. Analysis of Molecular Species and Intracellular Site(s) of Biosynthesis'. *Plant and Cell Physiology* 29 (4), 587–95.

Goff, K. L., Headley, J. V., Lawrence, J. R. & Wilson, K. E. (2013). 'Assessment of the Effects of Oil Sands Naphthenic Acids on the Growth and Morphology of *Chlamydomonas reinhardtii* Using Microscopic and Spectromicroscopic Techniques'. *Science of The Total Environment* 442, 116–22.

Gomes, M. P. & Juneau, P. (2016). 'Oxidative Stress in Duckweed (*Lemna minor* L.) Induced by Glyphosate: Is the Mitochondrial Electron Transport Chain a Target of this Herbicide?' *Environmental Pollution* 218, 402–9.

Gomes, M. P., Bicalho, E. M., Smedbol, É., Silva Cruz, F. V. da, Lucotte, M. & Garcia, Q. S. (2017). 'Glyphosate Can Decrease Germination of Glyphosate-Resistant Soybeans'. *Journal of Agricultural and Food Chemistry* 65 (11), 2279–86.

Gomes, M. P., Monteze Bicalho, E., Vieira da Silva Cruz, F., Souza, A. M., Rodrigues Silva, B. M., de Almeida Gonçalves, C., Silva dos Santos, T. R. & Souza Garcia, Q. (2019). 'Does Integrative Effects of Glyphosate, Gibberellin and Hydrogen Peroxide Ameliorate the Deleterious Effects of the Herbicide on Sorghum Seed Through its Germination?' *Chemosphere* 233, 905–12.

González-Torralva, F., Rojano-Delgado, A. M., Luque de Castro, M. D., Mülleder, N. & De Prado, R. (2012). 'Two Non-Target Mechanisms are Involved in Glyphosate-Resistant Horseweed (*Conyza canadensis* L. Cronq.) Biotypes'. *Journal of Plant Physiology* 169 (17), 1673–9.

Good, B. H., McDonald, M. J., Barrick, J. E., Lenski, R. E. & Desai, M. M. (2017). 'The Dynamics of Molecular Evolution over 60,000 Generations'. *Nature* 551 (7678), 45–50.

Goodwin, T. (1977). 'The Prenyllipids of the Membranes of Higher Plants'. In: *Lipids and Lipid Polymers in Higher Plants*. Springer, 29–47.

Gresham, D., Desai, M. M., Tucker, C. M., Jenq, H. T., Pai, D. A., Ward, A., DeSevo, C. G., Botstein, D. & Dunham, M. J. (2008). 'The Repertoire and Dynamics of Evolutionary Adaptations to Controlled Nutrient-Limited Environments in Yeast'. *PLOS Genetics* 4 (12), e1000303.

Gresham, D. & Dunham, M. J. (2014). 'The Enduring Utility of Continuous Culturing in Experimental Evolution'. *Genomics* 104 (6, Part A), 399–405.

Gresham, D. & Hong, J. (2014). 'The Functional Basis of Adaptive Evolution in Chemostats'. *FEMS Microbiology Reviews* 39, 2–16.

Gressel, J. & Segel, L. A. (1990). 'Modelling the Effectiveness of Herbicide Rotations and Mixtures as Strategies to Delay or Preclude Resistance'. *Weed Technology* 4 (1), 186–198.

Gressel, J. (2009). 'Evolving Understanding of the Evolution of Herbicide Resistance'. *Pest Management Science* 65 (11), 1164–73.

Gressel, J. (2011). 'Low Pesticide Rates May Hasten the Evolution of Resistance by Increasing Mutation Frequencies'. *Pest Management Science* 67 (3), 253–57.

Groeters, F., Tabashnik, B., Finson, N. & Johnson, M. (1994). 'Fitness Costs of Resistance to *Bacillus thuringiensis* in the Diamondback Moth (*Plutella xylostella*)'. *Evolution* 48 (1), 197–201.

Guerrero, I., Morales, M. B., Oñate, J. J., Geiger, F., Berendse, F., Snoo, G. de, Eggers, S., Pärt, T., Bengtsson, J., Clement, L. W., Weisser, W. W., Olszewski, A., Ceryngier, P., Hawro, V., Liira, J., Aavik, T., Fischer, C., Flohre, A., Thies, C. & Tscharntke, T. (2012). 'Response of Ground-Nesting Farmland Birds to Agricultural Intensification Across Europe: Landscape and Field Level Management Factors'. *Biological Conservation* 152, 74–80.

Halekoh, U. & Højsgaard, S. (2014). 'A Kenward-Roger Approximation and Parametric Bootstrap Methods for Tests in Linear Mixed Models – The R Package `pbkrtest`'. *Journal of Statistical Software* 59.9, 1–30. URL: `https://www.jstatsoft.org/v59/i09/`.

Hamm, C. E., Merkel, R., Springer, O., Jurkojc, P., Maier, C., Prechtel, K. & Smetacek, V. (2003). 'Architecture and Material Properties of Diatom Shells Provide Effective Mechanical Protection'. *Nature* 421 (6925), 841–3.

Hamill, A. S., Holt, J. S. & Mallory-Smith, C. A. (2004). 'Contributions of Weed Science to Weed Control and Management'. *Weed Technology* 18 (Invasive Weed Symposium), 1563–5.

Han, H., Vila-Aiub, M. M., Jalaludin, A., Yu, Q. & Powles, S. B. (2017). 'A double EPSPS gene mutation endowing glyphosate resistance shows a remarkably high resistance cost'. *Plant, Cell & Environment* 40 (12), 3031–42.

Hansson, E. M., Childs, D. Z. & Beckerman, A. P. (2022). 'Mesostats — A multiplexed, low-cost, do-it-yourself continuous culturing system for experimental evolution of mesocosms'. *PLoS ONE* 7 (17), e0272052.

Harvey, E. L., Bidle, K. D. & Johnson, M. D. (2015). 'Consequences of Strain Variability and Calcification in *Emiliania huxleyi* on Microzooplankton Grazing'. *Journal of Plankton Research*, 1137–48.

Hartnett, M. E., Newcomb, J. R. & Hodson, R. C. (1987). 'Mutations in *Chlamydomonas reinhardtii* Conferring Resistance to the Herbicide Sulfometuron Methyl'. *Plant Physiology* 85 (4), 898–901.

Harris, E. H., Stern, D. B. & Witman, G. B. (1989). *The Chlamydomonas Sourcebook*. Vol. 2. Academic Press San Diego.

Harper, J. (1956). 'The evolution of weeds in relation to resistance to herbicides'. *Proceedings of the 3rd British Weed Control Conference*, 179–188.

Häusler, R. E., Ludewig, F. & Krueger, S. (Dec. 2014). 'Amino Acids – A Life Between Metabolism and Signaling'. *Plant Science* 229, 225–37.

Healy-Fried, M. L., Funke, T., Priestman, M. A., Han, H. & Schönbrunn, E. (2007). 'Structural Basis of Glyphosate Tolerance Resulting from Mutations of Pro101 in *Escherichia coli* 5-Enolpyruvylshikimate-3-phosphate Synthase'. *Journal of Biological Chemistry* 282 (45), 32949–55.

Heap, I. (2022). *The International Herbicide-Resistant Weed Database*. Accessed: 18-01-2022. URL: `https://www.weedscience.org`.

Hébert, M.-P., Fugère, V. & Gonzalez, A. (2019). 'The Overlooked Impact of Rising Glyphosate Use on Phosphorus Loading in Agricultural Watersheds'. *Frontiers in Ecology and the Environment* 17 (1), 48–56.

Helander, M., Saloniemi, I. & Saikkonen, K. (2012). 'Glyphosate in Northern Ecosystems'. *Trends in Plant Science* 17 (10), 569–74.

Herms, D. A. & Mattson, W. J. (1994). 'Plant Growth and Defence'. *Trends in Ecology and Evolution* 9 (12), 488.

Hessen, D. O. & Van Donk, E. (1993). 'Morphological Changes in *Scenedesmus* Induced by Substances Released from *Daphnia*'. *Archiv für Hydrobiologie* 127 (2), 129–40.

Hiltunen, T., Hairston, N. G., Hooker, G., Jones, L. E. & Ellner, S. P. (2014). 'A Newly Discovered Role of Evolution in Previously Published Consumer-Resource Dynamics'. *Ecology Letters* 17 (8), 915–23.

Hildebrandt, T. M., Nunes Nesi, A., Araújo, W. L. & Braun, H.-P. (2015). 'Amino Acid Catabolism in Plants'. *Molecular Plant* 8 (11), 1563–79.

Hong, J. & Gresham, D. (2014). 'Molecular Specificity, Convergence and Constraint Shape Adaptive Evolution in Nutrient-Poor Environments'. *PLOS Genetics* 10 (1), e1004041.

Horai, H., Arita, M., Kanaya, S., Nihei, Y., Ikeda, T., Suwa, K., Ojima, Y., Tanaka, K., Tanaka, S., Aoshima, K., Oda, Y., Kakazu, Y., Kusano, M., Tohge, T., Matsuda, F., Sawada, Y., Hirai, M. Y., Nakanishi, H., Ikeda, K., Akimoto, N., Maoka, T., Takahashi, H., Ara, T., Sakurai, N., Suzuki, H., Shibata, D., Neumann, S., Iida, T., Tanaka, K., Funatsu, K., Matsuura, F., Soga, T., Taguchi, R., Saito, K. & Nishioka, T. (2010). 'MassBank: A Public Repository for Sharing Mass Spectral Data for Life Sciences'. *Journal of Mass Spectrometry* 45 (7), 703–14.

Hove-Jensen, B., Zechel, D. L. & Jochimsen, B. (2014). 'Utilization of Glyphosate as Phosphate Source: Biochemistry and Genetics of Bacterial Carbon-Phosphorus Lyase'. *Microbiology and Molecular Biology Reviews* 78 (1), 176–97.

HRAC (2022). *Herbicide Resistance Action Committee Mode of Action Classification Map 2022*. Accessed 19-04-2022. URL: `https://hracglobal.com`.

Hussain, S., Siddique, T., Saleem, M., Arshad, M. & Khalid, A. (2009). 'Chapter 5 Impact of Pesticides on Soil Microbial Diversity, Enzymes, and Biochemical Reactions'. *Advances in Agronomy*, 159–200.

Iwasa, K. & Murakami, S. (1968). 'Palmelloid Formation of Chlamydomonas. I. Palmelloid Induction by Organic Acids'. *Physiologia Plantarum* 21 (6), 1224–33.

James, S. W. & Lefebvre, P. A. (1989). 'Isolation and Characterization of Dominant, Pleiotropic Drug-resistance Mutants in *Chlamydomonas reinhardtii*'. *Current Genetics* 15 (6), 443–52.

James, S., Silflow, C., Stroom, P. & Lefebvre, P. (1993). 'A Mutation in the Alpha 1-Tubulin Gene of *Chlamydomonas reinhardtii* Confers Resistance to Anti-Microtubule Herbicides'. *Journal of Cell Science* 106 (1), 209–18.

Jander, G., Baerson, S. R., Hudak, J. A., Gonzalez, K. A., Gruys, K. J. & Last, R. L. (2003). 'Ethylmethanesulfonate Saturation Mutagenesis in Arabidopsis to Determine Frequency of Herbicide Resistance'. *Plant Physiology* 131 (1), 139–46.

Jasieniuk, M., Brûlé-Babel, A. L. & Morrison, I. N. (1996). 'The Evolution and Genetics of Herbicide Resistance in Weeds'. *Weed Science* 44 (1), 176–93.

Jugulam, M., Niehues, K., Godar, A. S., Koo, D.-H., Danilova, T., Friebe, B., Sehgal, S., Varanasi, V. K., Wiersma, A., Westra, P., Stahlman, P. W. & Gill, B. S. (2014). 'Tandem Amplification of a Chromosomal Segment Harboring 5-Enolpyruvylshikimate-3-Phosphate Synthase Locus Confers Glyphosate Resistance in *Kochia scoparia*'. *Plant Physiology* 166 (3), 1200–7.

Kadono, T., Kawano, T., Hosoya, H. & Kosaka, T. (2004). 'Flow Cytometric Studies of the Host-Regulated Cell Cycle in Algae Symbiotic with Green Paramecium'. *Protoplasma* 223 (2-4), 133–44.

Kao, K. C. & Sherlock, G. (2008). 'Molecular Characterization of Clonal Interference During Adaptive Evolution in Asexual Populations of *Saccharomyces cerevisiae*'. *Nature Genetics* 40 (12), 1499–1504.

Kasada, M., Yamamichi, M. & Yoshida, T. (2014). 'Form of an Evolutionary Tradeoff Affects Eco-Evolutionary Dynamics in a Predator-Prey System.' *Proceedings of the National Academy of Sciences of the United States of America* 111 (45), 16035–40.

Kaundun, S. S., Zelaya, I. A., Dale, R. P., Lycett, A. J., Carter, P., Sharples, K. R. & McIndoe, E. (2008). 'Importance of the P106S Target-Site Mutation in Conferring Resistance to Glyphosate in a Goosegrass (*Eleusine indica*) Population from the Philippines'. *Weed Science* 56 (5), 637–46.

Kawecki, T. J., Lenski, R. E., Ebert, D., Hollis, B., Olivieri, I. & Whitlock, M. C. (2012). 'Experimental Evolution'. *Trends in Ecology & Evolution* 27 (10), 547–60.

Kelly, D. W., Poulin, R., Tompkins, D. M. & Townsend, C. R. (2010). 'Synergistic Effects of Glyphosate Formulation and Parasite Infection on Fish Malformations and Survival'. *Journal of Applied Ecology* 47 (2), 498–504.

Kevan, P. G. (1999). 'Pollinators as Bioindicators of the State of the Environment: Species, Activity and Diversity'. *Invertebrate Biodiversity as Bioindicators of Sustainable Landscapes*, 373–93.

Khona, D. K., Shirolikar, S. M., Gawde, K. K., Hom, E., Deodhar, M. A. & D'Souza, J. S. (2016). 'Characterization of salt stress-induced palmelloids in the green alga, *Chlamydomonas reinhardtii*'. *Algal Research* 16, 434–48.

Kinnersley, M. A., Holben, W. E. & Rosenzweig, F. (2009). 'E Unibus Plurum: Genomic Analysis of an Experimentally Evolved Polymorphism in *Escherichia coli*'. *PLOS Genetics* 5 (11), e1000713.

Koo, D.-H., Molin, W. T., Saski, C. A., Jiang, J., Putta, K., Jugulam, M., Friebe, B. & Gill, B. S. (2018). 'Extrachromosomal Circular DNA-Based Amplification and Transmission of Herbicide Resistance in Crop Weed *Amaranthus palmeri*'. *Proceedings of the National Academy of Sciences* 115 (13), 3332–7.

Kostopoulou, S., Ntatsi, G., Arapis, G. & Aliferis, K. A. (2020). 'Assessment of the Effects of Metribuzin, Glyphosate, and Their Mixtures on the Metabolism of the Model Plant *Lemna minor* L. Applying Metabolomics'. *Chemosphere* 239, 124582.

Kvitek, D. J. & Sherlock, G. (2011). 'Reciprocal Sign Epistasis between Frequently Experimentally Evolved Adaptive Mutations Causes a Rugged Fitness Landscape'. *PLOS Genetics* 7 (4), e1002056.

Lagator, M., Vogwill, T., Colegrave, N. & Neve, P. (2013a). 'Herbicide Cycling has Diverse Effects on Evolution of Resistance in *Chlamydomonas reinhardtii*'. *Evolutionary Applications* 6 (2), 197–206.

Lagator, M., Vogwill, T., Mead, A., Colegrave, N. & Neve, P. (2013b). 'Herbicide Mixtures at High Doses Slow the Evolution of Resistance in Experimentally Evolving Populations of *Chlamydomonas reinhardtii*'. *New Phytologist* 198 (3), 938–45.

Lang, G. I. & Desai, M. M. (2014). 'The Spectrum of Adaptive Mutations in Experimental Evolution'. *Genomics* 104 (6), 412–6.

Landi, L., Cabrini, L., Sechi, A. M. & Pasquali, P. (1984). 'Antioxidative Effect of Ubiquinones on Mitochondrial Membranes'. *Biochemical Journal* 222 (2), 463–66.

Larson, S. J., Capel, P. D. & Majewski, M. S. (2019). *Pesticides in Surface Waters*. CRC Press.

Lemoine, Y. & Schoefs, B. (2010). 'Secondary Ketocarotenoid Astaxanthin Biosynthesis in Algae: A Multifunctional Response to Stress'. *Photosynthesis Research* 106 (1-2), 155–77.

Lenski, R. E., Rose, M. R., Simpson, S. C. & Tadler, S. C. (1991). 'Long-Term Experimental Evolution in *Escheria coli*. I. Adaptation and Divergence During 2,000 Generations'. *The American Naturalist* 138, 1315–41.

Lenth, R. V. (2022). '`emmeans`: Estimated Marginal Means, aka Least-Squares Means'. R package version 1.7.2. URL: `https://CRAN.R-project.org/package=emmeans`.

Less, H. & Galili, G. (2008). 'Principal Transcriptional Programs Regulating Plant Amino Acid Metabolism in Response to Abiotic Stresses'. *Plant Physiology* 147 (1), 316–30.

Leslie, T. & Baucom, R. S. (2014). '*De Novo* Assembly and Annotation of the Transcriptome of the Agricultural Weed *Ipomoea purpurea* Uncovers Gene Expression Changes Associated with Herbicide Resistance'. *G3 Genes|Genomes|Genetics* 4 (10), 2035–47.

Li, J., Peng, Q., Han, H., Nyporko, A., Kulynych, T., Yu, Q. & Powles, S. B. (2018). 'Glyphosate Resistance in *Tridax procumbens* via a Novel EPSPS Thr-102-Ser Substitution'. *Journal of Agricultural and Food Chemistry* 66 (30), 7880–8.

Liang, X., Zhang, L., Natarajan, S. K. & Becker, D. F. (2013). 'Proline Mechanisms of Stress Survival'. *Antioxidants & Redox Signaling* 19 (9), 998–1011.

Lichtenthaler, H. (1977). 'Regulation of Prenylquinone Synthesis in Higher Plants'. In: *Lipids and Lipid polymers in Higher Plants*. Springer, 231–58.

Liu, H., Chen, M., Zhu, F. & Harrison, P. J. (2016). 'Effect of Diatom Silica Content on Copepod Grazing, Growth and Reproduction'. *Frontiers in Marine Science* 3, 89.

Liu, W., Majumdar, S., Li, W., Keller, A. A. & Slaveykova, V. I. (2020). 'Metabolomics for Early Detection of Stress in Freshwater Alga *Poterioochromonas malhamensis* Exposed to Silver Nanoparticles'. *Scientific Reports* 10 (1), 20563.

Liu, J., Dong, C., Zhai, Z., Tang, L. & Wang, L. (2021). 'Glyphosate-Induced Lipid Metabolism Disorder Contributes to Hepatotoxicity in Juvenile Common Carp'. *Environmental Pollution* 269, 116186.

Lorraine-Colwill, D. F., Powles, S. B., Hawkes, T. R., Hollinshead, P. H., Warner, S. A. J. & Preston, C. (2002). 'Investigations into the Mechanism of Glyphosate Resistance in *Lolium rigidum*'. *Pesticide Biochemistry and Physiology* 74 (2), 62–72.

Love, A. C. & Wagner, G. P. (2022). 'Co-option of stress mechanisms in the origin of evolutionary novelties'. *Evolution*.

Lupwayi, N., Harker, K., Clayton, G., O'Donovan, J. & Blackshaw, R. (2009). 'Soil Microbial Response to Herbicides Applied to Glyphosate-Resistant Canola'. *Agriculture, Ecosystems & Environment* 129 (1-3), 171–6.

Lürling, M. & Beekman, W. (2006). 'Palmelloids Formation in *Chlamydomonas reinhardtii*: Defence Against Rotifer Predators?' *Annales de Limnologie - International Journal of Limnology* 42 (2), 65–72.

Lürling, M., Lange, H. J. de & Peeters, E. T. H. M. (2011). 'Effects of an Anionic Surfactant (FFD-6) on the Energy and Information Flow Between a Primary Producer (*Scenedesmus obliquus*) and a Consumer (*Daphnia magna*)'. *Ecotoxicology* 20 (8), 1881–9.

Lürling, M. & Van Donk, E. (1996). 'Zooplankton-Induced Unicell-Colony Transformation in *Scenedesmus acutus* and its Effect on Growth of Herbivore *Daphnia*'. *Oecologia* 108 (3), 432–7.

Lürling, M. & Van Donk, E. (1997). 'Morphological Changes in *Scenedesmus* Induced by Infochemicals Released In Situ from Zooplankton Grazers'. *Limnology and Oceanography* 42 (4), 783–8.

Lürling, M. (2011). 'Metribuzin Impairs the Unicell-Colony Transformation in the Green Alga *Scenedesmus obliquus*'. *Chemosphere* 82 (3), 411–7.

Maeda, H. & Dudareva, N. (2012). 'The Shikimate Pathway and Aromatic Amino Acid Biosynthesis in Plants'. *Annual Review of Plant Biology* 63 (1), 73–105.

Maharjan, R. P., Seeto, S., Notley-McRobb, L. & Ferenci, T. (2006). 'Clonal Adaptive Radiation in a Constant Environment'. *Science* 313 (5786), 514–7.

Maharjan, R. P., Ferenci, T., Reeves, P. R., Li, Y., Liu, B. & Wang, L. (2012). 'The Multiplicity of Divergence Mechanisms in a Single Evolving Population'. *Genome Biology* 13 (6), R41.

Mao, C., Xie, H., Chen, S., Valverde, B. E. & Qiang, S. (2016). 'Multiple Mechanism Confers Natural Tolerance of Three Lilyturf Species to Glyphosate'. *Planta* 243 (2), 321–35.

Maroli, A. S., Nandula, V. K., Dayan, F. E., Duke, S. O., Gerard, P. & Tharayil, N. (2015). 'Metabolic Profiling and Enzyme Analyses Indicate a Potential Role of Antioxidant Systems in Complementing Glyphosate Resistance in an *Amaranthus palmeri* Biotype'. *Journal of Agricultural and Food Chemistry* 63 (41), 9199–209.

Martin, S. L., Benedict, L., Sauder, C. A., Wei, W., Oliveira da Costa, L., Hall, L. M. & Beckie, H. J. (2017). 'Glyphosate Resistance Reduces *Kochia* Fitness: Comparison of Segregating Resistant and Susceptible F2 Populations'. *Plant Science* 261, 69–79.

Maroli, A. S., Nandula, V. K., Duke, S. O., Gerard, P. & Tharayil, N. (2018). 'Comparative Metabolomic Analyses of *Ipomoea lacunosa* Biotypes with Contrasting Glyphosate Tolerance Captures Herbicide-Induced Differential Perturbations in Cellular Physiology'. *Journal of Agricultural and Food Chemistry* 66 (8), 2027–39.

Marañón, E. (2015). 'Cell Size as a Key Determinant of Phytoplankton Metabolism and Community Structure'. *Annual Review of Marine Science* 7 (1), 241–64.

Melero-Jiménez, I. J., Bañares-España, E., Reul, A., Flores-Moya, A. & García-Sánchez, M. J. (2021). 'Detection of the Maximum Resistance to the Herbicides Diuron and Glyphosate, and Evaluation of its Phenotypic Cost, in Freshwater Phytoplankton'. *Aquatic Toxicology* 240, 105973.

Menchari, Y., Chauvel, B., Darmency, H. & Délye, C. (2007). 'Fitness Costs Associated with Three Mutant Acetyl-Coenzyme A Carboxylase Alleles Endowing Herbicide Resistance in Black-Grass *Alopecurus myosuroides*'. *Journal of Applied Ecology* 45 (3), 939–47.

Mendes, R. R., Takano, H. K., Leal, J. F., Souza, A. S., Morran, S., Oliveira, R. S., Adegas, F. S., Gaines, T. A. & Dayan, F. E. (2020). 'Evolution of EPSPS Double Mutation Impart-

ing Glyphosate Resistance in Wild Poinsettia (*Euphorbia heterophylla* L.)' *PLOS ONE* 15 (9), e0238818.
Michitte, P., Prado, R. D., Espinoza, N., Ruiz-Santaella, J. P. & Gauvrit, C. (2007). 'Mechanisms of Resistance to Glyphosate in a Ryegrass (*Lolium multiflorum*) Biotype from Chile'. *Weed Science* 55 (5), 435–40.
Miller, A. W., Befort, C., Kerr, E. O. & Dunham, M. J. (2013). 'Design and Use of Multiplexed Chemostat Arrays'. *Journal of Visualized Experiments* (72), 2–7.
Mithila, J., Hall, J. C., Johnson, W. G., Kelley, K. B. & Riechers, D. E. (2011). 'Evolution of Resistance to Auxinic Herbicides: Historical Perspectives, Mechanisms of Resistance, and Implications for Broadleaf Weed Management in Agronomic Crops'. *Weed Science* 59 (4), 445–57.
Mitra, A., Chatterjee, C. & Mandal, F. B. (2011). 'Synthetic Chemical Pesticides and Their Effects on Birds'. *Research Journal of Environmental Toxicology* 5 (2), 81–96.
Moe, L. A. (2013). 'Amino Acids in the Rhizosphere: From Plants to Microbes'. *American Journal of Botany* 100 (9), 1692–705.
Monod, J. (1950). 'La technique de culture continue: Théorie et applications'. *Annales De l'Institut Pasteur, Paris*, 390–410.
Moretti, M. L., Van Horn, C. R., Robertson, R., Segobye, K., Weller, S. C., Young, B. G., Johnson, W. G., Sammons, R. D., Wang, D., Ge, X., Avignon, A. d', Gaines, T. A., Westra, P., Green, A. C., Jeffery, T., Lespérance, M. A., Tardif, F. J., Sikkema, P. H., Hall, J. C., McLean, M. D., Lawton, M. B. & Schulz, B. (2018). 'Glyphosate Resistance in *Ambrosia trifida:* Part 2. Rapid Response Physiology and Non-Target-Site Resistance'. *Pest Management Science* 74 (5), 1079–88.
Motta, E. V. S., Raymann, K. & Moran, N. A. (2018). 'Glyphosate Perturbs the Gut Microbiota of Honey Bees'. *Proceedings of the National Academy of Sciences* 115 (41), 10305–10.
Murphy, B. P. & Tranel, P. J. (2019). 'Target-Site Mutations Conferring Herbicide Resistance'. *Plants* 8 (10), 382.
Nakamura, K., Bray, D. F. & Wagenaar, E. B. (1978). 'Ultrastructure of a Palmelloid-Forming Strain of *Chlamydomonas eugametos*'. *Canadian Journal of Botany* 56.19, 2348–56.
Nandula, V. K., Ray, J. D., Ribeiro, D. N., Pan, Z. & Reddy, K. N. (2013). 'Glyphosate Resistance in Tall Waterhemp (*Amaranthus tuberculatus*) from Mississippi is due to both Altered Target-Site and Nontarget-Site Mechanisms'. *Weed Science* 61 (3), 374–83.
Neve, P. & Powles, S. (2005). 'Recurrent Selection with Reduced Herbicide Rates Results in the Rapid Evolution of Herbicide Resistance in *Lolium rigidum*'. *Theoretical and Applied Genetics* 110 (6), 1154–66.
Neve, P., Vila-Aiub, M. M. & Roux, F. (2009). 'Evolutionary-Thinking in Agricultural Weed Management'. *New Phytologist* 184 (4), 783–93.
Neve, P., Norsworthy, J. K., Smith, K. L. & Zelaya, I. A. (2011). 'Modeling Glyphosate Resistance Management Strategies for Palmer Amaranth (*Amaranthus palmeri*) in Cotton'. *Weed Technology* 25 (3), 335–43.
Neve, P., Busi, R., Renton, M. & Vila-Aiub, M. M. (2014). 'Expanding the Eco-Evolutionary Context of Herbicide Resistance Research'. *Pest Management Science* 70 (9), 1385–93.
Neve, P. (2008). 'Simulation Modelling to Understand the Evolution and Management of Glyphosate Resistance in Weeds'. *Pest Management Science* 64 (4), 392–401.
Noctor, G., Lelarge-Trouverie, C. & Mhamdi, A. (2015). 'The Metabolomics of Oxidative Stress'. *Phytochemistry* 112, 33–53.
Norsworthy, J. K., Varanasi, V. K., Bagavathiannan, M. & Brabham, C. (2021). 'Recurrent Selection with Sub-Lethal Doses of Mesotrione Reduces Sensitivity in *Amaranthus palmeri*'. *Plants* 10 (7), 1293.
Novick, A. & Szilard, L. (1950). 'Description of the Chemostat'. *Science* 112 (2920), 715–6.
Oerke, E. (2006). 'Crop Losses to Pests'. *The Journal of Agricultural Science* 144 (1), 31–43.
Oikawa, A., Nakamura, Y., Ogura, T., Kimura, A., Suzuki, H., Sakurai, N., Shinbo, Y., Shibata, D., Kanaya, S. & Ohta, D. (2006). 'Clarification of Pathway-Specific Inhibition by Fourier Transform Ion Cyclotron Resonance/Mass Spectrometry-Based Metabolic Phenotyping Studies'. *Plant Physiology* 142 (2), 398–413.

Okamoto, O. K., Pinto, E., Latorre, L. R., Bechara, E. J. H. & Colepicolo, P. (2001). 'Antioxidant Modulation in Response to Metal-Induced Oxidative Stress in Algal Chloroplasts'. *Archives of Environmental Contamination and Toxicology* 40 (1), 18–24.

Olsen, Y., Knutsen, G. & Lien, T. (1983). 'Characteristics of Phosphorous Limitation in *Chlamydomonas reinhardtii* (Chlorophyceae) and its Palmelloids'. *Journal of Phycology* 19 (3), 313–9.

Orcaray, L., Zulet, A., Zabalza, A. & Royuela, M. (2012). 'Impairment of Carbon Metabolism Induced by the Herbicide Glyphosate'. *Journal of Plant Physiology* 169 (1), 27–33.

Orr, H. A. (June 2000). 'The Rate of Adaptation in Asexuals'. *Genetics* 155 (2), 961–8.

Osipitan, O. A. & Dille, J. A. (2017). 'Fitness Outcomes Related to Glyphosate Resistance in Kochia (*Kochia scoparia*): What Life History Stage to Examine?' *Frontiers in Plant Science* 8, 1090.

Overy, S. A., Walker, H. J., Malone, S., Howard, T. P., Baxter, C. J., Sweetlove, L. J., Hill, S. A. & Quick, W. P. (2005). 'Application of Metabolite Profiling to the Identification of Traits in a Population of Tomato Introgression Lines'. *Journal of Experimental Botany* 56 (410), 287–96.

Pančić, M. & Kiørboe, T. (2018). 'Phytoplankton Defence Mechanisms: Traits and Trade-Offs'. *Biological Reviews* 93 (2), 1269–303.

Pan, L., Yu, Q., Han, H., Mao, L., Nyporko, A., Fan, L., Bai, L. & Powles, S. B. (2019). 'Aldo-Keto Reductase Metabolizes Glyphosate and Confers Glyphosate Resistance in *Echinochloa colona*'. *Plant Physiology* 181 (4), 1519–34.

Paris, M., Roux, F., Bérard, A. & Reboud, X. (2008). 'The Effects of the Genetic Background on Herbicide Resistance Fitness Cost and its Associated Dominance in *Arabidopsis thaliana*'. *Heredity* 101 (6), 499–506.

Parsons, K. C., Mineau, P. & Renfrew, R. B. (Dec. 2010). 'Effects of Pesticide Use in Rice Fields on Birds'. *Waterbirds* 33 (sp1), 193–218.

Patti, G. J., Yanes, O. & Siuzdak, G. (2012). 'Metabolomics: The Apogee of the Omics Trilogy'. *Nature Reviews Molecular Cell Biology* 13 (4), 263–9.

Patterson, E. L., Pettinga, D. J., Ravet, K., Neve, P. & Gaines, T. A. (2018). 'Glyphosate Resistance and EPSPS Gene Duplication: Convergent Evolution in Multiple Plant Species'. *Journal of Heredity* 109 (2), 117–25.

Patterson, E. L., Saski, C., Sloan, D., Tranel, P., Westra, P. & Gaines, T. (2019). 'The Draft Genome of *Kochia scoparia* and the Mechanism of Glyphosate Resistance via Transposon-Mediated EPSPS Tandem Gene Duplication'. *BioRxiv*.

Pedersen, B. P., Neve, P., Andreasen, C. & Powles, S. B. (2007). 'Ecological Fitness of a Glyphosate-Resistant *Lolium rigidum* Population: Growth and Seed Production Along a Competition Gradient'. *Basic and Applied Ecology* 8 (3), 258–68.

Pedersen, E. J., Miller, D. L., Simpson, G. L. & Ross, N. (2019). 'Hierarchical Generalized Additive Models in Ecology: An Introduction with `mgcv`'. *PeerJ* 7, e6876.

Pelosi, C., Barot, S., Capowiez, Y., Hedde, M. & Vandenbulcke, F. (2014). 'Pesticides and Earthworms. A Review'. *Agronomy for Sustainable Development* 34 (1), 199–228.

Peng, Y., Abercrombie, L. L., Yuan, J. S., Riggins, C. W., Sammons, R. D., Tranel, P. J. & Stewart, C. N. (2010). 'Characterization of the Horseweed (*Conyza canadensis*) Transcriptome Using GS-FLX 454 Pyrosequencing and its Application for Expression Analysis of Candidate Non-Target Herbicide Resistance Genes'. *Pest Management Science* 66 (10), 1053–62.

Pereira, L., Fernandes, M. N. & Martinez, C. B. (2013). 'Hematological and Biochemical Alterations in the Fish *Prochilodus lineatus* Caused by the Herbicide Clomazone'. *Environmental Toxicology and Pharmacology* 36 (1), 1–8.

Perotti, V. E., Larran, A. S., Palmieri, V. E., Martinatto, A. K., Alvarez, C. E., Tuesca, D. & Permingeat, H. R. (2019). 'A Novel Triple Amino Acid Substitution in the EPSPS Found in a High-Level Glyphosate-Resistant *Amaranthus hybridus* Population from Argentina'. *Pest Management Science* 75 (5), 1242–51.

Pinto, E., Sigaud-kutner, T. C. S., Leitao, M. A. S., Okamoto, O. K., Morse, D. & Colepicolo, P. (2003). 'Heavy Metal-Induced Oxidative Stress in Algae'. *Journal of Phycology* 39 (6), 1008–18.

Pipke, R. & Amrhein, N. (1988). 'Degradation of the Phosphonate Herbicide Glyphosate by *Arthrobacter atrocyaneus* ATCC 13752'. *Applied and Environmental Microbiology* 54 (5), 1293–6.

Pizzul, L., Pilar Castillo, M. del & Stenström, J. (2009). 'Degradation of Glyphosate and Other Pesticides by Ligninolytic Enzymes'. *Biodegradation* 20 (6), 751–9.

Plaxton, W. C. (1996). 'The Organization and Regulation of Plant Glycolysis'. *Annual Review of Plant Physiology and Plant Molecular Biology* 47 (1), 185–214.
Pondaven, P., Gallinari, M., Chollet, S., Bucciarelli, E., Sarthou, G., Schultes, S. & Jean, F. (2007). 'Grazing-induced Changes in Cell Wall Silicification in a Marine Diatom'. *Protist* 158, 21–8.
Porter, K. G. (1975). 'Viable Gut Passage of Gelatinous Green Algae Ingested by *Daphnia*'. *SIL Proceedings, 1922-2010* 19 (4), 2840–50.
Powles, S. B. & Yu, Q. (2010). 'Evolution in Action: Plants Resistant to Herbicides'. *Annual Review of Plant Biology* 61, 317–47.
Powles, S. B. (2008). 'Evolved Glyphosate-Resistant Weeds Around The World: Lessons to be Learnt'. *Pest Management Science* 64 (4), 360–5.
Preston, C. & Powles, S. B. (2002). 'Evolution of Herbicide Resistance in Weeds: Initial Frequency of Target Site-Based Resistance to Acetolactate Synthase-Inhibiting Herbicides in *Lolium rigidum*'. *Heredity* 88 (1), 8–13.
Preston, C. & Wakelin, A. M. (2008). 'Resistance to Glyphosate from Altered Herbicide Translocation Patterns'. *Pest Management Science* 64 (4), 372–6.
Purrington, C. B. & Bergelson, J. (1999). 'Exploring the Physiological Basis of Costs of Herbicide Resistance in *Arabidopsis thaliana*'. *The American Naturalist* 154 (S1), S82–S91.
Purrington, C. B. (2000). 'Costs of Resistance'. *Current Opinion in Plant Biology* 3 (4), 305–8.
Quastel, J. H. (1950). '2,4-Dichlorophenoxyacetic Acid (2,4-D) as a Selective Herbicide', 244–9.
R Core Team (2021). *R: A Language and Environment for Statistical Computing*. R Foundation for Statistical Computing. Vienna, Austria. URL: `https://www.R-project.org/`.
Raatz, M., Schälicke, S., Sieber, M., Wacker, A. & Gaedke, U. (2018). 'One Man's Trash is Another Man's Treasure – The Effect of Bacteria on Phytoplankton–Zooplankton Interactions in Chemostat Systems'. *Limnology and Oceanography: Methods* 16, 629–39.
Rainey, P. B., Buckling, A., Kassen, R. & Travisano, M. (2000). 'The Emergence and Maintenance of Diversity: Insights from Experimental Bacterial Populations'. *Trends in Ecology & Evolution* 15 (6), 243–7.
Randolph-Anderson, B. L., Sato, R., Johnson, A. M., Harris, E. H., Hauser, C. R., Oeda, K., Ishige, F., Nishio, S., Gillham, N. W. & Boynton, J. E. (1998). 'Isolation and Characterization of a Mutant Protoporphyrinogen Oxidase Gene from *Chlamydomonas reinhardtii* Conferring Resistance to Porphyric Herbicides'. *Plant Molecular Biology* 38 (5), 839–59.
Raven, J. A. & Kubler, J. E. (2002). 'New Light on the Scaling of Metabolic Rate with the Size of Algae'. *Journal of Phycology* 38 (1), 11–6.
Reboud, X., Majerus, N., Gasquez, J. & Powles, S. B. (2007). '*Chlamydomonas reinhardtii* as a Model System for Pro-Active Herbicide Resistance Evolution Research'. *Biological Journal of the Linnean Society* 91 (2), 257–66.
Reboud, X. (2002). 'Response of *Chlamydomonas reinhardtii* to Herbicides: Negative Relationship Between Toxicity and Water Solubility Across Several Herbicide Families'. *Bulletin of Environmental Contamination and Toxicology* 69 (4), 554–61.
Relyea, R. A., Schoeppner, N. M. & Hoverman, J. T. (2005). 'Pesticides and Amphibians: The Importance of Community Context'. *Ecological Applications* 15 (4), 1125–34.
Relyea, R. A. (2003). 'Predator Cues and Pesticides: A Double Dose of Danger for Amphibians'. *Ecological Applications* 13 (6), 1515–21.
Relyea, R. A. (2005a). 'The Lethal Impact of Roundup on Aquatic and Terrestrial Amphibians'. *Ecological Applications* 15 (4), 1118–24.
Relyea, R. A. (2005b). 'The Impact of Insecticides and Herbicides on the Biodiversity and Productivity of Aquatic Communities'. *Ecological Applications* 15 (2), 618–27.
Relyea, R. A. (2012). 'New Effects of Roundup on Amphibians: Predators Reduce Herbicide Mortality; Herbicides Induce Antipredator Morphology'. *Ecological Applications* 22 (2), 634–47.
Reznick, D., Nunney, L. & Tessier, A. (2000). 'Big Houses, Big Cars, Superfleas and the Costs of Reproduction'. *Trends in Ecology & Evolution* 15 (10), 421–5.
Roccuzzo, S., Couto, N., Karunakaran, E., Kapoore, R. V., Butler, T. O., Mukherjee, J., Hansson, E. M., Beckerman, A. P. & Pandhal, J. (2020). 'Metabolic Insights Into Infochemicals Induced Colony Formation and Flocculation in *Scenedesmus subspicatus* Unraveled by Quantitative Proteomics'. *Frontiers in Microbiology* 11, 792.

Roux, F., Gasquez, J. & Reboud, X. (2004). 'The Dominance of the Herbicide Resistance Cost in Several *Arabidopsis thaliana* Mutant Lines'. *Genetics* 166 (1), 449–60.
Roux, F., Camilleri, C., Giancola, S., Brunel, D. & Reboud, X. (2005). 'Epistatic Interactions Among Herbicide Resistances in *Arabidopsis thaliana*: The Fitness Cost of Multiresistance'. *Genetics* 171 (3), 1277–88.
Roux, F. & Reboud, X. (2005). 'Is the Cost of Herbicide Resistance Expressed in the Breakdown of the Relationships Between Characters? A Case Study Using Synthetic-Auxin-Resistant *Arabidopsis thaliana* Mutants'. *Genetical Research* 85 (2), 101–10.
Rüegg, W. T., Quadranti, M. & Zoschke, A. (2007). 'Herbicide Research and Development: Challenges and Opportunities'. *Weed Research* 47 (4), 271–5.
Ryan, G. F. (1970). 'Resistance of Common Groundsel to Simazine and Atrazine'. *Weed Science* 18 (5), 614–16.
Salzmann, D., Handley, R. J. & Müller-Schärer, H. (2008). 'Functional Significance of Triazine-Herbicide Resistance in Defence of *Senecio vulgaris* Against a Rust Fungus'. *Basic and Applied Ecology* 9 (5).
Salomé, P. A. & Merchant, S. S. (2019). 'A Series of Fortunate Events: Introducing *Chlamydomonas* as a Reference Organism'. *The Plant Cell* 31 (8), 1682–707.
Sammons, R. D. & Gaines, T. A. (2014). 'Glyphosate Resistance: State of Knowledge'. *Pest Management Science* 70 (9), 1367–77.
Sathe, S. & Durand, P. M. (2016). 'Cellular Aggregation in *Chlamydomonas* (Chlorophyceae) is Chimaeric and Depends on Traits Like Cell Size and Motility'. *European Journal of Phycology* 51 (2), 129–38.
Saxton, M. A., Morrow, E. A., Bourbonniere, R. A. & Wilhelm, S. W. (2011). 'Glyphosate Influence on Phytoplankton Community Structure in Lake Erie'. *Journal of Great Lakes Research* 37 (4), 683–90.
Scholz, N. L., Fleishman, E., Brown, L., Werner, I., Johnson, M. L., Brooks, M. L., Mitchelmore, C. L. & Schlenk, D. (2012). 'A Perspective on Modern Pesticides, Pelagic Fish Declines, and Unknown Ecological Resilience in Highly Managed Ecosystems'. *BioScience* 62 (4), 428–34.
Sergiev, I. G., Alexieva, V. S., Ivanov, S. V., Moskova, I. I. & Karanov, E. N. (2006). 'The Phenylurea Cytokinin 4PU-30 Protects Maize Plants Against Glyphosate Action'. *Pesticide Biochemistry and Physiology* 85 (3), 139–46.
Servaites, J. C., Tucci, M. A. & Geiger, D. R. (1987). 'Glyphosate Effects on Carbon Assimilation, Ribulose Bisphosphate Carboxylase Activity, and Metabolite Levels in Sugar Beet Leaves'. *Plant Physiology* 85 (2), 370–4.
Sharma, S. S. & Dietz, K.-J. (2006). 'The Significance of Amino Acids and Amino Acid-Derived Molecules in Plant Responses and Adaptation to Heavy Metal Stress'. *Journal of Experimental Botany* 57 (4), 711–26.
Shaner, D. L. (2014). 'Lessons Learned From the History of Herbicide Resistance'. *Weed Science* 62 (2), 427–31.
Shaner, D. (1995). 'Herbicide Resistance: Where Are We? How Did We Get Here? Where Are We Going?' *Weed Technology* 9 (4), 850–56.
Shino, M., Hamada, T., Shigematsu, Y., Hirase, K. & Banba, S. (2018). 'Action Mechanism of Bleaching Herbicide Cyclopyrimorate, a Novel Homogentisate Solanesyltransferase Inhibitor'. *Journal of Pesticide Science* 43 (4), 233–9.
Sidhu, R. S., Hammond, B. G., Fuchs, R. L., Mutz, J.-N., Holden, L. R., George, B. & Olson, T. (June 2000). 'Glyphosate-Tolerant Corn: The Composition and Feeding Value of Grain from Glyphosate-Tolerant Corn Is Equivalent to That of Conventional Corn (*Zea mays* L.)' *Journal of Agricultural and Food Chemistry* 48 (6), 2305–2312.
Sikorski, Ł., Baciak, M., Bęś, A. & Adomas, B. (Apr. 2019). 'The Effects of Glyphosate-Based Herbicide Formulations on *Lemna minor*, a Non-Target Species'. *Aquatic Toxicology* 209, 70–80.
Skelding, D., Hart, S. F. M., Vidyasagar, T., Pozhitkov, A. E. & Shou, W. (2018). 'Developing a Low-Cost Milliliter-Scale Chemostat Array for Precise Control of Cellular Growth'. *Quantitative Biology* 6.2, 129–41.
Smyth, D. A., Wu, M.-X. & Black, C. C. (1984). 'Pyrophosphate and Fructose 2,6-Bisphosphate Effects on Glycolysis in Pea Seed Extracts'. *Plant Physiology* 76 (2), 316–20.

Sofo, A., Scopa, A., Dumontet, S., Mazzatura, A. & Pasquale, V. (2012). 'Toxic Effects of Four Sulphonylureas Herbicides on Soil Microbial Biomass'. *Journal of Environmental Science and Health, Part B* 47 (7), 653–9.

Solovchenko, A. E. (2013). 'Physiology and Adaptive Significance of Secondary Carotenogenesis in Green Microalgae'. *Russian Journal of Plant Physiology* 60 (1), 1–13.

Steinrücken, H. & Amrhein, N. (1980). 'The Herbicide Glyphosate is a Potent Inhibitor of 5-Enolpyruvylshikimic Acid-3-Phosphate Synthase'. *Biochemical and Biophysical Research Communications* 94 (4), 1207–12.

Strauss, S. Y., Rudgers, J. A., Lau, J. A. & Irwin, R. E. (2002). 'Direct and Ecological Costs of Resistance to Herbivory'. *Trends in Ecology and Evolution* 17 (6), 278–85.

Strilbyska, O. M., Tsiumpala, S. A., Kozachyshyn, I. I., Strutynska, T., Burdyliuk, N., Lushchak, V. I. & Lushchak, O. (2022). 'The Effects of Low-Toxic Herbicide Roundup and Glyphosate on Mitochondria'. *EXCLI journal* 21, 183–96.

Stupak, E. E., Migranova, I. G., Sharafieva, E. R., Egorova, N. N., Stupak, S. I. & Nikonov, V. I. (2019). 'The Glyphosate Influence on Cytogenetic and Biochemical Aspects of Wheat (*Triticum aestivum* L) Seedlings Development'. *IOP Conference Series: Earth and Environmental Science* 315 (4), 042018.

Sumner, L. W., Mendes, P. & Dixon, R. A. (2003). 'Plant Metabolomics: Large-Scale Phytochemistry in the Functional Genomics Era'. *Phytochemistry* 62 (6), 817–36.

Takano, H. K., Fernandes, V. N., Adegas, F. S., Jr, R. S. O., Westra, P., Gaines, T. A. & Dayan, F. E. (2020). 'A Novel TIPT Double Mutation in *EPSPS* Conferring Glyphosate Resistance in Tetraploid *Bidens subalternans*'. *Pest Management Science* 76 (1), 95–02.

Tierney, K. B., Baldwin, D. H., Hara, T. J., Ross, P. S., Scholz, N. L. & Kennedy, C. J. (2010). 'Olfactory Toxicity in Fishes'. *Aquatic Toxicology* 96 (1), 2–26.

Timmons, F. L. (1970). 'A History of Weed Control in the United States and Canada'. *Weed Science* 18 (2), 294–307.

Tonoyan, L., Guihéneuf, F., Friel, R. & O'Flaherty, V. (2020). 'Construction and Validation of A Low-Cost, Small-Scale, Multiplex Continuous Culturing System for Microorganisms'. *Bio-protocol* 10.21, e3813.

Toprak, E., Veres, A., Yildiz, S., Pedraza, J., Chait, R., Paulsson, J. & Kishony, R. (2013). 'Building a Morbidostat: An Automated Continuous-Culture Device for Studying Bacterial Drug Resistance Under Dynamically Sustained Drug Inhibition'. *Nature protocols* 8, 555–67.

Trenkamp, S., Eckes, P., Busch, M. & Fernie, A. R. (2009). 'Temporally resolved GC-MS-based metabolic profiling of herbicide treated plants treated reveals that changes in polar primary metabolites alone can distinguish herbicides of differing mode of action'. *Metabolomics* 5 (3), 277–91.

Unver, T., Bakar, M., Shearman, R. C. & Budak, H. (2010). 'Genome-Wide Profiling and Analysis of *Festuca arundinacea* miRNAs and Transcriptomes in Response to Foliar Glyphosate Application'. *Molecular Genetics and Genomics* 283 (4), 397–413.

Van Bruggen, A., He, M., Shin, K., Mai, V., Jeong, K., Finckh, M. & Morris, J. (2018). 'Environmental and Health Effects of the Herbicide Glyphosate'. *Science of The Total Environment* 616, 255–68.

Van den Bergh, B., Swings, T., Fauvart, M. & Michiels, J. (2018). 'Experimental Design, Population Dynamics, and Diversity in Microbial Experimental Evolution'. *Microbiology and Molecular Biology Reviews* 82 (3), e00008–18.

Van Horn, C. R., Moretti, M. L., Robertson, R. R., Segobye, K., Weller, S. C., Young, B. G., Johnson, W. G., Schulz, B., Green, A. C., Jeffery, T., Lespérance, M. A., Tardif, F. J., Sikkema, P. H., Hall, J. C., McLean, M. D., Lawton, M. B., Sammons, R. D., Wang, D., Westra, P. & Gaines, T. A. (2018). 'Glyphosate Resistance in *Ambrosia trifida*: Part 1. Novel Rapid Cell Death Response to Glyphosate'. *Pest Management Science* 74 (5), 1071–8.

Van Donk, E., Lürling, M., Hessen, D. O. & Lokhorst, G. M. (1997). 'Altered Cell Wall Morphology in Nutrient-Deficient Phytoplankton and its Impact on Grazers'. *Limnology and Oceanography* 42 (2), 357–64.

Vemanna, R. S., Vennapusa, A. R., Easwaran, M., Chandrashekar, B. K., Rao, H., Ghanti, K., Sudhakar, C., Mysore, K. S. & Makarla, U. (2017). 'Aldo-Keto Reductase Enzymes Detoxify

Glyphosate and Improve Herbicide Resistance in Plants'. *Plant Biotechnology Journal* 15 (7), 794–804.

Vervoort, L. M., Ronden, J. E. & Thijssen, H. H. (1997). 'The Potent Antioxidant Activity of the Vitamin K Cycle in Microsomal Lipid Peroxidation'. *Biochemical Pharmacology* 54 (8), 871–6.

Vila-Aiub, M. M., Neve, P. & Powles, S. B. (2005). 'Resistance Cost of a Cytochrome P450 Herbicide Metabolism Mechanism but not an ACCase Target Site Mutation in a Multiple Resistant *Lolium rigidum* Population'. *New Phytologist* 167 (3), 787–96.

Vila-Aiub, M. M., Neve, P. & Powles, S. B. (2009a). 'Fitness Costs Associated with Evolved Herbicide Resistance Genes in Plants'. *New Phytologist* 184, 751–67.

Vila-Aiub, M. M., Neve, P. & Powles, S. B. (2009b). 'Evidence for an Ecological Cost of Enhanced Herbicide Metabolism in *Lolium rigidum*'. *Journal of Ecology* 97 (4), 772–80.

Vila-Aiub, M. M., Balbi, M. C., Distéfano, A. J., Fernández, L., Hopp, E., Yu, Q. & Powles, S. B. (2012). 'Glyphosate Resistance in Perennial *Sorghum halepense* (Johnsongrass), Endowed by Reduced Glyphosate Translocation and Leaf Uptake'. *Pest Management Science* 68 (3), 430–6.

Vila-Aiub, M. M., Gundel, P. E., Yu, Q. & Powles, S. B. (2013). 'Glyphosate Resistance in *Sorghum halepense* and *Lolium rigidum* is Reduced at Suboptimal Growing Temperatures'. *Pest Management Science* 69 (2), 228–32.

Vila-Aiub, M. M., Goh, S. S., Gaines, T. A., Han, H., Busi, R., Yu, Q. & Powles, S. B. (2014). 'No Fitness Cost of Glyphosate Resistance Endowed by Massive EPSPS Gene Amplification in *Amaranthus palmeri*'. *Planta* 239 (4), 793–801.

Visviki, I. & Santikul, D. (2000). 'The pH Tolerance of *Chlamydomonas applanata* (Volvocales, Chlorophyta)'. *Archives of Environmental Contamination and Toxicology* 38 (2), 147–51.

Vogwill, T., Lagator, M., Colegrave, N. & Neve, P. (2012). 'The Experimental Evolution of Herbicide Resistance in *Chlamydomonas reinhardtii* Results in a Positive Correlation Between Fitness in the Presence and Absence of Herbicides'. *Journal of Evolutionary Biology* 25 (10), 1955–64.

Wahl, L. M. & Gerrish, P. J. (2001). 'The Probability that Beneficial Mutations are Lost in Populations with Periodic Bottlenecks'. *Evolution* 55.12, 2606–10.

Wakelin, A. M. & Preston, C. (2006). 'The Cost of Glyphosate Resistance: Is There a Fitness Penalty Associated with Glyphosate Resistance in Annual Ryegrass'. *Proceedings of the 15th Australian Weeds Conference. Adelaide, South Australia: Weed Management Society of South Australia*, 515–8.

Wang, T., Picard, J. C., Tian, X. & Darmency, H. (2010). 'A Herbicide-Resistant ACCase 1781 *Setaria* Mutant Shows Higher Fitness Than Wild Type'. *Heredity* 105 (4), 394–400.

Wang, C.-Y. (2001). 'Effect of Glyphosate on Aromatic Amino Acid Metabolism in Purple Nutsedge (*Cyperus rotundus*)'. *Weed Technology* 15 (4), 628–35.

Warwick, S. I. & Black, L. (1981). 'The Relative Competitiveness of Atrazine Susceptible and Resistant Populations of *Chenopodium album* and *C. strictum*'. *Canadian Journal of Botany* 59 (5), 689–93.

Wenger, J. W., Piotrowski, J., Nagarajan, S., Chiotti, K., Sherlock, G. & Rosenzweig, F. (2011). 'Hunger Artists: Yeast Adapted to Carbon Limitation Show Trade-Offs under Carbon Sufficiency'. *PLOS Genetics* 7.8, e1002202.

Werck-Reichhart, D., Hehn, A. & Didierjean, L. (2000). 'Cytochromes P450 for Engineering Herbicide Tolerance'. *Trends in Plant Science* 5 (3), 116–23.

Whitehead, C. W. & Switzer, C. M. (1963). 'The Differential Response of Strains of Wild Carrot to 2,4-D and Related Herbicides'. *Canadian Journal of Plant Science* 43 (3), 255–62.

Wong, B. G., Mancuso, C. P., Kiriakov, S., Bashor, C. J. & Khalil, A. S. (2018). 'Precise, Automated Control of Conditions for High-Throughput Growth of Yeast and Bacteria with eVOLVER'. *Nature biotechnology* 36.7, 614–23.

Wood, S. N. (2011). 'Fast Stable Restricted Maximum Likelihood and Marginal Likelihood Estimation of Semiparametric Generalized Linear Models'. *Journal of the Royal Statistical Society (B)* 73.1, 3–36.

Xi, Y.-L. & Feng, L.-K. (2004). 'Effects of Thiophanate-Methyl and Glyphosate on Asexual and Sexual Reproduction in the Rotifer *Brachionus calyciflorus* Pallas'. *Bulletin of Environmental Contamination and Toxicology* 73 (4), 644–51.

Xia, J., Psychogios, N., Young, N. & Wishart, D. S. (2009). 'MetaboAnalyst: A Web Server for Metabolomic Data Analysis and Interpretation'. *Nucleic Acids Research* 37 (Web Server), W652–60.

Yanniccari, M., Vila-Aiub, M. M., Istilart, C., Acciaresi, H. & Castro, A. M. (2016). 'Glyphosate Resistance in Perennial Ryegrass (*Lolium perenne* L.) is Associated with a Fitness Penalty'. *Weed Science* 64 (1), 71–9.

Yoshida, T., Jones, L. E., Ellner, S. P., Fussmann, G. F. & Hairston, N. G. (2003). 'Rapid Evolution Drives Ecological Dynamics in a Predator-Prey System'. *Nature* 424 (6946), 303–6.

Yu, Q., Cairns, A. & Powles, S. B. (2006). 'Glyphosate, Paraquat and ACCase Multiple Herbicide Resistance Evolved in a *Lolium rigidum* biotype'. *Planta* 225 (2), 499–513.

Yu, Q., Han, H., Vila-Aiub, M. M. & Powles, S. B. (2010). 'AHAS Herbicide Resistance Endowing Mutations: Effect on AHAS Functionality and Plant Growth'. *Journal of Experimental Botany* 61 (14), 3925–34.

Yu, Q., Jalaludin, A., Han, H., Chen, M., Sammons, R. D. & Powles, S. B. (2015). 'Evolution of a Double Amino Acid Substitution in the 5-Enolpyruvylshikimate-3-Phosphate Synthase in *Eleusine indica* Conferring High-Level Glyphosate Resistance'. *Plant Physiology* 167 (4), 1440–7.

Yu, H., Peng, J., Cao, X., Wang, Y., Zhang, Z., Xu, Y. & Qi, W. (2021). 'Effects of Microplastics and Glyphosate on Growth Rate, Morphological Plasticity, Photosynthesis, and Oxidative Stress in the Aquatic Species *Salvinia cucullata*'. *Environmental Pollution* 279, 116900.

Yuan, J. S., Tranel, P. J. & Stewart, C. N. (2007). 'Non-Target-Site Herbicide Resistance: A Family Business'. *Trends in Plant Science* 12 (1), 6–13.

Yuan, J. S., Abercrombie, L. L. G., Cao, Y., Halfhill, M. D., Zhou, X., Peng, Y., Hu, J., Rao, M. R., Heck, G. R., Larosa, T. J., Sammons, R. D., Wang, X., Ranjan, P., Johnson, D. H., Wadl, P. A., Scheffler, B. E., Rinehart, T. A., Trigiano, R. N. & Stewart, C. N. (2010). 'Functional Genomics Analysis of Horseweed (*Conyza canadensis*) with Special Reference to the Evolution of Non–Target-Site Glyphosate Resistance'. *Weed Science* 58 (2), 109–17.

Zabalza, A., Orcaray, L., Fernández-Escalada, M., Zulet-González, A. & Royuela, M. (2017). 'The Pattern of Shikimate Pathway and Phenylpropanoids After Inhibition by Glyphosate or Quinate Feeding in Pea Roots'. *Pesticide Biochemistry and Physiology* 141, 96–102.

Zhong, G., Wu, Z., Liu, N. & Yin, J. (2018). 'Phosphate Alleviation of Glyphosate-Induced Toxicity in *Hydrocharis dubia* (Bl.) Backer'. *Aquatic Toxicology* 201, 91–8.

Zhu, J., Patzoldt, W. L., Shealy, R. T., Vodkin, L. O., Clough, S. J. & Tranel, P. J. (2008). 'Transcriptome Response to Glyphosate in Sensitive and Resistant Soybean'. *Journal of Agricultural and Food Chemistry* 56 (15), 6355–363.

Appendices

APPENDIX A: CHAPTER 3 SUPPLEMENTARY MATERIAL

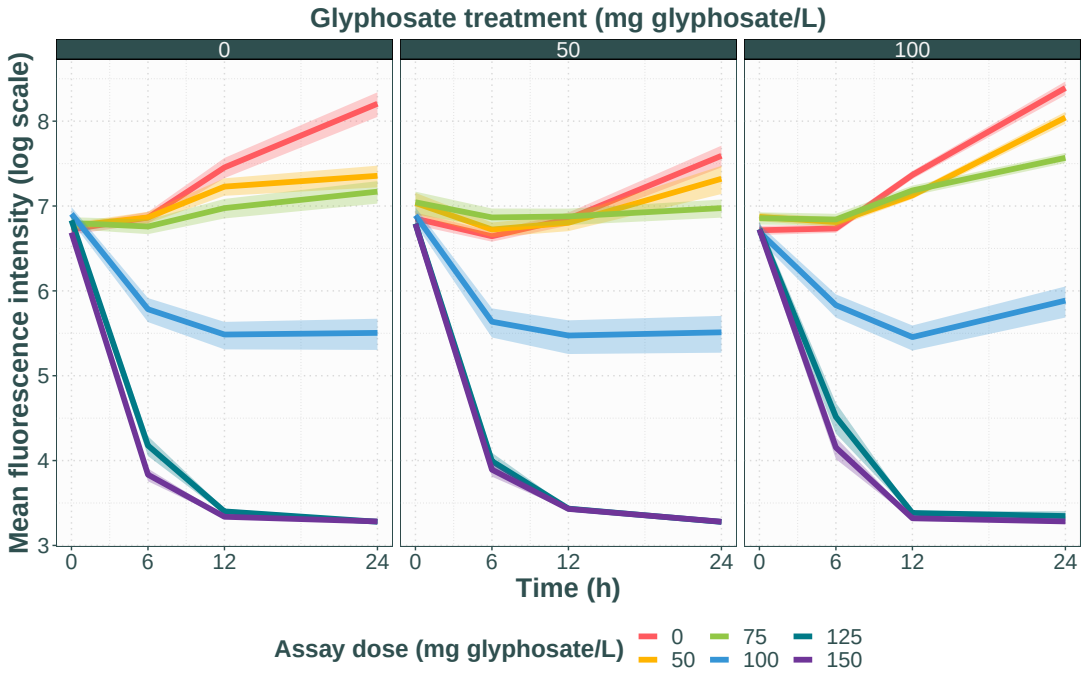

Figure A.2: Mean fluorescence intensity, a proxy for population density, through time in the growth assay 43 days after glyphosate introduction. Growth in each dose is represented as a separate colour. Each selection treatment is represented as a separate panel (0, 50, 100 mg/L glyphosate).

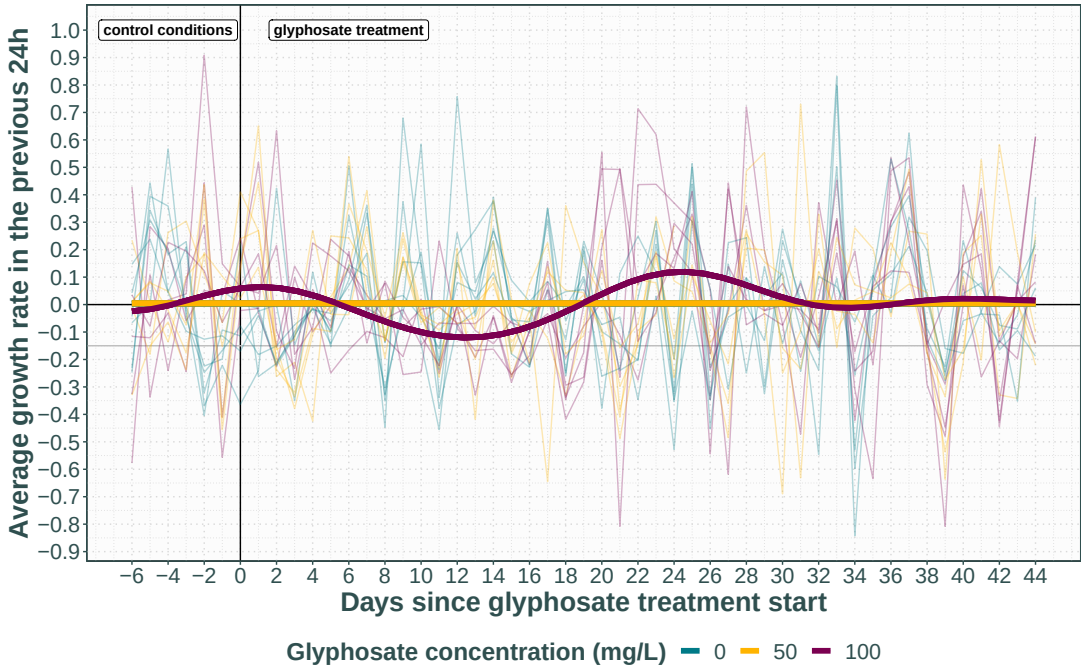

Figure A.3: Growth rate between days 8 and 57 of the experiment. Each thin line represents a population, thick lines display the predicted fit for each treatment by the hGAM. The horizontal grey line represents the dilution rate of 0.15.

Table A.1: Output for hGAM of day-to-day growth rate. edf refers to the effective degrees of freedom, i.e. the complexity of the smooth. The Ref.df, F and p-value are generated by an ANOVA to test the overall significance of the smooth, i.e. testing if it is different from a flat fit.

Smooth term	edf	Ref.df	F	p-value
s(exp_day):treatment_group0	0.000002	8	0	0.5
s(exp_day):treatment_group50	0.000009	8	0	0.7
s(exp_day):treatment_group100	5.7	8	7.9	0.001
s(treatment_group)	0.0000001	2	0	< 0.9
s(exp_day,chamber)	0.00001	158	0	< 0.9
s(dayID)	41.5	50	5	< 0.001

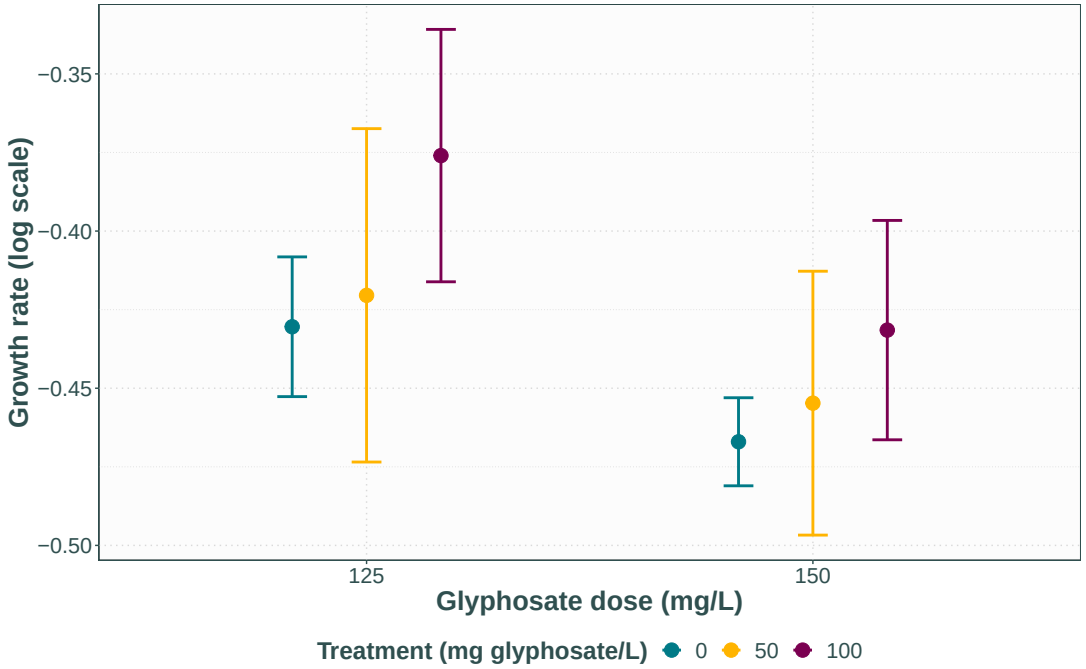

Figure A.4: Average growth rate over 6 hours in very high lethal doses of glyphosate 43 days after glyphosate introduction.

APPENDIX B: CHAPTER 5 SUPPLEMENTARY MATERIAL

Table B.1: Compounds targeted in MS/MS analysis, divided by hypothesis. Peaks from reference spectra have been excluded if below the detection limit of the instrument (<50 Da) or had a relative expected intensity below 30.

Compound	**Accurate mass**	**Target mass (mode)**	**Collision energy**	**MassBank reference spectrum**	**Major expected peaks**	**Present?**
Shikimate pathway						
D-Erythrose-4P (E4P)	200.0086	199(-)	10	PR100545	96.9703 ✓ 78.9602 ✓ 138.9800 ✓ 199.0008 ✓ 154.9088 ✓	✓
Phosphoenolpyruvate (PEP)	167.9824	167(-)	5	KO001571	167.0000 ✓ 78.9000 ✓ 138.9000 ✓	✓ ✓
Shikimate	174.0528	173(-)	30	KO001789	119.0000 ✓ 173.3000 ✓ 137.1000 ✓ 141.0000 ✓ 59.2000 ✗ 172.9000 ✓ 155.3000 ✓ 93.3000 ✗ 111.2000 ✓ 113.0000 ✓ 77.0000 ✗	✓
Amino acids						
Alanine (Ala)*	89.0477	88(-)	10	KO000021	88.2000 ✓	✓
Alanine (Ala)*	89.0477	90(+)	5	KO002053	90.0000 ✓	✓
Arginine (Arg)	174.1117	175(+)	10	CE000265	158.0923 ✓ 157.1083 ✓ 116.0705 ✓ 130.0975 ✓ 175.1190 ✓	✓
Arginine (Arg)	174.1117	173.2(-)	20	PR100578	131.0817 ✓ 173.1039 ✓	✓
Asparagine (Asn)	132.0535	131(-)	20	KO000025	114.0000 ✓ 113.3000 ✗ 70.0000 ✗ 95.3000 ✗ 131.0000 ✓ 70.8000 ✗ 71.9000 ✗ 58.2000 ✗	✓
Aspartate (Asp)	133.0375	132(-)	10	CE000453	132.0309 ✓ 88.0410 ✓ 115.0043 ✓ 114.0203 ✓	✓
Aspartate (Asp)	133.0375	134(+)	25	KO002065	74.0000 ✗ 70.2000 ✗ 88.2000 ✗ 71.0000 ✗ 72.1000 ✓	✗
Cysteine (Cys)	121.0197	122(+)	30	KO000848	58.9960 ✗ 76.0230 ✓ 86.9900 ✓	✗
Glutamate (Glu)	147.0532	146(-)	10	KO000848	146.1000 ✓ 127.9000 ✓ 102.0000 ✓	✓
Glutamine (Gln)‡	146.0691	145(-)	10	KO000843	145.0000 ✓ 144.6000 ✓ 127.0000 ✓	✓
Glycine (Gly)	75.032	74(-)	10	KO000829	74.0000 ✓	✓
Glycine (Gly)	75.032	76(+)	10	KO002934	76.0000 ✓	✓
Histidine (His)	155.0695	154(-)	20	BML01100	137.0347 ✓ 110.0720 ✓ 154.0613 ✓ 136.0498 ✓ 118.0387 ✓ 109.0375 ✓ 108.0607 ✓ 137.0719 ✓ 106.0393 ✓ 154.0373 ✓	✓

Continued on next page

Table B.1 – continued from previous page

Compound	Accurate mass	Target mass (mode)	Collision energy	MassBank reference spectrum	Major expected peaks	Accepted as present?
Histidine (His)	155.0695	156(+)	10	BML01070	114.9471 ✓ 111.9856 ✓ 155.9809 ✓	✓
Isoleucine (Iso)	131.0946	130(-)	30	KO001177	130.0000 ✓ 82.0000 ✗ 58.7000 ✗	
Isoleucine (Iso)	131.0946	132(+)	10	KO003173	86.2000 ✓ 69.2000 ✓ 115.3000 ✓ 98.0000 ✓	✓
Leucine (Leu)	131.0946	130(-)	30	KO001263	130.0000 ✓ 81.9000 ✗ 84.2000 ✗ 66.1000 ✗ 71.9000 ✗	
Leucine (Leu)	131.0946	132(+)	10	KO003278	86.2000 ✓ 115.1000 ✓	✓
Lysine (Lys)	146.1055	147(-)	30	RP001112	97.0781 ✓	✓
Methionine (Met)	149.051	150(+)	20	KO003333	104.1000 ✓ 56.3000 ✗ 133.1000 ✓ 101.8000 ✓ 61.1000 ✗ 73.0000 ✓ 74.0000 ✗ 87.3000 ✗ 150.3000 ✗ 114.4000 ✗ 86.2000 ✓ 84.2000 ✓ 85.0000 ✓ 115.4000 ✗ 101.0000 ✓ 105.0000 ✓	✓
Phenylalanine (Phe)	165.079	166(+)	20	RP000402	120.0807 ✓ 103.0541 ✓ 93.0694 ✓ 121.0840 ✓ 93.0694 ✓ 79.0538 ✓	✓
Phenylalanine (Phe)	165.079	164(-)	20	RP000412	103.0558 ✓ 147.0447 ✓ 164.0727 ✓ 104.0585 ✓ 148.0521 ✓	✓
Proline (Pro)	115.0633	116(+)	20	KO003673	70.0000 ✓	✓
Proline (Pro)	115.0633	114(-)	20	RP001712	114.0563 ✓	✓
Serine (Ser)	105.0426	104(-)	20	KO001781	74.2000 ✗ 103.9000 ✓	✗
Threonine (Thr)	119.0582	118(-)	20	KO001878	74.1000 ✗ 118.1000 ✓	✗
Tryptophan (Trp)	204.0899	205(+)	20	KO004073	188.2000 ✓ 146.1000 ✓ 144.1000 ✓ 159.1000 ✓ 118.1000 ✓ 170.1000 ✓	✓
Tryptophan (Trp)	204.0899	203(-)	20	KO001868	203.3000 ✓ 116.0000 ✓ 73.9000 ✓ 143.4000 ✗ 141.9000 ✓ 159.2000 ✓ 186.2000 ✓ 130.0000 ✓ 129.0000 ✓	✓
Tyrosine (Tyr)	181.0739	180(-)	20	KO001863	163.1000 ✓ 180.4000 ✗ 119.3000 ✗ 92.8000 ✓ 136.1000 ✓ 72.2000 ✗ 147.8000 ✗ 74.2000 ✗ 106.0000 ✓ 107.0000 ✓	✓
Tyrosine (Tyr)	181.0739	182(+)	10	KO004067	182.1000 ✓ 165.2000 ✓	✓

Continued on next page

Table B.1 – continued from previous page

Compound	Accurate mass	Target mass (mode)	Collision energy	MassBank reference spectrum	Major expected peaks	Accepted as present?
					136.0000 ✓ 122.2000 ✓ 121.0000 ✓	
Valine (Val)	117.079	116(-)	30	KO001990	116.2000 ✓	✓
Valine (Val)	117.079	118(+)	10	KO004251	118.1000 ✓ 72.0000 ✓ 101.0000 ✓ 50.1000 ✗ 117.6000 ✓	✓
Glyphosate and its degradation products						
Glyphosate	169.014	168(-)	4		167.9784 ✓ 149.9676 ✓ 123.9863 ✓ 180.0034 ✓	✓
Glyphosate	169.014	170(+)	4		173.9452 ✗ 129.9587 ✗ 175.9372 ✗ 170.0637 ✓ 163.9376 ✓	✗
Glyoxylate	74.0004	73(-)	10	KO000835	73.0000 ✗	✗
Sarcosine*	89.0477	88(-)	10	KO001799	88.2000 ✓	✓
Sarcosine*	89.0477	90(+)	5	KO003987	90.0000 ✓	✓
2-oxoglutarate‡	146.0215	145(-)	10	KO001528	145.1000 ✓ 101.1000 ✓	✓
Cinnamyl alcohol	134.0732	135(+)	10	PS044801	135.0000 ✓ 134.0000 ✓ 73.0000 ✓ 93.0000 ✓	✓
Exploratory analysis compounds						
D-ribose 5-phosphate	230.0192	229(-)	20	KO001751	97.2000 ✓ 78.9000 ✓ 139.2000 ✗ 99.1000 ✓ 229.3000 ✓ 137.3000 ✓ 147.0000 ✓ 169.0000 ✓ 59.1000 ✗ 165.4000 ✗	✓
D-ribulose 5-phosphate	230.0192	229(-)	20	PR100553	96.9677 ✓ 78.9590 ✓	✓
linoleate	280.2402	303(+)	20	PS027803	229.0114 ✓ 281.0000 ✓ 73.0000 ✓ 265.0000 ✓ 264.0000 ✓ 248.0000 ✓	✓
palmitoleate	254.2246	253(-)	40	KO001629	253.4000 ✗ 71.1000 ✗ 79.0000 ✓ 59.1000 ✗ 97.2000 ✗ 83.2000 ✗ 95.3000 ✗ 126.7000 ✗ 220.5000 ✗	✗
phosphate	97.9769	97(-)	40	RP022413	78.9591 ✓ 62.9641 ✗	✓
thiamine	266.1201	247(-)	20	KO001934	147.1000 ✓ 233.1000 ✓	✓
thyroxine	776.6867	777(+)	15	AU274306	731.6904 ✗ 604.7811 ✗ 350.9754 ✗ 379.9523 ✗ 323.9650 ✗ 633.7740 ✓	✗

Continued on next page

Table B.1 – continued from previous page

Compound	Accurate mass	Target mass (mode)	Collision energy	MassBank reference spectrum	Major expected peaks	Accepted as present?
					732.6928 ✓ 576.7651 ✓	
		759(+)			731.6904 ✗ 604.7811 ✗ 350.9754 ✗ 379.9523 ✓ 323.9650 ✗ 633.7740 ✗ 732.6928 ✓ 576.7651 ✗	✗
(2S)-2-isopropylmalate	176.0685	175(-)	20	KO001237	115.1000 ✗ 175.0000 ✓ 113.0000 ✓ 85.1000 ✗ 157.2000 ✗ 131.0000 ✗ 128.8000 ✗	✗
N-carbamoyl-L-aspartate	176.0433	175(-)		KO000412	131.8000 ✗ 114.8000 ✗ 88.1000 ✓ 93.3000 ✗	✗
AMP	347.0631	346(-)	20	PR100515	78.9598 ✓ 346.0553 ✓ 96.9698 ✓ 134.0470 ✓	✓
dGMP	347.0631	346(-)	20	PS048007	346.0000 ✓ 345.0000 ✓	✓
bilirubin	584.2635	583(-)	40	MT000136	285.1000 ✓ 539.2000 ✓ 241.2000 ✓ 253.2000 ✓ 286.1000 ✓ 213.2000 ✓	✓
GMP	363.058	362(-)	20	PR100567	78.9597 ✓ 362.0502 ✓ 211.0005 ✓ 96.9699 ✓ 150.0415 ✓ 133.0149 ✓	✓
medicagenate	502.3294	483(-)	40	BS003800	501.3200 ✗ 483.3079 ✓ 437.3043 ✗ 502.3245 ✗ 439.3184 ✗ 425.3060 ✗ 484.3129 ✗ 426.3095 ✗ 438.3101 ✗ 455.3126 ✗ 440.3184 ✗ 421.3097 ✗ 422.3162 ✗	✗

Table B.2: Mass bins and their putatively matched compounds, accurate masses, expected masses as given adducts, chemical formulas and expected roll in the cell metabolome. Compounds with the same monoisotopic mass are listed together. Compounds in **bold** were confirmed to be present through MS/MS analysis, all others could not be confirmed due to no reference spectra being available.

Mass-bin (mode)	Compound	Structure	Accurate mass	Expected mass and ion	Class
Pre-resistance					
97 (-)	(E)-2-hexenal	$C_6H_{10}O$	98.0732	97.0732 $[M-H]^-$	aldehyde
	(Z)-3-hexanal	$C_6H_{10}O$	98.0732	97.0732 $[M-H]^-$	aldehyde
	phosphate	HO_4P	97.9769	96.9769 $[M-H]^-$	inorganic phosphate
175 (-)	(2R,3S)-3-isopropylmalate	$C_7H_{10}O_5$	176.0685	175.0685 $[M-H]^-$	leucine precursor
	4-hydroxy-4-methyl-2-oxoglutarate	$C_6H_6O_6$	176.0321	175.0321 $[M-H]^-$	carboxylate
	L-ascorbate	$C_6H_7O_6$	176.0321	175.0321 $[M-H]^-$	Vitamin C
	L-*xylo*-hex-3-ulono-1,4-lactone	$C_6H_8O_6$	176.0321	175.0321 $[M-H]^-$	Vitamin C precursor
	N^5-formyl-N^5-hydroxy-L-ornithine	$C_6H_{12}N_2O_4$	176.0797	175.0797 $[M-H]^-$	modified amino acid
	6-hydroxy-*N*-methylmyosmine	$C_{10}H_{13}N_2O$	176.0950	175.0950 $[M-H]^-$	pyrroline
	serotonin	$C_{10}H_{13}N_2O$	176.0950	175.0950 $[M-H]^-$	signalling compound
223.2 (-)	5,6-epoxy-3-hydroxy-9-apo-β-caroten-9-one	$C_{13}H_{20}O_3$	224.1412	223.1412 $[M-H]^-$	carotenoid
	grasshopper ketone	$C_{13}H_{20}O_3$	224.1412	223.1412 $[M-H]^-$	carotenoid
228 (-)	4,5-*seco*-dopa	$C_9H_{10}NO_6$	229.0586	228.0586 $[M-H]^-$	betalain metabolite
	5-phospho-β-D-ribosylamine	$C_5H_{11}NO_7P$	229.0351	228.0351 $[M-H]^-$	purine and thiamine precursor
229 (-)	aldehydo-D-ribose 5-phosphate	$C_5H_9O_8P$	230.0192	229.0192 $[M-H]^-$	sugar phoshate
	α-D-ribose 5-phosphate	$C_5H_9O_8P$	230.0192	229.0192 $[M-H]^-$	sugar phoshate
	α-D-ribose-1-phosphate	$C_5H_9O_8P$	230.0192	229.0192 $[M-H]^-$	sugar phoshate
	β-D-ribose 5-phosphate	$C_5H_9O_8P$	230.0192	229.0192 $[M-H]^-$	sugar phoshate
	β-L-arabinose 1-phosphate	$C_5H_9O_8P$	230.0192	229.0192 $[M-H]^-$	sugar phoshate
	D-ribofuranose 5-phosphate	$C_5H_9O_8P$	230.0192	229.0192 $[M-H]^-$	sugar phoshate
	D-ribose 5-phosphate	$C_5H_9O_8P$	230.0192	229.0192 $[M-H]^-$	sugar phoshate
	D-ribulose 1-phosphate	$C_5H_9O_8P$	230.0192	229.0192 $[M-H]^-$	sugar phoshate
	D-ribulose 5-phosphate	$C_5H_9O_8P$	230.0192	229.0192 $[M-H]^-$	sugar phoshate
	D-xylulose 5-phosphate	$C_5H_9O_8P$	230.0192	229.0192 $[M-H]^-$	sugar phoshate
	L-ribulose 5-phosphate	$C_5H_9O_8P$	230.0192	229.0192 $[M-H]^-$	sugar phoshate
	L(or D)-ribulose 5-phosphate	$C_5H_9O_8P$	230.0192	229.0192 $[M-H]^-$	sugar phoshate
245 (-)	dimethylallyl diphosphate	$C_5H_9O_7P_2$	246.0058	245.0058 $[M-H]^-$	isoprenoid precursor
	glycerophosphoglycerol	$C_6H_{14}O_8P$	246.0505	245.0505 $[M-H]^-$	lipid
	isopentenyl diphosphate	$C_5H_9O_7P_2$	246.0058	245.0058 $[M-H]^-$	isoprenoid precursor
247.2 (-)	**thiamine**	$C_{12}H_{17}N_4OS$	266.1201	247.1101 $[M-H_2O-H]^-$	B vitamin
259 (-)	1D-*myo*-inositol 1-monophosphate	$C_6H_{11}O_9P$	260.0297	259.0297 $[M-H]^-$	polyol
	1D-*myo*-inositol 2-monophosphate	$C_6H_{11}O_9P$	260.0297	259.0297 $[M-H]^-$	polyol
	1D-*myo*-inositol 3-monophosphate	$C_6H_{11}O_9P$	260.0297	259.0297 $[M-H]^-$	polyol
	1D-*myo*-inositol 4-monophosphate	$C_6H_{11}O_9P$	260.0297	259.0297 $[M-H]^-$	polyol
	1D-*myo*-inositol 5-monophosphate	$C_6H_{11}O_9P$	260.0297	259.0297 $[M-H]^-$	polyol
	1D-*myo*-inositol 6-monophosphate	$C_6H_{11}O_9P$	260.0297	259.0297 $[M-H]^-$	polyol
	a D-galactopyranose 1-phosphate	$C_6H_{11}O_9P$	260.0297	259.0297 $[M-H]^-$	sugar phoshate

Continued on next page

Table B.2 – continued from previous page

Mass-bin (mode)	Compound	Structure	Accurate mass	Expected mass and ion	Class
	a hexose 1-phosphate	$C_6H_{11}O_9P$	260.0297	259.0297 $[M-H]^-$	sugar phoshate
	α-D-galactose 1-phosphate	$C_6H_{11}O_9P$	260.0297	259.0297 $[M-H]^-$	sugar phoshate
	α-D-galactose 6-phosphate	$C_6H_{11}O_9P$	260.0297	259.0297 $[M-H]^-$	sugar phoshate
	α-D-glucopyranose 1-phosphate	$C_6H_{11}O_9P$	260.0297	259.0297 $[M-H]^-$	sugar phoshate
	α-D-glucose 6-phosphate	$C_6H_{11}O_9P$	260.0297	259.0297 $[M-H]^-$	sugar phoshate
	α-D-mannopyranose 6-phosphate	$C_6H_{11}O_9P$	260.0297	259.0297 $[M-H]^-$	sugar phoshate
	α-D-mannose 1-phosphate	$C_6H_{11}O_9P$	260.0297	259.0297 $[M-H]^-$	sugar phoshate
	an α-hexose 1-phosphate	$C_6H_{11}O_9P$	260.0297	259.0297 $[M-H]^-$	sugar phoshate
	an inositol phosphate	$C_6H_{11}O_9P$	260.0297	259.0297 $[M-H]^-$	polyol
	β-D-fructofuranose 1-phosphate	$C_6H_{11}O_9P$	260.0297	259.0297 $[M-H]^-$	sugar phoshate
	β-D-fructofuranose 6-phosphate	$C_6H_{11}O_9P$	260.0297	259.0297 $[M-H]^-$	sugar phoshate
	β-D-galactose 6-phosphate	$C_6H_{11}O_9P$	260.0297	259.0297 $[M-H]^-$	sugar phoshate
	β-D-glucopyranose 1-phosphate	$C_6H_{11}O_9P$	260.0297	259.0297 $[M-H]^-$	sugar phoshate
	β-D-glucose 6-phosphate	$C_6H_{11}O_9P$	260.0297	259.0297 $[M-H]^-$	sugar phoshate
	β-D-mannopyranose 6-phosphate	$C_6H_{11}O_9P$	260.0297	259.0297 $[M-H]^-$	sugar phoshate
	β-L-galactose 1-phosphate	$C_6H_{11}O_9P$	260.0297	259.0297 $[M-H]^-$	sugar phoshate
	β-L-gulose 1-phosphate	$C_6H_{11}O_9P$	260.0297	259.0297 $[M-H]^-$	sugar phoshate
	D-fructofuranose 1-phosphate	$C_6H_{11}O_9P$	260.0297	259.0297 $[M-H]^-$	sugar phoshate
	D-fructofuranose 6-phosphate	$C_6H_{11}O_9P$	260.0297	259.0297 $[M-H]^-$	sugar phoshate
	D-galactopyranose 6-phosphate	$C_6H_{11}O_9P$	260.0297	259.0297 $[M-H]^-$	sugar phoshate
	D-glucopyranose 6-phosphate	$C_6H_{11}O_9P$	260.0297	259.0297 $[M-H]^-$	sugar phoshate
	D-glucose 1-phosphate	$C_6H_{11}O_9P$	260.0297	259.0297 $[M-H]^-$	sugar phoshate
	D-hexose 6-phosphate	$C_6H_{11}O_9P$	260.0297	259.0297 $[M-H]^-$	sugar phoshate
	D-mannopyranose 6-phosphate	$C_6H_{11}O_9P$	260.0297	259.0297 $[M-H]^-$	sugar phoshate
	D-mannose 6-phosphate	$C_6H_{11}O_9P$	260.0297	259.0297 $[M-H]^-$	sugar phoshate
	keto-D-fructose 6-phosphate	$C_6H_{11}O_9P$	260.0297	259.0297 $[M-H]^-$	sugar phoshate
274.2 (+)	normaritidine	$C_{16}H_{19}NO_3$	273.1365	274.1365 $[M+H]^+$	alkaloid
	oxomaritinamine	$C_{16}H_{19}NO_3$	273.1365	274.1365 $[M+H]^+$	alkaloid
289 (-)	D-glycero-D-manno-heptose 7-phosphate	$C_7H_{13}O_{10}P$	290.0403	289.0403 $[M-H]^-$	sugar phoshate
	D-sedoheptulose 7-phosphate	$C_7H_{13}O_{10}P$	290.0403	289.0403 $[M-H]^-$	sugar phoshate
291.2 (-)	(9Z,13S,15Z)-12,13-epoxyoctadeca-9,11,15-trienoate	$C_{18}H_{27}O_3$	292.2038	291.2038 $[M-H]^-$	fatty acid
	12-oxo-*cis*-10,15-phytodienoate	$C_{18}H_{27}O_3$	292.2038	291.2038 $[M-H]^-$	fatty acid
	androstan-3α,17β-diol	$C_{19}H_{32}O_2$	292.2402	291.2402 $[M-H]^-$	sterol
293.2 (-)	3-oxo-2-(*cis*-2'-pentenyl)-cyclopentane-1-octanoate	$C_{18}H_{29}O_3$	294.2195	293.2195 $[M-H]^-$	fatty acid
301.2 (-)	carlactone	$C_{19}H_{26}O_3$	302.1882	301.1882 $[M-H]^-$	lactone
	tributyrin	$C_{15}H_{26}O_6$	302.1729	301.1729 $[M-H]^-$	lipid
303.2 (+)	1-monomyristoyl-glycerol	$C_{17}H_{34}O_4$	302.2457	303.2457 $[M+H]^+$	lipid
	2-(6'-methylthio)hexyl-malate	$C_{11}H_{18}O_5S$	264.1031	303.1031 $[M+K]^+$	carboxylate
	2-*cis*-abs*cis*ate	$C_{15}H_{19}O_4$	264.1362	303.1362 $[M+K]^+$	hormone
	3-(6'-methylthio)hexyl-malate	$C_{11}H_{18}O_5S$	264.1031	303.1031 $[M+K]^+$	carboxylate

Continued on next page

Table B.2 – continued from previous page

Mass-bin (mode)	Compound	Structure	Accurate mass	Expected mass and ion	Class
	3"-deamino-3"-oxonicotianamine	$C_{12}H_{17}N_2O_7$	302.1114	303.1114 $[M+H]^+$	secondary metabolite
	8'-hydroxyabs*cis*ate	$C_{15}H_{19}O_5$	280.1311	303.1311 $[M+Na]^+$	hormone (abscisic acid derivative)
	carlactone	$C_{19}H_{26}O_3$	302.1882	303.1882 $[M+H]^+$	lactone
	linoleate	$C_{18}H_{31}O_2$	280.2402	303.2402 $[M+Na]^+$	fatty acid
	phaseic acid	$C_{15}H_{19}O_5$	280.1311	303.1311 $[M+Na]^+$	hormone (abscisic acid derivative)
304.2 (+)	pheophorbide b	$C_{35}H_{33}N_4O_6$	606.2478	304.1289 $[M+2H]^{2+}$	chlorin
309.2 (-)	13(S)-HPOTE	$C_{18}H_{29}O_4$	310.2144	309.2144 $[M-H]^-$	fatty acid
	a porphyrin	$C_{20}H_{14}N_4$	310.1218	309.1218 $[M-H]^-$	porphyrin
313.2 (+)	(9S)-HPODE	$C_{18}H_{31}O_4$	312.2301	313.2301 $[M+H]^+$	fatty acid
	13-HpODE	$C_{18}H_{31}O_4$	312.2301	313.2301 $[M+H]^+$	fatty acid
	(13S)-HPODE	$C_{18}H_{31}O_4$	312.2301	313.2301 $[M+H]^+$	fatty acid
	5-dihydrotestosterone	$C_{19}H_{30}O_2$	290.2246	313.2246 $[M+Na]^+$	steroid
	9-HpODE	$C_{18}H_{31}O_4$	312.2301	313.2301 $[M+H]^+$	fatty acid
	arachidate	$C_{20}H_{39}O_2$	312.3028	313.3028 $[M+H]^+$	fatty acid
346 (-)	2-hydroxy-dAMP	$C_{10}H_{12}N_5O_7P$	347.0631	346.0631 $[M-H]^-$	nucleotide
	AMP	$C_{10}H_{12}N_5O_7P$	347.0631	346.0631 $[M-H]^-$	nucleotide
362 (-)	8-oxo-dGMP	$C_{10}H_{12}N_5O_8P$	363.0580	362.0580 $[M-H]^-$	nucleic acid component
	GMP	$C_{10}H_{12}N_5O_8P$	363.0580	362.0580 $[M-H]^-$	nucleotie
425.2 (-)	deacetylmycothiol	$C_{15}H_{29}N_2O_{11}S$	444.1414	425.1314 $[M-H_2O-H]^-$	thiol
470.4 (+)	1-18:3-2-18:2-digalactosyldiacylglycerol	$C_{51}H_{86}O_{15}$	938.5967	470.3034 $[M+2H]^{2+}$	lipid
475.4 (+)	demethylphylloquinone	$C_{30}H_{44}O_2$	436.3341	475.3341 $[M+K]^+$	electron-transfer quinone
497.2 (-)	S-hydroxymethyl-mycothiol	$C_{18}H_{32}N_2O_{13}S$	516.1625	497.1525 $[M-H_2O-H]^-$	thiol
529.4 (-)	rhamnosyl tetracyclic spinosyn pseudoaglycone	$C_{30}H_{44}O_9$	548.2985	529.2885 $[M-H_2O-H]^-$	glycosylated macrolide
539.4 (+)	7,9,9'-*cis*-neurosporene	$C_{40}H_{58}$	538.4539	539.4539 $[M+H]^+$	carotenoid
	9'-*cis*-neurosporene	$C_{40}H_{58}$	538.4539	539.4539 $[M+H]^+$	carotenoid
	all-trans-neurosporene	$C_{40}H_{58}$	538.4539	539.4539 $[M+H]^+$	carotenoid
	α-zeacarotene	$C_{40}H_{58}$	538.4539	539.4539 $[M+H]^+$	carotenoid
	β-zeacarotene	$C_{40}H_{58}$	538.4539	539.4539 $[M+H]^+$	carotenoid
553.4 (-)	rhodopin	$C_{40}H_{58}O$	554.4488	553.4488 $[M-H]^-$	carotenoid
561.2 (-)	2'-O-methyl-rhamnosyl tetracyclic spinosyn pseudoaglycone	$C_{31}H_{46}O_9$	562.3142	561.3142 $[M-H]^-$	glycosylated macrolide
583.2 (-)	15,16-dihydrobiliverdin	$C_{33}H_{34}N_4O_6$	584.2635	583.2635 $[M-H]^-$	phytochrome precursor
	bilirubin	$C_{33}H_{34}N_4O_6$	584.2635	583.2635 $[M-H]^-$	bilin pigment
597.4 (-)	2-methoxy-6-all *trans*-heptaprenyl-2-methoxy-1,4-benzoquinol	$C_{42}H_{64}O_3$	616.4855	597.4755 $[M-H_2O-H]^-$	quinol
601.4 (+)	2-methoxy-6-(*all-trans*-heptaprenyl)phenol	$C_{42}H_{64}O_2$	600.4906	601.4906 $[M+H]^+$	ubiquinol-7 precursor
	3,4-dihydroxy-5-*all-trans*-hexaprenylbenzoate	$C_{37}H_{53}O_4$	562.4022	601.4022 $[M+K]^+$	lipid
607.4 (+)	1,2-dipalmitoylglycerol	$C_{35}H_{68}O_5$	568.5067	607.5067 $[M+K]^+$	lipid
	protoporphyrinogen IX	$C_{34}H_{38}N_4O_4$	568.3050	607.3050 $[M+K]^+$	porphyrin
	rhodovibrin	$C_{41}H_{60}O_2$	584.4593	607.4593 $[M+Na]^+$	carotenoid

Continued on next page

Table B.2 – continued from previous page

Mass-bin (mode)	Compound	Structure	Accurate mass	Expected mass and ion	Class
609.2 (-)	chlorophyllide b	$C_{35}H_{30}N_4O_6Mg$	628.2172	609.2072 $[M-H_2O-H]^-$	chlorophyllide
	primary fluorescent chlorophyll catabolite	$C_{35}H_{38}N_4O_7$	628.2897	609.2797 $[M-H_2O-H]^-$	bilin pigment
609.4 (+)	*all-trans*-hexaprenyl diphosphate	$C_{30}H_{49}O_7P_2$	586.3188	609.3188 $[M+Na]^+$	lipid
	presqualene diphosphate	$C_{30}H_{49}O_7P_2$	586.3188	609.3188 $[M+Na]^+$	lipid
625.4 (+)	*all-trans*-hexaprenyl diphosphate	$C_{30}H_{49}O_7P_2$	586.3188	625.3188 $[M+K]^+$	lipid
	presqualene diphosphate	$C_{30}H_{49}O_7P_2$	586.3188	625.3188 $[M+K]^+$	lipid
627.2 (-)	chlorophyllide b	$C_{35}H_{30}N_4O_6Mg$	628.2172	627.2172 $[M-H]^-$	chlorophyllide
	primary fluorescent chlorophyll catabolite	$C_{35}H_{38}N_4O_7$	628.2897	627.2897 $[M-H]^-$	bilin pigment
627.4 (+)	red chlorophyll catabolite	$C_{35}H_{36}N_4O_7$	626.2740	627.2740496 $[M+H]^+$	bilin pigment
637.4 (+)	*all-trans*-heptaprenyl diphosphate	$C_{35}H_{57}O_7P_2$	654.3814	637.3714 H2O-$[M+H]^+$	lipid
674.2 (-)	ferribactin	$C_{56}H_{91}N_{18}O_{21}$	1350.6528	674.3214 $[M-2H]^{2-}$	siderophore
674.4 (-)					
675.4 (+)	demethylmenaquinol-7	$C_{45}H_{64}O_2$	636.4906	675.4906 $[M+K]^+$	electron-transfer quinol
701.4 (-)	lipid IVA	$C_{68}H_{126}N_2O_{23}P_2$	1404.8540	701.4220 $[M-2H]^{2-}$	lipid
761.6 (+)	3-(*all-trans*-nonaprenyl)benzene-1,2-diol	$C_{51}H_{78}O_2$	722.6002	761.6002 $[M+K]^+$	ubiquinol-9 precursor
762.6 (+)	1-16:0-2-18:1-diacylglycerol-trimethylhomoserine	$C_{44}H_{83}NO_7$	739.6326	762.6326 $[M+Na]^+$	lipid
763.6 (+)	3-methoxy-4-hydroxy-5-*all-trans*-nonaprenylbenzoate	$C_{53}H_{79}O_4$	780.6057	763.5957 H2O-$[M+H]^+$	ubiquinol-9 precursor
793.6 (-)	ubiquinone-9	$C_{54}H_{82}O_4$	794.6213	793.6213 $[M-H]^-$	electron-transfer quinone
905.6 (-)	chlorophyll b	$C_{55}H_{70}N_4O_6Mg$	906.5146	905.5146 $[M-H]^-$	chlorophyll pigment
Post-resistance					
498.4 (+)	1-16:0-2-lysophosphatidylcholine	$C_{24}H_{50}NO_7P$	497.3481	498.3481 $[M+H]^+$	lipid
621.4 (+)	adonixanthin	$C_{40}H_{54}O_3$	582.4073	621.4073 $[M+K]^+$	carotenoid
	hydroxyspirilloxanthin	$C_{41}H_{58}O_2$	582.4437	621.4437 $[M+K]^+$	carotenoid
	menaquinol-6	$C_{41}H_{58}O_2$	582.4437	621.4437 $[M+K]^+$	electron-transfer quinol
734.6 (+)	1-16:0-2-18:4-diacylglycerol-trimethylhomoserine	$C_{44}H_{77}NO_7$	733.5857	734.5857 $[M+H]^+$	lipid
743.6 (-)	1-α-linolenoyl-2-palmitoyl-phosphatidylglycerol	$C_{40}H_{72}O_{10}P$	744.4941	743.4941 $[M-H]^-$	lipid/fatty acid
	1-linoleoyl-2-(3E)-hexadecenoyl-phosphatidylglycerol	$C_{40}H_{72}O10P1$	744.4941	743.4941 $[M-H]^-$	lipid/fatty acid
745.6 (-)	1-linoleoyl-2-palmitoyl-phosphatidylglycerol	$C_{40}H_{74}O_{10}P$	746.5098	745.5098 $[M-H]^-$	lipid/fatty acid
	1-oleoyl-2-(3E)-hexadecenoyl-phosphatidylglycerol	$C_{40}H_{74}O_{10}P$	746.5098	745.5098 $[M-H]^-$	lipid/fatty acid
795.6 (-)	ubiquinol-9	$C_{54}H_{84}O_4$	796.6370	795.6370 $[M-H]^-$	electron-transfer quinol
993.6 (-)	*all-trans*-dodecaprenyl diphosphate	$C_{60}H_{97}O_7P_2$	994.6944	993.6944 $[M-H]^-$	lipid
Persistent					
496.4 (+)	menaquinol-12	$C_{71}H_{106}O_2$	990.8193	496.4147 $[M+2H]^{2+}$	electron-transfer quinol
556.4 (-)	solasodine 3-O-β-D-glucoside	$C_{33}H_{53}NO_7$	575.3822	556.3722 $[M-H_2O-H]^-$	sterol
	Und-PP-Mur2Ac-L-Ala-γ-D-Glu-L-Lys-D-Ala-D-Ala	$C_{86}H_{140}N_7O_{21}P_2$	1671.9812	556.3204 $[M-3H]^{3-}$	glycoconjugate
557.4 (-)	2',3'-O-methyl-rhamnosyl tetracyclic spinosyn pseudoaglycone	$C_{32}H_{48}O_9$	576.3298	557.3198 $[M-H_2O-H]^-$	glycosylated macrolide

Continued on next page

Table B.2 – continued from previous page

Mass-bin (mode)	Compound	Structure	Accurate mass	Expected mass and ion	Class
	N-acetyl-β-D-glucosaminyl-(1→4)-*N*-acetyl-α-D-glucosaminyl-diphosphodolichol	$C_{96}H_{158}N_2O_{17}P_2$	1675.1192	557.3664 $[M\text{-}3H]^{3-}$	glycan
571.4 (-)	2',3',4'-O-methyl-rhamnosyl tetracyclic spinosyn pseudoaglycone	$C_{33}H_{50}O_9$	590.3455	571.3355 $[M\text{-}H_2O\text{-}H]^-$	glycosylated macrolide
583.4 (+)	adonixanthin	$C_{40}H_{54}O_3$	582.4073	583.4073 $[M+H]^+$	carotenoid
583.6 (+)	15-*cis*-phytoene	$C_{40}H_{64}$	544.5008	505.5008 $[M+K]^+$	carotenoid
736.6 (+)	1-16:0-2-18:3-diacylglycerol-trimethylhomoserine	$C_{44}H_{79}NO_7$	735.6013	736.6013 $[M+H]^+$	lipid
	1,2-dipalmitoyl-phosphatidylcholine	$C_{40}H_{80}NO_8P$	735.5778	736.5778 $[M+H]^+$	lipid
779.6 (-)	3-methoxy-4-hydroxy-5-all-*trans*-nonaprenylbenzoate	$C_{53}H_{79}O_4$	780.6057	779.6057 $[M\text{-}H]^-$	aromatic compound

Table B.3: Analysis of Deviance Table (Type II Wald χ^2-tests) for linear mixed effects model to test effect of glyphosate resistance evolution on shikimate pathway compounds with percentage ion count (arc sine transformed) of the putatively matched target compound as response.

Shikimate pathway functioning				
Compound	**Fixed effect**	χ^2	**DF**	**p**
E4P	day	40.1	6	< 0.001
	treatment	3.5	1	0.06
	day:treatment	81.3	6	< 0.001
PEP	day	13.8	6	0.03
	treatment	7.8	1	0.005
	day:treatment	6.1	6	0.4
DAHP	day	35.4	6	< 0.001
	treatment	1.1	1	0.3
	day:treatment	6.4	6	0.4
3-DHQ	day	17.1	6	0.009
	treatment	6.8	1	0.009
	day:treatment	4.9	6	0.6
3-dehydro-shikimate	day	20.9	6	0.002
	treatment	20.1	1	< 0.001
	day:treatment	57.4	6	< 0.001
Shikimate	day	88.9	6	< 0.001
	treatment	47.3	1	< .001
	day:treatment	78.7	6	< 0.001
Shikimate-3-phosphate	day	94.1	6	< 0.001
	treatment	60.4	1	< 0.001
	day:treatment	119.2	6	< 0.001
EPSP	day	16.1	6	0.01
	treatment	2.1	1	0.1
	day:treatment	27.6	6	< 0.001
Chorismate/Prephenate	day	41.9	6	< 0.001
	treatment	0.46	1	0.5
	day:treatment	45.4	6	< 0.001

Table B.4: Analysis of Deviance Table (Type II Wald χ^2-tests) for linear mixed effects model to test for presence of glyphosate and glyphosate breakdown products with percentage ion count (arc sine transformed) of the putatively matched target compound as response.

Glyphosate and its breakdown products – primary compounds				
Compound	**Fixed effect**	χ^2	**DF**	**p**
Glyphosate (-)	day	36.0	6	< 0.001
	treatment	0.07	1	0.8
	day:treatment	11.6	6	0.07.
AMPA (+)	day	124.5	6	< 0.001
	treatment	28.50	1	< 0.001
	day:treatment	11.1	6	0.09
Sarcosine (-)	day	10.7	6	0.1
	treatment	0.7	1	0.4
	day:treatment	19.4	6	0.004

Continued on next page

Table B.4 – continued from previous page

Glyphosate and its breakdown products – primary compounds				
Compound	**Fixed effect**	χ^2	**DF**	**p**
Sarcosine (+)	day	40.1	6	< 0.001
	treatment	10.0	1	0.002
	day:treatment	13.5	6	0.04

Table B.5: Selected pairwise contrasts, as estimated by the `emmeans` package for R, applied to linear mixed effects model to difference in presence of glyphosate and glyphosate breakdown products by day.

Glyphosate and its breakdown products – primary compounds				
Compound (mode)	**Contrast**	**t.ratio**	**DF**	**p**
Glyphosate (-)	day -3 0 - 100	-0.6	54.4	> 0.9
	day 1 0 - 100	2.5	54.4	0.44
	day 8 0 - 100	-1.6	54.4	> 0.9
	day 16 0 - 100	1.0	54.4	> 0.9
	day 22 0 - 100	-0.5	54.4	> 0.9
	day 29 0 - 100	-0.4	54.4	> 0.9
	day 36 0 - 100	0.5	54.4	> 0.9
AMPA (+)	day -3 0 - 100	2.3	43.5	0.54
	day 1 0 - 100	3.5	43.5	0.055
	day 8 0 - 100	3.3	43.5	0.1
	day 16 0 - 100	2.0	43.5	0.8
	day 22 0 - 100	5.2	43.5	< 0.001
	day 29 0 - 100	3.5	43.5	0.06
	day 36 0 - 100	1.7	43.5	> 0.9
Sarcosine (-)	day -3 0 - 100	3.3	52.7	0.09
	day 1 0 - 100	-1.6	52.7	> 0.9
	day 8 0 - 100	-0.9	52.7	> 0.9
	day 16 0 - 100	0	52.7	> 0.9
	day 22 0 - 100	1.3	52.7	> 0.9
	day 29 0 - 100	1.4	52.7	> 0.9
	day 36 0 - 100	-0.7	52.7	> 0.9
Sarcosine (+)	day -3 0 - 100	1.5	56	> 0.9
	day 1 0 - 100	1.4	56	> 0.9
	day 8 0 - 100	0.2	56	> 0.9
	day 16 0 - 100	-1.3	56	> 0.9
	day 22 0 - 100	1.0	56	> 0.9
	day 29 0 - 100	3.5	56	0.05
	day 36 0 - 100	2.0	56	0.8

Table B.6: Analysis of Deviance Table (Type II Wald χ^2-tests) for linear mixed effects model to test for presence of secondary glyphosate and AMPA breakdown products with percentage ion count (arc sine transformed) of the putatively matched target compound as response.

Glyphosate and its breakdown products – secondary compounds				
Compound	**Fixed effect**	χ^2	**DF**	**p**
α-D-ribose-1-[N-(phosphono-methyl)-glycine]5-phosphate(-)	day	8.9	6	0.2
	treatment	9.6	1	0.002
	day:treatment	2.9	6	0.8
α-D-ribose-1-[N-(phosphonomethyl)-glycine]5-phosphate(+)	day	6.6	6	0.4
	treatment	9.9	1	0.002
	day:treatment	0.6	6	> 0.9
α-D-ribose-1-[N-(phosphono-methyl)-glycine]5-triphosphate(-)	day	49.1	6	< 0.001
	treatment	10.1	1	0.002
	day:treatment	24.8	6	< 0.001
α-D-ribose-1-[N-(phosphonomethyl)-glycine]5-triphosphate(+)	day	5.2	6	0.5
	treatment	1.3	1	0.3
	day:treatment	5.7	6	0.5
α-D-ribose-1,5-bisphosphate(-)	day	15.7	6	0.02
	treatment	0.3	1	0.6
	day:treatment	6.4	6	0.4
α-D-ribose-1,5-bisphosphate(+)	day	8.2	6	0.2
	treatment	7.4	1	0.006
	day:treatment	18.8	6	0.005
5-phospho-α-D-ribose-1,2-cyclic phosphate(-)	day	39.1	6	< 0.001
	treatment	4.0	1	0.045
	day:treatment	18.8	6	0.004
5-phospho-α-D-ribose-1,2-cyclic phosphate(+)	day	31.3	6	< 0.001
	treatment	3.8	1	0.049
	day:treatment	11.0	6	0.09
5-phospho-α-D-ribose-1-diphosphate(-)	day	7.5	6	0.3
	treatment	12.8	1	< 0.001
	day:treatment	12.4	6	0.05

Continued on next page

Table B.6 – continued from previous page

Glyphosate and its breakdown products – secondary compounds				
Compound	**Fixed effect**	χ^2	**DF**	**p**
5-phospho-α-D-ribose-1-diphosphate(+)	day	11.2	6	0.08
	treatment	0.3	1	0.6
	day:treatment	5.8	6	0.4
α-D-ribose-1-(acetamidomethyl-phosphonate)5-triphosphate(-)	day	18.7	6	0.005
	treatment	0.7	1	0.4
	day:treatment	12.2	6	0.06
α-D-ribose-1-(acetamidomethyl-phosphonate)5-triphosphate(+)	day	19.1	6	0.004
	treatment	0.3	1	0.6
	day:treatment	7.7	6	0.3
α-D-ribose-1-(2-N-acetamidomethyl-phosphonate)5-phosphate(-)	day	14.7	6	0.02
	treatment	0.1	1	0.7
	day:treatment	1.8	6	0.9
α-D-ribose-1-(2-N-acetamidomethyl-phosphonate)5-phosphate(+)	day	4.5	6	0.6
	treatment	1.7	1	0.2
	day:treatment	4.3	6	0.6
Cinnamaldehyde(-)	day	44.4	6	< 0.001
	treatment	19.2	1	< 0.001
	day:treatment	5.9	6	0.4
Cinnamyl alcohol(-)	day	32.0	6	< 0.001
	treatment	2.4	1	0.1
	day:treatment	35.4	6	< 0.001
Cinnamyl alcohol(+)	day	74.0	6	< 0.001
	treatment	43.7	1	< 0.001
	day:treatment	68.5	6	< 0.001
2-oxoglutarate(-)	day	26.3	6	< 0.001
	treatment	39.1	1	< 0.001
	day:treatment	62.5	6	< 0.001

Table B.7: Selected pairwise contrasts, as estimated by the `emmeans` package for R, applied to linear mixed effects model to difference in presence of secondary glyphosate breakdown products by day.

Glyphosate and its breakdown products – secondary compounds				
Compound (mode)	**Contrast**	**t.ratio**	**DF**	**p**
α-D-ribose-1-[N-(phosphono-methyl)glycine]5-phosphate(-)	day -3 0 - 100	0.9	55.8	> 0.9
	day 1 0 - 100	1.2	55.8	> 0.9
	day 8 0 - 100	0	55.8	> 0.9
	day 16 0 - 100	1.7	55.8	> 0.9
	day 22 0 - 100	2.0	55.8	0.8
	day 29 0 - 100	1.1	55.8	> 0.9
	day 36 0 - 100	1.9	55.8	0.8
α-D-ribose-1-[N-(phosphono-methyl)glycine]5-phosphate(+)	day -3 0 - 100	1.4	56	> 0.9
	day 1 0 - 100	1.0	56	> 0.9
	day 8 0 - 100	0.8	56	> 0.9
	day 16 0 - 100	0.8	56	> 0.9
	day 22 0 - 100	1.5	56	> 0.9
	day 29 0 - 100	1.2	56	> 0.9
	day 36 0 - 100	1.6	56	> 0.9
α-D-ribose-1-[N-(phosphono-methyl)glycine]5-triphosphate(-)	day -3 0 - 100	-0.4	50.4	> 0.9
	day 1 0 - 100	-0.3	50.4	> 0.9
	day 8 0 - 100	1.5	50.4	> 0.9
	day 16 0 - 100	0.2	50.4	> 0.9
	day 22 0 - 100	2.3	50.4	0.6
	day 29 0 - 100	4.0	50.4	0.01
	day 36 0 - 100	4.0	50.4	0.01
α-D-ribose-1-[N-(phosphono-methyl)glycine]5-triphosphate(+)	day -3 0 - 100	1.5	54.4	> 0.9
	day 1 0 - 100	-0.2	54.4	> 0.9
	day 8 0 - 100	1.6	54.4	> 0.9
	day 16 0 - 100	-0.8	54.4	> 0.9
	day 22 0 - 100	0.3	54.4	> 0.9
	day 29 0 - 100	1.3	54.4	> 0.9
	day 36 0 - 100	0	54.4	> 0.9
α-D-ribose 1,5-bisphosphate(-)	day -3 0 - 100	0.7	56	> 0.9
	day 1 0 - 100	1.2	56	> 0.9
	day 8 0 - 100	-0.7	56	> 0.9
	day 16 0 - 100	0.5	56	> 0.9
	day 22 0 - 100	-1.1	56	> 0.9
	day 29 0 - 100	-0.7	56	> 0.9
	day 36 0 - 100	-1.5	56	> 0.9
α-D-ribose 1,5-bisphosphate(+)	day -3 0 - 100	-1.0	55.9	> 0.9
	day 1 0 - 100	-0.6	55.9	> 0.9
	day 8 0 - 100	1.6	55.9	> 0.9
	day 16 0 - 100	3.2	55.9	0.1
	day 22 0 - 100	1.8	55.9	0.9
	day 29 0 - 100	-0.4	55.9	> 0.9

Continued on next page

Table B.7 – continued from previous page

Glyphosate and its breakdown products – secondary compounds				
Compound (mode)	**Contrast**	**t.ratio**	**DF**	**p**
	day 36 0 - 100	3.0	55.9	0.2
5-phospho-α-D-ribose 1,2-cyclic phosphate(-)	day -3 0 - 100	2.0	55.7	0.8
	day 1 0 - 100	0.9	55.7	> 0.9
	day 8 0 - 100	-1.8	55.7	0.9
	day 16 0 - 100	-3.2	55.7	0.1
	day 22 0 - 100	-1.6	55.7	> 0.9
	day 29 0 - 100	-1.3	55.7	> 0.9
	day 36 0 - 100	-0.8	55.7	> 0.9
5-phospho-α-D-ribose 1,2-cyclic phosphate(+)	day -3 0 - 100	-1.4	56	> 0.9
	day 1 0 - 100	-1.9	56	0.8
	day 8 0 - 100	-1.1	56	> 0.9
	day 16 0 - 100	-2.1	56	0.7
	day 22 0 - 100	1.9	56	0.8
	day 29 0 - 100	-0.3	56	> 0.9
	day 36 0 - 100	-0.3	56	> 0.9
5-phospho-α-D-ribose 1-diphosphate(-)	day -3 0 - 100	-0.5	56	> 0.9
	day 1 0 - 100	0.9	56	> 0.9
	day 8 0 - 100	-2.8	56	0.2
	day 16 0 - 100	-3.4	56	0.06
	day 22 0 - 100	-0.9	56	> 0.9
	day 29 0 - 100	-1.2	56	> 0.9
	day 36 0 - 100	-1.5	56	> 0.9
5-phospho-α-D-ribose 1-diphosphate(+)	day -3 0 - 100	-0.7	52.6	> 0.9
	day 1 0 - 100	1.9	52.6	0.8
	day 8 0 - 100	-1.0	52.6	> 0.9
	day 16 0 - 100	0.5	52.6	> 0.9
	day 22 0 - 100	0.6	52.6	> 0.9
	day 29 0 - 100	0.2	52.6	> 0.9
	day 36 0 - 100	0.3	52.6	> 0.9
α-D-ribose 1-(acetamidomethylphosphonate)5-triphosphate(-)	day -3 0 - 100	-0.5	54.1	> 0.9
	day 1 0 - 100	-0.1	54.1	> 0.9
	day 8 0 - 100	-0.4	54.1	> 0.9
	day 16 0 - 100	-0.5	54.1	> 0.9
	day 22 0 - 100	-1.0	54.1	> 0.9
	day 29 0 - 100	2.2	54.1	0.6
	day 36 0 - 100	-2.4	54.1	0.5
α-D-ribose 1-(acetamidomethylphosphonate)5-triphosphate(+)	day -3 0 - 100	-1.2	54.2	> 0.9
	day 1 0 - 100	0.6	54.2	> 0.9
	day 8 0 - 100	-1.1	54.2	> 0.9
	day 16 0 - 100	-0.2	54.2	> 0.9
	day 22 0 - 100	0.6	54.2	> 0.9
	day 29 0 - 100	1.2	54.2	> 0.9
	day 36 0 - 100	1.7	54.2	> 0.9
α-D-ribose-1-(2-N-acetamidomethylphosphonate)5-phosphate(-)	day -3 0 - 100	0.3	55.2	> 0.9
	day 1 0 - 100	-1.0	55.2	> 0.9
	day 8 0 - 100	0.4	55.2	> 0.9
	day 16 0 - 100	0	55.2	> 0.9
	day 22 0 - 100	0.2	55.2	> 0.9
	day 29 0 - 100	0.7	55.2	> 0.9
	day 36 0 - 100	0.5	55.2	> 0.9
α-D-ribose-1-(2-N-acetamidomethylphosphonate)5-phosphate(+)	day -3 0 - 100	-0.8	56	> 0.9
	day 1 0 - 100	0.7	56	> 0.9
	day 8 0 - 100	0.7	56	> 0.9
	day 16 0 - 100	0.4	56	> 0.9
	day 22 0 - 100	1.9	56	0.8
	day 29 0 - 100	-0.2	56	> 0.9
	day 36 0 - 100	0.8	56	> 0.9
Cinnamaldehyde(-)	day -3 0 - 100	0.1	56	> 0.9
	day 1 0 - 100	1.0	56	> 0.9
	day 8 0 - 100	1.6	56	> 0.9
	day 16 0 - 100	3.1	56	0.1
	day 22 0 - 100	1.4	56	> 0.9
	day 29 0 - 100	2.6	56	0.4
	day 36 0 - 100	1.7	56	0.9
Cinnamyl alcohol(-)	day -3 0 - 100	1.5	54	> 0.9
	day 1 0 - 100	-1.4	54	> 0.9
	day 8 0 - 100	-2.6	54	0.4
	day 16 0 - 100	3.4	54	0.06
	day 22 0 - 100	3.3	54	0.08
	day 29 0 - 100	-0.6	54	> 0.9
	day 36 0 - 100	1.3	54	> 0.9
Cinnamyl alcohol(+)	day -3 0 - 100	0.1	56	> 0.9
	day 1 0 - 100	7.1	56	< 0.001
	day 8 0 - 100	6.3	56	< 0.001
	day 16 0 - 100	-1.9	56	0.8
	day 22 0 - 100	0	56	> 0.9
	day 29 0 - 100	3.7	56	0.03
	day 36 0 - 100	2,1	56	0.7
2-oxoglutarate	day -3 0 - 100	1.9	39.9	0.8

Continued on next page

Table B.7 – continued from previous page

Glyphosate and its breakdown products – secondary compounds				
Compound (mode)	**Contrast**	**t.ratio**	**DF**	**p**
	day 1 0 - 100	1.0	39.9	> 0.9
	day 8 0 - 100	3.8	39.9	0.03
	day 16 0 - 100	7.5	39.9	< 0.001
	day 22 0 - 100	7.8	39.9	< 0.001
	day 29 0 - 100	2.9	39.9	0.2
	day 36 0 - 100	1.7	39.9	> 0.9

Table B.8: Analysis of Deviance Table (Type II Wald χ^2-tests) for linear mixed effects model to test effect of glyphosate resistance evolution on amino acids with percentage ion count (arc sine transformed) of the putatively matched target compound as response.

Amino acid pool composition – negative mode				
Compound	**Fixed effect**	χ^2	**DF**	**p**
Ala	day	10.7	6	0.1
	treatment	0.7	1	0.4
	day:treatment	19.4	6	0.004
Arg	day	0.7	6	> 0.9
	treatment	0.6	1	0.4
	day:treatment	5.0	6	0.5
Asn	day	44.4	6	< 0.001
	treatment	19.2	1	< 0.001
	day:treatment	5.9	6	0.4
Asp	day	19.4	6	0.004
	treatment	0.2	1	0.7
	day:treatment	10.8	6	0.09
Glu	day	74.0	6	< 0.001
	treatment	15.3	1	< 0.001
	day:treatment	45.5	6	< 0.001
Gln	day	26.3	6	< 0.001
	treatment	39.1	1	< 0.001
	day:treatment	62.5	6	< 0.001
Gly	day	14.1	6	0.03
	treatment	2.8	1	0.1
	day:treatment	5.3	6	0.5
His	day	24.4	6	< 0.001
	treatment	0.001	1	> 0.9
	day:treatment	10.4	6	0.1
Iso/Leu	day	8.1	6	0.2
	treatment	12.1	1	< 0.001
	day:treatment	7.5	6	0.3
Lys	day	5.6	6	0.5
	treatment	0.9	1	0.4
	day:treatment	9.7	6	0.1
Phe	day	3.5	6	0.7
	treatment	2.9	1	0.09
	day:treatment	10.1	6	0.1
Pro	day	7.3	6	0.3
	treatment	0.9	1	0.3
	day:treatment	11.3	6	0.08
Trp	day	7.7	6	0.3
	treatment	11.1	1	< 0.001
	day:treatment	6.7	6	0.3
Tyr	day	53.9	6	< 0.001
	treatment	15.6	1	< 0.001
	day:treatment	23.4	6	< 0.001
Val	day	12.5	6	0.05
	treatment	5.7	1	0.02
	day:treatment	15.3	6	0.02
AA pool	day	47.4	6	< 0.001
	treatment	34.5	1	< 0.001
	day:treatment	31.3	6	< 0.001

Table B.9: Analysis of Deviance Table (Type II Wald χ^2-tests) for linear mixed effects model to test effect of glyphosate resistance evolution on amino acids with percentage ion count (arc sine transformed) of the putatively matched target compound as response.

Amino acid pool composition – positive mode				
Compound	**Fixed effect**	χ^2	**DF**	**p**
Ala	day	40.0	6	> 0.9
	treatment	10.0	1	0.002
	day:treatment	13.5	6	0.04

Continued on next page

Table B.9 – continued from previous page

Amino acid pool composition – positive mode				
Compound	**Fixed effect**	χ^2	**DF**	**p**
Arg	day	136.0	6	< 0.001
	treatment	31.0	1	< 0.001
	day:treatment	18.2	6	0.006
Gly	day	12.4	6	0.05
	treatment	0.6	1	0.5
	day:treatment	18.3	6	0.006
His	day	74.2	6	< 0.001
	treatment	20.0	1	< 0.001
	day:treatment	15.6	6	0.02
Iso/Leu	day	36.8	6	< 0.001
	treatment	0.4	1	0.6
	day:treatment	5.5	6	0.5
Met	day	78.8	6	< 0.001
	treatment	29.6	1	< 0.001
	day:treatment	6.4	6	0.4
Phe	day	35.9	6	< 0.001
	treatment	6.6	1	0.01
	day:treatment	29.3	6	< 0.001
Pro	day	234.1	6	< 0.001
	treatment	38.7	1	< 0.001
	day:treatment	9.0	6	0.2
Trp	day	40.5	6	< 0.001
	treatment	34.9	1	< 0.001
	day:treatment	13.8	6	0.03
Tyr	day	86.8	6	< 0.001
	treatment	10.9	1	< 0.001
	day:treatment	9.1	6	0.2
Val	day	74.7	6	< 0.001
	treatment	20.7	1	< 0.001
	day:treatment	12.2	6	0.06
AA pool	day	262.5	6	< 0.001
	treatment	51.6	1	< 0.001
	day:treatment	11.8	6	0.07

Table B.10: Selected pairwise contrasts, as estimated by the `emmeans` package for R, applied to linear mixed effects model to difference in presence of amino acids in negative mode by day.

Amino acid pool composition – negative mode				
Compound (mode)	**Contrast**	**t.ratio**	**DF**	**p**
Ala	day -3 0 - 100	3.3	52.8	0.09
	day 1 0 - 100	-1.6	52.8	> 0.9
	day 8 0 - 100	-0.9	52.8	> 0.9
	day 16 0 - 100	0	52.8	> 0.9
	day 22 0 - 100	1.3	52.8	> 0.9
	day 29 0 - 100	1.4	52.8	> 0.9
	day 36 0 - 100	-0.7	52.8	> 0.9
Arg	day -3 0 - 100	-0.9	56	> 0.9
	day 1 0 - 100	0.3	56	> 0.9
	day 8 0 - 100	0.1	56	> 0.9
	day 16 0 - 100	1.0	56	> 0.9
	day 22 0 - 100	1.5	56	> 0.9
	day 29 0 - 100	0.8	56	> 0.9
	day 36 0 - 100	-0.8	56	> 0.9
Asn	day -3 0 - 100	0.1	56	> 0.9
	day 1 0 - 100	1.0	56	> 0.9
	day 8 0 - 100	1.6	56	> 0.9
	day 16 0 - 100	3.1	56	0.1
	day 22 0 - 100	1.4	56	> 0.9
	day 29 0 - 100	2.6	56	0.4
	day 36 0 - 100	1.7	56	0.9
Asp	day -3 0 - 100	0.1	47.2	> 0.9
	day 1 0 - 100	0.6	47.2	> 0.9
	day 8 0 - 100	-2.1	47.2	0.7
	day 16 0 - 100	0.6	47.2	> 0.9
	day 22 0 - 100	-0.1	47.2	> 0.9
	day 29 0 - 100	1.9	47.2	0.8
	day 36 0 - 100	0.7	47.2	> 0.9
Glu	day -3 0 - 100	1.9	56	> 0.9
	day 1 0 - 100	1.0	56	0.01
	day 8 0 - 100	3.8	56	0.2
	day 16 0 - 100	7.5	56	0.02
	day 22 0 - 100	7.8	56	0.002
	day 29 0 - 100	2.9	56	> 0.9
	day 36 0 - 100	1.7	56	> 0.9
Gln	day -3 0 - 100	1.9	39.9	0.8
	day 1 0 - 100	1.0	39.9	> 0.9

Continued on next page

Table B.10 – continued from previous page

Amino acid pool composition – negative mode				
Compound (mode)	**Contrast**	**t.ratio**	**DF**	**p**
	day 8 0 - 100	3.8	39.9	0.03
	day 16 0 - 100	7.5	39.9	< 0.001
	day 22 0 - 100	7.8	39.9	< 0.001
	day 29 0 - 100	2.9	39.9	0.2
	day 36 0 - 100	1.7	39.9	> 0.9
Gly	day -3 0 - 100	-1.3	53.1	> 0.9
	day 1 0 - 100	-0.9	53.1	> 0.9
	day 8 0 - 100	-1.5	53.1	> 0.9
	day 16 0 - 100	-0.2	53.1	> 0.9
	day 22 0 - 100	0.4	53.1	> 0.9
	day 29 0 - 100	0	53.1	> 0.9
	day 36 0 - 100	-2.1	53.1	0.7
His	day -3 0 - 100	0.5	55.8	> 0.9
	day 1 0 - 100	-0.4	55.8	> 0.9
	day 8 0 - 100	0.5	55.8	> 0.9
	day 16 0 - 100	0.8	55.8	> 0.9
	day 22 0 - 100	-2.4	55.8	0.5
	day 29 0 - 100	-0.6	55.8	> 0.9
	day 36 0 - 100	1.6	55.8	> 0.9
Iso/Leu	day -3 0 - 100	0.6	56	> 0.9
	day 1 0 - 100	0.5	56	> 0.9
	day 8 0 - 100	0.4	56	> 0.9
	day 16 0 - 100	2.6	56	0.4
	day 22 0 - 100	2.8	56	0.3
	day 29 0 - 100	2.1	56	0.7
	day 36 0 - 100	0.2	56	> 0.9
Lys	day -3 0 - 100	2.0	55.2	0.8
	day 1 0 - 100	-1.3	55.2	> 0.9
	day 8 0 - 100	-0.6	55.2	> 0.9
	day 16 0 - 100	-0.3	55.2	> 0.9
	day 22 0 - 100	0.1	55.2	> 0.9
	day 29 0 - 100	-1.8	55.2	0.9
	day 36 0 - 100	-1.0	55.2	> 0.9
Phe	day -3 0 - 100	1.8	56	0.9
	day 1 0 - 100	1.2	56	> 0.9
	day 8 0 - 100	-1.0	56	> 0.9
	day 16 0 - 100	-0.3	56	> 0.9
	day 22 0 - 100	0	56	> 0.9
	day 29 0 - 100	2.7	56	0.3
	day 36 0 - 100	0	56	> 0.9
Pro	day -3 0 - 100	0.6	56	> 0.9
	day 1 0 - 100	-1.5	56	> 0.9
	day 8 0 - 100	-1.6	56	> 0.9
	day 16 0 - 100	0.4	56	> 0.9
	day 22 0 - 100	1.5	56	> 0.9
	day 29 0 - 100	1.7	56	> 0.9
	day 36 0 - 100	1.3	56	> 0.9
Trp	day -3 0 - 100	0.5	54.9	> 0.9
	day 1 0 - 100	0.5	54.9	> 0.9
	day 8 0 - 100	0.3	54.9	> 0.9
	day 16 0 - 100	1.7	54.9	> 0.9
	day 22 0 - 100	2.8	54.9	0.3
	day 29 0 - 100	1.8	54.9	0.9
	day 36 0 - 100	2.6	54.9	0.4
Tyr	day -3 0 - 100	-0.1	53.5	> 0.9
	day 1 0 - 100	0.3	53.5	> 0.9
	day 8 0 - 100	0	53.5	> 0.9
	day 16 0 - 100	3.3	53.5	0.08
	day 22 0 - 100	4.7	53.5	0.002
	day 29 0 - 100	1.7	53.5	> 0.9
	day 36 0 - 100	3.0	53.5	0.2
Val	day -3 0 - 100	-0.5	56	> 0.9
	day 1 0 - 100	3.6	56	0.04
	day 8 0 - 100	-0.3	56	> 0.9
	day 16 0 - 100	0.1	56	> 0.9
	day 22 0 - 100	1.5	56	> 0.9
	day 29 0 - 100	2.2	56	0.6
	day 36 0 - 100	-0.3	56	> 0.9
AA pool	day -3 0 - 100	1.5	54.2	> 0.9
	day 1 0 - 100	1.6	54.2	> 0.9
	day 8 0 - 100	-0.5	54.2	> 0.9
	day 16 0 - 100	5.0	54.2	< 0.001
	day 22 0 - 100	5.8	54.2	< 0.001
	day 29 0 - 100	3.4	54.2	0.07
	day 36 0 - 100	1.9	54.2	0.8

Table B.11: Selected pairwise contrasts, as estimated by the `emmeans` package for R, applied to linear mixed effects model to difference in presence of amino acids in positive mode by day.

Amino acid pool composition - positive mode				
Compound (mode)	**Contrast**	**t.ratio**	**DF**	**p**
Ala	day -3 0 - 100	1.5	56	> 0.9
	day 1 0 - 100	1.4	56	> 0.9
	day 8 0 - 100	0.2	56	> 0.9
	day 16 0 - 100	-1.3	56	> 0.9
	day 22 0 - 100	1.0	56	> 0.9
	day 29 0 - 100	3.5	56	0.05
	day 36 0 - 100	2.0	56	0.8
Arg	day -3 0 - 100	4.1	54.5	0.001
	day 1 0 - 100	2.4	54.5	0.5
	day 8 0 - 100	1.4	54.5	> 0.9
	day 16 0 - 100	2.6	54.5	0.4
	day 22 0 - 100	5.2	54.5	< 0.001
	day 29 0 - 100	1.5	54.5	> 0.9
	day 36 0 - 100	0.3	54.5	> 0.9
Gly	day -3 0 - 100	3.0	50.6	0.2
	day 1 0 - 100	0.4	50.6	> 0.9
	day 8 0 - 100	0.7	50.6	> 0.9
	day 16 0 - 100	-0.9	50.6	> 0.9
	day 22 0 - 100	1.6	50.6	> 0.9
	day 29 0 - 100	-0.1	50.6	> 0.9
	day 36 0 - 100	-1.9	50.6	0.8
His	day -3 0 - 100	1.4	54.1	> 0.9
	day 1 0 - 100	4.3	54.1	0.005
	day 8 0 - 100	3.3	54.1	0.1
	day 16 0 - 100	0.3	54.1	> 0.9
	day 22 0 - 100	0.5	54.1	> 0.9
	day 29 0 - 100	1.3	54.1	> 0.9
	day 36 0 - 100	3.3	54.1	0.1
Iso/Leu	day -3 0 - 100	-1.3	56	> 0.9
	day 1 0 - 100	1.7	56	> 0.9
	day 8 0 - 100	0.7	56	> 0.9
	day 16 0 - 100	0.4	56	> 0.9
	day 22 0 - 100	-0.5	56	> 0.9
	day 29 0 - 100	0.1	56	> 0.9
	day 36 0 - 100	0.6	56	> 0.9
Met	day -3 0 - 100	1.9	56	0.8
	day 1 0 - 100	3.2	56	0.1
	day 8 0 - 100	2.5	56	0.4
	day 16 0 - 100	1.0	56	> 0.9
	day 22 0 - 100	0.9	56	> 0.9
	day 29 0 - 100	1.9	56	0.8
	day 36 0 - 100	3.5	56	0.047
Phe	day -3 0 - 100	3.6	56	0.03
	day 1 0 - 100	3.2	56	0.1
	day 8 0 - 100	1.6	56	> 0.9
	day 16 0 - 100	-2.6	56	0.4
	day 22 0 - 100	-1.1	56	> 0.9
	day 29 0 - 100	1.2	56	> 0.9
	day 36 0 - 100	0.9	56	> 0.9
Pro	day -3 0 - 100	4.5	52.9	0.002
	day 1 0 - 100	3.7	52.9	0.03
	day 8 0 - 100	3.0	52.9	0.2
	day 16 0 - 100	1.2	52.9	> 0.9
	day 22 0 - 100	3.7	52.9	0.03
	day 29 0 - 100	2.8	52.9	0.3
	day 36 0 - 100	1.8	52.9	0.9
Trp	day -3 0 - 100	1.0	56	> 0.9
	day 1 0 - 100	4.4	56	0.003
	day 8 0 - 100	3.7	56	0.03
	day 16 0 - 100	2.6	56	0.4
	day 22 0 - 100	0	56	> 0.9
	day 29 0 - 100	2.2	56	0.6
	day 36 0 - 100	1.8	56	0.9
Tyr	day -3 0 - 100	1.1	49.3	> 0.9
	day 1 0 - 100	3.3	49.3	0.09
	day 8 0 - 100	1.3	49.3	> 0.9
	day 16 0 - 100	3.0	49.3	0.2
	day 22 0 - 100	1.1	49.3	> 0.9
	day 29 0 - 100	0.2	49.3	> 0.9
	day 36 0 - 100	2.1	49.3	0.7
Val	day -3 0 - 100	1.0	49.9	> 0.9
	day 1 0 - 100	4.4	49.9	0.004
	day 8 0 - 100	2.8	49.9	0.2
	day 16 0 - 100	0.5	49.9	> 0.9
	day 22 0 - 100	3.0	49.9	0.2
	day 29 0 - 100	2.6	49.9	0.4

Continued on next page

Table B.11 – continued from previous page

Amino acid pool composition - positive mode				
Compound (mode)	**Contrast**	**t.ratio**	**DF**	**p**
	day 36 0 - 100	2.2	49.9	0.6
AA pool	day -3 0 - 100	4.5	51.5	0.002
	day 1 0 - 100	5.6	51.5	< 0.001
	day 8 0 - 100	3.7	51.5	0.03
	day 16 0 - 100	2.0	51.5	0.8
	day 22 0 - 100	4.0	51.5	0.01
	day 29 0 - 100	3.0	51.5	0.2
	day 36 0 - 100	2.1	51.5	0.7

Table B.12: Discriminatory mass bins identified in exploratory analysis that did not match to a putative compound identity, along with the pattern. Data not shown, but available in repository listed in acknowledgements.

Pre-resistance			**Post-resistance**	**Persistent**
230 (-)	607.4 (-)	821.6 (-)	263.2 (-)	497.4 (+)
253.2 (-)	610.4 (+)	807.6 (-)	333 (-)	555.4 (-)
288.2 (+)	611.4 (+)	817.6 (-)	415.2 (-)	710.6 (+)
294.2 (-)	643.2 (-)	823.6 (-)	461.2 (-)	736.8 (+)
469.2 (+)	644.2 (-)	825.6 (-)	499.4 (+)	737.6 (+)
472.4 (+)	645.2 (-)	835.6 (-)	500.4 (+)	737.8 (+)
474.4 (+)	673.2 (-)	853.6 (-)	501.4 (+)	760.6 (+)
476.4 (+)	673.4 (-)	953.6 (-)	540.4 (-)	760.8 (+)
481.4 (-)	692.4 (+)	954.6 (-)	542.4 (-)	776.6 (+)
494.4 (+)	701.2 (-)	958.6 (-)	622.4 (+)	776.8 (+)
510.4 (+)	704.6 (+)	959.6 (-)	699.4 (-)	778.6 (-)
518.4 (-)	706.6 (+)	960.6 (-)	711.6 (+)	780.6 (-)
519.2 (-)	730.6 (+)	961.6 (-)	712.6 (+)	796.6 (-)
523.2 (+)	739.8 (+)	963.6 (-)	735.6 (+)	955.6 (-)
523.4 (+)	758.6 (+)	964.6 (-)	738.8 (+)	957.6 (-)
524.4 (+)	759.6 (+)		756.6 (+)	962.6 (-)
530.4 (-)	761.8 (+)		757.6 (+)	
539.2 (+)	762.8 (+)		794.6 (-)	
584.4 (+)	763.6 (+)		800.6 (+)	
587.6 (+)	763.8 (+)		956.6 (-)	

Table B.13: Analysis of Deviance Table (Type II Wald χ^2-tests) for linear mixed effects model for putatively identified discriminatory mass bins of interest from exploratory analysis with percentage ion count (arc sine transformed) of the putatively matched target compound as response.

Exploratory analysis – Putatively identified compounds				
Compound	**Fixed effect**	χ^2	**DF**	**p**
97 (-)	day	68.2	6	< 0.001
	treatment	7.6	1	0.006
	day:treatment	60.7	6	< 0.001
175 (-)	day	65.5	6	< 0.001
	treatment	26.8	1	< 0.001
	day:treatment	18.3	6	0.006
223.2 (-)	day	81.9	6	< 0.001
	treatment	17.0	1	< 0.001
	day:treatment	30.0	6	< 0.001
228 (-)	day	141.2	6	< 0.001
	treatment	2.3	1	0.1
	day:treatment	22.3	6	0.001
229 (-)	day	117.3	6	< 0.001
	treatment	5.5	1	0.02
	day:treatment	37.6	6	< 0.001
245 (-)	day	15.0	6	0.02
	treatment	1.0	1	0.3
	day:treatment	32.8	6	< 0.001
247.2 (-)	day	35.9	6	< 0.001
	treatment	31.4	1	< 0.001
	day:treatment	14.2	6	0.03
259 (-)	day	83.2	6	< 0.001
	treatment	0.1	1	0.8
	day:treatment	228.3	6	< 0.001
274.2 (+)	day	713.2	6	< 0.001
	treatment	229.5	1	< 0.001
	day:treatment	117.3	6	< 0.001
289 (-)	day	38.2	6	< 0.001
	treatment	2.4	1	0.1
	day:treatment	72.6	6	< 0.001

Continued on next page

Table B.13 – continued from previous page

Exploratory analysis – Putatively identified compounds				
Compound	**Fixed effect**	χ^2	**DF**	**p**
291.2 (-)	day	34.8	6	< 0.001
	treatment	17.0	1	< 0.001
	day:treatment	47.5	6	< 0.001
293.2 (-)	day	129.7	6	< 0.001
	treatment	29.2	1	< 0.001
	day:treatment	55.5	6	< 0.001
301.2 (-)	day	87.3	6	< 0.001
	treatment	195.5	1	< 0.001
	day:treatment	157.1	6	< 0.001
303.2 (+)	day	149.8	6	< 0.001
	treatment	203.78	1	< 0.001
	day:treatment	240.4	6	< 0.001
304.2 (+)	day	106.4	6	< 0.001
	treatment	139.3	1	< 0.001
	day:treatment	160.6	6	< 0.001
309.2 (-)	day	214.9	6	< 0.001
	treatment	12.5	1	< 0.001
	day:treatment	49.2	6	< 0.001
313.2 (+)	day	153.0	6	< 0.001
	treatment	30.9	1	< 0.001
	day:treatment	45.8	6	< 0.001
346 (-)	day	58.5	6	< 0.001
	treatment	6.4	1	0.01
	day:treatment	111.0	6	< 0.001
362 (-)	day	33.0	6	< 0.001
	treatment	14.9	1	< 0.001
	day:treatment	71.7	6	< 0.001
425.2 (-)	day	39.8	6	< 0.001
	treatment	127.9	1	< 0.001
	day:treatment	86.5	6	< 0.001
470.4 (+)	day	82.6	6	< 0.001
	treatment	14.2	1	< 0.001
	day:treatment	67.0	6	< 0.001
475.4 (+)	day	87.1	6	< 0.001
	treatment	1.0	1	0.3
	day:treatment	48.1	6	< 0.001
496.4 (+)	day	28.5	6	< 0.001
	treatment	21.4	1	< 0.001
	day:treatment	18.2	6	0.006
497.2 (-)	day	49.8	6	< 0.001
	treatment	25.8	1	< 0.001
	day:treatment	68.8	6	< 0.001
498.4 (+)	day	5.5	6	0.5
	treatment	20.3	1	< 0.001
	day:treatment	34.0	6	< 0.001
529.4 (-)	day	231.2	6	< 0.001
	treatment	49.4	1	< 0.001
	day:treatment	43.1	6	< 0.001
539.4 (+)	day	62.7	6	< 0.001
	treatment	119.8	1	< 0.001
	day:treatment	59.5	6	< 0.001
553.4 (-)	day	22.4	6	0.001
	treatment	7.4	1	0.007
	day:treatment	24.5	6	< 0.001
556.4 (-)	day	16.5	6	0.01
	treatment	12.7	1	< 0.001
	day:treatment	29.4	6	< 0.001
557.4 (-)	day	31.3	6	< 0.001
	treatment	13.7	1	< 0.001
	day:treatment	16.5	6	0.01
561.2 (-)	day	27.0	6	< 0.001
	treatment	2.8	1	0.09
	day:treatment	26.1	6	< 0.001
571.4 (-)	day	5.6	6	0.5
	treatment	9.5	1	0.002
	day:treatment	28.3	6	< 0.001
583.2 (-)	day	9.8	6	0.1
	treatment	7.5	1	0.006
	day:treatment	42.1	6	< 0.001
583.4 (+)	day	63.5	6	< 0.001
	treatment	206.4	1	< 0.001
	day:treatment	37.6	6	< 0.001
583.6 (+)	day	107.4	6	< 0.001
	treatment	329.5	1	< 0.001
	day:treatment	91.6	6	< 0.001
597.4 (-)	day	21.9	6	0.001
	treatment	15.7	1	< 0.001
	day:treatment	39.4	6	< 0.001

Continued on next page

Table B.13 – continued from previous page

Exploratory analysis – Putatively identified compounds				
Compound	**Fixed effect**	χ^2	**DF**	**p**
601.4 (+)	day	157.8	6	< 0.001
	treatment	125.5	1	< 0.001
	day:treatment	57.3	6	< 0.001
607.4 (+)	day	30.3	6	< 0.001
	treatment	3.6	1	0.06
	day:treatment	47.8	6	< 0.001
609.2 (-)	day	66.2	6	< 0.001
	treatment	38.2	1	< 0.001
	day:treatment	40.4	6	< 0.001
609.4 (+)	day	12.9	6	0.05
	treatment	11.4	1	< 0.001
	day:treatment	79.1	6	< 0.001
621.4 (+)	day	18.5	6	0.005
	treatment	36.4	1	< 0.001
	day:treatment	74.6	6	< 0.001
625.4 (+)	day	18.2	6	0.006
	treatment	3.0	1	0.09
	day:treatment	46.7	6	< 0.001
627.2 (-)	day	128.8	6	< 0.001
	treatment	12.9	1	< 0.001
	day:treatment	92.1	6	< 0.001
627.4 (+)	day	18.2	6	0.006
	treatment	33.2	1	< 0.001
	day:treatment	34.9	6	< 0.001
637.4 (+)	day	42.5	6	< 0.001
	treatment	6.3	1	0.01
	day:treatment	34.4	6	< 0.001
674.2 (-)	day	107.0	6	< 0.001
	treatment	97.9	1	< 0.001
	day:treatment	54.3	6	< 0.001
674.4 (-)	day	31.7	6	< 0.001
	treatment	88.1	1	< 0.001
	day:treatment	14.4	6	0.03
675.4 (+)	day	7.9	6	0.2
	treatment	16.5	1	< 0.001
	day:treatment	26.3	6	< 0.001
701.4 (-)	day	9.6	6	0.1
	treatment	110.6	1	< 0.001
	day:treatment	38.0	6	< 0.001
734.6 (+)	day	110.9	6	< 0.001
	treatment	16.2	1	< 0.001
	day:treatment	110.0	6	< 0.001
736.6 (+)	day	682.7	6	< 0.001
	treatment	1540.8	1	< 0.001
	day:treatment	1240.9	6	< 0.001
743.6 (-)	day	282.3	6	< 0.001
	treatment	33.7	1	< 0.001
	day:treatment	29.3	6	< 0.001
745.6 (-)	day	259.3	6	< 0.001
	treatment	41.6	1	< 0.001
	day:treatment	87.9	6	< 0.001
761.6 (+)	day	130.2	6	< 0.001
	treatment	49.7	1	< 0.001
	day:treatment	66.6	6	< 0.001
762.6 (+)	day	80.3	6	< 0.001
	treatment	0.9	1	0.3
	day:treatment	82.0	6	< 0.001
763.6 (+)	day	41.8	6	< 0.001
	treatment	1.9	1	0.2
	day:treatment	44.9	6	< 0.001
779.6 (-)	day	146.0	6	< 0.001
	treatment	36.8	1	< 0.001
	day:treatment	28.6	6	< 0.001
793.6 (-)	day	147.4	6	< 0.001
	treatment	13.8	1	< 0.001
	day:treatment	61.0	6	< 0.001
795.6 (-)	day	234.6	6	< 0.001
	treatment	34.0	1	< 0.001
	day:treatment	86.5	6	< 0.001
905.6 (-)	day	12.0	6	0.06
	treatment	12.2	1	< 0.001
	day:treatment	22.3	6	0.001
993.6 (-)	day	13.6	6	0.03
	treatment	14.9	1	< 0.001
	day:treatment	10.4	6	0.1

Table B.14: Selected pairwise contrasts, as estimated by the `emmeans` package for R, applied to linear mixed effects model to difference in presence of putatively identified mass bins for interest by day.

Exploratory analysis – Putatively identified compounds				
Compound (mode)	**Contrast**	**t.ratio**	**DF**	**p**
97 (-)	day -3 0 - 100	2.9	46.1	0.2
	day 1 0 - 100	-3.6	46.1	0.04
	day 8 0 - 100	-5.4	46.1	< 0.001
	day 16 0 - 100	-0.5	46.1	> 0.9
	day 22 0 - 100	1.1	46.1	> 0.9
	day 29 0 - 100	-2.6	46.1	0.4
	day 36 0 - 100	-2.7	46.1	0.3
175 (-)	day -3 0 - 100	-0.5	51.3	> 0.9
	day 1 0 - 100	3.8	51.3	0.02
	day 8 0 - 100	4.1	51.3	0.009
	day 16 0 - 100	3.5	51.3	0.06
	day 22 0 - 100	3.3	51.3	0.09
	day 29 0 - 100	2.3	51.3	0.6
	day 36 0 - 100	1.6	51.3	> 0.9
223.2 (-)	day -3 0 - 100	-1.1	56	> 0.9
	day 1 0 - 100	1.2	56	> 0.9
	day 8 0 - 100	0.8	56	> 0.9
	day 16 0 - 100	-4.5	56	0.002
	day 22 0 - 100	-4.2	56	0.006
	day 29 0 - 100	-2.0	56	0.8
	day 36 0 - 100	-1.1	56	> 0.9
228 (-)	day -3 0 - 100	0.3	40.7	> 0.9
	day 1 0 - 100	-1.2	40.7	> 0.9
	day 8 0 - 100	0.2	40.7	> 0.9
	day 16 0 - 100	2.3	40.7	0.6
	day 22 0 - 100	3.8	40.7	0.03
	day 29 0 - 100	1.2	40.7	> 0.9
	day 36 0 - 100	-0.1	40.7	> 0.9
229 (-)	day -3 0 - 100	0.8	40.4	> 0.9
	day 1 0 - 100	-0.9	40.4	> 0.9
	day 8 0 - 100	-0.6	40.4	> 0.9
	day 16 0 - 100	3.6	40.4	0.05
	day 22 0 - 100	4.9	40.4	0.001
	day 29 0 - 100	1.8	40.4	0.9
	day 36 0 - 100	0.2	40.4	> 0.9
245 (-)	day -3 0 - 100	0.9	42.6	> 0.9
	day 1 0 - 100	-3.8	42.6	0.02
	day 8 0 - 100	-1.1	42.6	> 0.9
	day 16 0 - 100	0.1	42.6	> 0.9
	day 22 0 - 100	2.4	42.6	0.5
	day 29 0 - 100	-0.2	42.6	> 0.9
	day 36 0 - 100	-2.3	42.6	0.5
247.2 (-)	day -3 0 - 100	-2.4	56	0.5
	day 1 0 - 100	-0.5	56	> 0.9
	day 8 0 - 100	-4.4	56	0.003
	day 16 0 - 100	-2.9	56	0.2
	day 22 0 - 100	0.2	56	> 0.9
	day 29 0 - 100	-2.6	56	0.4
	day 36 0 - 100	-2.1	56	0.7
259 (-)	day -3 0 - 100	3.6	35.9	0.05
	day 1 0 - 100	-4.0	35.9	0.02
	day 8 0 - 100	-5.8	35.9	< 0.001
	day 16 0 - 100	7.6	35.9	< 0.001
	day 22 0 - 100	5.0	35.9	0.001
	day 29 0 - 100	-2.6	35.9	0.4
	day 36 0 - 100	-2.6	35.9	0.4
274.2 (+)	day -3 0 - 100	8.3	56	< 0.001
	day 1 0 - 100	0.5	56	> 0.9
	day 8 0 - 100	6.4	56	< 0.001
	day 16 0 - 100	9.0	56	< 0.001
	day 22 0 - 100	11.7	56	< 0.001
	day 29 0 - 100	4.4	56	0.003
	day 36 0 - 100	-0.2	56	> 0.9
289 (-)	day -3 0 - 100	4.5	49	0.003
	day 1 0 - 100	-0.4	49	> 0.9
	day 8 0 - 100	-1.6	49	> 0.9
	day 16 0 - 100	4.1	49	0.009
	day 22 0 - 100	3.8	49	0.03
	day 29 0 - 100	-3.0	49	0.2
	day 36 0 - 100	-1.8	49	0.9
291.2 (-)	day -3 0 - 100	0.3	56	> 0.9
	day 1 0 - 100	0.6	56	> 0.9
	day 8 0 - 100	2.0	56	0.8
	day 16 0 - 100	-5.4	56	< 0.001
	day 22 0 - 100	-4.9	56	< 0.001

Continued on next page

Table B.14 – continued from previous page

Exploratory analysis – Putatively identified compounds				
Compound (mode)	**Contrast**	**t.ratio**	**DF**	**p**
	day 29 0 - 100	-1.5	56	> 0.9
	day 36 0 - 100	-1.9	56	0.8
293.2 (-)	day -3 0 - 100	1.2	56	> 0.9
	day 1 0 - 100	0.6	56	> 0.9
	day 8 0 - 100	0.8	56	> 0.9
	day 16 0 - 100	-6.6	56	< 0.001
	day 22 0 - 100	-4.7	56	0.001
	day 29 0 - 100	-2.7	56	0.3
	day 36 0 - 100	-3.0	56	0.2
301.2 (-)	day -3 0 - 100	-1.0	55.9	> 0.9
	day 1 0 - 100	2.3	55.9	0.6
	day 8 0 - 100	8.0	55.9	< 0.001
	day 16 0 - 100	11.1	55.9	< 0.001
	day 22 0 - 100	12.0	55.9	< 0.001
	day 29 0 - 100	6.0	55.9	< 0.001
	day 36 0 - 100	0.8	55.9	> 0.9
303.2 (+)	day -3 0 - 100	0.1	52.6	> 0.9
	day 1 0 - 100	2.7	52.6	0.3
	day 8 0 - 100	10.9	52.6	< 0.001
	day 16 0 - 100	12.2	52.6	< 0.001
	day 22 0 - 100	14.9	52.6	< 0.001
	day 29 0 - 100	7.1	52.6	< 0.001
	day 36 0 - 100	0.3	52.6	> 0.9
304.2 (+)	day -3 0 - 100	1.6	50.5	> 0.9
	day 1 0 - 100	2.9	50.5	0.2
	day 8 0 - 100	7.2	50.5	< 0.001
	day 16 0 - 100	11.6	50.5	< 0.001
	day 22 0 - 100	12.8	50.5	< 0.001
	day 29 0 - 100	5.5	50.5	< 0.001
	day 36 0 - 100	0.4	50.5	> 0.9
309.2 (-)	day -3 0 - 100	-0.1	56	> 0.9
	day 1 0 - 100	1.5	56	> 0.9
	day 8 0 - 100	2.5	56	0.4
	day 16 0 - 100	-4.8	56	< 0.001
	day 22 0 - 100	-4.8	56	< 0.001
	day 29 0 - 100	-2.1	56	0.7
	day 36 0 - 100	-1.6	56	> 0.9
313.2 (+)	day -3 0 - 100	0.4	46.0	> 0.9
	day 1 0 - 100	6.4	46.0	< 0.001
	day 8 0 - 100	5.8	46.0	< 0.001
	day 16 0 - 100	3.0	46.0	0.2
	day 22 0 - 100	3.1	46.0	0.1
	day 29 0 - 100	3.0	46.0	0.2
	day 36 0 - 100	-0.2	46.0	> 0.9
346 (-)	day -3 0 - 100	-1.4	21.5	> 0.9
	day 1 0 - 100	0.1	21.5	> 0.9
	day 8 0 - 100	-1.9	21.5	0.8
	day 16 0 - 100	4.8	21.5	0.005
	day 22 0 - 100	5.1	21.5	0.002
	day 29 0 - 100	4.3	21.5	0.01
	day 36 0 - 100	2.4	21.5	0.5
362 (-)	day -3 0 - 100	2.9	49.0	0.2
	day 1 0 - 100	-2.3	49.0	0.5
	day 8 0 - 100	-6.3	49.0	< 0.001
	day 16 0 - 100	-4.9	49.0	< 0.001
	day 22 0 - 100	-2.7	49.0	0.3
	day 29 0 - 100	0.9	49.0	> 0.9
	day 36 0 - 100	-1.7	49.0	0.9
425.2 (-)	day -3 0 - 100	-0.3	56	> 0.9
	day 1 0 - 100	-1.1	56	> 0.9
	day 8 0 - 100	-3.6	56	0.04
	day 16 0 - 100	-11.1	56	< 0.001
	day 22 0 - 100	-7.3	56	< 0.001
	day 29 0 - 100	-4.5	56	0.003
	day 36 0 - 100	-2.1	56	0.7
470.4 (+)	day -3 0 - 100	-0.2	31.1	> 0.9
	day 1 0 - 100	0.1	31.1	> 0.9
	day 8 0 - 100	-2.3	31.1	0.6
	day 16 0 - 100	-6.8	31.1	< 0.001
	day 22 0 - 100	-5.6	31.1	< 0.001
	day 29 0 - 100	-2.0	31.1	0.8
	day 36 0 - 100	-1.0	31.1	> 0.9
475.4 (+)	day -3 0 - 100	-1.8	56	0.9
	day 1 0 - 100	-0.1	56	> 0.9
	day 8 0 - 100	-1.7	56	0.9
	day 16 0 - 100	5.1	56	< 0.001
	day 22 0 - 100	3.4	56	0.07
	day 29 0 - 100	-2.3	56	0.6
	day 36 0 - 100	-0.1	56	> 0.9

Continued on next page

Table B.14 – continued from previous page

Exploratory analysis – Putatively identified compounds				
Compound (mode)	**Contrast**	**t.ratio**	**DF**	**p**
496.4 (+)	day -3 0 - 100	-1.4	25.3	> 0.9
	day 1 0 - 100	-2.1	25.3	0.7
	day 8 0 - 100	-4.0	25.3	0.02
	day 16 0 - 100	-3.7	25.3	0.05
	day 22 0 - 100	-2.9	25.3	0.2
	day 29 0 - 100	-4.8	25.3	0.004
	day 36 0 - 100	-4.7	25.3	0.005
497.2 (+)	day -3 0 - 100	-2.7	55.3	0.3
	day 1 0 - 100	2.0	55.3	0.8
	day 8 0 - 100	2.2	55.3	0.7
	day 16 0 - 100	-5.6	55.3	< 0.001
	day 22 0 - 100	-6.4	55.3	< 0.001
	day 29 0 - 100	-2.7	55.3	0.3
	day 36 0 - 100	-2.0	55.3	0.8
498.4 (+)	day -3 0 - 100	-1.8	44.2	0.9
	day 1 0 - 100	-2.5	44.2	0.4
	day 8 0 - 100	-3.6	44.2	0.04
	day 16 0 - 100	-0.2	44.2	> 0.9
	day 22 0 - 100	0.1	44.2	> 0.9
	day 29 0 - 100	-4.7	44.2	0.002
	day 36 0 - 100	-5.3	44.2	< 0.001
529.4 (-)	day -3 0 - 100	0.3	55.4	> 0.9
	day 1 0 - 100	-1.7	55.4	> 0.9
	day 8 0 - 100	-7.9	55.4	< 0.001
	day 16 0 - 100	-4.4	55.4	0.004
	day 22 0 - 100	-2.0	55.4	0.7
	day 29 0 - 100	-3.6	55.4	0.04
	day 36 0 - 100	-1.7	55.4	> 0.9
539.4 (+)	day -3 0 - 100	0.5	56	> 0.9
	day 1 0 - 100	-3.6	56	0.4
	day 8 0 - 100	-4.8	56	< 0.001
	day 16 0 - 100	-9.3	56	< 0.001
	day 22 0 - 100	-6.5	56	< 0.001
	day 29 0 - 100	-2.5	56	0.4
	day 36 0 - 100	-2.6	56	0.3
553.4 (-)	day -3 0 - 100	0	42.3	> 0.9
	day 1 0 - 100	-0.5	42.3	> 0.9
	day 8 0 - 100	-0.6	42.3	> 0.9
	day 16 0 - 100	-5.2	42.3	< 0.001
	day 22 0 - 100	-2.4	42.3	0.5
	day 29 0 - 100	-1.2	42.3	> 0.9
	day 36 0 - 100	-1.2	42.3	> 0.9
556.4 (-)	day -3 0 - 100	0.9	29.5	> 0.9
	day 1 0 - 100	-3.0	29.5	0.2
	day 8 0 - 100	-1.2	29.5	> 0.9
	day 16 0 - 100	-3.0	29.5	0.2
	day 22 0 - 100	-3.3	29.5	0.1
	day 29 0 - 100	-3.8	29.5	0.03
	day 36 0 - 100	-3.8	29.5	0.03
557.4 (-)	day -3 0 - 100	0	28.8	> 0.9
	day 1 0 - 100	-2.3	28.8	0.5
	day 8 0 - 100	-2.1	28.8	0.7
	day 16 0 - 100	-3.5	28.8	0.07
	day 22 0 - 100	-2.8	28.8	0.3
	day 29 0 - 100	-3.9	28.8	0.03
	day 36 0 - 100	-3.3	28.8	0.1
561.2 (-)	day -3 0 - 100	-3.2	56	0.1
	day 1 0 - 100	0.9	56	> 0.9
	day 8 0 - 100	3.6	56	0.04
	day 16 0 - 100	0.7	56	> 0.9
	day 22 0 - 100	1.5	56	> 0.9
	day 29 0 - 100	-0.4	56	> 0.9
	day 36 0 - 100	1.4	56	> 0.9
571.4 (-)	day -3 0 - 100	1.1	28.2	> 0.9
	day 1 0 - 100	-2.1	28.2	0.7
	day 8 0 - 100	-1.5	28.2	> 0.9
	day 16 0 - 100	-2.7	28.2	0.3
	day 22 0 - 100	-2.5	28.2	0.5
	day 29 0 - 100	-3.8	28.2	0.04
	day 36 0 - 100	-3.7	28.2	0.046
583.2 (-)	day -3 0 - 100	-3.7	56	0.03
	day 1 0 - 100	2.2	56	0.6
	day 8 0 - 100	2.9	56	0.2
	day 16 0 - 100	-3.8	56	0.02
	day 22 0 - 100	-1.3	56	> 0.9
	day 29 0 - 100	-1.7	56	0.9
	day 36 0 - 100	-1.9	56	0.8
583.4 (+)	day -3 0 - 100	0	56	> 0.9
	day 1 0 - 100	5.9	56	< 0.001

Continued on next page

Table B.14 – continued from previous page

Exploratory analysis – Putatively identified compounds				
Compound (mode)	**Contrast**	**t.ratio**	**DF**	**p**
	day 8 0 - 100	7.7	56	< 0.001
	day 16 0 - 100	6.3	56	< 0.001
	day 22 0 - 100	6.6	56	< 0.001
	day 29 0 - 100	5.6	56	< 0.001
	day 36 0 - 100	5.9	56	< 0.001
583.6 (+)	day -3 0 - 100	0	55.4	> 0.9
	day 1 0 - 100	-7.1	55.4	< 0.001
	day 8 0 - 100	-8.4	55.4	< 0.001
	day 16 0 - 100	-11.2	55.4	< 0.001
	day 22 0 - 100	-11.6	55.4	< 0.001
	day 29 0 - 100	-7.6	55.4	< 0.001
	day 36 0 - 100	-8.0	55.4	< 0.001
597.4 (-)	day -3 0 - 100	0.5	55.4	> 0.9
	day 1 0 - 100	1.4	55.4	> 0.9
	day 8 0 - 100	-4.8	55.4	< 0.001
	day 16 0 - 100	-2.6	55.4	0.3
	day 22 0 - 100	-2.9	55.4	0.2
	day 29 0 - 100	-4.0	55.4	0.01
	day 36 0 - 100	0.7	55.4	> 0.9
601.4 (+)	day -3 0 - 100	0.7	56	> 0.9
	day 1 0 - 100	5.9	56	< 0.001
	day 8 0 - 100	8.4	56	< 0.001
	day 16 0 - 100	5.7	56	< 0.001
	day 22 0 - 100	6.1	56	< 0.001
	day 29 0 - 100	2.5	56	0.4
	day 36 0 - 100	0.2	56	> 0.9
607.4 (+)	day -3 0 - 100	0.4	55.6	> 0.9
	day 1 0 - 100	3.6	55.6	0.03
	day 8 0 - 100	1.1	55.6	> 0.9
	day 16 0 - 100	-3.6	55.6	0.04
	day 22 0 - 100	-4.4	55.6	0.004
	day 29 0 - 100	-1.4	55.6	> 0.9
	day 36 0 - 100	-1.3	55.6	> 0.9
609.2 (+)	day -3 0 - 100	-2.0	56	0.8
	day 1 0 - 100	5.5	56	< 0.001
	day 8 0 - 100	5.1	56	< 0.001
	day 16 0 - 100	3.1	56	0.2
	day 22 0 - 100	2.7	56	0.3
	day 29 0 - 100	1.5	56	> 0.9
	day 36 0 - 100	0.5	56	> 0.9
609.4 (+)	day -3 0 - 100	-1.2	48.5	> 0.9
	day 1 0 - 100	1.1	48.5	> 0.9
	day 8 0 - 100	3.7	48.5	0.04
	day 16 0 - 100	-2.4	48.5	0.5
	day 22 0 - 100	-6.2	48.5	< 0.001
	day 29 0 - 100	-4.4	48.5	0.004
	day 36 0 - 100	3.0	48.5	0.2
621.4 (+)	day -3 0 - 100	-1.1	50.3	> 0.9
	day 1 0 - 100	-1.0	50.3	> 0.9
	day 8 0 - 100	1.0	50.3	> 0.9
	day 16 0 - 100	-1.0	50.3	> 0.9
	day 22 0 - 100	-6.3	50.3	< 0.001
	day 29 0 - 100	-6.2	50.3	< 0.001
	day 36 0 - 100	-7.0	50.3	< 0.001
625.4 (+)	day -3 0 - 100	0.1	47.8	> 0.9
	day 1 0 - 100	1.5	47.8	> 0.9
	day 8 0 - 100	2.9	47.8	0.2
	day 16 0 - 100	-1.4	47.8	> 0.9
	day 22 0 - 100	-4.3	47.8	0.006
	day 29 0 - 100	-3.2	47.8	0.1
	day 36 0 - 100	-1.9	47.8	0.8
627.2 (-)	day -3 0 - 100	-4.7	56	0.001
	day 1 0 - 100	7.9	56	< 0.001
	day 8 0 - 100	4.3	56	0.005
	day 16 0 - 100	0.1	56	> 0.9
	day 22 0 - 100	1.2	56	> 0.9
	day 29 0 - 100	0	56	> 0.9
	day 36 0 - 100	0.6	56	> 0.9
627.4 (+)	day -3 0 - 100	2.0	55.4	0.8
	day 1 0 - 100	-3.1	55.4	0.1
	day 8 0 - 100	-1.3	55.4	> 0.9
	day 16 0 - 100	-3.8	55.4	0.02
	day 22 0 - 100	-4.9	55.4	< 0.001
	day 29 0 - 100	-4.4	55.4	0.004
	day 36 0 - 100	-1.7	55.4	> 0.9
637.4 (+)	day -3 0 - 100	-1.4	50.3	> 0.9
	day 1 0 - 100	0.6	50.3	> 0.9
	day 8 0 - 100	2.0	50.3	0.7
	day 16 0 - 100	-1.3	50.3	> 0.9

Continued on next page

Table B.14 – continued from previous page

Exploratory analysis – Putatively identified compounds				
Compound (mode)	**Contrast**	**t.ratio**	**DF**	**p**
	day 22 0 - 100	-4.6	50.3	0.002
	day 29 0 - 100	-3.3	50.3	0.09
	day 36 0 - 100	-1.1	50.3	> 0.9
674.2 (-)	day -3 0 - 100	-1.4	56	> 0.9
	day 1 0 - 100	7.5	56	< 0.001
	day 8 0 - 100	6.1	56	< 0.001
	day 16 0 - 100	5.2	56	< 0.001
	day 22 0 - 100	5.3	56	< 0.001
	day 29 0 - 100	3.1	56	0.1
	day 36 0 - 100	2.3	56	0.6
674.4 (-)	day -3 0 - 100	-0.8	56	> 0.9
	day 1 0 - 100	-4.2	56	0.006
	day 8 0 - 100	-2.4	56	0.5
	day 16 0 - 100	-4.4	56	0.004
	day 22 0 - 100	-5.4	56	< 0.001
	day 29 0 - 100	-4.4	56	0.004
	day 36 0 - 100	-3.2	56	0.1
675.4 (+)	day -3 0 - 100	0.3	55.9	> 0.9
	day 1 0 - 100	-1.1	55.9	> 0.9
	day 8 0 - 100	1.0	55.9	> 0.9
	day 16 0 - 100	-4.1	55.9	0.01
	day 22 0 - 100	-3.1	55.9	0.1
	day 29 0 - 100	-4.0	55.9	0.01
	day 36 0 - 100	-0.4	55.9	> 0.9
701.4 (-)	day -3 0 - 100	-0.2	56	> 0.9
	day 1 0 - 100	-3.1	56	0.1
	day 8 0 - 100	-2.7	56	0.3
	day 16 0 - 100	-4.7	56	0.002
	day 22 0 - 100	-6.8	56	< 0.001
	day 29 0 - 100	-7.5	56	< 0.001
	day 36 0 - 100	-2.8	56	0.2
734.6 (+)	day -3 0 - 100	1.0	36.4	> 0.9
	day 1 0 - 100	-2.9	36.4	0.2
	day 8 0 - 100	-0.7	36.4	> 0.9
	day 16 0 - 100	3.9	36.4	0.02
	day 22 0 - 100	7.6	36.4	< 0.001
	day 29 0 - 100	4.7	36.4	0.003
	day 36 0 - 100	4.2	36.4	0.009
736.6 (+)	day -3 0 - 100	1.0	31.9	> 0.9
	day 1 0 - 100	26.6	31.9	< 0.001
	day 8 0 - 100	26.9	31.9	< 0.001
	day 16 0 - 100	30.4	31.9	< 0.001
	day 22 0 - 100	31.4	31.9	< 0.001
	day 29 0 - 100	31.8	31.9	< 0.001
	day 36 0 - 100	35.6	31.9	< 0.001
743.6 (-)	day -3 0 - 100	2.3	49.5	0.6
	day 1 0 - 100	-0.1	49.5	> 0.9
	day 8 0 - 100	0.8	49.5	> 0.9
	day 16 0 - 100	3.9	49.5	0.02
	day 22 0 - 100	5.3	49.5	< 0.001
	day 29 0 - 100	4.3	49.5	0.006
	day 36 0 - 100	4.6	49.5	0.002
745.6 (-)	day -3 0 - 100	1.5	53.5	> 0.9
	day 1 0 - 100	-3.4	53.5	0.07
	day 8 0 - 100	0.6	53.5	> 0.9
	day 16 0 - 100	6.8	53.5	< 0.001
	day 22 0 - 100	6.3	53.5	< 0.001
	day 29 0 - 100	5.0	53.5	< 0.001
	day 36 0 - 100	4.2	53.5	0.007
761.6 (+)	day -3 0 - 100	1.6	55.4	> 0.9
	day 1 0 - 100	7.0	55.4	< 0.001
	day 8 0 - 100	7.6	55.4	< 0.001
	day 16 0 - 100	4.1	55.4	0.01
	day 22 0 - 100	0.3	55.4	> 0.9
	day 29 0 - 100	0.2	55.4	> 0.9
	day 36 0 - 100	0.1	55.4	> 0.9
762.6 (+)	day -3 0 - 100	1.3	51.2	> 0.9
	day 1 0 - 100	6.8	51.2	< 0.001
	day 8 0 - 100	1.9	51.2	0.8
	day 16 0 - 100	-3.7	51.2	0.03
	day 22 0 - 100	-2.7	51.2	0.3
	day 29 0 - 100	-0.7	51.2	> 0.9
	day 36 0 - 100	0.4	51.2	> 0.9
763.6 (+)	day -3 0 - 100	1.0	56	> 0.9
	day 1 0 - 100	4.9	56	< 0.001
	day 8 0 - 100	1.7	56	> 0.9
	day 16 0 - 100	-3.9	56	0.02
	day 22 0 - 100	-1.6	56	> 0.9
	day 29 0 - 100	0.5	56	> 0.9

Continued on next page

Table B.14 – continued from previous page

Exploratory analysis – Putatively identified compounds				
Compound (mode)	**Contrast**	**t.ratio**	**DF**	**p**
	day 36 0 - 100	1.2	56	> 0.9
779.6 (-)	day -3 0 - 100	1.5	50.9	> 0.9
	day 1 0 - 100	-0.8	50.9	> 0.9
	day 8 0 - 100	3.3	50.9	0.08
	day 16 0 - 100	3.9	50.9	0.02
	day 22 0 - 100	4.1	50.9	0.009
	day 29 0 - 100	4.1	50.9	0.01
	day 36 0 - 100	5.3	50.9	< 0.001
793.6 (-)	day -3 0 - 100	1.1	44.7	> 0.9
	day 1 0 - 100	-2.6	44.7	0.3
	day 8 0 - 100	-0.1	44.7	> 0.9
	day 16 0 - 100	3.1	44.7	0.1
	day 22 0 - 100	5.8	44.7	< 0.001
	day 29 0 - 100	4.0	44.7	0.01
	day 36 0 - 100	3.3	44.7	0.09
795.6 (-)	day -3 0 - 100	0.1	37	> 0.9
	day 1 0 - 100	-0.7	37	> 0.9
	day 8 0 - 100	2.2	37	0.6
	day 16 0 - 100	5.3	37	< 0.001
	day 22 0 - 100	8.0	37	< 0.001
	day 29 0 - 100	5.9	37	< 0.001
	day 36 0 - 100	4.7	37	0.002
905.6 (-)	day -3 0 - 100	-0.2	56	> 0.9
	day 1 0 - 100	0.3	56	> 0.9
	day 8 0 - 100	-0.8	56	> 0.9
	day 16 0 - 100	-3.8	56	0.03
	day 22 0 - 100	-4.3	56	0.005
	day 29 0 - 100	-1.0	56	> 0.9
	day 36 0 - 100	0.5	56	> 0.9
993.6 (-)	day -3 0 - 100	0.3	56	> 0.9
	day 1 0 - 100	1.6	56	> 0.9
	day 8 0 - 100	2.5	56	0.4
	day 16 0 - 100	1.5	56	> 0.9
	day 22 0 - 100	-0.4	56	> 0.9
	day 29 0 - 100	1.2	56	> 0.9
	day 36 0 - 100	3.6	56	0.04

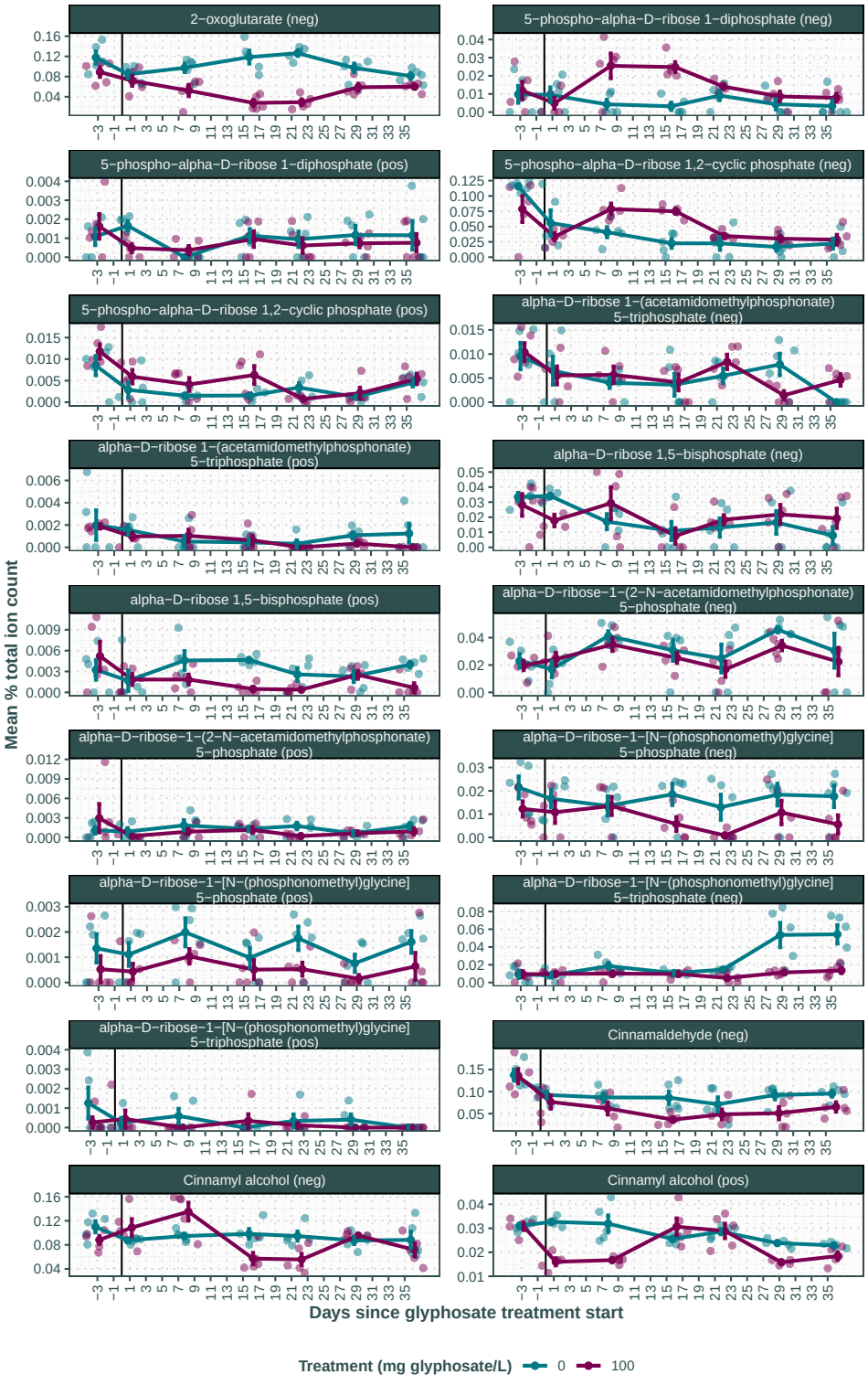

Figure B.1: Mean % ion counts for mass bins matched to secondary glyphosate and AMPA degradation products and related compounds in negative and positive mode. The raw data is shown in the background as transparent points and the black vertical line indicates introduction of the glyphosate treatment.